2024

Volume : 13
Issue : 3
Page : 179 - 283

e-ISSN : 2147-4249

Eurasian Journal of Soil Science

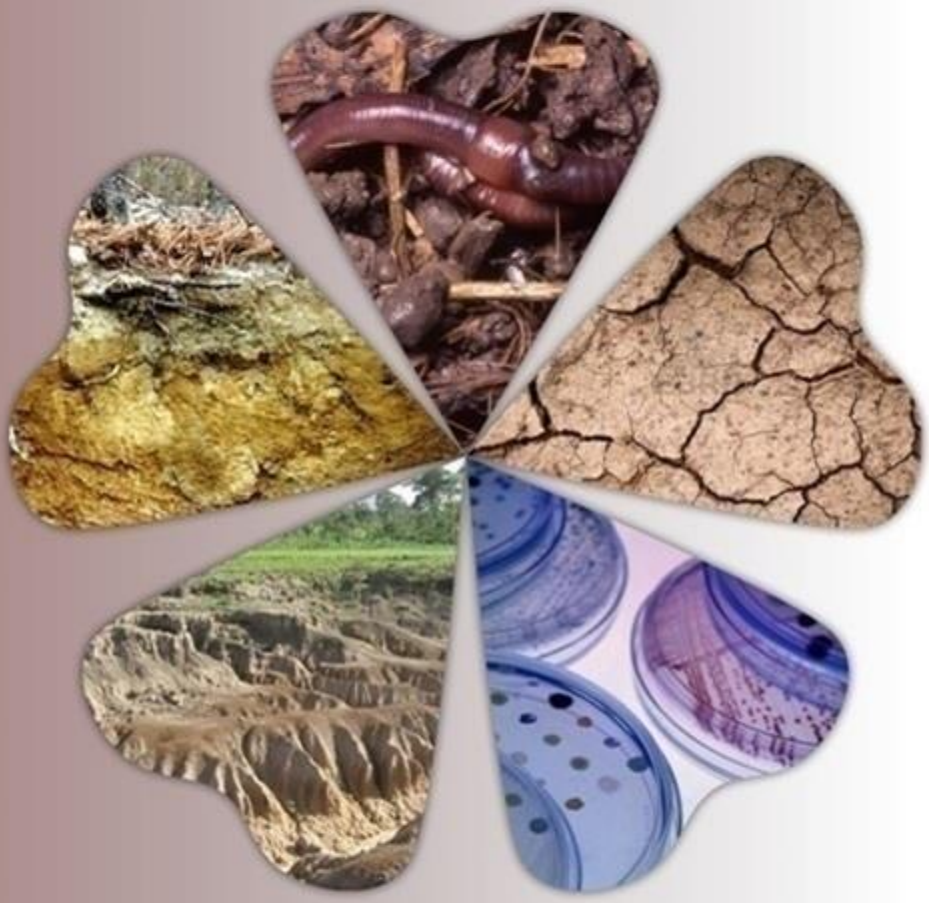

Federation of Eurasian Soil Science Societies

Editor(s)-in-chief
Dr.Rıdvan KIZILKAYA
Dr.Evgeny SHEIN
Dr.Coskun GULSER

http://ejss.fesss.org

Published by Federation of Eurasian Soil Science Societies

EURASIAN JOURNAL OF SOIL SCIENCE

(Peer Reviewed Open Access Journal)

Published by Federation of Eurasian Soil Science Societies

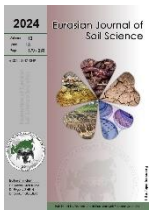

EDITORS-IN-CHIEF

Dr.Rıdvan KIZILKAYA
Ondokuz Mayıs University, Türkiye

Dr.Evgeny SHEIN
Moscow State University, Russia

Dr.Coşkun GÜLSER
Ondokuz Mayıs University, Türkiye

EDITORIAL BOARD

Dr.Amrakh I. MAMEDOV, Azerbaijan
Dr.Brijesh Kumar YADAV, India
Dr.Carla FERREIRA, Sweden
Dr.Guilhem BOURRIE, France
Dr.Guy J. LEVY, Israel
Dr.Gyozo JORDAN, Hungary
Dr.Haruyuki FUJIMAKI, Japan
Dr.Hayriye IBRIKCI, Türkiye
Dr.İbrahim ORTAŞ, Türkiye
Dr.Jae YANG, South Korea
Dr.Jun YAO, China
Dr.Mohammad A. HAJABBASI, Iran
Dr.Nicolai S. PANIKOV, USA
Dr.Shamshuddin JUSOP, Malaysia
Dr.Sokrat SINAJ, Switzerland
Dr.Tatiana MINKINA, Russia
Dr.Vít PENIZEK, Czech Republic
Dr.Yakov PACHEPSKY, USA
Dr.Yury N. VODYANITSKII, Russia

DIVISION EDITORS

Dr.Aminat UMAROVA, Soil Physics and Mechanic, Russia
Dr.David PINSKY, Soil Chemistry, Russia
Dr.Hassan EL-RAMADY, Soil Fertility, Egypt
Dr.İmanverdi EKBERLİ, Applied Mathematic in Soil Science, Türkiye
Dr.Kadir SALTALI, Soil Degradation and Reclamation, Türkiye
Dr.Metin TURAN, Plant Nutrition, Türkiye
Dr.Mustafa BOLCA, Soil Survey and Mapping, Türkiye
Dr.Nikolay KHITROV, Soil Genesis and Classification, Russia
Dr.Orhan DENGİZ, Remote Sensing and GIS in Soil Science, Türkiye
Dr.Sait GEZGİN, Fertilizer and Fertilization, Türkiye
Dr.Sezai DELİBACAK, Soil Health and Quality, Türkiye
Dr.Svatopluk MATULA, Soil Hydrology, Czech Republic
Dr.Svetlana SUSHKOVA, Soil Pollution, Russia
Dr.Taşkın ÖZTAŞ, Soil Erosion and Conservation, Türkiye
Dr.Tayfun AŞKIN, Geostatistics, Türkiye
Dr.Tomasz ZALESKI, Soil Mineralogy & Micromorphology, Poland
Dr.Victor B. ASIO, Soil Management, Philippines
Dr.Vishnu D. RAJPUT, Soil Biology and Biochemistry, Russia

SCIENTIFIC EDITORS

Dr.Alexander MAKEEV, Russia
Dr.Benyamin KHOSHNEVİSAN, China
Dr.Fariz MIKAILSOY, Türkiye
Dr.Füsun GÜLSER, Türkiye
Dr.Galina STULINA, Uzbekistan
Dr.H. Hüsnü KAYIKÇIOĞLU, Türkiye
Dr.İzzet AKÇA, Türkiye
Dr.János KÁTAI, Hungary
Dr.Lia MATCHAVARIANI, Georgia
Dr.Marketa MIHALIKOVA, Czech Republic
Dr.Maja MANOJLOVIC, Serbia
Dr.Niyaz Mohammad MAHMOODI, Iran
Dr.Ramazan ÇAKMAKCI, Türkiye
Dr.Ritu SINGH, India
Dr.Saglara MANDZHIEVA, Russia
Dr.Saoussen HAMMAMI, Tunusia
Dr.Srdjan ŠEREMEŠİĆ, Serbia
Dr.Velibor SPALEVIC, Montenegro

ADVISORY EDITORIAL BOARD

Dr.Ajit VARMA, India
Dr.David MULLA, USA
Dr.Donald GABRIELS, Belgium
Dr.İsmail ÇAKMAK, Türkiye
Dr.Nicola SENESI, Italy

HONORARY BOARD

Dr.Ayten NAMLI, Türkiye
Dr.Beibut SULEIMENOV, Kazakhstan
Dr.Ermek BAIBAGYSHOV, Kyrgyzstan
Dr.Garib MAMMADOV, Azerbaijan
Dr.Hamid ČUSTOVIĆ, Bosnia & Herzegovina
Dr.Irina Carmen CALCIU, Romania
Dr.Mihajlo MARKOVİĆ, Serbia
Dr.Pavel KRASILNIKOV, Russia

LINGUISTIC EDITOR

Birol KURT, Türkiye
Gregory T. SULLIVAN, Australia
Oksana FOTINA, Russia
Yelena KANDALINA, Kazakhstan

ABOUT THIS JOURNAL: Eurasian Journal of Soil Science is the official English language journal of the Federation of Eurasian Soil Science Societies. Eurasian Journal of Soil Science peer-reviewed open access journal that publishes research articles, critical reviews of basic and applied soil science in all related to soil and plant studies and general environmental soil science.

ABSTRACTING AND INDEXING: SCOPUS, CABI, FAO-Agris, EBSCOhost, ProQuest, DOAJ, OAJI, TR Dizin, TURKISH Journalpark, CrossRef, CiteFactor, CAS, etc.

Year: 2024, Volume: 13, Issue: 3, Page: 179 - 283 **e-ISSN 2147-4249**

EURASIAN JOURNAL OF SOIL SCIENCE

(Peer Reviewed Open Access Journal)

Published by Federation of Eurasian Soil Science Societies

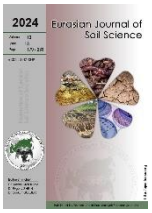

YEAR: 2024 **VOLUME : 13** **ISSUE : 3** **PAGE : 179 – 283**

CONTENTS

Eurasian Journal of Soil Science 2024, 13(3), 179 - 189

Eurasian Journal of Soil Science

Journal homepage : http://ejss.fesss.org

Efficacy of solid and liquid Biolistics in improving the nutrients in latosol soil from Bali, Indonesia

Ni Luh Gede Sudaryati, I Made Dwi Mertha Adnyana *

Department of Biology, Faculty of Information Technology and Science, Hindu University of Indonesia, East Denpasar, Denpasar City, Indonesia

Article Info
Received : 17.06.2022
Accepted : 30.01.2024
Available online: 06.02.2024

Author(s)
N.L.G.Sudaryati
I.M.D.M.Adnyana *

* Corresponding author

Abstract

The increase in household organic waste during the COVID-19 pandemic was a source of pollution, especially in soil. The high pollution intensity in various sectors causes the soil to degrade and lose nutrients. This study aimed to analyze the efficacy of solid and liquid biolistics for improving the nutritional status of latosol soil collected from Bali, Indonesia. The experimental design was a completely randomized design. Efficacy testing by providing solid and liquid *biolistics* to latosol soils in polybags at different concentrations was performed five times. Macro- and micronutrient testing was carried out three months after the application of the treatments. One-way ANOVA and the LSD test (p<0.05) were used to assess the results. The results revealed significant differences between the treatment groups in terms of N, P, K, the C/N ratio, water content, and pH, with a probability value of 0.000 (p<0.05). Thus, solid and liquid biolistics s are efficacious at increasing the fertility of latosol soils. The contents of N, P, K, moisture content, pH, macronutrients (P_2O_5, K_2O, C-Organic, N-Total, and C/N ratio) and micronutrients (Fe, Mg, Mn, Na, Zn) contribute significantly to improving soil aggregates and structures; improving the physical, chemical, and biological properties of the soil; and improving the bioavailability of nutrients and soil quality. The presence of microorganisms is involved in accelerating the process of biodegradation and decomposition in soil. Thus, solid and liquid biolistics s deserve to be developed as natural soil repairers.

Keywords: Biofertilizer, Biolistics, soil repairer, local microorganisms, domestic waste.

© 2024 Federation of Eurasian Soil Science Societies. All rights reserved

Introduction

The COVID-19 pandemic has harmed the environment, especially through the increase in household domestic waste quality caused by large-scale social restrictions throughout Indonesia, including the Province of Bali (Putro, 2020). The work-from-home policy contributes to an increase in organic waste and food every day (Pappalardo et al., 2020; Arumugam et al., 2021). In addition, the impact of the COVID-19 pandemic reportedly resulted in a decrease in waste management and management by relevant agencies (Roy et al., 2021). According to data from the National Waste Management Information System in 2020, waste generation in 9 districts/cities in Bali reached 904,924.34 tons/year, with an average of 2,479.24 tons/day. Waste generation increased in 2021, reaching 915,482.46 tons/year, with an average of 2,508.17 tons/day (Ministry of Environment and Forestry, 2020, 2022). Household organic waste accounted for 40.91%, the market accounted for 16.04%, and other waste accounted for 43.05%, with 1,178.13 tons/day left untreated (Waste for Change, 2021), resulting in environmental pollution, including a decrease in soil fertility rates (El-Ramady et al., 2020; Adnan et al., 2022; Yang et al., 2022).

Every day, an increase in waste generation negatively impacts soil quality (Putro, 2020). This is because poorly handled domestic organic wastewater enters and permeates the soil, worsens soil conditions, threatens the survival of soil microbiota, and has implications for decreasing soil nutrients and causing environmental degradation (Tsukiji et al., 2020; Waste for Change, 2021). Recent research reveals that the pollution intensity from various sectors results in soil degradation and nutrient loss (Dehghani et al., 2021; Suriyaprakash et al.,

: https://doi.org/10.18393/ejss.1432873
: http://ejss.fesss.org/10.18393/ejss.1432873
Publisher : Federation of Eurasian Soil Science Societies
e-ISSN : 2147-4249

2021). Furthermore, inorganic fertilizers containing nitrogen and phosphorus significantly contribute to soil pollutants, lowering physical, chemical, biological, and soil permeability (Eugenio et al., 2018; El-Ramady et al., 2020). Continuous degradation of soil results in a low number of remodeled microorganisms in the soil, resulting in a decrease in agricultural land productivity (Geisseler and Scow, 2014; Kashyap et al., 2017; Pappalardo et al., 2020).

In light of these concerns, it is crucial to implement integrated waste management, including agricultural land, to minimize land degradation in Bali. The use of synthetic fertilizers in the community harms the environment, so new efforts have been made to use household and market organic waste (leaves, fruits, and vegetables) enriched with local microorganisms and fungi (*Trichoderma* sp.) as soil repellents and soil fertility enhancers called *biolistics*. Solid and liquid *biolistics* products were made to stop the use of inorganic fertilizers, which kill microorganisms in the soil and cause the nutrients in the soil to run out (Du et al., 2020). Raw materials are sourced from waste and passed through the fermentation system (Suthar et al., 2017; Vassileva et al., 2021). They are useful for increasing microbial biomass and bioconversion of microbial substrates, enzymes, and primary and secondary metabolites (Vassileva et al., 2021). In addition, bacterial and fungal inoculations of the main ingredients of biofertilizers reportedly increase the bioavailability of soil nutrients through nitrogen fixation and mobilization of phosphorus, potassium, and iron nutrients and improve the soil structure by improving its aggregation and stability (Rashid et al., 2016).

This study aimed to evaluate and analyze the efficacy of solid and liquid *biolistics* for improving the nutritional status of latosol soil in Bali, Indonesia. Type land latosols are spread throughout the Bali region and have a relatively low fertility rate. This research is expected to contribute to the use of waste as a useful soil remediation agent.

Material and Methods

Study design: This study utilized an experimental design with a completely randomized design. There were six treatment groups, and each group was replicated five times, as determined using the Federer equation (Darwin et al., 2021). In this study, solid and liquid biolistics were applied at different levels in latosol soils with low fertility rates in large polybags; 20 polybags were given solid biolistics with different levels of P1 (157 g/polybag), P2 (314 g/polybag), P3 (471 g/polybag), and P4 (628 g/polybag); five pure positive controls (PCs) were given 100% NPK; and five negative controls (NCs) were given without treatment. Moreover, liquid biolices that are ready for use are then applied to the soil utilizing 1 L of liquid biolases mixed in 5 L of clean water and poured into 20 polybags at different concentrations, namely, P1 (208.4 mL/polybag), P2 (417 mL/polybag), P3 (533.8 mL/polybag) and P4 (834 mL/polybag). Moreover, five pure positive controls (PCs) were given 100% NPK, and five negative controls (NCs) were not treated. A total of 60 polybags with a total of 30 polybags were given solid biolistics, and 30 polybags were given liquid biolistics. The intensity of soil fertilization was carried out once every two weeks for a duration of three months. The soil fertility rates were measured using the parameters nitrogen (N), phosphorus (P), potassium (K), the C/N ratio, moisture content, and acidity level (pH) one week after the treatment ended. Macro- and micronutrients in solid and liquid biolistics were measured in integrated testing laboratories.

Sample: Federer's formula was used to determine the number of samples and tests used (Adnyana, 2021). The formula used was (n-1) (t-1) ≥ 15, and the results were obtained for six treatment groups with five replicates each; 30 samples were used for solid biochemical testing, and 30 samples were used for liquid biochemical testing.

Laboratory testing: After solid and liquid *biolistics were applied*, soil nutrient testing was conducted in the laboratory via several tests. The soil N (%) levels were determined using a spectrophotometer set to a wavelength of 636 nm and the following standards for testing organic fertilizer. At a wavelength of 651 nm, Walkley and Black used a spectrophotometer to measure the levels of C-organic (%). The amounts of significant (P and K) and minor (Fe, Mn, Zn, and Na) nutrients in the soil were measured using Morgan Wolf extract. Spectrometry was used to measure P_2O_5, K_2O total, and N-total (Kjeldahl), and a pH meter was used to measure the pH. The Regulation Number 01 of 2019 of the Minister of Agriculture of the Republic of Indonesia on organic fertilizers, biological fertilizers, and soil reformers was used to guide all tests (Ministry of Agriculture, 2019).

Time and Location: This research was conducted at Greenhouse Tanam.id, Denpasar, for six months (January–June 2021) at the Treatment and Technical Implementation Unit of the Biosciences and Biotechnology Laboratory and the Soil Chemistry and Fertility Laboratory of Udayana University to test macro, micro, and soil fertility nutrients based on predetermined parameters.

Instruments and Materials: The instruments used in this study consisted of personal protective equipment, needles, trays, hoes, punches, analytical scales, acid chambers, buckets, hammers, hacksaws, paralons, knives,

measuring cups, electric stoves, destilators, spectrophotometers, beker glasses, Erlenmeyer flasks, ovens, hanging scales, digital scales, large polybags, timba, gadgets, and stationery. The research materials used were 40 kg of kitchen and market organic waste (fruit, leaf, and vegetable), 5 kg of bamboo leaf, 5 kg of rice laundry water, coconut water, sack, trash bag, plastic, Trichoderma sp. isolate, methyl red-methyl blue, 40% boric acid, granulated sugar, 0.1 N NaOH, 0.1 N HCl, H_2SO_4 and latosol soil taken from Suwung landfill, Denpasar, Bali.

Research procedures

1. In the media preparation, latosol soil was inserted into a large polybag (40 cm) with a filling of 3/4 of the total polybag weighing 4-6 kg. There were 60 polybags per row of media provided.
2. At this stage, the preparation of *the biolistic* materials was performed. It consists of preparing kitchen organic waste and markets in the form of rotten fruit waste, vegetables, and leaves obtained from various places, weighing as much as 20 kg. Isolate samples were obtained from the Food and Horticulture Plant Protection Center (BPTPH) Semarang. A 250 g isolate of *Trichoderma* sp. mushrooms was propagated in rice media.
3. At this stage, as much as 5 kg of fruit and vegetable waste was weighed and then refined using a blender. Subsequently, 1 kg of granulated sugar and one bunch of leaves were chopped as a source of microbes, 2 L of coconut water, and 15 L of rice laundry water. The material is a microbial growth medium containing carbohydrates (source C), proteins (source N), minerals, and vitamins. The media was subsequently added, and the plants were curdled for 3-5 days until fragrance. The solution was filtered and stored in a bottle, after which the resulting gas was discharged. If the gas is removed, a solution containing microorganisms from the area is ready to use.
4. At this stage, 20 kg of organic waste is prepared. A large bucket was prepared, and then, organic waste, *Trichoderma* sp., and MOL were isolated so that the volume was as high as 0.2 L. Dopped organic waste was spread, covered with sacks or other materials, and fermented for 2-3 weeks. The mixture was opened every ten days, a local microorganism solution was added, and the mixture was closed again. After three weeks, the fertilizer is disassembled by paying attention to the black or brown color of the soil, after which the solid *biolistics* are ready to use.
5. At this stage, 15 kg of organic waste was chopped, and as much as 500 mL of *Trichoderma* sp. isolates and local microorganism solutions were added. The mixture was subsequently squeezed for one week, after which the fragrant fragrance was filtered, after which the liquid *biolistics* were ready to use.
6. To test the soil and *biolistics* that are ready for use, polybags filled with latosol soil were added. Twenty polybags were given solid *biolistics* at different concentrations—25% (157 g/polybag), 50% (314 g/polybag), 75% (471 g/polybag), and 100% (628 g/polybag); five pure positive controls were administered 100% NPK, and five negative controls were administered without treatment. Moreover, liquid *biolases* that are ready for use are then applied to the soil utilizing 1 L of liquid *biolases* mixed in 5 L of clean water and poured into 20 polybags at different concentrations, namely, 25% (208.4 mL/polybag), 50% (417 mL/polybag), 75% (533.8 mL/polybag) and 100% (834 mL/polybag). Moreover, five pure positive controls were given 100 NPK, and 5 negative controls were not treated. Solid and liquid biologics were added once every two weeks, and the experiments were carried out in the afternoon. Fertilization rates were based on guidelines for the use of biological fertilizers and soil repellents. After three months of testing the fertility of the soil, the fertility level was determined.
7. Fertility rate testing was performed by submitting soil samples and solid and liquid *biolistics* to an integrated testing laboratory, after which the data were further analyzed and test results obtained; this process ended with statistical analysis and interpretation of the data.

Data analysis

The soil fertility rates in each group were determined using statistical analysis to assess the efficacy of solid and liquid biolistics at different levels. Parameters The following elements were analyzed using SPSS, Inc., software version 25.0, with one-way ANOVA and LSD tests: nitrogen (N), phosphorus (P), potassium (K), carbon/nitrogen ratio, moisture content, and acidity level (pH). The macro- and micronutrient contents were analyzed descriptively and are presented in the graphs and narratives. The interpretation of the laboratory results followed the standard guidelines of the National Standardization Agency of the Republic of Indonesia (SNI) 19-7030-2004 on composting from domestic organic waste (National Standardization Agency of the Republic of Indonesia, 2004) and the Regulation of the Minister of Agriculture of the Republic of Indonesia No. 01 of 2019 concerning organic fertilizers, biological fertilizers, and soil repairers (Ministry of Agriculture, 2019).

Results and Discussion

Efficacy of solid biolistics in increasing the fertility of latosol soils

Based on solid *biolistics* efficacy test findings on the fertility rate of latosol soil collected in Bali, Indonesia, Table 1 shows five parameters, namely, N, P, K, the C/N ratio, and the moisture content. The results of the one-way ANOVA test showed that nitrogen content (N) had an F value of 32,151, with a probability value of p= 0.000<0.05. Therefore, there was a significant difference between the treatment groups. The least significant difference (LSD) was obtained only with the P3 treatment. This was very true for P4, whereas the other treatments did not significantly differ. An F count of 33.683 was obtained for the phosphorus content (P), with a probability of p= 0.000<0.05. Thus, there were significant differences between the treatment groups. The LSD test results revealed significant differences between the NC treatment and the PC, P2 treatment and P3, and P3 treatment and P4. K was tested, and an F count of 28,540 was obtained, with a probability value of p= 0.000 <0.05. Thus, there was a significant difference between the treatment groups. The LSD test results showed a noticeable difference in the PC treatment with P1, P2 with P3, and P3 with P4. Testing the ratio of carbon to nitrogen (C/N) yielded a calculated F count of 21,844, with a probability value **of p**= 0.000 < 0.05. Thus, there was a significant difference between the treatment groups. The LSD test results revealed significant differences between the NC and PC groups and between the P3 and P4 groups. Furthermore, the water content test obtained an F value of 168,499 with a probability value of p= 0.000 < 0.05. Thus, there were significant differences between the treatment groups. The LSD test revealed significant differences among the NC+PC treatment, PC+P1 treatment, PC+P2 treatment, and PC+P3 treatment groups.

Table 1. Fertility of the latosol soil caused by the addition of solid *biolistics*

Parameter/Unit	Treatment	Mean ± SD	Shapiro-Wilk	Levene Statistic	F	p value
N (%)	Negative control (NC)	0.240 ± 0.089^{a}	0.831	9.021	32.151	0.000*
	Positive control (PC)	0.774 ± 0.261^{a}				
	P1 (157 g/polybag)	0.884 ± 0.185^{a}				
	P2 (314 g/polybag)	1.894 ± 0.351^{a}				
	P3 (471 g/polybag)	3.304 ± 0.666^{b}				
	P4 (628 g/polybag)	6.014 ± 1.923^{c}				
P (%)	Negative control (NC)	0.320 ± 0.192^{a}	0.904	2.397	33.683	0.000*
	Positive control (PC)	3.344 ± 0.831^{b}				
	P1 (157 g/polybag)	3.606 ± 0.196^{b}				
	P2 (314 g/polybag)	3.714 ± 0.391^{b}				
	P3 (471 g/polybag)	4.580 ± 0.540^{c}				
	P4 (628 g/polybag)	5.594 ± 1.261^{d}				
K (%)	Negative control (NC)	0.162 ± 0.087^{a}	0.888	3.858	28.540	0.000*
	Positive control (PC)	1.666 ± 0.150^{a}				
	P1 (157 g/polybag)	0.724 ± 0.595^{c}				
	P2 (314 g/polybag)	0.570 ± 0.155^{c}				
	P3 (471 g/polybag)	2.292 ± 0.894^{d}				
	P4 (628 g/polybag)	3.452 ± 0.643^{e}				
C/N Ratio	Negative control (NC)	2.506 ± 0.879^{a}	0.902	15.205	21.844	0.000*
	Positive control (PC)	5.980 ± 0.238^{b}				
	P1 (157 g/polybag)	6.480 ± 0.571^{b}				
	P2 (314 g/polybag)	7.000 ± 0.748^{b}				
	P3 (471 g/polybag)	7.760 ± 0.876^{b}				
	P4 (628 g/polybag)	11.358 ± 2.959^{c}				
Water Content (% [w/w])	Negative control (NC)	6.456 ± 0.741^{a}	0.843	2.835	168.499	0.000*
	Positive control (PC)	20.004 ± 2.251^{b}				
	P1 (157 g/polybag)	22.052 ± 1.093^{c}				
	P2 (314 g/polybag)	21.896 ± 1.306^{c}				
	P3 (471 g/polybag)	25.354 ± 0.759^{d}				
	P4 (628 g/polybag)	28.740 ± 1.154^{e}				

Abbreviations: * = significant difference (p<0.05); different letters = significant difference according to the LSD test (p<0.05); same letter = no significant difference according to the LSD test (p> 0.05); N= nitrogen; P= phosphorus; K= potassium; C/N = carbon-to-nitrogen ratio.

Efficacy of liquid biolistics in increasing the fertility of latosol soils

The efficacy of liquid *biolistics* on the fertility rate of latosol soil collected from Bali, Indonesia, was evaluated using five criteria, namely, the concentration of N, P, and K; the C/N ratio; and the acidity level (pH), as shown in Table 2. The statistical test results showed that the nitrogen content (N) obtained from the F count was 140,511 ($p = 0.000 < 0.05$). Thus, there was a significant difference between the treatment groups. The LSD test results showed a very noticeable difference in all treatment groups, NC, PC, P1, P2, P3, and P4, with values of $p<0.05$. The phosphorus content (P) was tested, and a calculated F count value of 35,380 was obtained, with a probability of $p = 0.000 < 0.05$. Thus, there was a significant difference between the treatment groups. The LSD test results revealed noticeable differences between P2 and P3 and between P3 and P4. K was obtained from an F count of 111,935, with a probability value of $p = 0.000 < 0.05$. Thus, there was a significant difference between the treatment groups. According to the LSD tests, there were clear differences between the negative control (NC) and positive control (PC) groups and between the PC treatment and P1, P1 treatment and P2, and P3 treatment and P4. Testing the ratio of carbon to nitrogen (C/N) yielded an F count of 188,959 with a probability value of $p = 0.000 < 0.05$. Thus, there was a significant difference between the treatment groups. The LSD test results showed very noticeable differences in the negative control treatment (NC) compared to the positive control (PC), P1 treatment with P2, P2 treatment with P3, and P3 treatment with P4. Furthermore, acidity level (pH) testing yielded a calculated F value of 11,555, with a probability value of $p = 0.000 < 0.05$. Thus, there was a significant difference between the treatment groups. The LSD test results showed a noticeable difference between the negative control treatment (NC) and the positive control (PC).

Table 2. Fertility of the latosol soil caused by the addition of liquid biolistics

Parameter/ Unit	Treatment	Mean ± SD	Shapiro-Wilk	Levene Statistic	F	p value
N (%)	Negative control (NC)	0.560 ± 0.181^{a}	0.933	3.233	140.511	0.000*
	Positive control (PC)	12.586 ± 0.805^{b}				
	P1 (208.4 mL/polybag)	6.418 ± 1.516^{c}				
	P2 (417 mL/polybag)	7.922 ± 1.321^{d}				
	P3 (533.8 mL/polybag)	12.874 ± 1.331^{e}				
	P4 (834 mL/polybag)	16.698 ± 0.727^{f}				
P (%)	Negative control (NC)	0.802 ± 0.272^{a}	0.913	6.804	35.380	0.000*
	Positive control (PC)	8.338 ± 0.842^{a}				
	P1 (208.4 mL/polybag)	5.818 ± 1.810^{a}				
	P2 (417 mL/polybag)	7.864 ± 1.150^{b}				
	P3 (533.8 mL/polybag)	13.196 ± 4.591^{c}				
	P4 (834 mL/polybag)	17.106 ± 1.023^{d}				
K (%)	Negative control (NC)	1.300 ± 0.187^{a}	0.823	2.437	111.935	0.000*
	Positive control (PC)	14.658 ± 1.960^{b}				
	P1 (208.4 mL/polybag)	8.986 ± 0.406^{c}				
	P2 (417 mL/polybag)	12.516 ± 0.626^{d}				
	P3 (533.8 mL/polybag)	12.546 ± 0.956^{d}				
	P4 (834 mL/polybag)	14.050 ± 1.159^{e}				
C/N Ratio	Negative control (NC)	5.540 ± 1.054^{a}	0.955	0.129	188.959	0.000*
	Positive control (PC)	13.124 ± 0.706^{b}				
	P1 (208.4 mL/polybag)	14.382 ± 1.360^{b}				
	P2 (417 mL/polybag)	16.598 ± 1.072^{c}				
	P3 (533.8 mL/polybag)	19.720 ± 0.955^{d}				
	P4 (834 mL/polybag)	25.090 ± 6.189^{e}				
pH	Negative control (NC)	4.540 ± 0.763^{a}	0.961	0.632	11.555	0.000*
	Positive control (PC)	6.000 ± 0.612^{b}				
	P1 (208.4 mL/polybag)	5.900 ± 0.418^{b}				
	P2 (417 mL/polybag)	6.200 ± 0.836^{b}				
	P3 (533.8 mL/polybag)	7.000 ± 0.790^{b}				
	P4 (834 mL/polybag)	7.500 ± 0.500^{b}				

Abbreviations: * = significant difference ($p< 0.05$); different letters = significant difference according to the LSD test ($p<0.05$); same letter = no significant difference according to the LSD test ($p> 0.05$); N= nitrogen; P= phosphorus; K= potassium; C/N = ratio of carbon to nitrogen; pH = hydrogen power.

Macro and micronutrient contents in solid and liquid biolistic

The results of laboratory tests on the content of solid and liquid biolistic macro- and micronutrients are presented in Figures 1 and 2. The macronutrients contained in solid and liquid biologics include C-organic substances; total N, P_2O_5, and K_2O; the C/N ratio; and hydrogen. The micronutrients contained in solid and liquid biolistics include iron (Fe), magnesium (Mg), mangan (Mn), sodium (Na), and zinc (Zn). The results indicate that all the parameters tested related to the contents of macro- and micronutrients contained in solid and liquid *biolistics* meet the minimum standards required for biological fertilizers, soil repairers, and solid organic fertilizers; the raw materials used are from domestic organic waste according to the Indonesian National Standard 19-7030-2004 and the Regulation of the Minister of Agriculture of the Republic of Indonesia number 01 of 2019. The content is very useful for increasing soil fertility; improving the microbiological, physical, and chemical structure of the soil; and accelerating the growth of organisms to help improve the process of biodegradation and the availability of nutrients in the soil.

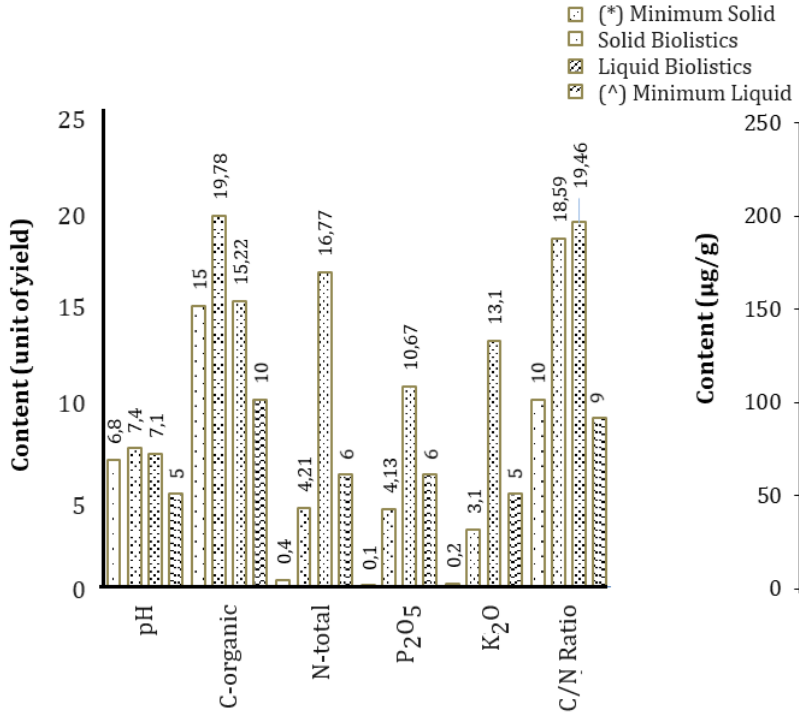

Figure 1. The macronutrients contained in *biolistics* are solids and liquids.
Information: (*) = Indonesian National Standard (SNI) Reference 19-7030-2004; (^) Minister of Agriculture of the Republic of Indonesia Number 01 of 2019; pH = Power of Hydrogen; P_2O_5 = Phosphorus pentaxide; K2O = Potassium Oxide; C/N = Ratio of carbon to nitrogen.

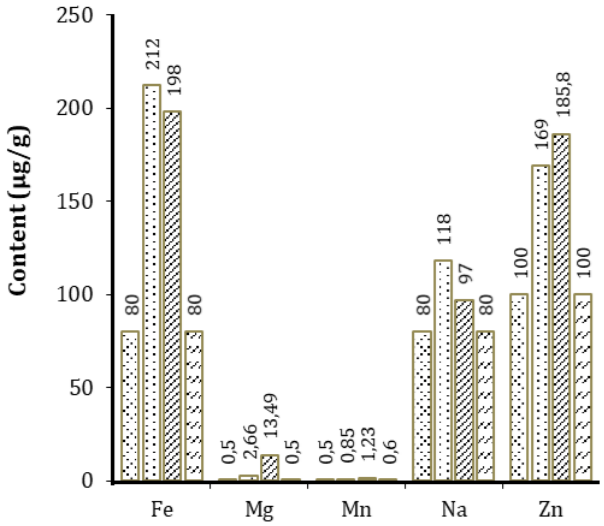

Figure 2. The micronutrients contained in the *biolistics* are solids and liquids.
Information: (*) = Indonesian National Standard (SNI) Reference 19-7030-2004; (^) Minister of Agriculture of the Republic of Indonesia Number 01 of 2019; Fe = Iron (µg/g); Mg = Magnesium (%); Mn = Manganese (µg/g); Na = Sodium (%); and Zn = Zinc (µg/g).

Discussion

Research on the efficacy of solid and liquid *biolistics* in latosol soils showed that nitrogen (N), phosphorus (P), potassium (K), the C/N ratio, moisture content, and acidity level (pH) in all treatment groups significantly improved the aggregation and biological structure of the soil, increasing the capacity and number of microorganisms for organic matter biodegradation and opening up the soil. These results are in line with the findings of Lazcano et al. (2021) and Rashid et al. (2016), who revealed that the inoculation of bacteria and microorganisms in organic fertilizers can improve physical, chemical, and microbiological properties and improve soil aggregates so that they can be applied.

Tables 1 and 2 show that there is a significant difference between soils given solid and liquid *biolistics* treatments at different concentrations and those given a negative control (NC) or positive control (PC). The N, P, K, C/N ratio, water content, and pH positively affected the fertility of the latosol soil. This occurs because of the enrichment of local microorganisms and fungi by *Trichoderma* sp., which can increase nutrients from solid and liquid biolistics. When applied to the soil, biochar can increase the availability of nutrients and increase aggregation (Mahanty et al., 2016; Mitter et al., 2021). Enrichment by adding *Trichoderma* sp. isolates were enriched by the addition of biological fertilizer products, organic fertilizers, and soil repellents because this

fungus has many advantages and positive impacts on soil improvement (Pandey and Chandra, 2016; Mącik et al., 2020; Fasusi et al., 2021).

Trichoderma spp. can produce antibiotics that are used naturally to kill parasites found in the soil (Al-Suhaibani et al., 2020; Bhandari et al., 2021). This fungus produces several secondary metabolites in the form of nonribosomal peptides, terpenoids, pyrones, and indolic derivatives with toxic effects on breeding soil parasites (Kashyap et al., 2017). In addition, *Trichoderma* sp. can produce indole-3-acetate acid, which contributes to plant acceleration and increased growth time (Asghar and Kataoka, 2021). *The* organic matter of *Trichoderma* can accelerate the process of nitrogen mineralization by increasing the effectiveness of soil phosphatase (Al-Suhaibani et al., 2020; Asghar and Kataoka, 2021; Mayo-Prieto et al., 2021), increasing nutrient absorption, and increasing soil tolerance to abiotic and biotic acidity (Bhardwaj et al., 2014; Fasusi et al., 2021).

In solid and liquid *biolistics*, pollination with local microorganisms and *Trichoderma* sp. increases the activity of microbial exoenzymes that help to breakdown carbon, nitrogen, and phosphorus (Abbasi and Yousra, 2012; Francioli et al., 2016). Scientists are attempting to accelerate the breakdown of nutrients, biomass growth, and absorption of organic and inorganic substances (Mehetre and Mukherjee, 2015; Bononi et al., 2020). This efficiency in the use of microand macronutrients culminates in increased soil productivity (Zhao et al., 2018; Szczałba et al., 2019; Vassileva et al., 2021), transforming the soil environment of the rhizosphere, plant growth-boosting agents, natural decomposition agents, and bioremediation biological agents (Halifu et al., 2019; Zin and Badaluddin, 2020), increasing the provision of soil nutrients in the form of N, P, and K, and other nutrients such as antibiotics, auxin hormones, cytokinins, and vitamins that enrich the root rhizosphere (Contreras-Cornejo et al., 2016; Yadav and Sarkar, 2019; Bhandari et al., 2021), and improving the biological properties of soils by dissolving phosphate compounds, nitrogen propagation, and phosphate activity (Fitriatin et al., 2021).

The macronutrients in the biolistic solid and liquid contents met the quality standards of fertilizers and soil reformers required by the Regulation of the Minister of Agriculture of the Republic of Indonesia number 01 of 2019. Figure 1 shows that the pH in solid *biolistics* is classified as neutral to alkaline (7.4), while in liquid *biolistics*, it is classified as neutral (7.1). The C-organic content was very high at 19.78% in solid *biolistics* and 15.22% in liquid *biolistics*. The N-total value in liquid *biolistics* (16.77%) is higher than that in solid *biolistics* (4.21%) but is classified as meeting the minimum requirements. Furthermore, for the P_2O_5 content, the same result was obtained, namely, from liquid *biolistics* (10.67%) and a high length from solid *biolistics* (4.13%). At K_2O, the content of solid *biolistics* (K) was 3.1% lower than that of liquid *biolistics* (13.1%), and the C/N ratios in solid *biolistics* (18.59) and liquid *biolistics* (19.46) were very high.

Relatively good results were obtained for improving the soil nutrients in the latosol soils. In line with the findings of Arthanawa et al. (2022), research on the effects of natural biofertilizers with a pH of H_2O (8.19), C-organic material (25.18%), N-total material (1.49%), P (2.01%), and K (1.99%) was classified as very high, with a field capacity of 29.16%, so that the use of natural materials can increase soil fertility. Kai and Tamaki (2020) revealed that obtaining similar higher total cholesterol (TC), total nitrogen (TN), and C/N ratios in soils fed organic fertilizers seems to increase bacterial biomass, leading to improved nutrient circulation through N and P circulation.

The macro- and micronutrients contained in solid and liquid *biolistics* indicate that *biolistics*, both solid and liquid, are suitable for use as soil repellents and soil fertility enhancers, especially in latosol soils that have low fertility rates. Both solid and liquid *biolistics* can add C-organic matter to soils and plants. Thomas and Singh (2019) revealed that high or low levels of C-organic matter in the soil are influenced by the amount of organic matter contained in fertilizers. Soil organic matter can be maintained, which contributes to an increase in the biological activity of soil, nutrients, and water transportation so that the decomposition process progresses well (Siddiquee et al., 2017). The total N content also contributes to the need for nutrients in the soil. Nitrogen is useful for increasing the growth of roots, stems, and leaves; for increasing chlorophyll production; for increasing protein levels; and for accelerating the growth of shoots at the roots (Yadav and Sarkar, 2019; Beeby et al., 2020; Bononi et al., 2020).

Elemental N in solid and liquid *biolistics* can improve and control the growth and development of microorganisms in low-fertility soils (Raimi et al., 2017; Lazcano et al., 2021). In addition, the P_2O_5 and phosphorus contents of *biolistics* are important for the bioconversion of sunlight into chemical energy via photosynthetic absorption of CO, which has an impact on the availability of carbohydrate sources in soils with an abundance of organic matter (Islam et al., 2014; Fitriatin et al., 2021). Furthermore, carbohydrates under abundant conditions are synthesized into proteins with the elements N and S. Thus, the formation of cells, tissues, and organs in the soil and in prospective shoots will occur faster, contributing to improved soil quality

(Li et al., 2017). An increase in K_2O in solid and liquid *biolistics* deregulates the translocation of assimilated K_2O to all plant roots. This represents the accumulation of N in the soil, which triggers a decrease in soil quality (Baldi et al., 2016).

The micronutrients contained in the solid and liquid *biolistics* met the quality standards of fertilizers and soil reformers required according to the Regulation of the Minister of Agriculture of the Republic of Indonesia number 01 of 2019. Figure 2 shows that the Fe (iron) content is greater in solid *biolistics* (212 µg/g) than in liquid *biolistics* (198 µg/g). The content of magnesium (Mg) was greater in liquid *biolistics* (13.49%) than in solid *biolistics* (2.66%). Furthermore, for manganese (Mn), the same results are obtained for both liquid biolistic (1.23 µg/g) and solid biolistic (0.85 µg/g) sorbents. For Na, the solid biolistic content (118%) was greater than the liquid biolistic content (97%). Finally, the zinc (Zn) content was greater in liquid *biolistics* (185.8 µg/g) than in solid *biolistics* (169 µg/g).

The micronutrients contained in solid and liquid *biolives* have functions and benefits when their quantities meet normal standards. Iron (Fe) is indispensable for enzymes in the soil (Mitter et al., 2012; Mitter et al., 2021). Fe functions in soil oxidation, respiration, and photosynthesis. As an enzyme catalyst, Fe is associated with the formation of chlorophyll and soil aggregates. In addition, Mn aids in the formation of chloroplasts. Mn is involved in the activity of enzymes involved in photosynthesis and respiration and in the metabolism of N. Mn can inhibit the formation of phenolic and lignin materials for the defense of plants from fungal infections (Contreras-Cornejo et al., 2016; Zhao et al., 2018; Mącik et al., 2020). Furthermore, magnesium (Mg) plays a role in nitrogen metabolism (Lazcano et al., 2021). Ca and Zn in solid and liquid *biolistics* are obtained from the market and from household waste in the form of leaves, vegetables, and fruits that contain many minerals that are good for increasing soil nucleation. Ca, Zn, and Na synergize and are involved in water (osmosis) movement and ion balance in the soil (Abbasi and Yousra, 2012; Mayo-Prieto et al., 2021).

In this study, we found that all parts of the solid and liquid biosystems improved the quality of the latosol soils. This finding is new because the development of organic waste alone as a soil improvement agent has not been able to directly provide good results. Nutrients such as N, P, and K need to be stable for a long time, so improvements in the quality of *biolistics* need to be evaluated. In addition, the results of this study are different from those of previous studies in which substantial amounts of Effective Microorganism-4 (EM-4) were used as a fertilizer decomposition inoculant; however, these studies obtained less significant results in improving soil nutrients but focused on the yield of the plant produced (Chantal et al., 2010; Hidalgo et al., 2022). In this study, the use of macronutrients such as carbon and potassium was improved by maintaining the quality of the raw materials used in biolistic manufacturing, while the use of microelements such as manganese and naphthalene was improved by maintaining the quality of the production materials used. The hope is that the *biolistics* produced comply with established quality standards and can improve soil nutrients appropriately and efficiently.

The use of solid and liquid *biolistics* to increase soil fertility is better than the use of synthetic fertilizers. Physically, organic matter improves the structure and increases the capacity of the soil to store water. Chemically, organic matter increases the resistance of soil to pH changes, increases the exchange capacity of cations, decreases fixation factors, and acts as a reservoir of secondary nutrients and microelements. Biologically, as an energy source for soil microorganisms, nitrogen plays an important role in the decomposition and release of nutrients in soil ecosystems. The microbial community contained in the *biolistics* was determined through microbiological examination; these included *Rhizobium* sp., *Azospirillum* sp., *Bacillus* sp., and *Trichoderma* sp. All the nutrient components met the Indonesian National Standard (SNI) 19-7030-2004 (National Standardization Agency of the Republic of Indonesia, 2004) and the Regulation of the Minister of Agriculture of the Republic of Indonesia Number 01 of 2019 (Ministry of Agriculture, 2019).

Conclusion

Solid and *liquid biolistics* are effective at increasing the fertility of latosol soils. The nitrogen content (N), phosphorus (P), potassium (K), carbon-to-nitrogen ratio (C/N ratio), moisture content, and pH contribute significantly to improving soil aggregates and structures; improving the physical, chemical, and biological properties of soils; and improving the bioavailability of nutrients in the soil. Macro- and micronutrients are beneficial for maintaining and improving soil quality, and the presence of *Rhizobium* sp., *Azospirillum* sp., *Bacillus* sp., and *Trichoderma* sp. is involved in accelerating the process of biodegradation and decomposition in soil. However, further research is needed to determine the stability of macro- and micronutrients in relation to biologics and their impact on the soil. In addition, it is necessary to compare the length of time needed to store nutrients in biolistic-treated soils with that needed for other soil reformers on latosol soils or other soils. Moreover, related research is needed on how well solid and liquid *biolistics* work in soils with different fertility levels and how they can be used directly in soil and plant care on a larger scale.

Acknowledgment

Many thanks go to the Department of Biology, The Hindu University of Indonesia, and anyone who supported and contributed to this research.

References

Abbasi, M.K., Yousra, M., 2012. Synergistic effects of biofertilizer with organic and chemical N sources in improving soil nutrient status and increasing growth and yield of wheat grown under greenhouse conditions. *Plant Biosystems* 146: 181–189.

Adnan, M., Xiao, B., Xiao, P., Zhao, P., Bibi, S., 2022. Heavy metal, waste, COVID-19, and rapid industrialization in this modern era-fit for sustainable future. *Sustainability* 14(8): 4746.

Adnyana, I.M.D.M., 2021. Populasi dan Sampel. In: Metode penelitian pendekatan kuantitatif. Darwin, M. (Ed.), CV. Media Sains Indonesia, Bandung, pp. 103–116.

Al-Suhaibani, N., Selim, M., Alderfasi, A., El-Hendawy, S., 2020. Comparative performance of integrated nutrient management between composted agricultural wastes, chemical fertilizers, and biofertilizers in improving soil quantitative and qualitative properties and crop yields under arid conditions. *Agronomy* 10(10): 1503.

Arthanawa, I.G.N., Astika, I.N., Darmawan, I.K., Yana, D.P.S., Situmeang, Y.P., Sudita, I.D.N., 2022. The effects of organic and inorganic fertilizers on red chili plants. *SEAS (Sustainable Environment Agricultural Science)* 6(1): 70–80.

Arumugam, V., Abdullah, I., Yusoff, I.S.M., Abdullah, N.L., Tahir, R.M., Nasir, A.M., Omar, A.E., Ismail, M.H., 2021. The impact of COVID-19 on solid waste generation in the perspectives of socioeconomic and people's behavior: A case study in Serdang, Malaysia. *Sustainability* 13(23): 13045.

Asghar, W., Kataoka, R., 2021. Effect of coapplication of *Trichoderma* spp. with organic composts on plant growth enhancement, soil enzymes and fungal community in soil. *Archives of Microbiology* 203(7): 4281–4291.

Baldi, E., Amadei, P., Pelliconi, F., Tosell, M., 2016. Use of *Trichoderma* spp. and arbuscular mycorrhizal fungi to increase soil beneficial population of bacteria in a nectarine commercial orchard: Effect on root growth, nutrient acquisition and replanting disease. *Journal of Plant Nutrition* 39(8): 1147–1155.

Beeby, J., Moore, S., Taylor, L., Nderitu, S., 2020. Effects of a one-time organic fertilizer application on long-term crop and residue yields, and soil quality measurements using biointensive agriculture. *Frontiers in Sustainable Food Systems* 4: 67.

Bhandari, S., Pandey, K.R., Joshi, Y.R., Lamichhane, S.K., 2021. An overview of multifaceted role of *Trichoderma* spp. for sustainable agriculture. *Archives of Agriculture and Environmental Science* 6(1): 72–79.

Bhardwaj, D., Ansari, M.W., Sahoo, R.K., Tuteja, N., 2014. Biofertilizers function as key player in sustainable agriculture by improving soil fertility, plant tolerance and crop productivity. *Microbial Cell Factories* 13(1): 1–10.

Bononi, L., Chiaramonte, J.B., Pansa, C.C., Moitinho, M.A., Melo, I.S., 2020. Phosphorus-solubilizing Trichoderma spp. from Amazon soils improve soybean plant growth. *Scientific Reports* 10: 2858.

Chantal, K., Xiaohou, S., Weimu, W., Iro Ong'or, B.T., 2010. Effects of effective microorganisms on yield and quality of vegetable cabbage comparatively to nitrogen and phosphorus fertilizers. *Pakistan Journal of Nutrition* 9(11): 1039–1042.

Contreras-Cornejo, H.A., Macías-Rodríguez, L., Del-Val, E., Larsen, J., 2016. Ecological functions of *Trichoderma* spp. and their secondary metabolites in the rhizosphere: interactions with plants. *FEMS Microbiology Ecology* 92(4): fiw036.

Darwin, M., Mamondol, M.R., Sormin, S.A., Nurhayati, Y., Tambunan, H., Sylvia, D., Adnyana, I.M.D.M., Prasetiyo, B., Vianitati, P., Gebang, A.A., 2021. Quantitative approach research method, 1st ed. CV Media Sains Indonesia, Bandung. 178p.

Dehghani, M.H., Omrani, G.A., Karri, R.R., 2021. Solid waste-sources, toxicity, and their consequences to human health. In: Soft computing techniques in solid waste and wastewater management. Karri, R.R., Ravindran, G., Dehghani, M.H. (Eds.). Elsevier, pp. 205–213.

Du, C., Munir, S., Abad, R., Lu, D., 2020. Valorization of organic waste into biofertilizer and its field application. In: Waste Biorefinery. Bhasbar, T., Pandey, A., Tsang, D.C.W. (Eds.). Elsevier, pp. 179–198.

El-Ramady, H., Brevik, E., Amer, M., Elsakhawy, T., Omara Ahmed, A.E.-D., Elbasiouny, H., Elbehiry, F., Mosa, A., El-Ghamry, A., Bayoumi, Y., Shalaby, T., 2020. Soil and air pollution in the era of COVID-19: A global issue. *Egyptian Journal of Soil Science* 60(4): 437–448.

Eugenio, N.R., McLaughlin, M., Pennock, D., 2018. Soil pollution: a hidden reality. Food and Agriculture Organization of the United Nations (FAO), Rome. 142p. Available at [Access date: 13.04.2022]: https://www.fao.org/3/i9183en/i9183en.pdf

Fasusi, O.A., Cruz, C., Babalola, O.O., 2021. Agricultural sustainability: Microbial biofertilizers in rhizosphere management. *Agriculture* 11(2): 163.

Fitriatin, B.N., Amanda, A.P., Kamaluddin, N.N., Khumairah, F.H., Sofyan, E.T., Yuniarti, A., Turmuktini, T., 2021. Some soil biological and chemical properties as affected by biofertilizers and organic ameliorants application on paddy rice. *Eurasian Journal of Soil Science* 10(2): 105–110.

Francioli, D., Schulz, E., Lentendu, G., Wubet, T., Buscot, F., Reitz, T., 2016. Mineral vs. organic amendments: Microbial community structure, activity and abundance of agriculturally relevant microbes are driven by long-term fertilization strategies. *Frontiers in Microbiology* 7(1446): 1–16.

Geisseler, D., Scow, K.M., 2014. Long-term effects of mineral fertilizers on soil microorganisms - A review. *Soil Biology and Biochemistry* 75: 54–63.

Halifu, S., Deng, X., Song, X., Song, R., 2019. Effects of two Trichoderma strains on plant growth, rhizosphere soil nutrients, and fungal community of *Pinus sylvestris* var. mongolica annual seedlings. *Forests* 10(9): 758.

Hidalgo, D., Corona, F., Martín-Marroquín, J.M., 2022. Manure biostabilization by effective microorganisms as a way to improve its agronomic value. *Biomass Conversion and Biorefinery* 12(10): 4649–4664.

Islam, M.A., Mostafa, M.G., Rahman, M.R., 2014. Conversion of solid organic waste into compost using Trichoderma spp. And its application on some selected vegetables. *International Journal of Environment and Waste Management* 14(3): 211–221.

Kai, T., Tamaki, M., 2020. Effect of organic and chemical fertilizer application on growth, yield, and soil biochemical properties of landrace *Brassica napus* L. leaf-and-stem vegetable and landrace (Norabona). *Journal of Agricultural Chemistry and Environment* 9(4): 314–330.

Kashyap, P.L., Rai, P., Srivastava, A.K., Kumar, S., 2017. *Trichoderma* for climate resilient agriculture. *World Journal of Microbiology and Biotechnology* 33(155): 1–18.

Lazcano, C., Zhu-Barker, X., Decock, C., 2021. Effects of organic fertilizers on the soil microorganisms responsible for N_2O emissions: A review. *Microorganisms* 9(5): 983.

Li, S., Li, J., Zhang, B., Li, D., Li, G., Li, Y., 2017. Effect of different organic fertilizers application on growth and environmental risk of nitrate under a vegetable field. *Scientific Reports* 7: 17020.

Mącik, M., Gryta, A., Frąc, M., 2020. Biofertilizers in agriculture: An overview on concepts, strategies and effects on soil microorganisms. In: Advances in Agronomy. Sparks, D.L. (Ed.). Vol. 162. Elsevier, pp. 31–87.

Mahanty, T., Bhattacharjee, S., Goswami, M., Bhattacharyya, P., Das, B., Ghosh, A., Tribedi, P., 2016. Biofertilizers: a potential approach for sustainable agriculture development. *Environmental Science and Pollution Research* 24: 1–21.

Malusá, E., Sas-Paszt, L., Ciesielska, J., 2012. Technologies for beneficial microorganisms inocula used as biofertilizers. *The Scientific World Journal* Article ID 491206.

Mayo-Prieto, S., Porteous-Álvarez, A.J., Mezquita-García, S., Rodríguez-González, Á., Carro-Huerga, G., del Ser-Herrero, S., Gutiérrez, S., Casquero, P.A., 2021. Influence of physicochemical characteristics of bean crop soil in *Trichoderma* spp. development. *Agronomy* 11(2): 274.

Mehetre, S.T., Mukherjee, P.K., 2015. *Trichoderma* improves nutrient use efficiency in crop plants. In: Nutrient use efficiency: from basics to advances. Rakshit, A., Singh, H.B., Sen, A.. (Eds.). Springer India. pp. 173–180.

Ministry of Agriculture, 2019. Regulation of the Minister of Agriculture of the Republic of Indonesia Number 01 of 2019 concerning Registration of Organic Fertilizers, Biological Fertilizers, and Soil Improvements. pp. 1-44.

Ministry of Environment and Forestry, 2022. National Waste Management Information System. pp.14-50. Available at [Access date: 13.04.2022]: https://sipsn.menlhk.go.id/sipsn/public/data/timbulan

Ministry of Environment and Forestry, 2020. Status of Environment and Forestry 2020. Ministry of Environment and Forestry of the Republic of Indonesia. Available at [Access date: 13.04.2022]: https://www.menlhk.go.id/cadmin/uploads/SLHI_2022_upload_final_77f9948571.pdf

Mitter, E.K., Tosi, M., Obregón, D., Dunfield, K.E., Germida, J.J., 2021. Rethinking Crop Nutrition in Times of Modern Microbiology: Innovative Biofertilizer Technologies. *Frontiers in Sustainable Food Systems* 5: 606815.

National Standardization Agency of the Republic of Indonesia, 2004. Indonesian National Standard 19-7030-2004 concerning Specifications of compost from domestic organic waste. Available at [Access date: 13.04.2022]: http://inswa.or.id/wp-content/uploads/2012/07/Spesifikasi-kompos-SNI.pdf

Pandey, V., Chandra, K., 2016. Agriculturally important microorganisms as biofertilizers: commercialization and regulatory requirements in Asia. In: Agriculturally important microorganisms. Singh, H.B., Sarma, B.K., Keswani, C. (Eds.). Springer Singapore. pp. 133–145.

Pappalardo, G., Cerroni, S., Nayga, R.M., Yang, W., 2020. Impact of COVID-19 on Household Food Waste: The Case of Italy. *Frontiers in Nutrition* 7: 585090.

Putro, B.D., 2020. Double burdens: the condition of woman scavengers during the pandemic at the monang maning waste processing site, Denpasar. *Journal of Bali Studies* 10(2): 537–556.

Raimi, A., Adeleke, R., Roopnarain, A., 2017. Soil fertility challenges and biofertilizer as a viable alternative for increasing smallholder farmer crop productivity in sub-Saharan Africa. *Cogent Food and Agriculture* 3(1): 1400933.

Rashid, M.I., Mujawar, L.H., Shahzad, T., Almeelbi, T., Ismail, I.M.I., Oves, M., 2016. Bacteria and fungi can contribute to nutrients bioavailability and aggregate formation in degraded soils. *Microbiological Research* 183: 26–41.

Roy, P., Mohanty, A.K., Wagner, A., Sharif, S., Khalil, H., Misra, M., 2021. Impacts of COVID-19 outbreak on the municipal solid waste management: now and beyond the pandemic. *ACS Environmental Au* 1: 32–45.

Siddiquee, S., Shafawati, S.N., Naher, L., 2017. Effective composting of empty fruit bunches using potential *Trichoderma* strains. *Biotechnology Reports* 13: 1–7.

Suriyaprakash, R., Dowlath, M.J.H., Karuppannan, S.K., Arunachalam, K.D., 2021. Soil contamination, risk assessment and nanobioremediation, In: Nanomaterials for soil remediation. Amrane, A., Mohan, D., Nguyen, T.A., Assadi, A.A., Yasin, G. (Eds.). Elsevier, pp. 239–258.

Suthar, H., Hingurao, K., Vaghashiya, J., Parmar, J., 2017. Fermentation: a process for biofertilizer production. In: Microorganisms for green revolution, microorganisms for sustainability. Panpatte, D.G., Jhala, Y.K., Vyas, R.V., Shelat, H.N. (Eds.). Springer Singapore. pp. 229–252.

Szczałba, M., Kopta, T., Gąstoł, M., Sękara, A., 2019. Comprehensive insight into arbuscular mycorrhizal fungi, *Trichoderma* spp. and plant multilevel interactions with emphasis on biostimulation of horticultural crops. *Journal of Applied Microbiology* 127: 630–647.

Thomas, L., Singh, I., 2019. Microbial biofertilizers: types and applications. In: Biofertilizers for Sustainable Agriculture and Environment. Giri, B., Prasad, R., Wu, Q.S., Varma, A. (Eds.). Soil Biology, vol 55. Springer, Cham. pp. 1–19.

Tsukiji, M., Gamaralalage, P.J.D., Pratomo, I.S.Y., Onogawa, K., Alverson, K., Honda, S., Ternald, D., Dilley, M., Fujioka, J., Condrorini, D., 2020. Waste management during the COVID-19 pandemic from response to recovery. United Nations Environment Programme, International Environmental Technology Centre (IETC), and IGES Center Collaborating with UNEP on Environmental Technologies (CCET), Kenya. Available at [Access date: 13.04.2022]: https://reliefweb.int/attachments/a874ef9b-5236-3cbd-ad06-1a18b0dca8d7/WMC-19.pdf

Vassileva, M., Malusà, E., Sas-Paszt, L., Trzcinski, P., Galvez, A., Flor-Peregrin, E., Shilev, S., Canfora, L., Mocali, S., Vassilev, N., 2021. Fermentation strategies to improve soil bio-inoculant production and quality. *Microorganisms* 9(6): 1254.

Waste for Change, 2021. Waste management emergency during the COVID-19 Pandemic. Association of Cities and Regions for Sustainable Resource Management. Available at [Access date: 13.04.2022]: https://waste4change.com/blog/waste-management-emergency-during-the-covid-19-pandemic/

Yadav, K.K., Sarkar, S., 2019. Biofertilizers, impact on soil fertility and crop productivity under sustainable agriculture. *Environment and Ecology* 37(1): 89–93.

Yang, M., Chen, L., Msigwa, G., Tang, K.H.D., Yap, P.S., 2022. Implications of COVID-19 on global environmental pollution and carbon emissions with strategies for sustainability in the COVID-19 era. *Science of the Total Environment* 809: 151657.

Zhao, J., Zhou, X., Jiang, A., Fan, J., Lan, T., Zhang, J., Cai, Z., 2018. Distinct impacts of reductive soil disinfestation and chemical soil disinfestation on soil fungal communities and memberships. *Applied Microbiology and Biotechnology* 102: 7623–7634.

Zin, N.A., Badaluddin, N.A., 2020. Biological functions of *Trichoderma* spp. for agriculture applications. *Annals of Agricultural Sciences* 65: 168–178.

Eurasian Journal of Soil Science 2024, 13(3), 190 - 201

Eurasian Journal of Soil Science

Journal homepage : http://ejss.fesss.org

Characterization of humic acids from soil of Delhi regions and their impact on plant growth

Charu Singh [a], Abhishek Chauhan [b], Jayati Arora [a], Anuj Ranjan [b,c], Vishnu D. Rajput [c], Svetlana Sushkova [c], Tatiana Minkina [c], Sambasivan Venkat Eswaran [d], Tanu Jindal [b,*]

[a] Amity Institute of Environmental Sciences, Amity University, Noida, Uttar Pradesh, India
[b] Amity Institute of Environmental Toxicology, Safety, and Management, Amity University, Noida, Uttar Pradesh, India
[c] Academy of Biology and Biotechnology, Southern Federal University, Rostov-On-Don, Russia
[d] St Stephen's College, Delhi, 110007; Amity University, Noida, Uttar Pradesh-201313, India

Article Info
Received : 02.11.2023
Accepted : 31.01.2024
Available online: 07.02.2024

Author(s)
C.Singh
A.Chauhan
J.Arora
A.Ranjan
V.D.Rajput
S.Sushkova
T.Minkina
S.V.Eswaran
T.Jindal *

* Corresponding author

Abstract

Humus materials are considered complex organic substances generated through a chain of chemical reactions and responsible for many processes in soil that ultimately govern soil health. The structural and functional characteristics of humus depend upon the location, quality, and microbial abundance of the soils. However, the differential characteristics of soil organic matter, seasonal changes, parent rock, plant cover, microbial abundance, and anthropogenic activities majorly affect it. The present study has aimed toward the extraction of humus from five different locations in the Delhi region of India and their characteristics were investigated through elemental analysis, Fourier Transform infrared (FT-IR) spectroscopy, and UV spectroscopy. The results showed that there was a higher degree of unsaturation detected in the Forest soil sample. The results of FT-IR showed the presence of characteristic peaks of humus in the samples however the intensity of bands was weak in sample disposable site soil sample and clayey soil sample due to the variation in soil physicochemical properties. The study also aimed to assess the growth of *Oryza sativa* (rice) plants observed in the hydroponics system. The significant finding was observed with the forest soil sample in 1000 mgL^{-1} and treatment in which the growth was minimum in clayey soil of 1500 mgL^{-1}. Our investigation infers the diverse nature of humus in different soils and its implications for plant growth, highlighting the importance of understanding soil organic matter for sustainable agriculture and soil health management.

Keywords: Humus, humic acid, fulvic acid, organic matter, soil health.

© 2024 Federation of Eurasian Soil Science Societies. All rights reserved

Introduction

Soil organic matter is the key component of soil that affects the physicochemical properties of soil. The organic matter is made up of non-living heterogeneous material derived from microbial and chemical degradation of the organic pool in the soil (Lal, 2020). These processes are termed as humification process which generates humus which is further resistant to degradation. Humus substances are mainly associated with soil nutrient flux, carbon restoration, pollutants movements, soil aggregation behaviour, and soil fertility (Körschens, 2002). Humus is mainly composed of fulvic acids, humic acids (HAs), and humin materials. It features a network of single strands connecting clusters of humic material and minerals, forming a carbonaceous structure (Jackson, 1993). They exist as groups of peptide amphiphiles, carbohydrates, N-heterocyclics, and alkyl-aromatics. Although some polysaccharides, proteins, lipids nucleic acids were also found in the humus (Enev et al., 2014). The clay fractions predominantly consist of phenols, lignin, lipids, and fatty acids. The primary functional groups within the HAs molecule include carboxylic, phenolic, and alcoholic, along with minor groups like hydroxy, methoxy, thiol, etc. The Humic substances (HS) represent around 80% of organic matter. The structures and compositions of humus largely depend on the quality of organic matter, soil properties, and microbial activity, involving several polymerization, degradation, and transformation

: https://doi.org/10.18393/ejss.1433418
: http://ejss.fesss.org/10.18393/ejss.1433418
Publisher : Federation of Eurasian Soil Science Societies
e-ISSN : 2147-4249

processes leading to the generation of humus materials in soils (Wei et al., 2019). The composition of marine humus is generally composed of aliphatic compounds while the presence of certain carboxylic acids and phenolics in humus was due to input of lignin, and tannins from terrestrial materials (Hayes et al., 2017). Humus derived from coal exhibits significant variations in mineral components (aluminosilicate), the number of functional groups, and water content (Volkov et al., 2021).

Several theories were earlier presented for the determination of humus structures (Ndzelu et al., 2020, Chen et al., 2020). According to Stevenson (1994)'s study, they are composed of heterogeneous organic macromolecules similar to the original material. There is significant concern in controlling the commercial potential of humic acids due to their ability to enhance plant growth (Thakur et al., 2023). Few studies have reported that HAs are composed of hydrophobic materials stabilized by neutral pH and hydrophobic forces while fulvic acids are mainly formed from hydrophilic compounds derived at any pH (Kolchanova et al., 2021). However, detailed structural characterization of humus materials has been discussed less, and thus a critical extraction procedure is essential for the derivation of proper structures.

For the determination of qualitative and quantitative features of humus, fractionation of organic matter is preferred as it can generate more valuable information about the humus produced. Previously, various extraction techniques like the use of chelating agents, cationic exchange resins, organic solvents, aqueous saline solutions, and alkaline solvents were employed. Due to the establishment of multiple procedures, there was a lack of proper determination of humus composition and humus characteristics. Hence, the International Humic Substances Society (IHSS) has implemented an extraction method involving the treatment of samples with a potent base (typically 0.1 or 0.5 mol L^{-1} NaOH) within a nitrogen-rich environment (Li et al., 2022). Despite numerous chemical alterations in the structural compositions, this methodology successfully yielded an optimal composition and provided representative compositions similar to those found in the original material.

Characterizing the HAs is vital for understanding their structural composition and applications in agriculture, environmental science, and biotechnology. Analytical techniques like Elemental Analyzer, UV spectrophotometry, and FTIR spectroscopy reveal molecular characteristics and interactions, providing insights into the organic nature of HAs. UV spectrophotometry examines ultraviolet light absorption, identifying functional groups and the aromatic nature of HAs. FTIR spectroscopy helps by identifying the specific functional groups. These methods collectively offer a comprehensive understanding of HA's chemical composition, facilitating its use in diverse applications, from soil improvement to wastewater treatment.

The growth-promoting activity of plants in response to varying concentrations of HAs extracted from soil is a subject of keen scientific interest in agriculture. The Has are evident to influence plant growth through multiple mechanisms. When applied to plants at different concentrations, HA can enhance root development, nutrient uptake, and overall plant vigour (Adani et al., 1998) . Studies have shown that lower concentrations of HAs can stimulate root growth and improve nutrient absorption by facilitating ion exchange processes in the root zone. Conversely, higher concentrations of HAs might exert different effects, potentially leading to improved photosynthetic efficiency, increased biomass, and enhanced resistance to environmental stresses (Castro et al., 2022). However, the response of plants to varying HAs concentrations is complex and can be species-specific, as different plants possess varying capacities to respond to these organic compounds (Stuijfzand et al., 1999) . As such, investigations into the growth-promoting potential of HAs at different concentrations contribute to our understanding of soil components and plant development, extending the pursuit for sustainable agricultural practices.

In the present study, we aimed towards the determination of spectral and chemical characteristics of HAs obtained from soil of five different locations. Characterization of the extracted HA was performed through FT-IR, UV-Vis spectrophotometry, and an elemental analyzer. This study was also aimed at the assessment of the growth-promoting potential of the extracted HAs from different locations. For this purpose, *Oryza sativa* was used as model plants using a reliable hydroponic rice seedling culture system to examine the various plant physiology parameters.

Material and Methods

Chemicals and Reagents

All the chemicals used in the extraction and characterization stages were of high purity and analytical research grade. Reagents and chemicals used in the study include hydrochloric acid (HCl), sodium hydroxide (NaOH), distilled water, potassium bromide (KBr), sodium pyrophosphate ($Na_4P_2O_7$), sodium hypochlorite (NaClO)and deuterium oxide (Merck). Hoagland solution macronutrients- magnesium sulphate heptahydrate ($MgSO4{\cdot}7H_2O$), calcium nitrate ($Ca(NO_3)_2$), potassium dihydrogen phosphate (KH_2PO_4), potassium nitrate

(KNO_3), ethylenediaminetetraacetic acid iron (III) sodium salt ($C_{10}H_{12}FeN_2NaO_8 \cdot H_2O$) and micronutrients-boric acid (H_3BO_3), manganese chloride tetrahydrate ($MnCl_2 \cdot 4H_2O$), zinc sulphate heptahydrate ($ZnSO_4 \cdot 7H_2O$), sodium molybdate dihydrogen monoxide ($Na_2MoO_4 \cdot H_2O$), copper sulphate pentahydrate ($CuSO_4.5H_2O$), the Technical-grade HA was obtained from Sigma-Aldrich. *Oryza sativa* seeds were purchased from Indian Agriculture Research Institute (IARI).

Sampling Site

Soil samples were collected from 0-20 cm depths at five diverse locations within the Delhi-NCR region, India. The collected samples represented various soil types, including forest soil, agricultural field soil, riverbank soil from the Yamuna, landfill soil near Ghazipur landfill site, and clayey soil from a pond in Gautam Buddha Nagar, Uttar Pradesh, India. Specifically, the soil from the forest area near Gwal Pahadi, Gurugram, Haryana, situated in the Aravalli Hills, was classified as 'undisturbed' due to its minimal human impact and was located 17 km from Gurugram, India. The agricultural field soil was collected from Bulandshahr District, Uttar Pradesh, India, while riverbank soil was obtained from the Yamuna bank at Kalindi Kunj, Delhi, India. The soil near the Ghazipur landfill site of Ghaziabad, Uttar Pradesh, and the clayey soil near a pond in Bulandshahr District, Uttar Pradesh, India were also part of the study. The collected samples were designated as S1, S2, S3, S4, and S5 labels respectively (Figure 1). These locations were chosen based on significant differences in pedogenetic factors, parent material, landform, land use, and management practices (Table 1). The selection process also carefully considered the molecular-level diversity within the soil samples (Senesi and Loffredo, 1999; Lehmann and Kleber, 2015). Multiple sub-samples were gathered, air-dried, and sifted through a 2.0 mm mesh for subsequent chemical analysis, following the methodology as explained by Xiao et al. (2021).

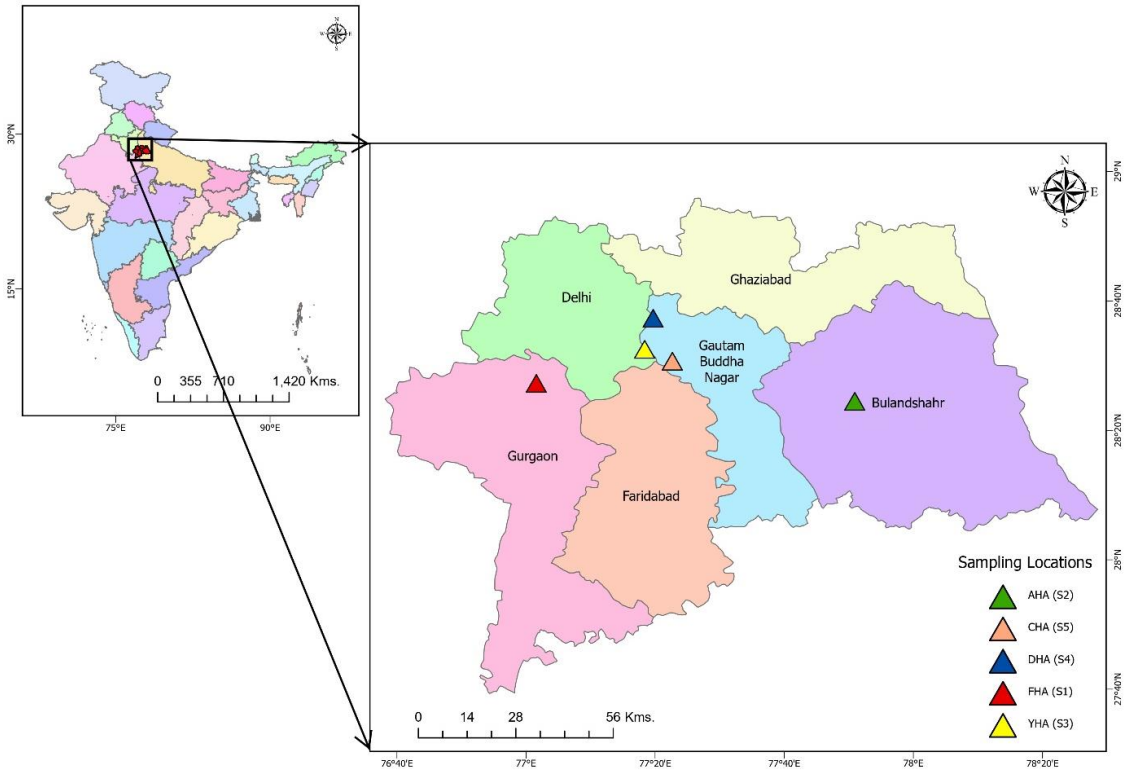

Figure 1. Soil sampling location on the map of Delhi NCR, India

All experiments were conducted at a room temperature of 25±1°C and humidity 50%.

Table 1. Soil sampling locations and their geo-coordinates in and around Delhi National Capital Region (NCR) of India

S. No.	Sampling Site	Location	Latitude	Longitude
1	S1 (Forest HA-FHA)	Gwal Pahadi, Gurgaon, Haryana, India	28.457523	77.026344
2	S2 (Agriculture HA-AHA)	Bulandshahr District, Uttar Pradesh, India	28.411331	77.848434
3	S3 (Yamuna HA-YHA)	Yamuna bank at Kalindi Kunj, Delhi, India	28.545267	77.306092
4	S4 (Disposal HA-DHA)	Ghazipur landfill site of Ghaziabad, Uttar Pradesh, India	28.625242	77.327989
5	S5 (Clay HA-CHA)	Gautam Buddha Nagar, Uttar Pradesh, India	28.514580	77.377594

Extraction and Purification of HA

The extraction of HAs in the soil was done corresponding to the standard method of the International Humic Substance Society (IHSS) (IHHS, 2024). The extraction was performed using 0.1 M HCl, and subsequently extracting during the night with 0.1 M NaOH under an atmosphere of N_2. The pH was set to 2.0 by adding 6.0

M HCl. Then, the remnants were collected and further extracted again. The contents existed centrifuged at 5,000 RCF for 10 minutes before being redissolved in a solution containing 0.1 M KOH under a N_2 atmosphere The clustered colloidal particles were then collected by subjecting it to centrifugation at 40,000 RCF for 15 minutes after this solution was adjusted to 0.3 M using KCl. The precipitated HAs were retrieved through centrifugation after the supernatant was centrifugally acidified by adjusting the pH to 2.0 using 6.0 M HCl. After being treated twice for 24 hours with 0.5% HF + HCl, the HAs were centrifuged at 5,000 RCF. The material that precipitated was dialyzed and subsequent freeze-drying following a rinse with 200 ml of 0.01 M HCl. The treated samples were then obtained through centrifugation at 5,000 RCF (Figure 2).

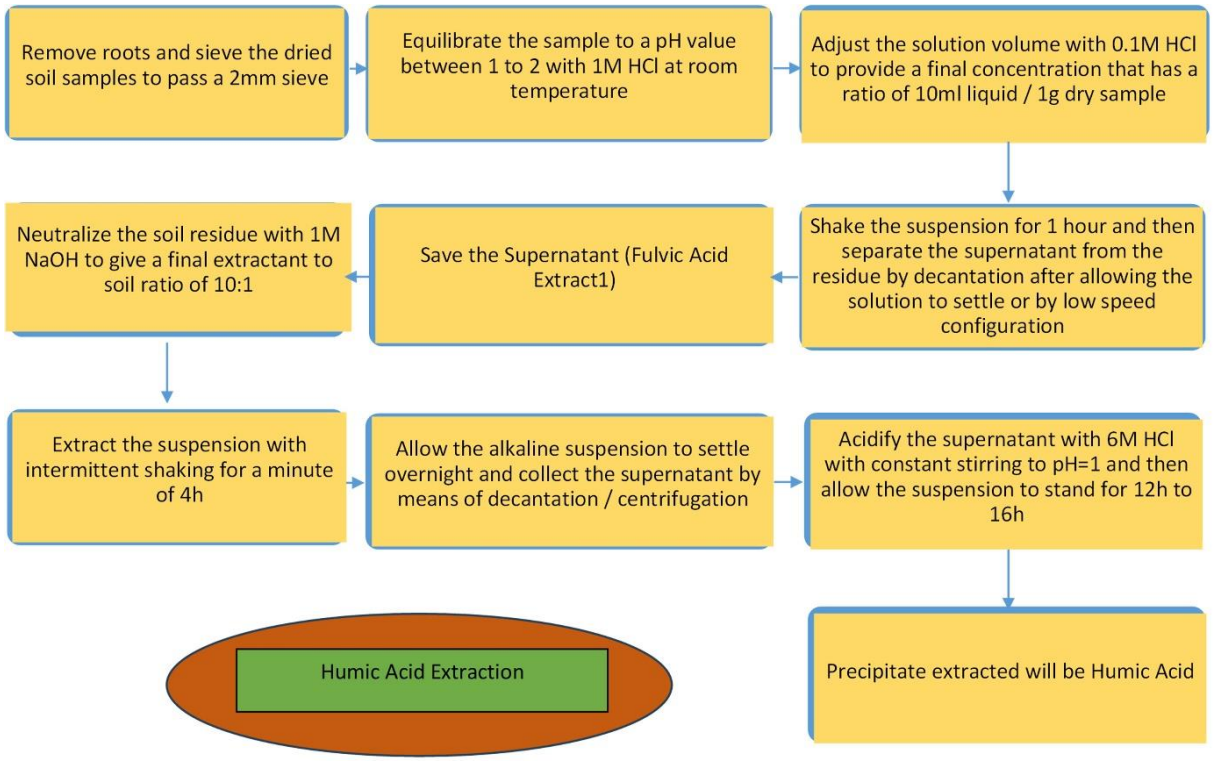

Figure 2. Flow chart illustrating the methodology of Humic Acid extraction steps.

Characterization of Humic Samples

Elemental Analysis

After extraction and purification, the obtained HAs fractions, elemental compositions of the HAs were determined by the elemental analyser (CHNS-O EA 3000). The percentage of O content was determined by subtracting the percentages of C, H, N, and S after making corrections for moisture and ash content in the data. The following formula was used for the calculations: $\%O = [100 - (\%C + \%H + \%N + \%S)$

UV-Visible Spectrophotometry

UV-VIS spectroscopy was done using AJX-1600 spectrophotometer where the spectra were taken corresponding to the methods described by Datta et al. (2022) using a wavelength range of 200 to 800nm, at 25°C, with a 1 cm optical path in a solution created by diluting 20mg of HAs in 1 L of $NaHCO_3$ (0.05 $molL^{-1}$), with a pH 8.0. To calculate the relationship coefficient E4 /E6, the absorbance at 465 nm was divided by that obtained at 665 nm (Datta et al. 2022) .

A separate stock solution of HA (10 mgL^{-1}) was prepared using $Na_4P_2O_7$ alkali solvent. Using this solution, multiple standards working solutions with HA concentrations ranging from 0.002% to 0.012% were also prepared in solvent. The absorbance of HA in the UV-VIS spectral range was measured in the mixture of $Na_4P_2O_7$ alkali solvent. To establish the calibration series, each standard working solution was transferred into a spectrophotometric cell, and its absorbance was recorded at two wavelengths, 465 and 665 nm.

Fourier Transform Infrared Spectroscopy (FT-IR)

The spectral analysis was performed using a Bruker Vertex 70 FTIR spectrophotometer equipped with a Platinum attenuated total reflection (ATR) module. To achieve this, the lyophilized and purified samples were converted into tablets and compressed together with KBr. Subsequently, FT-IR spectra ranging from 400 to 4000 cm^{-1} were generated. A resolution of 4 cm^{-1} was utilized, and 10 scans were performed to generate the set of 10 spectra. Origin software (version 5.0, 2007) was used to assess these spectra.

Plant Materials and Growth Conditions

Rice seeds (*Oryza sativa* L.) were procured from Indian Agriculture Research Institute (IARI), New Delhi, India. Before use, seeds of consistent size underwent surface sterilization using solution of NaClO at a concentration of 10% (v/v) was applied for a period of 10 minutes. Following this, they were thoroughly rinsed with distilled water and immersed for a duration of 4 hours. Subsequently, the healthy and seeds of consistent size were placed in 150 mm petri dishes, covered with filter paper of Whatman no. 1, and moistened with Hoagland's solution at half-strength with a pH of 6.5 as described by Arditti and Dunn (1969). The seeds were further allowed for germination in the absence of light at a temperature of 28 ± 2°C and for 4 days. The ensuing young seedlings were grown under a photon flux density (PFD) of 150 µmol photons m^2 s^{-1} and kept within a relative humidity range of 50–60%. This environment followed a day/night cycle lasting 12 hours each at a consistent temperature of 28 ± 2°C for a duration of 8 days inside a growth chamber. Following this period, seedlings of consistent size were selected and relocated into half-strength Hoagland's solution at half-strength for a 7-day acclimatization period. Subsequently, the leaves were carefully stored at −86 °C until further analyses. After the 7-day treatment period, root and shoot samples were gathered from both treated and untreated (control) seedlings, and different parameters were measured for analysis.

Determination of Growth Parameters and Photosynthetic Pigment

The parameters related to growth, such as fresh and dry weight, along with root and shoot length, were assessed following the random harvest of both untreated (control) and treated rice seedlings. From each sample, 10 seedlings were selected at random, and then divided into root and shoot portions for subsequent measurement of their respective length and fresh weight. To ascertain the dry weight, the root and shoot segments were enclosed in butter paper and underwent oven drying at a temperature range of 65-75°C for 48 hours, following which their weights were measured. To assess total chlorophyll and carotenoids, 25 mg of fresh leaves were extracted in 5 ml of 80% (v/v) acetone for each sample. The quantification of chlorophyll and carotenoids was conducted following the procedures outlined by Arnon (1949) and Ikan (1969), respectively. There were total of 16 treatments viz, T1 (control) to T16, and three concentrations were taken, 500 mg L^{-1}, 1000 mg L^{-1}, and 1500 mgL^{-1} as per the description of the treatments is given in the table 2.

Table 2. Description of treatments

Treatment Code	Doses (mg L^{-1})	Treatment Details
T1	Not Applicable	Control (Nutrient Broth)
T2	500	
T3	1000	FHA (Forest HA)
T4	1500	
T5	500	
T6	1000	AHA (Agriculture HA)
T7	1500	
T8	500	
T9	1000	YHA (Yamuna HA)
T10	1500	
T11	500	
T12	1000	DHA (Disposal HA)
T13	1500	
T14	500	
T15	1000	CHA (Clayey HA)
T16	1500	

Results and Discussion

Elemental Analysis

The elemental composition is the most fundamental trait of the organic compound of any sample. The results of the elemental analysis, along with the atomic ratios (C/H and C/N) and the ash content of the samples are provided in Figure 3. The results were obtained after corrected the moisture and remaining ash contents were assessed through thermogravimetric analysis. The content of %C was highest in S1 followed by S2, S3, S4, and S5. However, the %H was maximum in S2. %N was followed the different trend S2>S1>S3>S4>S5. %O and %S was highest in S1.

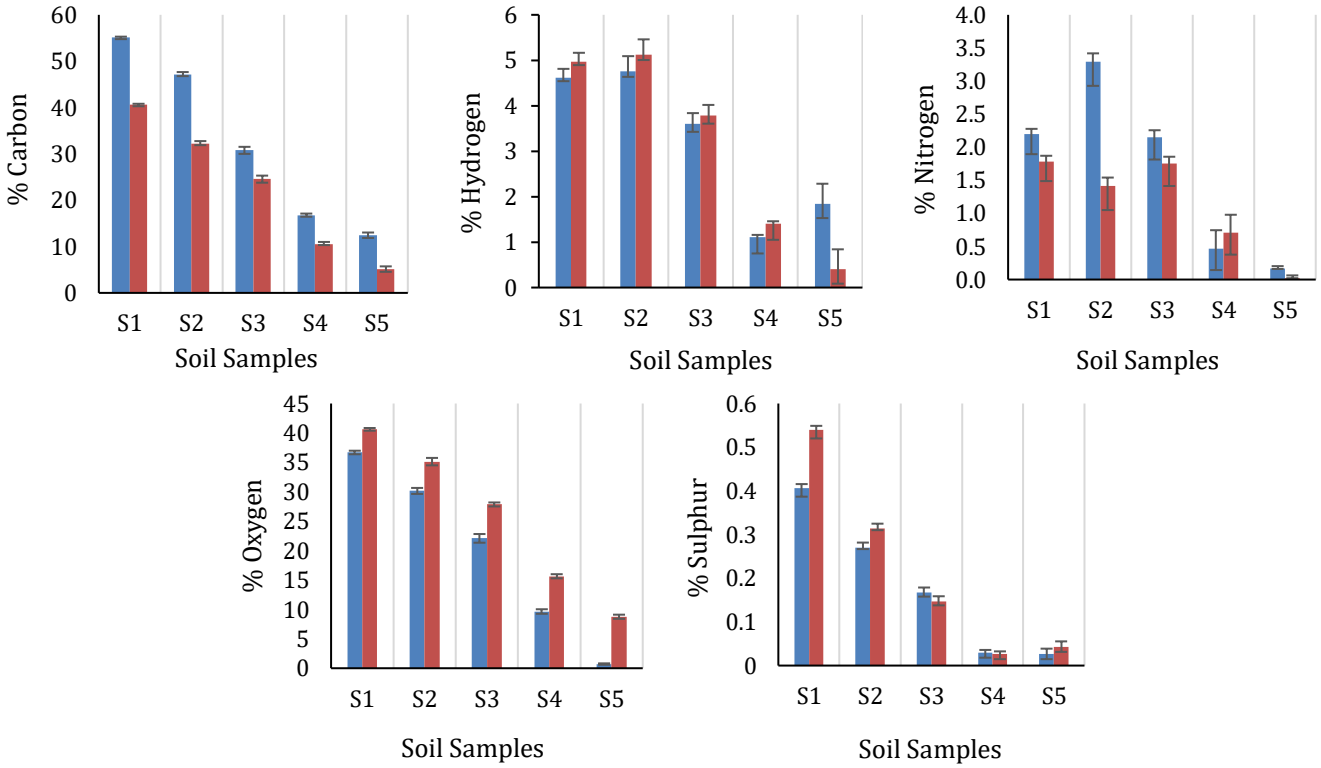

Figure 3. Elemental analysis of the samples for percent content of Carbon, hydrogen Nitrogen, oxygen and sulphur

UV-Vis Spectroscopy

The UV absorption serves as an effective indicator of the unsaturated carbon content in samples, presenting a rapid, simple, and highly sensitive approach for molecular characterization (Figure 4). The spectra of the samples were showing higher absorbance (200-300 nm) for sample S2, due to the presence of more chromophores of double bonds (C=C, C=O). These results were corroborating the above section with higher aromatic structures (higher H/C) in sample S1. The percentage HA was maximum in S1 that is 0.089% followed by S2, S3, S4 and S5 (Figure 5).

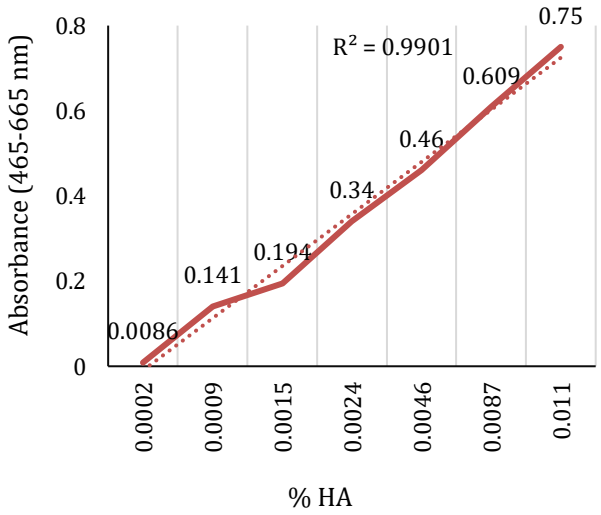

Figure 4. Calibration curve of the standard Humic Acid prepared at the absorbance of 465-665 nm

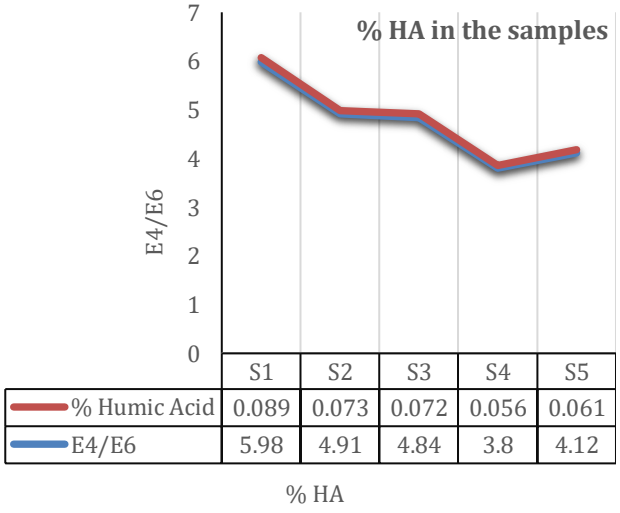

Figure 5. Percentage of Humic Acid in the soil samples selected for the studies

FT-IR Analysis

To identify the conformational alterations and content fluctuations of functional groups of HAs from various locations, FTIR spectra were collected. The spectroscopic data about tested samples has been provided in Figure 6. The spectrum was divided into two bandwidth regions for a wider understanding of bands. All the samples were showing almost similar absorption patterns due to the basic skeleton structures of the HAs. However, few differences in the intensity and band shifting were found owing to their origin sites. The spectra existing 3500-3000 cm^{-1} were showing the bands of stretching of O–H, minor stretching of N–H, and displaying

hydrogen-bonded –OH groups (Cocozza et al., 2003). The intensity of these bands was prominent in S1, S2 and S3 however it gets decreased in S4 and S5 due to the presence of less matured humus substances. Since in the S4 major organic reactions owing to humus formation were absent therefore it is showing immature humus substances. The groups that appeared between 2900-2300 cm^{-1} were major due to involving asymmetric and symmetric stretching of C–H in CH_2 groups. These groups were absent in S4 and S5, and very prominent intensity was detected in S2 due to a chemical reaction that occurred at that site. The absorption bands at 1740 were corresponding to the stretching of C=O in COOH and other carbonyl groups. The bands occurring between 1600-1690 cm^{-1} were arising from vibrations in the aromatic C=C skeleton, stretching of C=O in amide groups (designated as amide I band), and C=O in quinone and/or hydrogen-bonded conjugated ketones. Additionally, the presence of a peak at 1550 cm^{-1} was associated with N–H deformation and C=N stretching (referred to as amide II band), as well as stretching of aromatic C=C. There were several absorption bands detected between 1200-1400 cm^{-1} were denoting the presence of asymmetric bending of C–H in CH3 groups, deformation of O–H, and stretching of C–O in phenolic OH, bending of C–H in CH_2 and CH_3 groups, anti-symmetric stretching of COO–, and stretching of C–O in aryl esters. The extra peak observed at 1130 cm^{-1}, associated with the skeletal vibration of C–O–C stretching, could possibly be attributed to the presence of cellulose residues in the sample (Ertani et al., 2011). Many peaks between 500-1000 cm^{-1} were denoting the existence of lignin residues in the samples, as reported by Rodríguez-Lucena et al. (2009). There was a remarkable shift in the intensity was detected at each peak. In sample S1 the peaks were more prominent followed by S2, S3, S4 and S5.

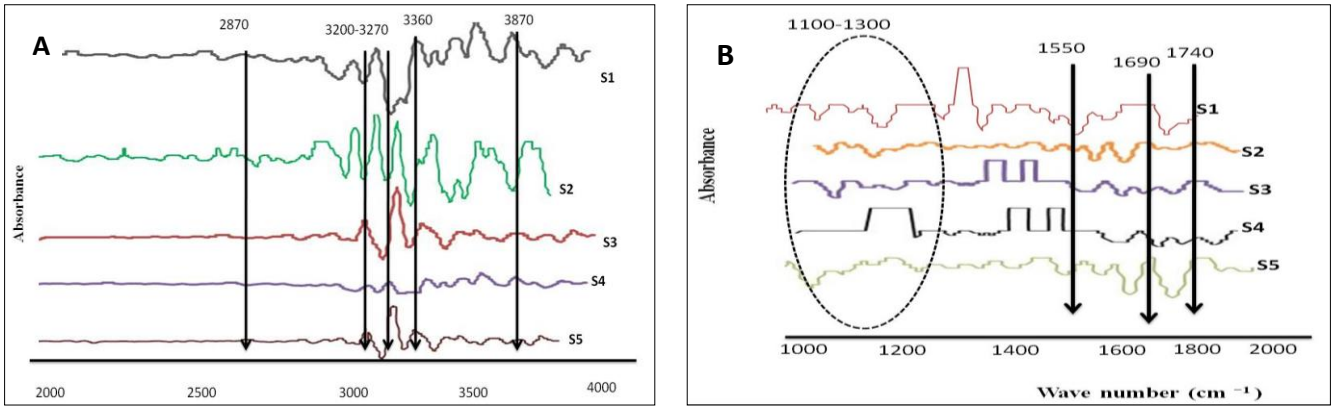

Figure 6: FT-IR spectra of the Humic Acids samples extracted from soil of the five different locations across Delhi, NCR, India (A) illustrate the diverse functional groups present in the range 2000 to 4000 cm^{-1},and (B) illustrate the diverse functional groups present in the range 1000 to 2000 cm^{-1}

A higher percentage of C, and H in S1and S2 were suggesting a lower degree of humification than that of S3, S4, and S5. The H/C, N/C, values were almost similar for S2 and S3 however they were highest for S2, suggesting a higher degree of unsaturation. The higher values in S2 were denoting the presence of less substituted aromatic rings due to shorter transformation reactions.

Hydroponics Setup with Rice Using Various Concentrations of HA

Treatments significantly affected the fresh mass, length, protein content, chlorophyll content and carotenoids content of the rice seedlings. All the treatments gave significantly higher values. The best treatment for all the parameters was T3 in which the value of the shoot fresh mass was 0.79 g/seedling, and the fresh root mass was 0.325 g/seedling. The value of maximum total protein content is 19.1 mg g^{-1} FW, maximum chlorophyll content is 29 mg g^{-1} FW and the maximum carotenoids is 551 mg g^{-1} FW. The least values of all the parameters were observed in T11.

Discussion

The elemental composition serves as a fundamental aspect that unveils the organic makeup of each sample. Carbon, nitrogen, hydrogen, oxygen, and sulfur work together in organic compounds, showing how important the elemental composition is in understanding how systems function. Our study assess the elemental composition's core role in describing the organic composition of examined samples. This comprehensive analysis focusses on essential ratio of element (C/H and C/N) alongside ash content. The adjustments for water content and remaining ash content, executed through analysis using thermogravimetric, contribute to these outcomes. Aligned with Amir et al. (2004), composting induced substantial nitrogen content (%N) reduction and a higher carbon-to-nitrogen (C/N) ratio. Parallel to their findings, our study indicates increased oxygen content (%O) and a slightly elevated oxygen-to-carbon (O/C) ratio post-composting, collectively

suggesting compositional transformations. It's important that hydrogen (%H) and carbon (%C) content experienced limited variation during this process, aligning with Amir et al.'s observations. The distribution of carbon content (%C) across sampling stations resonates with Tadini et al. (2022), revealing higher %C in S1, followed by S2, S3, S4, and S5. Their study demonstrated declining soil carbon content (%C) with depth across integrated agricultural systems, paralleling our depth-related trend.

Table 3. Impact of different treatments on seedling length and fresh biomass, total chlorophyll, carotenoid, and protein content in rice seedlings

Treatments	Fresh mass (g/ seedling)		Length (cm/seedling)		Total Protein	Total chlorophyll	Carotenoids
	Shoot	Root	Shoot	Root	(mg g^{-1} FW)	(mg g^{-1} FW)	(mg g^{-1} FW)
T1(Control)	0.68±.0.006	0.291±0.008	16.1±0.47	8.58±0.35	15.8 ± 0.19	25 ± 1.76	463.0 ± 5.19
T2	0.52±.0.008	0.212±0.032	13.1±0.66	6.40±0.70	12.8 ± 0.15	21 ± 1.43	383.2 ± 4.29
T3	0.79±.0.029	0.325±0.010	18.3±0.45	9.36±0.90	19.1 ± 0.23	29 ± 1.99	551.0 ± 6.17
T4	0.60±.0.004	0.253±0.023	14.2±0.62	7.40±0.59	14.4 ± 0.17	23 ± 1.61	427.5 ± 4.79
T5	0.48±.0.004	0.183±0.007	12.1±0.53	5.90±0.34	12.3 ± 0.15	20 ± 1.38	378.0 ± 4.23
T6	0.62±0.014	0.244±0.009	14.9±0.38	7.65±0.12	14.6 ± 0.18	22 ± 1.54	412.0 ± 4.61
T7	0.51±0.012	0.195±0.012	12.8±0.81	6.33±0.28	12.1 ± 0.15	20 ± 1.41	373.1 ± 4.18
T8	0.62±0.007	0.263±0.006	14.4±0.78	7.93±0.44	14.2 ± 0.17	23 ± 1.57	384.5 ± 4.31
T9	0.68±.0.006	0.165±0.008	16.1±0.47	8.58±0.35	15.8 ± 0.19	25 ± 1.76	463.0 ± 5.19
T10	0.49±.0.029	0.321±0.010	17.3±0.44	8.36±0.80	15.1 ± 0.23	29 ± 1.99	561.0 ± 6.81
T11	0.20±.0.008	0.126±0.032	11.1±0.66	5.40±0.70	11.8 ± 0.15	19 ± 1.43	356.2 ± 4.29
T12	0.30±.0.002	0.242±0.023	12.6±0.61	5.70±0.54	13.4 ± 0.17	25 ± 1.31	438.5 ± 4.58
T13	0.38±.0.004	0.173±0.007	13.1±0.53	6.90±0.34	14.3 ± 0.14	22 ± 1.34	385.8 ± 3.68
T14	0.42±0.014	0.144±0.009	16.9±0.38	6.95±0.17	13.6 ± 0.18	21 ± 1.36	321.0 ± 3.25
T15	0.48±0.012	0.205±0.012	11.8±0.81	6.45±0.28	12.1 ± 0.11	21 ± 1.48	328.8 ± 3.85
T16	0.31±0.007	0.011±0.006	11.2±0.78	5.63±0.44	14.2 ± 0.17	23 ± 1.57	329.5 ± 4.02

Mirroring Polyakov et al. (2019), our %N analysis reveals a distinctive trend among sampling stations: S2>S1>S3>S4>S5. Their focus on HAs underscores the relationship between nitrogen (%N) and hydrogen (%H) content within HAs, aligned with our observations. Additionally, the heightened oxygen (%O) and sulphur (%S) content in S1 resonates with Polyakov et al. (2019)'s emphasis on HAs' elemental composition. Despite differing sample types, our study's elevated oxygen and sulphur content in S1 echoes similar organic composition trends.

Our study demonstrates that UV absorption serves as quickly and highly responsive for characterizing the molecular composition of samples, particularly in terms of unsaturated carbon content. The UV spectra exhibited elevated absorbance within the 200-300 nm range for sample S2, indicating a higher presence of chromophores associated with double bonds (C=C, C=O). These findings align with the observation of greater aromatic structures (evidenced by a higher H/C ratio) in sample S1. The analysis revealed that sample S1 had the highest percentage of HA at 0.089%, followed by decreasing percentages in the order of S2, S3, S4, and S5. Our research underscores the utility of UV absorption analysis as a valuable tool for assessing the unsaturated carbon content in samples and provides valuable insights into the relative HA content among the tested samples.

In a series of studies on the characterization of HS, UV-Vis spectroscopy has emerged as a valuable analytical tool. Enev et al. (2014) compared HS from various sources, including soil, compost, and lignite, and employed UV-Vis spectroscopy to assess their structural differences. They found that the existence of O-containing functional groups followed a distinct order across these materials. Additionally, the study by Chen et al. (2002) focused on natural organic matter (NOM) fractions and reference soil HA (SHA) and utilized UV-Vis spectroscopy to reveal variations in the excess of aromatic C=C and methoxyl ($-OCH_3$) functional groups. Furthermore, Chen et al. (1977) emphasized the significance of the E4/E6 ratio, a key UV-Vis parameter, for characterizing humic and fulvic acids, highlighting its relationship with particle size, pH, and various chemical properties. Pedra et al. (2008) explored the effects of organic amendments on soil HAs using UV-Vis spectroscopy, particularly noting alterations in the E4/E6 ratio and the aliphatic and aromatic characteristics of soil HAs. Altogether, these studies underscore the versatility and applicability of UV-Vis spectroscopy in elucidating the structural characteristics of HS from various sources.

The FT-IR analysis conducted on various samples of HAs from diverse locations has revealed critical insights into their compositional and structural characteristics. These findings can be discussed in conjunction with relevant studies, focuses on the complexity of HAs in different environmental contexts. In the spectral zone of 3500-3000 cm^{-1}, bands associated with O-H stretching, minor N-H stretching, and the presence of hydrogen-bonded -OH groups were observed, consistent with previous studies (Woelki et al., 1997). The intensity of

these bands was notably higher in samples S1, S2, and S3, suggesting a greater presence of matured HS, while S4 and S5 exhibited lower intensities, indicating the presence of less matured humic compounds.

The bands in the 2900-2300 cm^{-1} range corresponded to asymmetric and symmetric C-H stretching of CH_2 groups. This aligns with the absence of these bands in S4 and S5, where unique chemical reactions may be occurring, as reported by Tu et al. (1993). Absorption bands at 1740 cm^{-1} were attributed to the C=O stretching of COOH and other carbonyl groups, consistent with the presence of these functional groups (Woelki et al., 1997). The range of 1600-1690 cm^{-1} indicated aromatic C=C skeletal vibrations and C=O stretching of amide groups (amide I band), consistent with observations in previous studies (Tu et al., 1993). The peak at 1550 cm^{-1} was linked to N-H deformation and C=N stretching (amide II band) as well as aromatic C=C stretching, corroborating findings by Senesi et al. (1999).

Additional absorption bands between 1200-1400 cm^{-1} pointed to various functional groups, including C-H asymmetric bending in CH_3 groups, O-H deformation, C-O stretching of phenolic OH, C-H bending of CH_2 and CH_3 groups, anti-symmetric stretching of COO-, and C-O stretching of aryl esters aligning with the results observed by Senesi et al. (1999). The presence of cellulose residues in the sample was suggested by an additional band at 1130 cm^{-1} (C-O-C stretching skeletal vibration), similar to findings by Senesi et al. (1999). The detection of lignin residues aligns with the presence of similar aromatic components observed in previous studies (Senesi et al., 1999).Variations in the intensity of these spectral features were observed among the different samples. S1 exhibited the most prominent peaks, followed by S2, S3, S4, and S5. This variance suggests differences in the degree of humification and the degree of unsaturation, as reported by previous research (Tu et al., 1993; Senesi et al., 1999). The FT-IR analysis of HAs presented in this study parallels and extends the findings of previous research. The characterization of functional groups and spectral features provides valuable insights into the diverse composition and structural characteristics of HAs across various environmental sectors. These findings contribute to an enhanced comprehension of the role of HAs in organic matter decomposition and nutrient cycling (Tu et al., 1993; Woelki et al., 1997; Senesi et al., 1999).

In our study, we have found that the various treatments significantly influenced the growth and biochemical composition of rice seedlings. Specifically, all treatments yielded significantly higher values compared to the control group, indicating their positive impact on the seedlings. Treatment T3 stood out as the most effective, with the highest shoot and root fresh mass, maximum total protein content, chlorophyll content, and carotenoid content. In contrast, treatment T11 consistently exhibited the lowest values across all parameters. These findings emphasize the substantial influence of the treatments on rice seedling growth and biochemical composition, with T3 demonstrating the most favourable outcomes.

Our research aligns with previous studies on HS and their role in promoting plant growth and enhancing biochemical composition. Nardi et al. (2021) highlighted the importance of understanding the connection between the chemical structure of humic substances (HS) and their impact on biological activity is crucial. They highlighted the significance of specific functional groups in HS that could elicit favorable physiological responses in plants including hormone-like signalling pathways. This aligns with our findings where treatment T3 significantly increased protein content, chlorophyll content, and carotenoid content in rice seedlings, indicating its positive impact on biochemical composition. Our results are also consistent with the study by Vaccaro et al. (2015), which examined the effects of HS on maize seedlings. They found that HS positively influenced nitrate metabolism, leading to increased soluble protein and amino acid synthesis, as well as the activity and transcription of enzymes involved in nitrogen assimilation. Similarly, in our study, treatment T3 significantly increased protein content, suggesting improved biochemical composition in rice seedlings.

The study by García et al. (2014) investigated the effects of HA under water stress conditions on rice plants. They observed that peroxidase activity was maintained by HA, reduced lipid peroxidation, and regulated abscisic acid levels, indicating its protective effects on plants. In our study, treatment T3 consistently outperformed other treatments across various parameters, suggesting its potential to promote rice seedling growth and biochemical enhancement, which is in line with the protective effects demonstrated by HA in the study.

This study discusses about the elemental composition, UV absorption and FTIR analysis of humic acids (HAs). The study explores compositional changes during composting and highlights the utility of UV-Vis spectroscopy and FTIR analysis in characterizing HAs. It also connects these findings with some previous reported literature. Additionally, the research investigates the impact of various treatments on rice seedling growth and biochemical composition. These results align with previous studies emphasizing the positive effects of humic substances on plant growth and biochemical composition.

Conclusion

Humic acids play a significant role in the fertility of soil and plant health. In present study, assessment of diverse characteristics of HAs from various locations of Delhi NCR has been done. Through elemental analysis, we determined that the samples exhibited variations in C, H, N_2, O_2 and S content, with sample S1 showing the highest C and S levels. UV-Vis spectroscopy highlighted differences in the unsaturated carbon content among samples, with sample S2 displaying the highest absorbance in the 200-300 nm range, indicative of more double bonds. Moreover, our FT-IR analysis focuses on the structural and compositional disparities among HA samples, with S1 and S2 exhibiting more intense bands, suggesting a lower degree of humification. The hydroponics experiments revealed significant effects of different treatments of HAs on rice seedlings' growth and biochemical characteristics. Treatment T3 has been found to be the most effective by promoting significant growth in root and shoot length, increased root and shoot fresh mass increased protein, chlorophyll, and carotenoid content in rice seedlings. On the contrary, treatment T11 consistently showed the least helpful to the seedling health across all parameters. The findings contribute to a understanding of the HAs and their role in organic matter composition in the various soil. This study also emphasizes the potential for optimizing promoting and utilization of HAs to enhance sustainable crop growth by ensuring soil and plant health for sustainable agriculture practices.

Acknowledgment

The authors are grateful to the Founder President of Amity University, Dr. Ashok K Chauhan for his constant support and encouragement. The study was also supported by the Southern Federal University with the financial support of the Ministry of Science and Higher Education of the Russian Federation, agreement no. 075-15-2022-1122 and funded by the Strategic Academic Leadership Program of the Southern Federal University ("Priority 2030").

References

Adani, F., Genevini, P., Zaccheo, P., Zocchi, G., 1998. The effect of commercial humic acid on tomato plant growth and mineral nutrition. *Journal of Plant Nutrition* 21(3): 561–575.

Almendros, G., Guadalix, M.E., González-Vila, F.J., Martin, F., 1996. Preservation of aliphatic macromolecules in soil humins. *Organic Geochemistry* 24(6–7): 651–659.

Amir, S., Hafidi, M., Merlina, G., Hamdi, H., Revel, J.-C., 2004. Elemental analysis, FTIR and ^{13}C-NMR of humic acids from sewage sludge composting. *Agronomie* 24(1): 13–18.

Arnon, D.I., 1949. Copper enzymes in isolated chloroplasts. Polyphenoloxidase in beta vulgaris. *Plant Physiology* 24(1): 1–15.

Castro, T.A.V.T., García, A.C., Tavares, O.C.H., Pereira, E.G., Souza, C.C.B., Torchia, D.F.O., Pinho, C.F., Castro, R.N., 2022. Humic acids affect photosynthetic quantum efficiency in rice under water deficit. *Theoretical and Experimental Plant Physiology* 34(4): 463–483.

Chang, R.R., Mylotte, R., Hayes, M.H.B., Mclnerney, R., Tzou, Y.M., 2014. A comparison of the compositional differences between humic fractions isolated by the IHSS and exhaustive extraction procedures. *Naturwissenschaften* 101(3): 197–209.

Chen, J., Gu, B., LeBoeuf, E. J., Pan, H., Dai, S., 2002. Spectroscopic characterization of the structural and functional properties of natural organic matter fractions. *Chemosphere* 48(1): 59–68.

Chen, X., Wu, J., Opoku-Kwanowaa, Y., 2020. Effects of returning granular corn straw on soil humus composition and humic acid structure characteristics in saline-alkali soil. *Sustainability* 12(3): 1005.

Chen, Y., Senesi, N., Schnitzer, M., 1977. Information provided on humic substances by e4/e6 ratios. *Soil Science Society of America Journal* 41(2): 352–358.

Cocozza, C., D'Orazio, V., Miano, T. M., Shotyk, W., 2003. Characterization of solid and aqueous phases of a peat bog profile using molecular fluorescence spectroscopy, ESR and FT-IR, and comparison with physical properties. *Organic Geochemistry* 34(1): 49–60.

Dębska, B., Szombathova, N., Banach-Szott, M., 2009. Properties of humic acids of soil under different management regimes. *Polish Journal of Soil Science* 42(2): 131-138.

Enev, V., Pospíšilová, Ľ., Klučáková, M., Liptaj, T., Doskočil, L. 2014. Spectral characterization of selected humic substances. *Soil and Water Research* 9(1): 9–17.

Ertani, A., Francioso, O., Tugnoli, V., Righi, V., Nardi, S., 2011. Effect of commercial lignosulfonate-humate on zea mays l. Metabolism. *Journal of Agricultural and Food Chemistry* 59(22): 11940–11948.

García, A.C., Santos, L.A., Izquierdo, F.G., Rumjanek, V.M., Castro, R.N., Dos Santos, F.S., De Souza, L.G.A., Berbara, R.L.L., 2014. Potentialities of vermicompost humic acids to alleviate water stress in rice plants (Oryza sativa L.). *Journal of Geochemical Exploration* 136: 48–54.

González Pérez, M., Martin-Neto, L., Saab, S.C., Novotny, E.H., Milori, D.M.B.P., Bagnato, V.S., Colnago, L.A., Melo, W.J., Knicker, H., 2004. Characterization of humic acids from a Brazilian Oxisol under different tillage systems by EPR, ^{13}C NMR, FTIR and fluorescence spectroscopy. *Geoderma* 118(3–4): 181–190.

Guggenberger, G., 2005. Humification and mineralization in soils. In: Microorganisms in Soils: Roles in Genesis and Functions. Varma, A., Buscot, F., (Eds.) Vol. 3. Springer-Verlag. pp. 85–106.
Hayes, M.H.B., Mylotte, R., Swift, R.S., 2017. Humin: Its composition and importance in soil organic matter. *Advances in Agronomy* 143: 47–138.
IHHS, 2024. Isolation of ihss soil fulvic and humic acids. Available at [Access date: 25.01.2024]: https://humic-substances.org/isolation-of-ihss-soil-fulvic-and-humic-acids/
Ikan, R., 1991. Natural products: a laboratory guide. Academic Press. 316p.
Jackson, W.R., 1993. Humic, fulvic and microbial balance: organic soil conditioning Evergreen: Jackson Research Center. 329p.
Javanshah, A., Saidi, A., 2016. Determination of humic acid by spectrophotometric analysis in the soils. *International Journal of Advanced Biotechnology and Research* 7: 19-23.
Jindo, K., Hernández, T., García, C., Sánchez-Monedero, M.A., 2011. Influence of stability and origin of organic amendments on humification in semiarid soils. *Soil Science Society of America Journal* 75(6): 2178–2187.
Kelleher, B.P., Simpson, A.J., 2006. Humic substances in soils: Are they really chemically distinct? *Environmental Science and Technology* 40(15): 4605–4611.
Kolchanova, K., Tolpeshta, I., Izosimova, Y., 2021. Adsorption of fulvic acid and water extractable soil organic matter on kaolinite and muscovite. *Agronomy* 11(12): 2420.
Kononova, M.M., 1961. Soil organic matter: Its nature, its role in soil formation and in soil fertility. Soil organic matter, its nature, its role in soil formation and in soil fertility. Pergamon Press. 450p.
Kononova, M.M., 1981. Materia orgánica del suelo: su naturaleza, propiedades y métodos de investigación. Oikos-Tau, Barcelona, Spain. 365p. [in Spanish]
Kögel-Knabner, I., Zech, W., Hatcher, P.G., 1988. Chemical composition of the organic matter in forest soils: The humus layer. *Zeitschrift Für Pflanzenernährung Und Bodenkunde* 151(5): 331–340.
Körschens, M., 2002. Importance of soil organic matter (SOM) for biomass production and environment (A review). *Archives of Agronomy and Soil Science* 48(2): 89–94.
Lal, R., 2020. Soil organic matter content and crop yield. *Journal of Soil and Water Conservation* 75(2): 27A-32A.
Lehmann, J., Kleber, M., 2015. The contentious nature of soil organic matter. *Nature* 528(7580): 60–68.
Li, J.-J., Ji, H.-B., Wang, W.-J., Dong, F., Yin, C., Zhang, L., Li, R., Gao, J., 2022. Study on the profile distribution and morphology of soil humic substances in Karst area of Zunyi city, China. *Sustainability* 14(10): 6145.
Nardi, S., Schiavon, M., Francioso, O., 2021. Chemical structure and biological activity of humic substances define their role as plant growth promoters. *Molecules* 26(8): 2256.
Ndzelu, B. S., Dou, S., Zhang, X., 2020. Changes in soil humus composition and humic acid structural characteristics under different corn straw returning modes. *Soil Research* 58(5): 452-460.
Pedra, F., Plaza, C., Fernández, J. M., García-Gil, J. C., Polo, A., 2008. Effects of municipal solid waste compost and sewage sludge on chemical and spectroscopic properties of humic acids from a sandy Haplic Podzol and a clay loam Calcic Vertisol in Portugal. *Waste Management* 28(11): 2183–2191.
Peña-Méndez, E. M., Gajdošová, D., Novotná, K., Prošek, P., Havel, J., 2005. Mass spectrometry of humic substances of different origin including those from Antarctica. *Talanta* 67(5): 880–890.
Polyakov, V.I., Chegodaeva, N.A., Abakumov, E.V., 2019. Molecular and elemental composition of humic acids isolated from selected soils of the Russian Arctic. *Bulletin of Tomsk State University, Biology* 47: 6-21.
Pospíšilová, Ľ., Fasurová, N., 2009. Spectroscopic characteristics of humic acids originated in soils and lignite. *Soil and Water Research* 4(4): 168–175.
Qiang, T., Xiao-quan, S., Zhe-ming, N., 1993. Comparative characteristic studies on soil and commercial humic acids. *Fresenius Journal of Analytical Chemistry* 347: 330-336.
Ribeiro, J.S., Ok, S.S., Garrigues, S., De La Guardia, M., 2001. FTIR tentative characterization of humic acids extracted from organic materials. *Spectroscopy Letters* 34(2): 179–190.
Rodríguez-Lucena, P., Lucena, J.J., Hernández-Apaolaza, L., 2009. Relationship between the structure of Fe-Lignosulfonate complexes determined by FTIR spectroscopy and their reduction by the leaf Fe reductase. UC Davis: Department of Plant Sciences. Available at [Access date: 02.11.2023]: https://escholarship.org/uc/item/9k69q71d
Senesi, N., Loffredo, E., 1999. The chemistry of soil organic matter. In: Soil Physical Chemistry. Spark, D.L. (Ed.). CRC Press, pp. 239-370.
Senesi, N., Miano, T.M., 1994. Humic substances in the global environment and implications on human health. Proceedings of the 6th International Meeting of the International Humic Substances Society, 20-25 September 1992, Monopoli (Bari), Italy, Elsevier. 1368p.
Stevenson, F.J., 1982. Humus chemistry: Genesis, composition, reactions. John Wiley & Sons. Inc. 496p.
Stuijfzand, S.C., Jonker, M.J., Van Ammelrooy, E., Admiraal, W., 1999. Species-specific responses to metals in organically enriched river water, with emphasis on effects of humic acids. *Environmental Pollution* 106(1): 115–121.
Tadini, A.M., Bernardi, A.C.C., Milori, D.M.B.P., Oliveira, P.P.A., Pezzopane, J.R.M., Martin-Neto, L. 2022. Spectroscopic characteristics of humic acids extracted from soils under different integrated agricultural production systems in tropical regions. *Geoderma Regional* 28: e00476.

Tadini, A.M., Nicolodelli, G., Mounier, S., Montes, C.R., Milori, D.M.B.P., 2015. The importance of humin in soil characterisation: A study on Amazonian soils using different fluorescence techniques. *Science of The Total Environment* 537: 152–158.

Thakur, S.K., Goswami, K., Kumar, A., Bhattacharjee, S., Eswaran, S.V., 2023. Gwal pahari acid: Isolation, characterization of a new soil based plant growth promoting humic acid. *Sustainable Development Research* 5(1): 44-65.

Thurman, E.M., Malcolm, R.L., 1981. Preparative isolation of aquatic humic substances. *Environmental Science and Technology* 15(4): 463–466.

Timofeevna Shirshova, L., Ghabbour, E.A., Davies, G., 2006. Spectroscopic characterization of humic acid fractions isolated from soil using different extraction procedures. *Geoderma* 133(3–4): 204–216.

Tzou, Y.-M., Wang, S.-L., Liu, J.-C., Huang, Y.-Y., Chen, J.-H., 2008. Removal of 2,4,6-trichlorophenol from a solution by humic acids repeatedly extracted from a peat soil. *Journal of Hazardous Materials* 152(2): 812–819.

Vaccaro, S., Ertani, A., Nebbioso, A., Muscolo, A., Quaggiotti, S., Piccolo, A., Nardi, S., 2015. Humic substances stimulate maize nitrogen assimilation and amino acid metabolism at physiological and molecular level. *Chemical and Biological Technologies in Agriculture* 2(1): 5.

Volkov, D., Rogova, O., Proskurnin, M., 2021. Temperature dependences of IR spectra of humic substances of brown coal. *Agronomy* 11(9): 1822.

Wei, S., Li, Z., Sun, Y., Zhang, J., Ge, Y., Li, Z., 2022. A comprehensive review on biomass humification: Recent advances in pathways, challenges, new applications, and perspectives. *Renewable and Sustainable Energy Reviews* 170: 112984.

Woelki, G., Friedrich, S., Hanschmann, G., Salzer, R., 1997. HPLC fractionation and structural dynamics of humic acids. *Fresenius' Journal of Analytical Chemistry* 357(5): 548–552.

Wolf, B., Snyder, G., 2003. Sustainable soils: The place of organic matter in sustaining soils and their productivity. CRC Press. 376p.

Xiao, L., Zhang, W., Hu, P., Xiao, D., Yang, R., Ye, Y., Wang, K., 2021. The formation of large macroaggregates induces soil organic carbon sequestration in short-term cropland restoration in a typical karst area. *Science of The Total Environment* 801: 149588.

Eurasian Journal of Soil Science 2024, 13(3), 202 - 209

Eurasian Journal of Soil Science

Journal homepage : http://ejss.fesss.org

Assessing the impact of biofertilizer on soil microbial dynamics and metabolic activity in a controlled maize pot-grown experiment

Katya Dimitrova [a,*], Tursynbek Kaiyrbekov [a], Dobrinka Balabanova [b]

[a] Agricultural University – Plovdiv, Faculty of Plant Protection and Agroecology, Department of Microbiology and Environmental Biotechnologies, Plovdiv, Bulgaria

[b] Agricultural University – Plovdiv, Faculty of Agronomy, Department of Plant Physiology, Biochemistry and Genetics, Plovdiv, Bulgaria

Article Info

Received : 15.12.2023
Accepted : 11.02.2024
Available online: 19.02.2024

Author(s)

K.Dimitrova *
T.Kaiyrbekov
D.Balabanova

* Corresponding author

Abstract

Biofertilizers, consisting of carefully selected microorganisms across various species and genera, exhibit distinct features that enhance soil fertility and promote plant growth. Embracing the principles of eco-friendly agriculture, the use of biofertilizers emerges as a pivotal strategy for sustainable farming, contributing to environmental preservation and the overall health and biodiversity of the soil. In this study, a commercially available biofertilizer, containing a specialized strain of *Priestia megatherium* with nitrogen-fixing capabilities, was employed alongside chemical fertilizers at two different doses (30 and 40 mg per kg of soil). The primary objective was to evaluate the impact of biofertilizer on the metabolic activity and structure of microbial communities in a short-term experiment involving potted maize plants, utilizing the BIOLOG® EcoPlates technique. Parameters such as average well-color development (AWCD) and substrate utilization across six guilds (SAWCD) were assessed to gauge microbial metabolic activity. Additionally, functional indexes, including Shannon diversity, Shannon evenness, and Simpson diversity, were calculated as indicators of soil microbial community functionality. While statistically significant differences in AWCD among the studied variants were not observed, all estimated functional indexes consistently revealed heightened microbial diversity and evenness following the application of biofertilizer. This noteworthy finding, achieved within a relatively short period of plant cultivation, underscores the necessity for further research to explore the biofertilizer's enduring effects on soil communities, both in controlled laboratory environments and under real-world field conditions.

Keywords: Biofertilizer, BIOLOG® EcoPlate, functional indexes, metabolic activity, microbial communities, *Priestia megaterium*.

© 2024 Federation of Eurasian Soil Science Societies. All rights reserved

Introduction

Biofertilizers contain living microorganisms which can affect plant growth and productivity by activating processes in the soil and in the plant. The use of biofertilizers is considered an eco-friendly approach, which complies with the aims set in the “farm to fork” strategy of the EU for 20% reduction of mineral fertilisers (Kurniawati et al., 2023). The biofertilizers usually contain either a single strain or a combination of different strains and species belonging to the genera *Azotobacter* spp., *Rhizobium* spp. and *Azospirillum* spp., and mycorrhizal fungi (AMF). The list of species applied as biofertilizers is constantly expanding and currently included strains from the genera *Aeromonas*, *Arthrobacter*, *Bacillus*, *Clostridium*, *Enterobacter*, *Gluconacetobacter*, *Klebsiella*, *Pseudomonas*, and *Serratia*. The microbial biofertilizers can be applied in the soil, on the leaves or seeds. One of the main goals of their application is towards increased microbial activity, diversity of beneficial microorganisms, and change in the ratio between different species which can boost soil processes and organic matter turnover (Bargaz et al., 2018; Vessey, 2003). Despite the expanding interest on the application of AMF and beneficial bacteria their mechanisms of action are not fully revealed (Backer et al., 2018; Ramakrishna et al., 2019). The effectiveness of biofertilizers would depend on the properties of the

: https://doi.org/10.18393/ejss.1439846
: http://ejss.fesss.org/10.18393/ejss.1439846
Publisher : Federation of Eurasian Soil Science Societies
e-ISSN : 2147-4249

selected species and strains but the combined use of biofertilizers and the mineral fertilisers would require both laboratory and field data in order to establish the optimal ratio, to optimize the way of application and to reveal the possible mechanisms of interactions between microorganisms and plants. The justification of such approach should also take into account financial resources, available machinery and other intrinsic factors (Bargaz et al., 2018).

The primary objective of this study was to investigate the impact of biofertilizer on the metabolic activity of soil microorganisms and alterations in the structure of soil microbial communities. This investigation was conducted through a short-term laboratory experiment involving potted maize plants, carefully controlled to maintain constant conditions

Material and Methods

Maize variety

In the study was used maize hybrid - Kneja 307. The plants were grown in a climate-controlled chamber set at the following conditions: a photosynthetic photon flux density (PPFD) - 200 µmol m^{-2} s^{-1}, an average temperature - 25°C ± 1°C, an average relative humidity – 65% and 13/11 hours day/night photoperiod. After one-month cultivation, the plants were taken off from the pots and plant material and soil was used for further analyses.

Soil

The soil used in the pot experiment, 0 to 10 cm depth, was collected from the Experimental field of the Agricultural University-Plovdiv, Bulgaria. The soil type was classified as silty clay loam (mollic fluvisols) - 19.9% sand, 46.9% silt, 33.2% clay with 2.66% organic matter and high lime content (Table 1).

Table 1. Physicochemical characteristics of bulk soil

Soil parameters	Value	Units
Nitrogen	7.94	ppm
Phosphorus (P_2O_5)	214.60	ppm
Potassium (K_2O)	423.50	ppm
$CaCO_3$	8.75	g/kg
Exchangeable cations (ca+mg)	16.20	meq/100 g
Electrical conductivity	108.10	µS/cm
Soil organic matter	2.66	%
pH	8.80	logarithmic units

Mineral fertilizer and biofertilizer

Ammonium nitrate was used as mineral fertilizer. The biofertilizer is a product available on the market under commercial name NUPTAK (Daymsa, Spain) and is comprised of a selected strain of gram-positive, spore-forming rod bacterium - *Priestia megatherium CB2001.*

Experimental design

The experiment was comprised of four treatments (Table 2), with five replicates (pots) with 4 plants per pot. The collected bulk soil was sieved, split in two and half of it was sprayed with a freshly prepared suspension of biofertilizer in a dose of 0.33 mg per kg soil. The other soil was sprayed with the same quantity of tap water and all soil samples were thoroughly mixed. The biofertilizer inoculated soil and the control (uninoculated soil) were further split in two and were fertilized either with 30 or with 45 mg ammonium nitrate per kg soil, respectively. After fertilization the soil samples were mixed with perlite at 3:1 volume ratio and each pot was filled with 1 kg of soil.

Table 2. Experimental variants - descriptions and abbreviations

Variants abbreviation	Variants description	
	Mineral fertilizer - ammonium nitrate, mg kg^{-1}	Biofertilizer – Priestia megaterium, mg kg^{-1}
30 ppm N	30	-
30 ppm N+PM	30	0.33
45 ppm N	45	-
45 ppm N+PM	45	0.33

The rizhospheric soil was carefully brushed from the plant roots and was used for metabolic analysis. The other soil in the pots was used for soil respiration and physicochemical analyses.

Soil analyses

Available mineralized forms of nitrogen (ammonium and nitrate) were determined by modified Kjeldahl method. Soil phosphorus analysis was conducted Egner-Riehm DL method according to Egner and Riehm (1955). The applied method, with slight modification, includes $SnCl_2$ dissolved in hydrosulfuric acid as an indicator and measurement of wavelength at 700 nm. The analysis for available potassium was done with 5 g of soil sample dissolved in 50 ml of 2N HCl acid and the suspension was shaken and filtered before reading on a flame photometer.

Soil respiration

The soil respiration was determined according to Isermeyer method described by Alef (1995).

Metabolic activity of microbial soil communities

Metabolic activity of soil communities was assessed using the 96-well Eco MicroPlates™ of BIOLOG® (Biolog Inc., USA). Each EcoPlate is comprised of 31 different substrates organized in the following guilds - carbohydrates (ten substrates), carboxylic acids (seven substrates), polymers (four substrates), amino acids (six substrates), amines (two substrates) and phenolic compounds (two substrates). The EcoPlate contains three replicates of guilds.

One gram of the rhizospheric soil was suspended in 9 ml sterile distilled water, thoroughly mixed and left to settle for 5 min, after which a 10^{-3} dilution was prepared. The inoculation of Biolog® EcoPlates was done with 150 µl and plates were incubated at 25±1°C. The plates were read spectrophotometrically immediately after inoculation and consequently at 24 hour intervals for 7 days (168h) with the MicroStation™ Reader provided by the BIOLOG® System. The calculations for average well-color development (AWCD) and separately for each guilds were based on the optical density (OD) measured at 590 nm and 750 nm according to the procedure described by Sofo and Ricciuti (2019) except the formula for AWCD which was according to Huang et al. (2012) as follows:

$$\mathrm{AWCD} = \sum (C_i - R)/31$$

where R is the control well (water) and C_i is the value of carbon substrate well

Functional indexes

The wells with an average OD ≤0.250 were not taken as a positive response for substrates utilization according to Sofo and Ricciuti (2019) and was set to zero in calculation. Shannon richness was calculate by the following formula:

$$H' = -\sum(P_i \times lnP_i),$$

where $P_i = (C_i - R)/\sum C_i - R)$

The Shannon evenness index (E) which was derived from the Shannon index used the formula:

$$E = H'/lnS$$

where S was the substrate richness (the number of wells which showed positive threshold OD≥0.250)

Simpson diversity index (D) was calculated according to Ge et al. (2018):

$$D = 1 - \sum P_i^2,$$

where P_i is the same as in the Shannon index calculation.

Data analysis

AWCD values calculations and the graph visualization was done with Microsoft Excel using the three replicates on each ecoplate as independent measurements (n=3). In order to compare functional indexes of the different treatments one-way analysis of variance (ANOVA) was performed with SPSS program (IBM, ver. 26) with the level of significance $p<0.05$.

Results and Discussion

Effect of mineral fertilization and biofertilizer on soil parameters

The application of mineral fertilizer and biofertilizer affected the soil pH – a slight decrease from 8.80 to 8.45. Additionally, the level of available phosphorus oxide has increased after treatments which could be explained by solubilisation of the fixed phosphorus which correspond to the phosphorus solubilization activity assigned to the strain present in the biofertilizer according to information provided by the manufacturer. The increase of available phosphorus in the soil is often associated with the presence of phosphorus solubilizing microorganisms (Mehnaz, 2016). The analysis showed a higher level (8%) of ammonium in the soil treated with the lower dose of mineral fertilizer supplemented with biofertilizer – 30 ppm N+PM when compared to the non-supplemented with a biofertizer variant – 30 ppm N. However, there was not significant difference of available ammonium in the soil between 45 ppm N and 45 ppm N+PM treatment. The potassium (K_2O) level

declined from 423.5 ppm (Table 1) to 345 ppm due to its utilization by plants and the used chemical fertilizer does not provide potassium. The soil used in the current experiment, showed a relatively low nitrogen content which also declined for all variants at the end of plant cultivation. The study (data not shown) also included assessment of plant biometrics, photosynthetic activity, antiradical activity and analyses of leaf and root mineral content. In general, analyses of estimated parameters did not reveal statistically significant differences between experimental treatments which can be explained by the short duration of the performed pot experiment (Table 3).

Table 3. Mineral content of soil at the end of plant cultivation

Variant	pH	Mineral content, ppm			
		P_2O_5	K_2O	NH_4	NO_3
30 ppm N	8.52	296.4	326.0	2.93	5.65
30 ppm N+PM	8.43	300.1	346.0	3.19	5.68
45 ppm N	8.47	282.8	346.6	3.83	4.56
45 ppm N+PM	8.40	302.6	346.0	3.92	8.49

The inoculated with biofertilizer soils showed higher respiration rate (Table 2) in comparison to soils without biofertilizer.

Table 4. Soil respiration (mg CO_2/g dry soil/24 h)

Variants	Soil respiration
30 ppm N	0.062^{b} ±0.012
30 ppm N+PM	0.096^{ab} ±0.012
45 ppm N	0.078^{b} ±0.015
45 ppm N+PM	0.129^{a} ±0.021

Legend: The soil respiration is presented as mean ± SD, n=3; the different superscript letters indicate statistical difference at $p<0.05$

The average well-color development (AWCD) (Figure 1) which was used to assess the metabolic activity of soil microorganisms revealed a presence of a lag phase till 24th hour and highest activity between 48th hour and 96th hour; after that the changes in the optical density were moderate. There was not significant difference between different variants till 96th hour, however, the variants 30 ppm N+PM and 45 ppm N showed higher activity in comparison to other variants. Similar observation, which included a lag phase and a gradual increase in the metabolic activity of microorganisms, was made by Ge at al. (2018). The OD change could be assigned predominantly to bacterial activity because the reading of the EcoPlate started from 24th hour which is insufficient time for fungi development and their contribution to the color in the wells could be ignored (Figure 1). In fact, either in natural or in experimental conditions, if there is no inhibitory factors that could suppress the growth and metabolic activity of microorganisms the curve of AWCD usually keeps a typical sigmoid shape (Stefanowicz, 2006, Lima et al., 2015).

In order to obtain more detailed information about specific metabolic activity of bacteria the AWCD was also calculated separately for the six guilds of substrates (amino acids, carbohydrates, carboxylic acids, amines, polymers, and phenolic compounds) provided by the Biolog® EcoPlate.

The utilization of amino acids (Figure 2) showed a distinct dynamics for different variants, especially after the 96th hour of incubation, despite the lack of statistical difference. After 72nd hour of inoculation until the end of the incubation period the variant 30 ppm N + PM showed a higher metabolic activity in comparison to the other variants.

The utilization of amines, on the contrary to the utilization of all other guilds, was more active only for the variants that were not supplemented with biofertilizer and there was a clear difference between variants in the created graph (Figure 3). Ge et al. (2018) observed the low utilization of amines and considered that among all substrates provided in the Ecoplate these substrates were less preferable. However, the authors reported an optical density of 1.600 on the 7th day of incubation, and in the current experiment the maximum values for the same period was only 1.097 for variant 30 ppm N and this value was comparable with the value of carbohydrates utilization (1.193). The observed mean values were accompanied with a notable standard deviation which restrained any reliable conclusions about microbial metabolism of amines in the variants.

There was not significant difference of carboxylic acid utilization between variants (Figure 4). However, the utilization of this guild of ten different carboxylic acids was detected, even at a relatively low level, on the 24th hour measurement only for the two variants that were treated with biofertilizer. According to some authors utilization of carboxylic acids could be considered as the most representative substrate guild of the Ecoplate and they associated the better utilization of carboxylic acids to improved plant health. The authors found that the higher carboxylic acids utilization of microbial communities was related to the lower level of damages to the trees which were objects of the study (Cai et al., 2010).

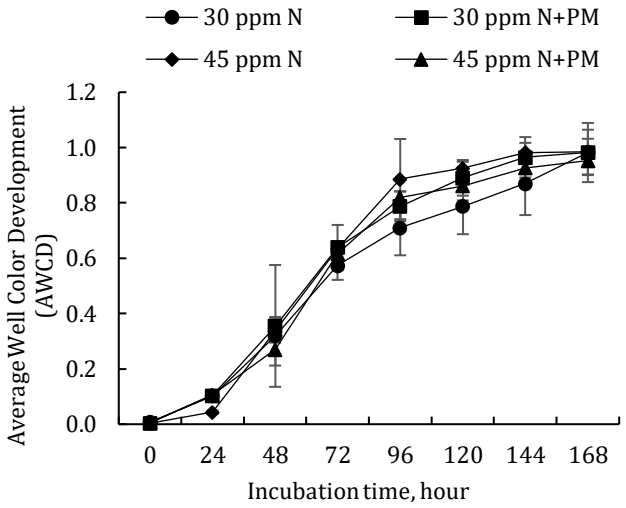

Figure 1. Microbial metabolic activity in the Biolog® EcoPlate

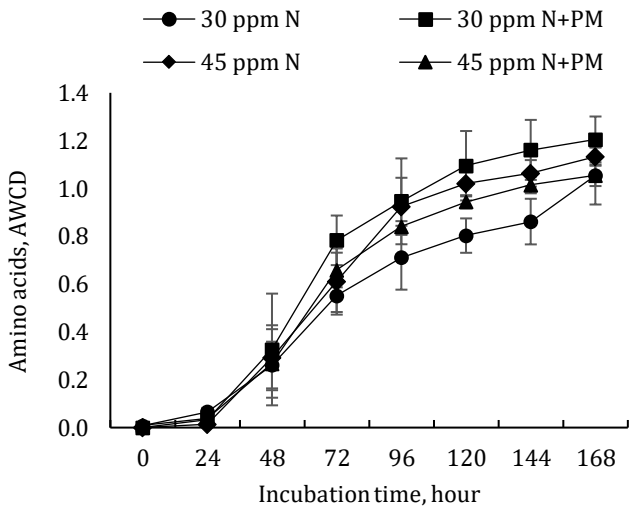

Figure 2. Dynamics of amino acids utilization in the Biolog® EcoPlate

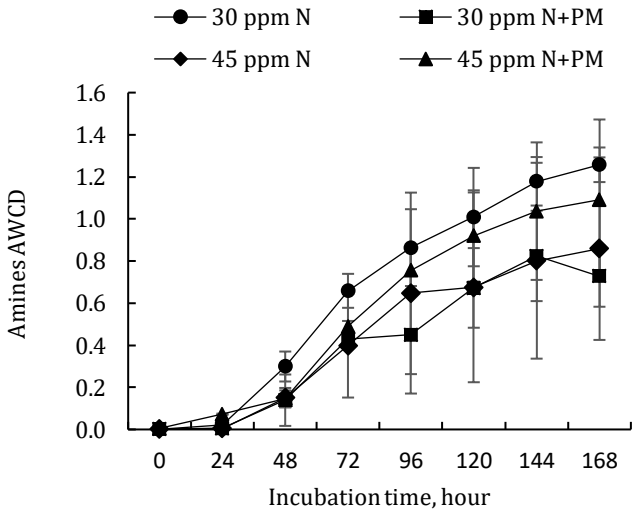

Figure 3. Dynamics of amines utilization in the Biolog® EcoPlate

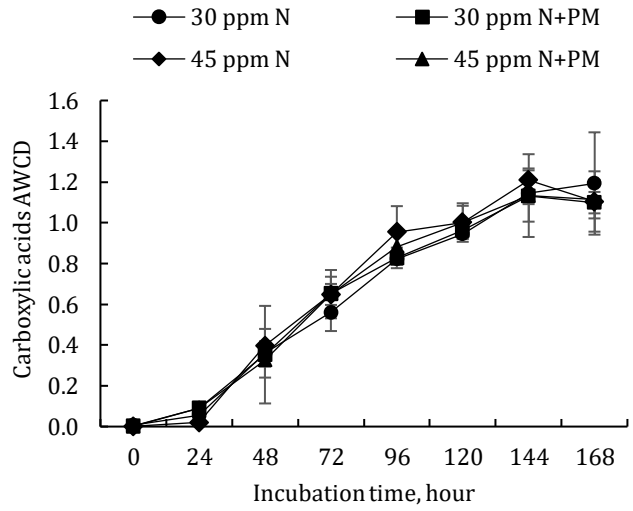

Figure 4. Dynamics of carboxylic acids utilization in the Biolog® EcoPlate

The carbohydrates were utilized (Figure 5) intensively up to 72nd hour. The variant 40 ppm N showed a relatively low value (0.104) at the 24th hour but reached OD of 0.487 at the measurement on 48th hour. After 120th hour until the end of the incubation the variants 30 ppm N+Priestia and 45 ppm N showed a higher metabolic activity in comparison to the other variants. The optical density varied between 0.716 to 0.800 on 72nd hour, but after that the curve tend to flat and at the end of the incubation the values ranged between 0.889 and 1.006 and there was no significant difference between variants.

In comparison to the other substrates, utilization of polymers began slowly and very uniformly among the variants and the same uniformity remained up to 96th hour despite that the curve became steep after 48th. Only after 120th hour the different variants could be distinguished one from another (Figure 6). In general, the utilization of polymers is not a very common characteristic for bacterial metabolism. This is especially true for the included in the *Ecoplate cyclodextrin*, wells (E 1-5-9), which metabolization was related to the existence of a relatively rare metabolic path in bacterial cells. The metabolic path has been described in the cells of hyperthermophilic archaea such as *Thermococcus* sp., *Pyrococcus furiosus* and *Archaeoglobus fulgidus* and other studies found it only in a few species of mesophilic bacteria such as *Klebsiella oxytoca* and *Bacillus subtilis* (Centeno-Leija et al., 2022). As a result the polymer utilization is assigned mainly to some bacteria with a relatively low abundance in the soil.

Xiao et al. (2022) used in their study *Rhodopseudomonas palustris* and *Bacillus subtilis* as microbial inoculants and found that they not only positively influenced the rice yield (17.73%) but there was also a synergy

between inoculants. Additionally, the inoculants have an influence on the structure of microbial communities and this effect concerned predominantly the rare species than the typical ones. The changes in the rare species authors explained with the increase of beneficial microorganisms in the soil and with the intensification of some essential soil processes (Xiao et al., 2022).

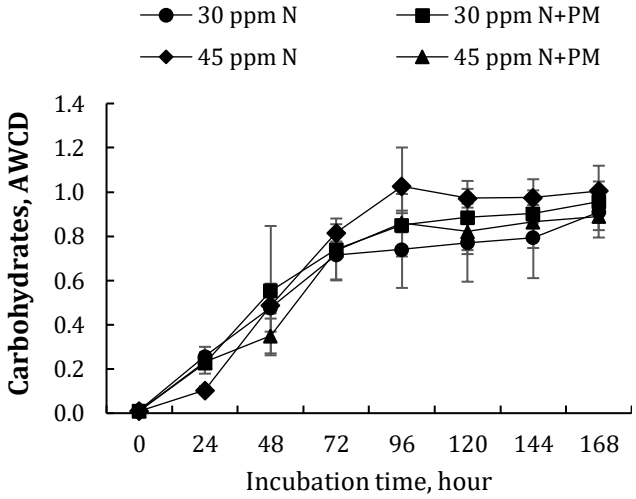

Figure 5. Dynamics of carbohydrates utilization in the Biolog® EcoPlate

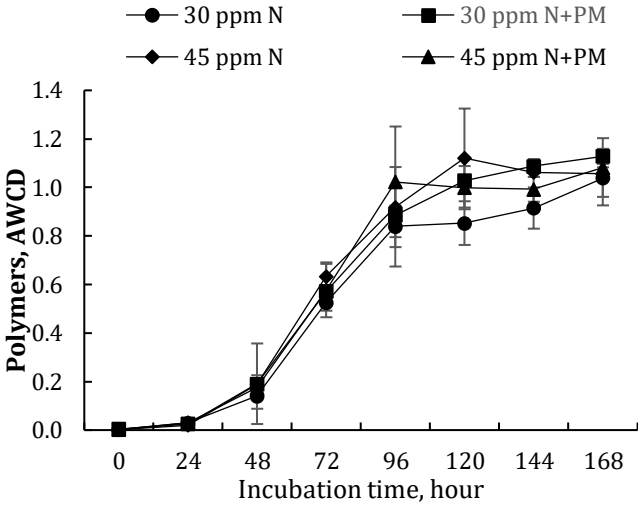

Figure 6. Dynamics of polymers utilization in the Biolog® EcoPlate

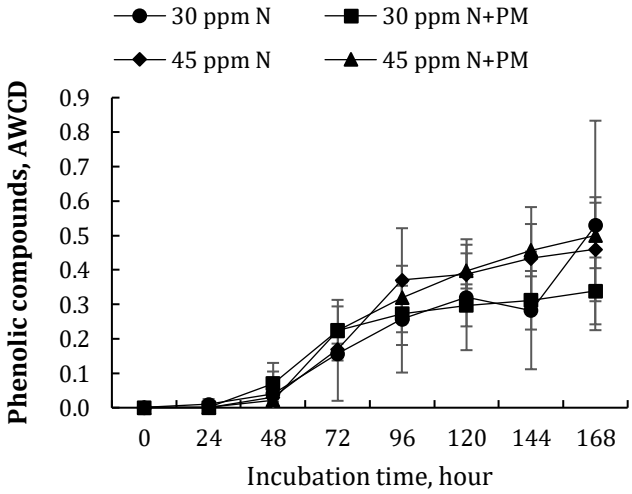

Figure 7. Dynamics of phenolic compounds utilization in the Biolog® EcoPlate

The utilization of phenolic compounds (2- hydroxy benzoic acid and 4- hydroxy benzoic acid) was lowest in comparison to all other guilds present in the Ecoplate. It was especially true for 2- hydroxy benzoic acid since the optical density in the corresponding wells (C 3-7-11) was either very low or the estimated values were even negative after correction with the control well which additionally contributed to the relatively larger standard deviation during calculations. At the end of the incubation period, the highest mean value was observed for the variant 30 ppm N - 0.529 with a standard deviation of 0.304.

After taking into account the values for optical density above 0.250 which were considered as a positive response towards substrates utilization the measurement taken on the 72nd hour was used for functional indexes calculation. The Shannon richness is related to species abundance and in the current study it has the higher values for variants supplemented with biofertilizer - 3.245 and 3.236 for variants 45 ppm + PM and 30 ppm N + PM, respectively (Table 3). Additionally, the Shannon evenness and Simpson diversity indices also showed higher values for biofertilizer-supplemented variants. However, none of the observed differences was statistically significant but the consistent trend across the calculated indexes could be considered as a clear indication that the biofertilizer has a positive effect on soil microbial communities. The effect of biofertilizer on microbial communities in the current study could be restrained to some extend due to the relatively short duration of the experiment, low organic matter content in the soil, high carbonate content or other factors. On the contrary to the presented results are findings of Roesti et al. (2006) who reported a significant modification in the structure of microbial communities after biofertilizer application.

Table 5. Metabolic functional diversity indices of soil samples treated with mineral fertilizer and Priestia megatherium-based biofertilizer

Variant	Indices		
	Shannon diversity (H´)	Shannon evenness (E)	Simpson diversity index (D)
30 ppm N	3.157 ± 0.202	0.962 ± 0.025	0.955 ± 0.006
30 ppm N+PM	3.236 ± 0.032	0.978 ± 0.007	0.958 ± 0.002
45 ppm N	3.181 ± 0.070	0.973 ± 0.007	0.955 ± 0.003
45 ppm N+PM	3.245 ± 0.082	0.978 ± 0.002	0.959 ± 0.003

Legend: Indexes are presented as: mean ± stand. deviation, n=3

Some studies did not find a significant effect of biofertilizer on soil microbial communities or the effect was very limited (Baldi et al., 2021, Wang et al., 2021). Other authors reported that biofertilizers did not provided the expected changes of the observed parameters or their effect was highly dependent on the applied doses (Al-Zubade et al., 2021, Siswanti and Riesty, 2021). Hou et al. (2023) used in their study three doses of mineral fertilizer (0, 200 and 400 kg N $ha^{-1}yr^{-1}$) and found that different doses of fertilizer affected variously microbial communities structure but fertilization at a moderate dose triggered higher diversity. Such data have practical importance because they offer information that can be used in the process for establishment of optimal ratio of mineral fertilizer and biofertilizer. The proper ratio would provide the expected positive effect of biofertilizer application along with the low input of mineral fertilizer. In their study Adesemoye et al. (2009) also tried to solve the question if the reduced doses of mineral fertilizer combined with a biofertilizer on tomato plants could provide the plant development comparable to those at optimal mineral fertilization and to what extend could be reduced fertilizer when it is supplemented with biofertilizer. The authors used biofertilizer that contained bacteria (*Bacillus amyloliquefaciens* IN937a and *Bacillus pumilus* T4), and arbuscular mycorrhizal fungi - AMF (*Glomus intraradices*). The results indicated that when the biofertilizer was added the reduction in the doses of mineral fertilizer could be up to 75% and the plant growth and yield was equivalent to the use of recommended doses of mineral fertilizer alone. When the doses of mineral fertilzer was further reduced below 75% the trend of positive effects were no longer convincing or consistent across the estimated parameters. According to the authors, when the doses of mineral fertilizer were reduced to 70% the combined use of both bacteria and AMF seemed mandatory. The results of the study showed the positive effect of biofertilizer but authors recommended furhter estimation of applied in the study microorganisms before they could become a part of the intergraded agricultural management (Adesemoye et al., 2009).

Conclusion

In conclusion, this study revealed notable shifts in soil composition and a favorable impact on soil microbial communities following the application of biofertilizer. The microbial metabolic activity demonstrated the ability of microorganisms to utilize EcoPlate substrates, displaying certain preferences for specific guilds. Although no statistically significant differences were observed among the variants at this stage, the consistent positive effects of the biofertilizer across estimated functional indexes suggest its potential benefits. This observation underscores the need for further research to explore the potential long-term effects and broader applications of biofertilizers in soil management practices.

Acknowledgment

This study, part of the Project 03/23 activities, was financially supported by the Centre for Science research, Technology Transfer and Protection of Intellectual Property of Agricultural University – Plovdiv.

References

Adesemoye, A.O., Torbert, H.A., Kloepper, J.W., 2009. Plant growth-promoting rhizobacteria allow reduced application rates of chemical fertilizers. *Microbial Ecology* 58(4): 921-929.

Alef, K., 1995. Soil respiration. In: Methods in applied soil microbiology and biochemistry. Alef, K., Nannipieri, P. (Eds.). Harcourt Brace & Company, Academic Press, UK, pp. 215-216.

Al-Zubade, A., Phillips, T.D., Williams, M.A., Jacobsen, K.L., Van Sanford, D. 2021. Effect of biofertilizer in organic and conventional systems on growth, yield and baking quality of hard red winter wheat. *Sustainability* 13(24): 13861.

Baldi, E., Gioacchini, P., Montecchio, D., Mocali, S., Antonielli, L., Masoero, G., Toselli, M., 2021. Effect of biofertilizers application on soil biodiversity and litter degradation in a commercial apricot orchard. *Agronomy* 11(6): 1116.

Backer, R., Rokem, J.S., Ilangumaran, G., Lamont, J., Praslickova, D., Ricci, E., Subramanian, S., Smith, D.L., 2018. Plant growth-promoting rhizobacteria: Context, mechanisms of action, and roadmap to commercialization of biostimulants for sustainable agriculture. *Frontiers in Plant Science* 9: 1473.

Bargaz, A., Lyamlouli, K., Chtouki, M., Zeroual, Y., Dhiba, D., 2018. Soil microbial resources for ımproving fertilizers efficiency in an ıntegrated plant nutrient management system. *Frontiers in Microbiology* 9: 1606.

Cai, Y.F., Barber, P., Dell, B., O'Brien, P., Williams, N., Bowen, B., Hardy, G., 2010. Soil bacterial functional diversity is associated with the decline of *Eucalyptus gomphocephala*. *Forest Ecology and Management* 260(6): 1047–1057.

Centeno-Leija, S., Espinosa-Barrera, L., Velazquez-Cruz, B., Cárdenas-Conejo, Y., Virgen-Ortíz, R., Valencia-Cruz, G., Saenz, R.A., Marín-Tovar, Y., Gómez-Manzo, S., Hernández-Ochoa, B., Rocha-Ramirez, L.M., Zataraín-Palacios, R., Osuna-Castro, J.A., López-Munguía, A., Serrano-Posada, H., 2022. Mining for novel cyclomaltodextrin glucanotransferases unravels the carbohydrate metabolism pathway via cyclodextrins in *Thermoanaerobacterales*. *Scientific Reports* 12(1): 730.

Egner, H., Riehm, H., 1955. Die doppellaktatmethode (The double lactate method). In: Die Untersuchung von Böden. VDLUFA (Verbande Deutscher Landwirtschaftlicher Untersuchungs-und Forschungsanstalten), Methodenbuch Band 1. Hermann, T.R., Nuemann, K.E., (Eds.) Verlag, Radebeul and Berlin, Germany.

Ge, Z., Du, H., Gao, Y., Qiu, W., 2018. Analysis on metabolic functions of stored rice microbial communities by BIOLOG ECO microplates. *Frontiers in Microbiology* 9: 1375.

Hou, S., Ren, K., Fan, F., Zhao, M., Zhou, W., Zhou, B., Li, C., 2023. The effects of plant density and nitrogen fertilization on maize yield and soil microbial communities in the black soil region of Northeast China. *Geoderma* 430: 116325.

Huang, H.Y., Zhou, P., Shi, W.W., Liu, Q.L., Wang, N., Feng, H.W., Zhi, Y.E., 2012. Microbial functional diversity in facilities cultivation soils of nitrate accumulation. *Procedia Environmental Sciences* 13: 1037–1044.

Kurniawati, A., Stankovics, P., Hilmi, Y.S., Toth, G., Smol, M., Toth, Z., 2023. Understanding the future of bio-based fertilisers: The EU's policy and implementation. *Sustainable Chemistry for Climate Action* 3: 100033.

Lima, A.B., Cannavan, F.D.S., Germano, M.G., Dini-Andreote, F., Frabchini, J.C., de Paula, A.M., Teixeira, W.G.,Tsai, S.M., 2015. Effects of vegetation and seasonality on bacterial communities in Amazonian dark earth and adjacent soils. *African Journal of Microbiology Research* 9(40): 2119-2134.

Mehnaz, S., 2016. An overview of globally available bioformulations. In: Bioformulations: For sustainable agriculture. Arora, N.K, Mehnaz, S., Balestrini, R. (Eds.). Springer, pp. 267–281.

Ramakrishna, W., Yadav, R., Li, K., 2019. Plant growth promoting bacteria in agriculture: Two sides of a coin. *Applied Soil Ecology* 138: 10-18.

Roesti, D., Gaur, R., Johri, B., Imfeld, G., Sharma, S., Kawaljeet, K., Aragno, M., 2006. Plant growth stage, fertiliser management and bio-inoculation of arbuscular mycorrhizal fungi and plant growth promoting rhizobacteria affect the rhizobacterial community structure in rain-fed wheat fields. *Soil Biology and Biochemistry* 38(5): 1111–1120.

Siswanti, D.U., Riesty, O.S., 2021. Effects of biofertilizer and manure application on growth rate and chlorophyll content of spinach (*Amaranthus tricolor* L.) under salinity stress condition. BIO Web of Conferences. The 1st International Conference of Advanced Veterinary Science and Technologies for Sustainable Development (ICAVESS 2021) 33: 05003.

Sofo, A., Ricciuti P.A., 2019. Standardized method for estimating the functional diversity of soil bacterial community by Biolog® EcoPlates™ assay - the case study of a sustainable olive orchard. *Applied Sciences* 9(19): 4035.

Stefanowicz, A., 2006. The Biolog plates technique as a tool in ecological studies of microbial communities. *Polish Journal of Environmental Studies* 15(5): 669-676.

Vessey, J.K., 2003. Plant growth promoting rhizobacteria as biofertilizers. *Plant and Soil* 255: 571–586.

Wang, J., Liu, L., Gao, X., Hao, J., Wang, M., 2021. Elucidating the effect of biofertilizers on bacterial diversity in maize rhizosphere soil. *PLoS One* 16(4): e0249834.

Xiao, X., Zhu, Y., Gao, C., Zhang, Y., Gao, Y., Zhao, Y., 2022. Microbial inoculations improved rice yields by altering the presence of soil rare bacteria. *Microbiological Research* 254: 126910.

Eurasian Journal of Soil Science 2024, 13(3), 210 - 223

Eurasian Journal of Soil Science

Journal homepage : http://ejss.fesss.org

Nomograph development for water erosion quantification in Wadi Cheliff's catchment, Northern Algeria

Ilhem Bouaichi *, Bénina Touaibia

Mobilization and Valorization of Water Resources Laboratory (MVRE), National Higher School for Hydraulics (ENSH), Soumaa road 29, Blida, Algeria

Article Info

Received : 18.09.2023
Accepted : 15.03.2024
Available online: 19.03.2024

Author(s)

I.Bouaichi *
B.Touaibia

* Corresponding author

Abstract

Water erosion study is regarded as one of the most important axes in scientific researches. The erosive effect of water on the surface layers can have major consequences on soil loss and land degradation. The objective of our work was the development of a water erosion nomograph that represents a practical and precise tool that is adapted to local conditions for a direct quantification of erosive action in the absence of basic data. Regarding the magnitude of the phenomenon in Algeria, the catchment of Wadi Cheliff was taken as an experimental site where a significant spatio-temporal variability of liquid and solid flows was observed and the measurement network in different locations was either dispersed or non-existent. The developed methodological approach permitted the identification of 149 experimental sites (20 hydrometric stations, 15 large dams and 114 hill dams) where existing data allowed the erosion quantification. A flow coefficient variography was performed in addition to a principal component analysis (PCA), leading to the identification of three distinct groups. Moreover, the modeling of the studied variable was achieved through the application of multivariate analysis to the third group of 100 observations. Applying the principles of nomography on the final model, a nomograph of the semi-arid area of Wadi Cheliff catchment was realized for surfaces ranging from 500 to 25 000 ha. This nomograph enabled the direct quantification of water erosion from the product ($Es_1 \times Es_2$), taking into account the area of the catchment, its average slope and its flow coefficient with a mean absolute percentage error (MAPE) of 2%.

Keywords: Multivariate analysis, nomograph, PCA, variography, Wadi Cheliff, water erosion.

© 2024 Federation of Eurasian Soil Science Societies. All rights reserved

Introduction

The frequent presence of excessive suspended sediment in streams is a relevant indicator of water erosion problems within a catchment. In order to assess the extent of these problems and understand their consequences, it is crucial to measure the sedimentation rates reaching the outlet. From the perspective of sustainable management and preservation of natural water and soil resources at the catchment, it becomes essential to quantify water erosion accurately, which allows the identification of areas likely to produce high levels of sediment.

In North Africa, erosive action is a significant threat. The majority of catchments in Algeria, Tunisia and Morocco are characterized by a strong degradation, exceeding 20 T ha^{-1} per year (Remini and Remini, 2003).

The erosion rate quantification is a complex and challenging task in practice due to the various factors contributing to its increase (Megnounif et al., 2007; Ochoa et al., 2016; Dengiz and Demirkaya, 2022; Najafova, 2022). This task becomes particularly difficult in practice especially when watersheds are not gauged with the absence of a well-established monitoring network that provides the basic data, so it gets challenging to measure spatial-temporal variability of erosion processes. Without these data, it is also difficult to establish references for comparing changes over time. Indeed, the lack of these essential elements significantly complicates the direct quantification; thus, the use of other methods is essential for a precise measurement of

: https://doi.org/10.18393/ejss.1455407
: http://ejss.fesss.org/10.18393/ejss.1455407
Publisher : Federation of Eurasian Soil Science Societies
e-ISSN : 2147-4249

the water erosive action on the soil. Among the most widely used methods today, Digital Terrain Model and Geographic Information System, remote sensing space, models based on physical processes of soil particle detachment, geophysical techniques and hydrological models. Various erosion modelling studies, including Touaibia et al. (2001), López-Tarazón et al. (2010), Eisazadeh et al. (2012), Meddi et al. (2014) and Heng and Suestugi (2015), have contributed to the understanding of the erosive process rate, despite the absence of data.

Nowadays, although numerical and computational methods have become predominant in hydrology, nomography remains an interesting technique for understanding the relationships between different variables and performing rapid calculations. The earliest nomographs originated in the late 19th and early 20th centuries, and they are still very useful. However, the advent of nomographic science and its use on hydrological modeling remains poorly employed today. In the 1840s, there was an emergence of articles discussing the effect of deformation on graphic representations known as nomographs, in order to enhance their readability. Over the following decades, documents on analytical criteria for graphical representation were produced. The initial documentation by d'Ocagne in 1884, detailing various types of nomographs, serves as a reference point, as mentioned by Jahnke (2012).

When performing intricate numerical calculations, it is beneficial to utilize a nomograph. This graphic representation is depicted through lines or fixed points with appropriately marked scales, whether mobile or not. According to Tournès (2000), a simple reading provides the intended value based on the parameters. Additionally, their adaptability and flexibility to a wide range of situations support their utilization (Tran Van, 1961). Thus, nomographs or abacus represent graphic tables playing the same role as numerical tables. They are often based on empirical equations that were developed from field observations and experimental data.

In this context, the objective of our work was the application of nomography which represents a discipline less frequently used nowadays, and its association with new computational methods such as numerical modeling, variograph and statistical methods for quantifying the complex phenomenon of water erosion of a watershed. Indeed, only the nomograph of Wischmeier and Smith developed in 1960 and updated in 1978, provides a graphical representation of the universal soil loss equation that allows users to directly read the estimated values of the various parameters of the equation for the quantification of the erosive rate.

The Wadi Cheliff catchment is considered as a study area given its large territory and the weakness of its measurement network. With the absence of hydrometric stations and their concentration in the north of the basin, it is crucial to identify every structure that is susceptible to silting. Hence, 149 sites were listed with 20 hydrometric stations measuring liquid and solid flows, as well as 15 large dams and 114 hill dams contributing to the calculation of the erosion rate from their siltation rate. This identification permitted the establishment of a particular methodology for the development of an erosion nomograph that links it to the basin's flow coefficient as well as its morphometric coefficients (slope and surface). The methodology that was adopted included the following:

- Identification of 149 experimental sites throughout the basin,
- Quantification of specific erosion at site watershed level,
- Determination of the different influencing factors, namely the surface area of each site, its drainage density, its average slope, its vegetation cover and its flow coefficient. This last parameter was variographed,
- PCA application for the identification of homogeneous areas,
- Search for a regressive model via multivariate analysis,
- Trace and validate the nomograph using a programming algorithm.

Material and Methods

Presentation of the study area

The Wadi Cheliff's catchment, with its main stream extending 759 km and draining an area of 4 375 000 ha at its mouth, is an important Wadi in North Africa due to its annual water supply. It plays a major role in the hydrographic system of Algeria since it is the only river that drains part of the highlands to cross the Cheliff valley and join at its outlet the Mediterranean Sea near Mostaganem. It owes its character to the deep structure of the landscapes it crosses.

The study area extends between longitudes 0° 7' and 3° 31' East and between latitudes 33° 53' and 36° 26' North. It is bordered to the North by the coastal catchments of Algiers and Oran, to the East by the catchments of Isser, Hodna, Zahrez, and the high plateaus of Constantine, to the West by the basins of Macta and the high

plateaus of Oran, in addition to the Saharan Atlas to the South (Figure 1a). It is divided into two distinct regions:

- The upstream part of the Cheliff with an area of 2 050 000 ha, limited to the south by the mountains of Jebel Amour and to the north by the Ouarsenis mountains;
- The downstream part of the Cheliff, which covers an area of 2 325 000 ha, bounded to the south by the mountain ranges of Tiaret, Saida and Ouarsenis, and by the Dahra and Beni Menacer to the north.

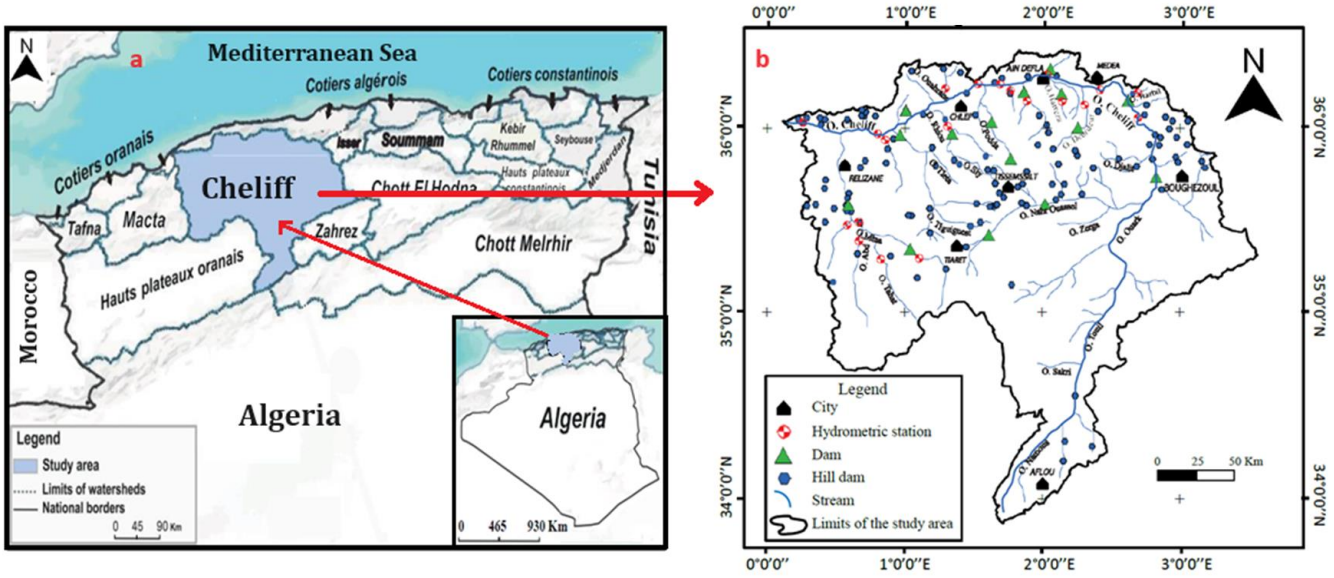

Figure 1. Catchment of Wadi Cheliff and its network measures
(a: Location of the study area; b: Location of experimental sites in the study area)

Its altitudes range from 0 to 1983 m. Almost all of its soils are alluvial, consisting mainly of fine components derived from marls or clays, making soils more vulnerable to erosion (Bouchelkia and Remini, 2003).

Additionally, its climate is semi-arid Mediterranean characterized by irregular spatio-temporal rainfall patterns. Furthermore, the average annual precipitation is 357 mm, it oscillates between values less than 150 mm in the South and values close to 700 mm in the Northeast sector. While the average annual temperature for the entire basin is estimated at 19.2°C. The surface runoff obviously undergoes the influence of the marine rain regime which is characterized by the succession of a rainy and cold season with considerable floods and a very marked dry and hot summer season with a non-significant flow, thus the average annual runoff varies from 3% to 35% at the outlet of the basin.

Moreover, the measurement network identified for our study includes 149 experimental sites that were distributed homogeneously as follow: 20 hydrometric stations, 15 large dams and 114 hill dams, in order to cover the entire study area (Figure 1b).

Database

The used data for water erosion quantification are gathered from the National Agency of Water Resources for hydrometric stations (13 to 56 years of operation), from the National Agency of Dams and Transfers for dams, and from the Agency of Hydrographic Basin Cheliff-Zahrez for hill dams. They are presented under shape:

For data from hydrometric stations, the files include:

- Instantaneous liquid flows Ql ($m^3\ s^{-1}$).
- Instantaneous concentrations C ($g\ L^{-1}$).
- Instantaneous solid flows Qs ($kg\ s^{-1}$).
- Average daily flows Qad ($m^3\ s^{-1}$).

For dams and hill reservoirs, the files gather:

- Bathymetric surveys of the dams.
- Data of dams releases: date, inputs, total consumption (drinking water supply, irrigation, other), distributaries (leakage, bottom outlet, discharge, desludging and evaporation), available water volume and so the filling rate.
- Identification of hill reservoirs: code, name, structure nature, geographic coordinates (X, Y and Z), Wadi, catchment surface, year into service, initial capacity, destination, actual state and operational duration.

Quantification approach of the specific erosion

At hydrometric station level

Building on the scientific work of Touaibia et al. (2001), Ammari (2012) and Kheniche et al. (2019), our approach is based on homogenisation and data extension via a functional relationship of solid flow – liquid flow. Regressive models requested are of type: linear, logarithmic, power, exponential and polynomial. The monthly-scale scatter diagram identified the power-like regressive pattern as follows:

$$Q_s = a \times Q_l^b \quad (1)$$

With: Qs : solid flow (kg s^{-1}); Ql : liquid flow (m^3 s^{-1}); a , b : coefficients.

The explained variance by determination coefficient is satisfactory. This latter represents 57% to 87% of the total variance.

Relationship (1) allowed quantifying the solid transport Qs in suspension at daily, monthly and annual scales on the whole observation period (Bouchelkia and Remini, 2003; Bouanani, 2004; Lee and Kang, 2014).

For thrust, works of Mokhtari (2005), Larfi and Remini (2006) and Elahcène (2013) estimated it to 19%, 32% and 11% respectively for some similar basins. An average of 20% is retained; it is supported by works of Touaibia (2000) on tributaries of the considered basin (O.Mina).

The release of dams contributed to the erosive phenomenon. On the 20 hydrometric stations, 10 among them are located below the 15 considered dams. These releases contribute from 2% to 70% to the annual sediments inputs, which varies from one station to another according to the dams' number located upstream and their activity state. On average, we estimate that 40% of the annual sediments quantities are transited or deposited only for tributary stations of the dams.

The annual values of the specific erosion (Es) vary considerably passing from 2.64 to 13.91 T ha^{-1}, corresponding to areas of 253 700 ha and 47 000 ha, respectively. The surface effect is to be taken into consideration because its influence is direct on the quantification of Es.

At dam's level

The quantification of Qs (sediment and thrust) was carried out at the level of 15 catchment dams from the latest bathymetric campaigns carried out between 2018 and 2019.

The Boughezoul dam records the lowest annual soil loss, i.e. Es = 0.26 T ha^{-1}, for an estimated annual siltation volume of 0.489 Mm^3 and corresponding to a surface of 1 873 000 ha. Likewise, for the Deurdeur dam, which loses annually a volume of 0.470 Mm^3 of its storage capacity, Es is estimated to 10.05 T ha-1 for a surface of 46 800 ha. This reflects directly the surface effect on quantification of the phenomenon under study.

The dam's watershed of Wadi Fodda presents the maximum annual degradation of soil of about 48.28 T ha^{-1}. This corresponds to an annual silting volume and to a surface estimated, respectively, to 1.738 Mm^3 and 36 000 ha. Otherwise, for the Gargar's dam, which receives in its basin an annual mud volume that is 3 times upper than its previous volume, i.e. 5.717 Mm^3, Es is equal to 23.92 T ha^{-1} for a surface of 239 000 ha. This confirms the surface effect which intervenes once again on the Es values.

At hill dam's level

Hillside reservoirs mobilize surface water structures intended for irrigation. With 114 structures, they make up over 75% of the monitoring network. Their representative spatial distribution of the watershed allowed scanning the whole study area. Knowing capacity storage, surface of their watershed and their expected lifetime, Es is calculated directly (Abdellaoui et al., 2002).

Specific erosion multivariate analysis

Identification of explanatory variables

According to Touaibia and Achite (2003), Zhou et al. (2008), Bouchnak et al. (2009) and Shen et al. (2016), five explanatory variables are selected for multivariate analysis, it is about:

- Surface of the catchment (S ; ha): It has a direct effect and it is inversely proportional to the specific erosion. As for 149 sites, surface varies from 480 ha to 1 873 000 ha, with a variation coefficient (Cv) of 3.55.
- Draining density (Dd ; km km^{-2}): It is the ratio of the length sum of a catchment's water courses on its surface. Its values vary from 0.40 to 1.87 km km^{-2}, with a Cv of 0.36.
- Average slope of the catchment (P ; %): Expressed in %, it allows determination and classification of the relief. Its increase proportionally causes that of water erosion (El Kateb et al., 2013). Slope is determined from the Digital Elevation Model (DEM) with a resolution of 30 m, downloaded from ASTER GDEM. Average values vary from 4.15% to 21.48%.

- Flow coefficient (Cf ; %): It is the ratio between the average death of runoff and the effective rainfall. Used database includes 50 measurements, where Cf is calculated based on hydrometric and rainfall data. Study of variography and its interpolation by Krigeage method have identified the spherical model, for representation of Cf variography (Figure 3c). Its function γ(h) is given by the following formula (2). Values of Cf vary from 2.2% to 35%.

$$\gamma(h) = 54 + 25\left[\frac{3}{2}\left(\frac{h}{41.5}\right) - \frac{1}{2}\left(\frac{h}{41.5}\right)^3\right] \quad (2)$$

- Vegetation cover rate (Cveg ; %):

It is considered as one of the variables playing an important role against water erosion (Rey et al. 2004). Its determination required collection of 12 land use maps of the wilayas covering the study area, obtained from National Institute of Soil, Irrigation and Drainage. These maps were assembled in order to produce the land use map of the Wadi Cheliff's catchment. The resulting map demonstrated that the vegetation cover rate of the 149 sites varies from 1.03% to 88.24%.

On Figure 2, an organizational chart is developed explaining different determination phases of explanatory variables corresponding to different measure sites. The resulting maps are illustrated in Figure 3.

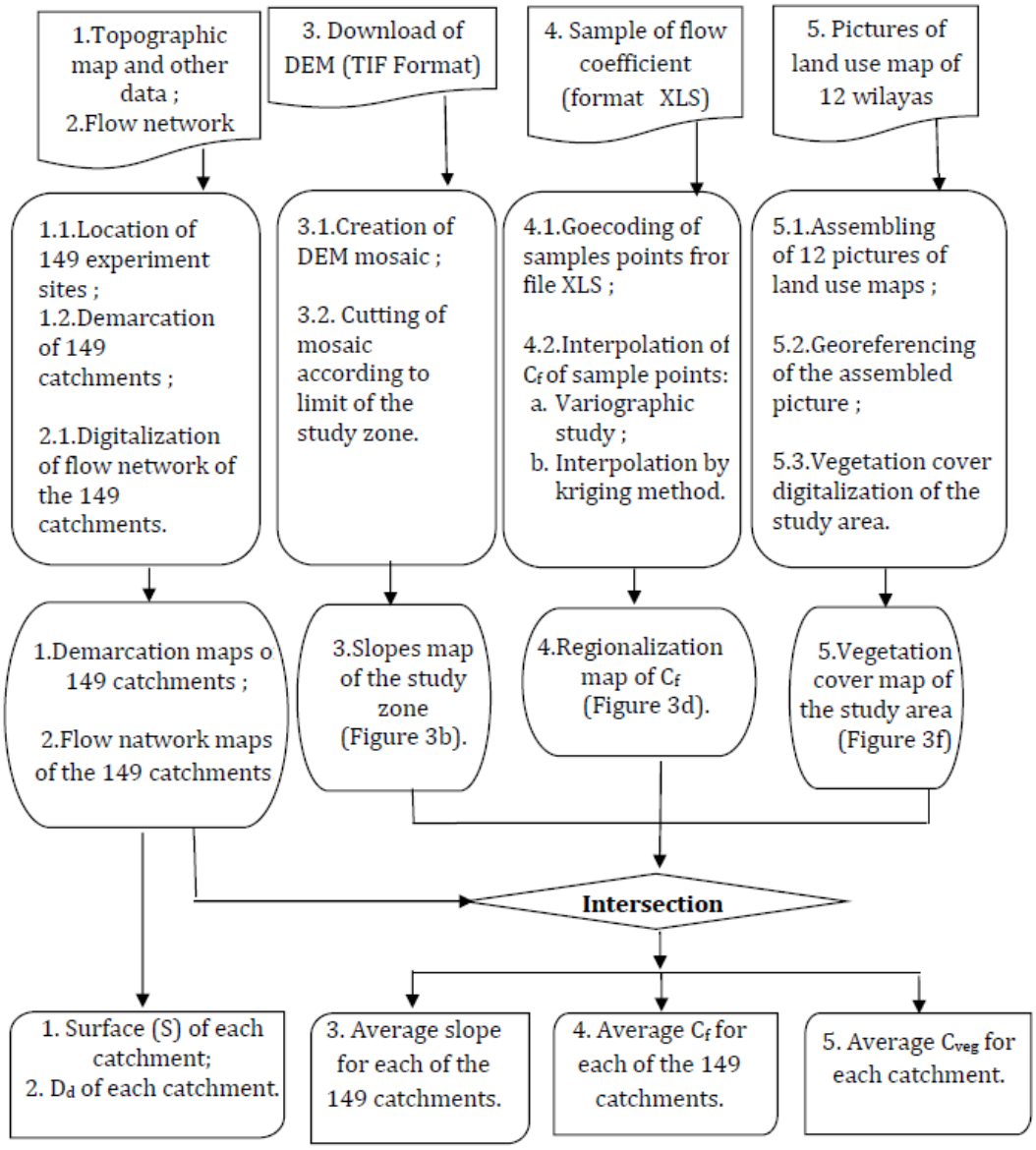

Figure 2. Organizational chart adopted for determination of explanatory variables.

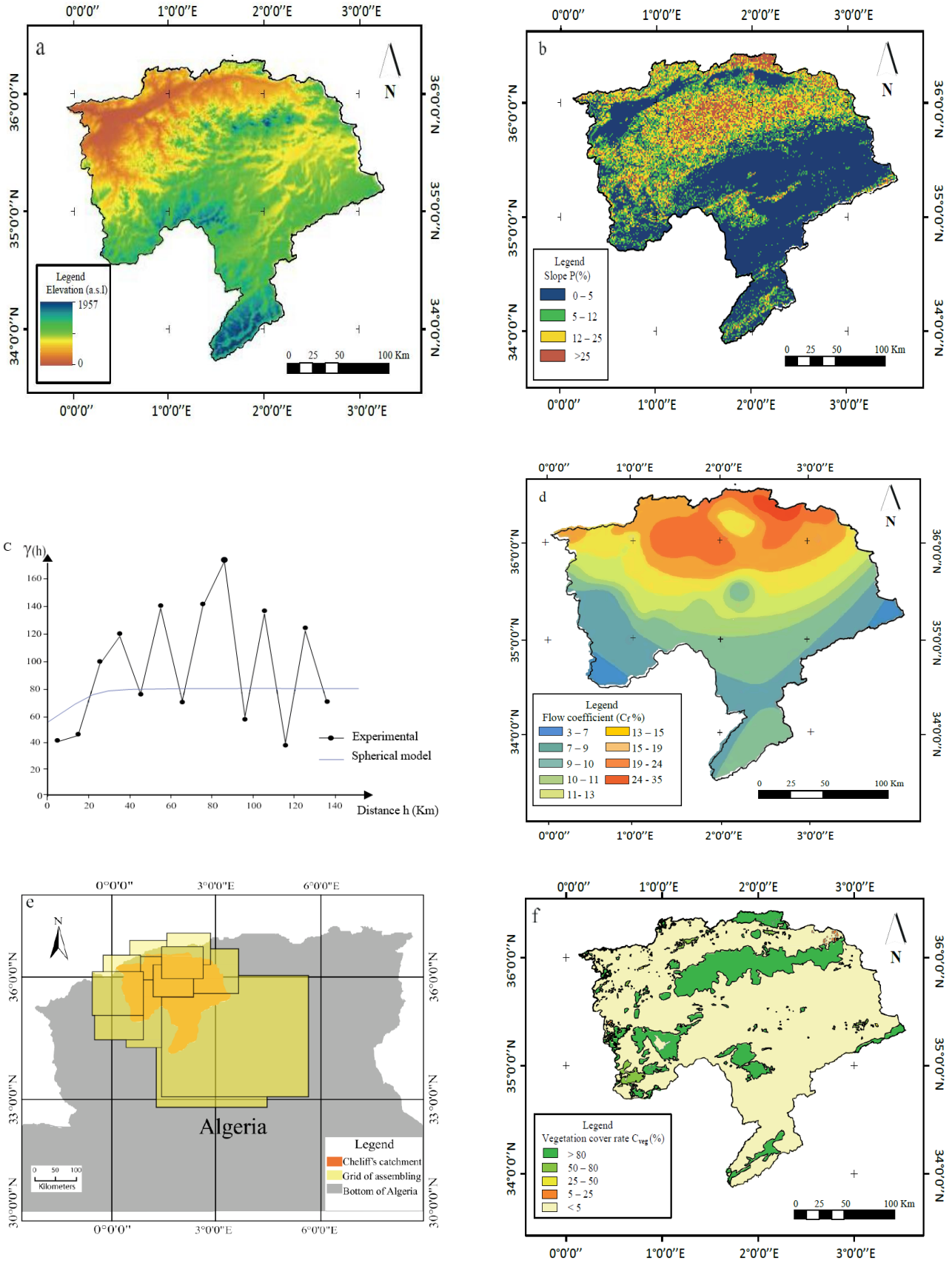

Figure 3. Determination maps of explanatory variables of Wadi Cheliff's catchment
(a: Digital Elevation Model (DEM), b: Slopes map, c: Variogram of flow coefficient, d: Flow coefficient regionalization, e: Basin map for assembly of 12 wilayas, f: Vegetation cover rate)

Principal Components Analysis (PCA)

It is considered as being a very powerful method to explore structure of a high number "P" of quantitative data by observed element (Hotelling, 1933). PCA is applied on a matrix of 149 lines and 6 columns. Two cases are taken into consideration; with and without varimax rotation of orthogonal axes. Correlation matrix (Table 1) shows that between Es and explanatory variables Dd, P and Cf, the relationships are the most significant at the tolerance level of 5% with correlation coefficients estimated respectively at 0.66, 0.70 and 0.73.

Sites assembly allowed identification of the factorial axes responsible of spatial distribution. This underlines heterogeneities between groups and deduces variables that best characterize each group. Percentages of cumulative variances show that the three first components C1, C2 and C3, explaining 85.21% of the total data, are retained. Contributions of projected variables after varimax rotation (Table 1) show dominance of S on axe C3 and of Cveg on axe C2 (Figure 4e) where 37.35% of inertia is cumulated.

Projection of individuals on axes C2-C3 (Figure 4f), makes three distinct groups:

- The first group of 23 individuals is characterized by surfaces relatively large associated to weak values of Es and inversely. It highlights the direct effect of the surface on its qualification according to its magnitude order.
- The second group, where 22 individuals are gathered, is characterized by very dense Cveg rates to which correspond relatively important Es values.
- As for the third group, which gather 104 individuals, it is characterized by a positive proportionality, on the first hand, between Es and variables Dd, P and Cf, and on other hand, negative proportionality between Es and variables S and Cveg. This group avoids influence of the surface and rate of vegetation cover on the specific erosion estimate. It will be subject of a multivariate analysis.

Table 1. Correlation matrix of PCA and variables contribution according to the axes

Variables	Correlation matrix before PCA						Contribution of the variables according to the axes C_1, C_2 and C_3 (%)		
	Es	S	D_d	P	C_f	C_{veg}	C_1	C_2	C_3
Es	1						27.18	4.46	0.32
S	-0.17	1					0.46	0.00	95.85
D_d	0.66	-0.15	1				15.87	18.97	0.26
P	0.70	-0.24	0.41	1			27.63	3.71	2.24
C_f	0.73	-0.21	0.52	0.82	1		28.84	0.02	1.33
C_{veg}	-0.17	-0.01	-0.27	0.13	-0.03	1	0.01	72.83	0.00

Multivariate analysis: application of multiple regressions

1st case: 3rd group (104 values)

Research of a functional relationship between the studied variable and explanatory variables is done by stepwise regression, allowing to eliminate each time the less correlated variation based on correlation coefficient (r) for error P = 5% (Dagnelie, 1992). The non-linearity of the studied relationship duly demonstrated (Borges, 1993; Achite and Meddi, 2005). Its application highlights the matrix of variables correlation (Table 2). The correlation coefficients are clearly improved between Es and variables S and Cveg going from -0.17 to -0.87 and from -0.17 to -0.53, respectively. The resulting regression models show that the regression fit lies between Es and all other variables, with R^2 at its highest value of 0.83 (Table 2). The adjustment of the predicted values by the selected model compared to the measured values presents four observations outside the confidence intervals fixed at 95%. Application of Kolmogorov-Smirnov's test becomes indispensable to make up mind whether these observations are to be taken into account or not.

Results display D statistic test which represents the highest difference between the two cumulated frequency curves of the two samples, and thus the p-value (to be compared to the meaning threshold, *P, generally fixed at 5%). This latter is the probability to have the same values under the hypothesis Ho (null hypothesis that two samples come from the same distribution), otherwise an alternative hypothesis H1 (that these same samples come from distribution having different apportionments). With D = 1 and p-value = 2.86% (which is inferior to *P), the Ho hypothesis is rejected in favour of the alternative H1 hypothesis. Measured values are very different from those predicted. These four comments are to be excluded from the series, with a size of 100 measurements, and the regression restudied.

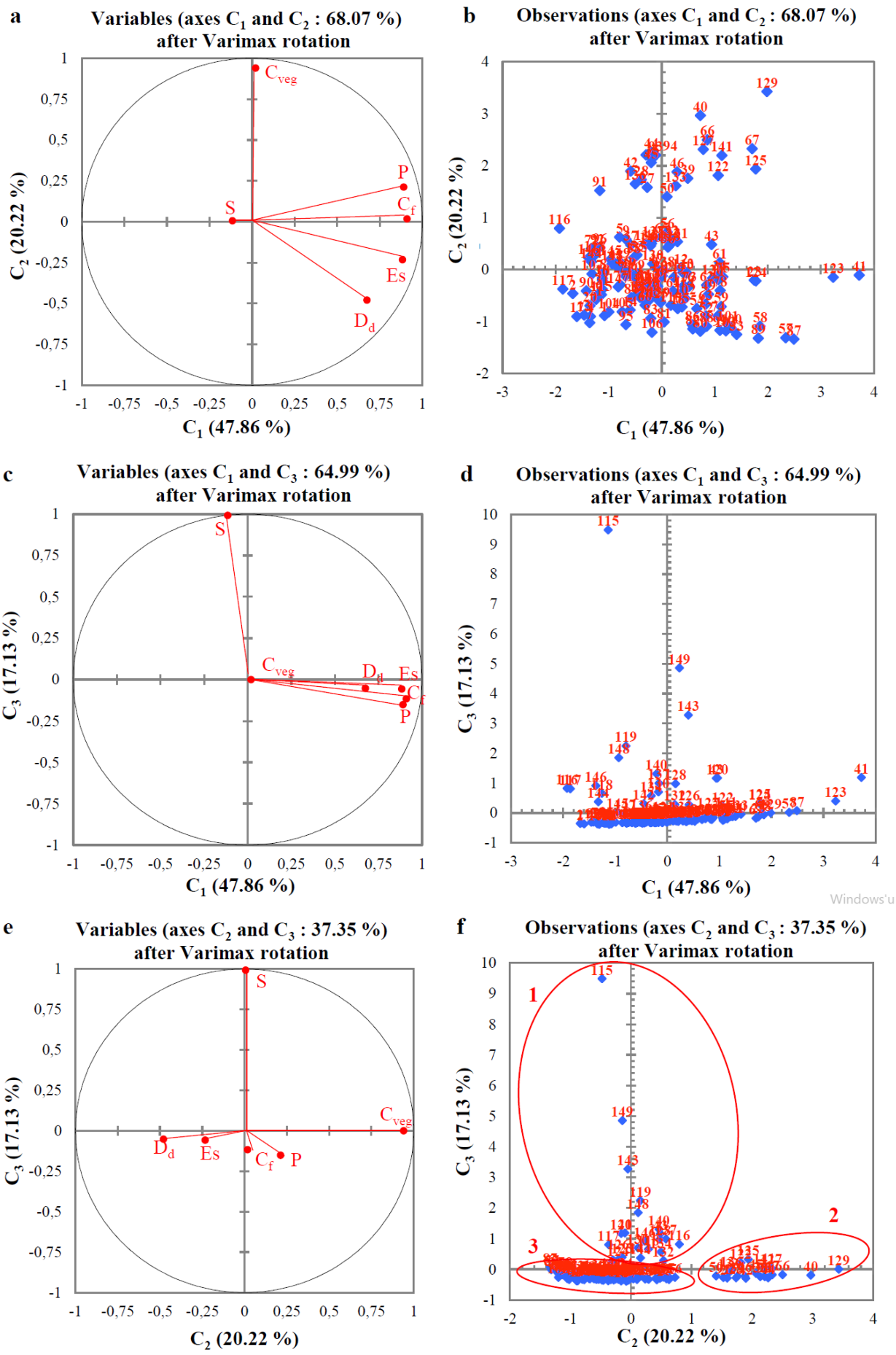

Figure 4. Correlation circles and projection of individuals on different axes

Table 2. Correlation matrix of multivariate analysis and regressive models (3rd group, 1st case).

Correlation matrix (1st case)						
Variables	Es	S	D_d	P	C_f	C_{veg}
Es	1					
S	-0.87	1				
D_d	0.66	-0.63	1			
P	0.84	-0.81	0.47	1		
C_f	0.82	-0.77	0.49	0.85	1	
C_{veg}	-0.53	0.58	-0.40	-0.35	-0.42	1
Regressive models (1st case)						
Variables	R^2	Models				
5 (S, D_d, P, C_f, C_{veg})	0.83	$Es = 2.85 \times S^{-0.132} \times D_d^{0.265} \times P^{0.493} \times C_f^{0.29} \times C_{veg}^{-0.037}$				
4 (S, D_d, P, C_f)	0.82	$Es = 3.23 \times S^{-0.16} \times D_d^{0.27} \times P^{0.164} \times C_f^{0.316}$				
3 (S, P, C_f)	0.80	$Es = 3.98 \times S^{-0.215} \times P^{0.362} \times C_f^{0.348}$				
2 (S, P)	0.79	$Es = 5.29 \times S^{-0.238} \times P^{0.661}$				
1 (S)	0.74	$Es = 41.35 \times S^{-0.368}$				

2nd Case: 3rd truncated group (100 values)

The correlation matrix (Table 3) shows clearly a general improvement of its corresponding coefficients. The obtained related models demonstrate that Es regression with five, four and three variables is constant in the sense that R^2 is too (R^2 = 0.97). The model with three variables is retained for nomograph development; it is formulated according to expression 3.

$$Es\ (T\ ha-1\ per\ year) = 16.68 \times S^{-0.375} \times P^{0.164} \times C_f^{0.204} \quad (3)$$

Table 3. Correlation matrix of multivariate analysis and regressive models (3rd group, 2nd case)

Correlation matrix (2nd case)						
Variables	Es	S	D_d	P	C_f	C_{veg}
Es	1					
S	-0.97	1				
D_d	0.66	-0.68	1			
P	0.88	-0.83	0.48	1		
C_f	0.86	-0.80	0.50	0.85	1	
C_{veg}	-0.55	0.57	-0.40	-0.32	-0.40	1
Regressive models (2nd case)						
Variables	R^2	Models				
5 (S, D_d, P, C_f, C_{veg})	0.97	$Es = 15.8 \times S^{-0.365} \times D_d^{0.015} \times P^{0.181} \times C_f^{0.191} \times C_{veg}^{-0.005}$				
4 (S, D_d, P, C_f)	0.97	$Es = 16.3 \times S^{-0.37} \times D_d^{0.014} \times P^{0.169} \times C_f^{0.193}$				
3 (S, P, C_f)	0.97	$Es = 16.68 \times S^{-0.375} \times P^{0.164} \times C_f^{0.204}$				
2 (S, P)	0.96	$Es = 21.1 \times S^{-0.394} \times P^{0.309}$				
1 (S)	0.95	$Es = 56.21 \times S^{-0.461}$				

Statistical analysis

The quality and reliability of the traced nomograph depend on the values of the calculated precision indices, it is often recommended to utilize a combination of these indices in order to obtain an accurate and complete evaluation of the numerical or graphic representation for quantifying water erosion. According to Isik (2013), Felegari et al. (2014) and Shirzadi et al. (2022), we chose the following indices: Mean Absolute Percentage Error (MAPE), Mean Square Deviation (MSD), Willmott Index (d), Coefficient of Determination (R^2) and the NASH criterion (NS), where each index contributed to decision-making regarding the validation and utilization of the developed graphical tool.

- MAPE is calculated according to the expression 4 based on deviations in absolute value between observations' measurements and those predicted compared to the measured values. It is expressed in %. A model representing perfectly the measured data will present a MAPE that is equal to 0.

$$MAPE = \sum_{i=1}^{N} \frac{\left|Es_{mes(i)} - Es_{pred(i)}\right|}{Es_{mes(i)}} \times \frac{100}{N};\ \left(MAPE \in [0, +\infty[\right) \quad (4)$$

With: Esmes represents the specific measured erosion; Espred is the specific predicted erosion by the nomograph and N is the observations' number.

- ASD, given by expression 5, is the value to be minimised for a prediction of values close to 0; the nomograph is considered as perfect.

$$ASD = \frac{\sum_{i=1}^{N}\left(Es_{pred(i)} - Es_{mes(i)}\right)^2}{N};\ \left(ASD \in [0, +\infty[\right) \quad (5)$$

- Index d, according to formula 6, measures the degree where predictions are exempt of errors. d varies between 0 and 1 where a value close to 1 indicates a perfect agreement between measured and predicted observations, while for a value close to 0, the prediction is in complete disagreement (Willmott, 1981).

$$d = 1 - \frac{\sum_{i=1}^{N}\left(P_i - O_i\right)^2}{\sum_{i=1}^{N}\left[\left|\left(P_i - \bar{O}\right)\right| + \left|\left(O_i - \bar{O}\right)\right|\right]^2};\left(0 \le d \le 1\right) \quad (6)$$

With: P(i) represents predicted values, O(i) and $\bar{O}$ are respectively values and average of measured observations.

- R2, determined by formula 7, measures prediction quality and ad adequacy between measured and predicted values by abacus, as it approaches to 1 and more abacus explains better the distribution of measured points.

$$R^2 = \frac{\sum_{i=1}^{N}\left(\left(Es_{pred(i)} - \overline{Es_{pred}}\right) \times \left(Es_{mes(i)} - \overline{Es_{mes}}\right)\right)}{\sqrt{\sum_{i=1}^{N}\left(Es_{pred(i)} - \overline{Es_{pred}}\right)^2} \times \sqrt{\sum_{i=1}^{N}\left(Es_{mes(i)} - \overline{Es_{mes}}\right)^2}};\left(0 \le R^2 \le 1\right) \quad (7)$$

- NS was defined in 1969 by Nash and improved in 1970 by Nash and Sutcliffe. It allows evaluating improvement brought by the used model compared to the reference model, generally average estimator. If Nash = 1, the abacus perfectly represents the data. When it is less than 0, this latter is a less-good estimator of measured data than their average, it is given by expression 8.

$$NS = 1 - \frac{\sum_{i=1}^{N}\left(Es_{mes(i)} - Es_{pred(i)}\right)^2}{\sum_{i=1}^{N}\left(Es_{mes(i)} - \overline{Es_{mes}}\right)^2};\left(NS \in]-\infty, 1]\right) \quad (8)$$

Results and Discussion

Nomograph elaboration

At the end of this work, a nomograph (or abacus) is established. The layout of this latter is based on abacus theory which corresponds to the graphic representation listed by mathematical laws defined by equations to any variable number (D'ocagne, 1899). Today, this discipline is designated under the name of "Nomography". It is natural to think that it is not possible in practice to nomograph with reasonable manner an equation of more than three variables while remaining in the two-dimensional plane (Pirio, 2010).

In our case, it is about an equation with four variables (Es, S, Cf and P) to be represented in a plane axis system. A transformation of equation (3) by separating it into two auxiliary functions easily nomografiable on the plan (Es1 and Es2 with three variables each) is indispensable, with:

$$Es_1 = f(S, C_f) = 4.084 \times S^{-0.375} \times C_f^{0.102} \quad (9)$$

$$Es_2 = f(P, C_f) = 4.084 \times P^{0.164} \times C_f^{0.102} \quad (10)$$

$$Es = Es_1 \times Es_2 \quad (11)$$

The developed nomograph is illustrated in Figure 5.

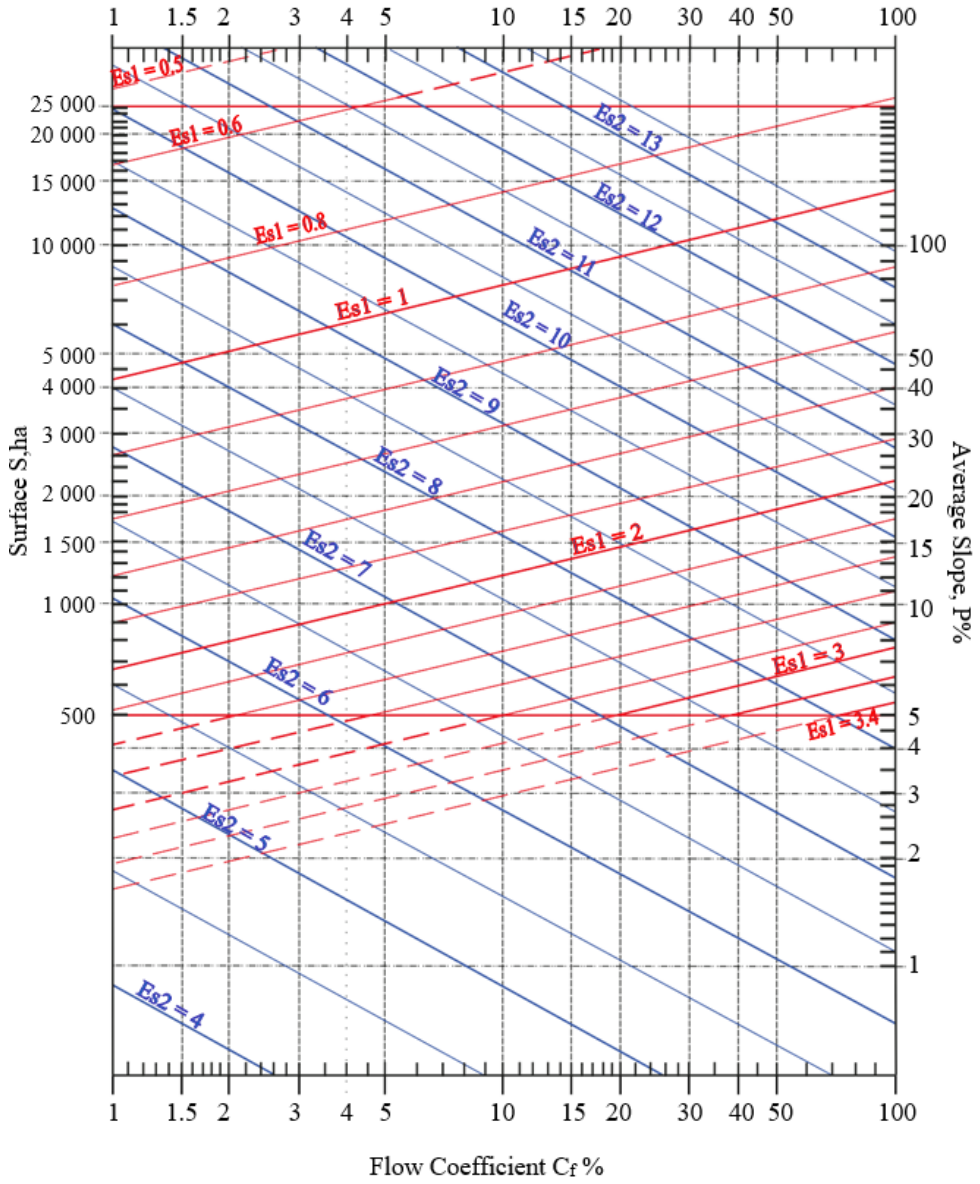

Figure 5. Nomograph of the specific erosion according to surface, average slope and flow coefficient for the Wadi Cheliff catchment

Nomograph validation

This validation step is a systematic process by which the reliability and accuracy of the developed nomograph was evaluated. Based on the 3rd group data resulting from the PCA for the plot, only 03 hydrometric stations and 97 hill dams out of a total of 20 and 114 structures were respectively selected, while all the 15 experimental sites of the dams were eliminated. Further, 20 sites of the remaining 100 were token as an example (Table 4) where we mentioned 03 different results, the 1st quantification of water erosion was based on experimental data, the second is performed since the multivariate analysis of the erosive action in relation to the involved factors, whereas the third was realized from the traced nomograph, which contributes to the determination of Es by knowing the Es1 and Es2 quantities calculated respectively by simple interpolation from the following couples of characteristics (S, Cf) and (P, Cf) of the corresponding catchment. However, this step must be accompanied by the calculation of the precision indices (Table 5) for a decision on the final result validation.

Table 4. Validation of Es (T ha^{-1} per year) results from nomographic quantification

Experimantal sites	Catchment caracteristics			Es_{exp}	Es_{ma}	$Es_{nmgrph} = Es_1 \times Es_2$		
	S (ha)	P (%)	C_f (%)			Es	E	Es_{nmgrph}
Hydrometric Station	16 300	13.12	21.52	7.34	6.83	0.82	8.39	6.88
	10 600	9.44	15.32	7.52	7.12	0.93	7.72	7.18
	12 550	11.39	17.06	7.53	7.04	0.89	8.00	7.12
Hill dams	20 540	6.81	5.02	4.64	4.24	0.65	6.50	4.23
	2 700	14.03	17.74	12.82	13.06	1.56	8.35	13.03
	2 585	12.66	16.05	13.09	12.80	1.60	8.06	12.90
	16 890	5.52	9.00	4.71	4.94	0.74	6.72	4.96
	632	17.88	22.26	23.73	24.47	2.70	8.96	24.19
	3 141	10.53	16.26	12.04	11.57	1.47	7.88	11.58
	1 166	13.26	16.61	17.89	17.50	2.17	8.18	17.75
	617	16.71	22.08	24.21	24.38	2.76	8.85	24.43
	24 980	6.55	9.70	4.05	4.45	0.65	6.90	4.46
	6 619	8.95	11.93	8.23	8.02	1.09	7.42	8.10
	4 453	10.95	13.58	9.52	9.87	1.27	7.77	9.87
	502	14.24	25.55	27.16	26.40	3.03	8.78	26.60
	21 150	5.85	8.68	4.79	4.55	0.68	6.73	4.58
	10 310	7.03	9.53	5.95	6.25	0.87	7.10	6.19
	767	13.81	19.55	21.12	21.27	2.53	8.38	21.23
	8 328	8.64	8.13	6.75	6.79	0.95	7.15	6.76
	4 787	10.48	15.66	9.40	9.80	1.25	7.82	9.78

E_{Sexp}: Specific erosion from experimental data; E_{Sma}: Specific erosion from multivariate analysis; $E_{Snmgrph}$: Specific erosion from the developed nomograph.

The experimental results of specific erosion vary from 27.16 to 4.05 (T ha^{-1} per year) for respective areas from 502 to 24 980 ha, these same values were estimated by the nomograph at 26.60 and 4.46 (T ha^{-1} per year). On the one hand, we noted that all sites with catchment area > 25 000 ha were previously eliminated by the PCA, including some hydrometric stations and hill dams, but also all dams in the study area due to the impact of these structures on rivers and their downstream flow regimes (Assani et al., 2007; Yang et al., 2011). Thus, the influence of the watershed surface for the determination of the erosive action rate is decisive as well as the choice of sites because it plays a determining role in the regulation of precipitation concentration, the distribution of flows and therefore in the modulation of specific erosion. Moreover, because of elevated rates of sedimentation that do not adequately reflect actual quantities, places with catchment areas smaller than 500 ha were excluded. Therefore, the surface effect for our study was not significant regarding values between 500 and 25 000 ha in the Wadi Cheliff catchment.

In consideration of the precision indicators (Table 5) established for a 100 values samples distributed homogeneously over the entire study area, we found that the prediction of the values measured from the nomograph was very satisfactory. Furthermore, a low percentage of MAPE of 2% suggests that the graph estimated and the experimental values are matching and with more accuracy. Similarly, an excellent compatibility between the experimental observations and their predictions was indicated with values of R^2, d and NS equal to 0.99, which means that the nomograph has a remarkable ability to accurately reproduce observed or measured conditions by having an excellent fit to the field data and local conditions of the study area. This was confirmed by an ASD of 0.07 which indicated that absolute errors between nomographic predictions and their observations were relatively small, with limited dispersion.

Table 5. Accuracy index of specific erosion nomograph

Indexes	MAPE (%)	ASD	d	R^2	NS
Values	2	0.07	0.99	0.99	0.99

Conclusion

Due to the complexity of assessing water erosion rates at the catchment level especially the ungauged. The combination of a thorough analysis of hydrological, topographic and pedological factors with scientific and technological advances offers an integrated approach to estimate erosive risks and develop strategies for water and agricultural resource management.

Upon completion of our study, the findings indicate that the specific erosion varies annually from 4.46 to 26.60 T ha-1 on the catchment of Wadi Cheliff, classifying it as one of the Mediterranean rivers with the highest solid

inputs in the world relative to their average flow depth (Milliman, 2006). This magnitude is due to the fragility of the Mediterranean soils caused by irregular and often violent rainfall favoring erosion. In addition, significant slopes in many areas of hills and mountains exacerbate the phenomenon, while high temperatures accelerate the organic matter mineralization, as well as the often-reduced vegetation cover due to the climate and anthropogenic actions; therefore the soils are poorly protected (Plan Bleu, 2003; Özdemir, 2020).

Multivariate analysis allowed a regression model generation with nomographed functions, having as explanatory variables the surface, the flow coefficient and the average slope of the catchment with $R^2 = 0.99$. The nomograph was drawn according to the abacus theory, The product ($Es_1 \times Es_2$) provides the overall specific erosion values for the considered watershed, where each of the two quantities is obtained from the abacus by interpolation in function of the corresponding data. The tool is designed to be applied in the Wadi Cheliff catchment, for a Mediterranean climate with a semi-arid tendency and for areas between 500 and 25 000 ha which delineate the surface interval limits. Beyond this range, erosive action cannot be calculated due to the significant effect of the catchment area on specific erosion that takes into consideration the influence of rainfall distribution, topography, land use, soil type and management practices.

The nomograph is validated with a MAPE equal to 2%. Its reliability depends entirely on the availability of a credible, representative and precise database to ensure the validity of mathematical relationships and adjust its parameters to better adapt to the specific hydrological conditions of a given region. This graphic tool is recommended for its use simplicity, fast field estimation and decision support for territorial planning, which should be supported by identifying areas vulnerable to sediment production for appropriate treatment.

References

Abdellaoui, B., Merzouk, M., Aberkan, M., Albergel, J., 2002. Hydrological balance and siltation of the Saboun dam (Morocco). *Journal of Water Science* 5(4): 737-748.

Achite, M., Meddi, M., 2005. Spatial and temporal variability of streamflow and solid yields in semiarid areas. Case of the oued Mina basin (Northwest Algeria). *Journal of Water Science* 18: 37-56.

Ammari, A., 2012. Vulnérabilité à l'Envasement des Barrages (cas du bassin Hydrographique des Côtiers Algérois). PhD thesis. University of Biskra, Algeria. 195p. Available at [Access date: 18.09.2023]: http://thesis.univ-biskra.dz/id/eprint/68

Assani, A.A., Lajoie, F., Laliberté, C., 2007. The effects of dams on mean anual flow characteristics according to management mode and basin drainage area in Québec *Journal of Water Science* 20(1): 127-146.

Borges, A.L., 1993. Modélisation de l'érosion sur deux bassins versants expérimentaux des Alpes du Sud. PhD thesis. University of Grenoble I, France. 258p. Available at [Access date: 18.09.2023]: https://these.hal.science/tel-00764428

Bouanani, A., 2004. Hydrologie, transport solide et modélisation. Etude de quelques sous bassins de la Tafna (NW–Algérie). PhD thesis. University of Tlemcen, Algeria. 250p. Available at [Access date: 18.09.2023]: http://dspace1.univ-tlemcen.dz/handle/112/15094

Bouchelkia, H., Remini, B., 2003. Quantification du transport solide dans le bassin versant Algérien du Chellif. Ingénieries 33: 45-56. Available at [Access date : 18.09.2023]: https://hal-science/hal-00466014

Bouchnak, H., Felfoul, M.S., Boussema, M.R., Snane, M.H., 2009. Slope and rainfall effects on the volume of sediment yield by gully erosion in the Souar lithologic formation (Tunisia). *Catena* 78: 170-177.

D'ocagne, M., 1884. Procède Nouveau de calcul Graphique. Annales des Ponts et Chaussées 8, 531–540.

D'ocagne, M., 1899. Traité de la nomographie. Théorie des abaques, applications pratiques ; Gauthier-Villars, Paris. 496p.

Dagnelie, P., 1992. Statistique Théorique et Appliquée, Tome 1 – Les bases théoriques. Gembloux Agronomic Presses, vol 2, Belgique. 492p.

Dengiz, O., Demirkaya, S., 2022. Estimation and spatial distribution of some soil erodibility parameters in soils of Ilgaz Nationale Park. *Eurasian Journal of Soil Science* 11(1): 1-9.

Eisazadeh, L., Sokouti, R., Homaee, M., Pazira, E., 2012. Comparison of empirical models to estimate soil erosion and sediment yield in micro catchments. *Eurasian Journal of Soil Science* 1(1): 28-33.

El Kateb, H., Zhang, H., Zhang, P., Mosandl, R., 2013. Soil erosion and surface runoff on different vegetation covers and slope gradients: A field experiment in Southern Shaanxi Province, China. *Catena* 105: 1-10.

Elahcène, O., 2013. Etude du transport solide par charriage et en suspension dans le bassin versant de l'Oued Bellah (tipaza). PhD thesis. ENSA, El-Harrach, Algeria. 109 p.

Felegari, M., Talebi, A., Dastorani, M.T., Rangavar, A. S., 2014. Efficiency Assessment of Rangeland Hydrology and Erosion Model (RHEM) for water erosion quantification (Case study: Sangane Waterched-Iran). *Environmental Resources Research* 2(2): 134-146.

Heng, S., Suestugi, T., 2015. Regionalization of sediment rating curve for sediment yield prediction in ungauged catchments. *Hydrology Research* 46(1): 26-38.

Hotelling, H., 1933. Analysis of a complex of statistical variables into principal components. *Journal of Educational Psychology* 24: 417-441.

Isik, S., 2013. Regional rating curve models of suspended sediment transport for Turkey. *Earth Science Informatics* 6: 87–98.

Jahnke, H.N., 2012. Cauchy's Cours d'analyse. An Annotated Translation By Robert E. Bradley, and C. Edward Sandifer. Sources and Studies in the History of Mathematics and Physical Sciences. Dordrecht (Springer) 2009. *Historia Mathematica* 39: 460-479.

Kheniche, S., Louamri, A., Taabni, M., 2019. Estimation du transport solide et évolution de la relation "Débit liquid – debit solide" dans un basin semi-aride (Cas de l'oued Mellegue amont). *Algérie Orientale. Sciences & Technologie* D 50: 71-80.

Larfi, B., Remini, B., 2006. Le transport solide dans le bassin versant de l'Oued Isser. Impact sur l'envasement du barrage de Beni Amrane (Algérie). *Larhyss Journal* 5: 63-73.

Lee, S.E., Kang, S.H., 2014. Geographic information system-coupling sediment delivery distributed modeling based on observed data. *Water Science & Technology* 70(3): 495-501.

López-Tarazón, J.A., Batalla, R.J., Vericat, D., Balasch, J.C., 2010. Rainfall, runoff and sediment transport relations in a meso scale mountainous catchment: The River Isábena (Ebro basin). *Catena* 82: 23-34.

Meddi, M., Toumi, S., Assani, A.A., Eslamian, S., 2014. Regionalisation of rainfall erosivity in northern Algeria. *International Journal Hydrology Science and Technology* 4(2) :155-175.

Megnounif, A., Terfous, A., Ghenaim, A., Poulet, J.B., 2007. Key processes influencing erosion and sediment transport in a semi-arid Mediterranean area: the Upper Tafna catchment, Algeria. *Hydrological Sciences Journal* 52(6): 1271-1284.

Milliman, J.D., Sediment delivery from Mediterranean rivers: regional, global and temporal perspectives. Fluxes of small and medium-size Mediterranean rivers: Impact on coastal areas. In: Proceedings of the Mediterranean Science Commission, CIESM Workshop. 29 Mars-1 Avril 2006. Trogir, Croatia. pp. 67-71.

Mokhtari, E., 2005. Etude du transport solide par charriage dans l'Oued Mina et son impact sur l'envasement du barrage de Sidi M'hamed Ben Aouda (W, Relizane). Master's thesis. ENSH, Blida, Algeria. 95 p.

Najafova, N., 2022. System of measurs for soil erosion and protection. In: Proceedings of the International Soil Science Symposium on "Soil Science and Plant Nutrition". 2-3 December 2022. Samsun, Türkiye. pp. 195-198.

Ochoa, P.A., Fries, A., Mejía, D., Burneo, J.I., Ruíz-Sinoga, J.D., Cerdà, A., 2016. Effects of climate, land cover and topography on soil erosion risk in a semiarid basin of the Andes. *Catena* 140: 31–42.

Özdemir, N., 2020. Effects of land and plant managements on soil erodibility in the Turhal District of Tokat, Turkey. *Eurasian Journal of Soil Science* 9(4): 362-367.

Pirio, L., 2010. Géométrie anamorphique I : Abaques et Nomogrammes. Images des Mathématiques. CNRS, France. 21 p. Available at [Access date: 18.09.2023]: http://dml.mathdoc.fr/item/hal-00609226/

Plan Bleu, 2003. Les menaces sur les sols dans les pays méditerranéens. Etude bibliographique. Plan bleu pour la Méditerranée, Valbonne, France. 80p.

Remini, W., Remini, B., 2003. La sédimentation dans les barrages de l'Afrique du Nord. Courrier du Savoir 04: 65-69. Available at [Access date: 18.09.2023]: https://www.asjp.cerist.dz/en/article/77926

Rey, F., Ballais, J.L., Marre, A., Rovéra, G., 2004. Role of vegetation in protection against surface hydric erosion. *Comptes Rendus Géoscience* 336: 991–998.

Shen, H., Zheng, F., Wen, L., Han, Y., Hu, W., 2016. Impacts of rainfall intensity and slope gradient on rill erosion processes at loessial hillslope. *Soil and Tillage Research* 155: 429-436.

Shirzadi, A., Shahabi, H., Nabiollahi, K., Taghizadeh-Mehrjardi, R., Lizaga, I., Clague, J. J., Sushant, S. K., Golmohamadi, F., Ahmad, A., 2022. Towards robust smart data-driven soil erodibility index prediction under different scenarios. *Geocarta International* 37(26): 13176-13209.

Touaibia, B., 2000. Erosion- Transport solide- Envasement de barrage. Cas du bassin versant de l'Oued Mina (Wilaya de Relizane). PhD thesis, I.N.A. El Harrach, Algeria. 175p. Available at [Access date: 18.09.2023]: http://localhost:8080/xmlui/handle/123456789/2405

Touaibia, B., Achite, M., 2003. Contribution to the mapping of specific erosion in the Wadi Mina basin in the semiarid zone of northern Algeria. *Hydrological Sciences Journal* 48(2): 235-242.

Touaibia, B., Aidaoui, A., Gomer, D., Achite, M., 2001. Temporal quantification and variability of sediment discharge in a semiarid area in northern Algeria. *Hydrological Sciences Journal* 46(1): 41-53.

Tournès, D., 2000. NOTES & DEBATS pour une histoire du calcul graphique. Revue d'histoire des mathématiques 6 : 127-161. Available at [Access date : 18.09.2023]: http://www.numdam.org/item/RHM_2000__6_1_127_0

Tran Van, Q., 1961. Nomographie et statistique. Revue de statistique appliquée 9(3): 47-76. Available at [Access date: 18.09.2023]: http://www.numdam.org/item?id=RSA_1961__9_3_47_0

Willmott, C. J., 1981. On the validation of models. *Physical Geography* 2(2): 184-194.

Yang, S.L., Milliman, D.J., Li, P., Xu, K., 2011. 50,000 dams later: Erosion of the Yangtze River and its delta. *Global and Planetary Change* 75: 14-20.

Zhou, P., Luukkanen, O., Tokola, T., Nieminen, J., 2008. Effect of vegetation cover on soil erosion in a mountainous watershed. *Catena* 75: 319–325.

Eurasian Journal of Soil Science 2024, 13(3), 224 - 233

Eurasian Journal of Soil Science

Journal homepage : http://ejss.fesss.org

Investigating the possibility of using subcritical water for extracting polycyclic aromatic hydrocarbons from soils of the dry-steppe zone

Svetlana Sushkova *, Tamara Dudnikova, Tatiana Minkina, Andrey Barbashev, Elena Antonenko, Evgenyi Shuvaev, Anastasia Nemtseva

Southern Federal University, Rostov-on-Don, 344090, Russia

Article Info

Received : 02.09.2023
Accepted : 15.04.2024
Available online: 23.04.2024

Author(s)

S.Sushkova*
T.Dudnikova
T.Minkina
A.Barbashev
E.Antonenko
E.Shuvaev
A.Nemtseva

* Corresponding author

Abstract

In the course of the model experiment, extraction conditions of 16 priority PAHs in subcritical water medium were selected for soils of the chestnut-solonetz complex. For low molecular weight 2-ringed naphthalene and 3-ringed acenaphthene, acenaphthylene, anthracene, phenanthrene and fluorene, the optimal extraction conditions correspond to 10 minutes at a temperature of 200°C. For high molecular weight 4- and 5-ring benz(a)anthracene, fluoranthene, pyrene, chrysene, benz(b)fluoranthene, benz(k)fluoranthene, dibenz(a,h)anthracene, as well as the pollutant of the first hazard class - benz(a)pyrene, the optimal extraction time reached 20 minutes at a temperature of 250°C. For 6-ring benz(g,h,i)perylene and indeno(1,2,3-cd)pyrene, the optimum extraction time increased to 30 minutes and the temperature to 300°C. When comparing the methods of extraction of pollutants from soils, it is shown that the extraction methods can be placed in the following descending order by the value of the extraction coefficient of priority PAHs from the studied types of soils: ultrasonic extraction (1.05) > subcritical extraction (1.13) > saponification method (1.25). Using multivariate analysis of dispersion it is shown that the efficiency of subcritical aqueous extraction decreases with increasing number of benzene rings in the PAH molecule, as well as with increasing soil salinity in the following order: Gleyic Kastanozems < Endosalic Kastanozems < Kastanozems Sodic < Solonets.

Keywords: Priority PAHs, subcritical technologies, organic pollutants, Kastanozems, Solonets, PAH extraction method.

© 2024 Federation of Eurasian Soil Science Societies. All rights reserved

Introduction

Polycyclic aromatic hydrocarbons are a class of hazardous widespread organic compounds, many of which exhibit carcinogenic and teratogenic properties (ATSDR, 1995; IARC, 2020; Sushkova et al., 2021). The main sources of PAHs introduction into the environment include enterprises of extraction, processing and usage of liquid and solid fuels, motor and ship transportation, municipal wastes (Tsibart and Gennadiev, 2013). Despite the diversity of pathways and sources of pollutants, up to 90% of all emitted PAHs accumulate in the soil (Qu et al. 2020), which is a serious threat in areas with developed agricultural production. This is especially dangerous for vulnerable saline soils in the dry-steppe zone, which require special reclamation measures for stable high yields (Kalinitchenko et al., 2022).

To date, there is no unified concept for assessing the ecological status of PAH-contaminated soils. The International Agency for Research on Cancer publishes an annual list of substances and factors contributing to carcinogenesis. In this list, more than 30 PAHs are marked as substances likely to contribute to cancer formation (IARC, 2020). Nevertheless, only benz(a)pyrene is subject to control and regulation of its content in soils in Russia (GN 2.1.7.2041-06, 2006, 2017). In world practice, when assessing and forecasting the ecological state of soils, the content of 16 PAHs from the list of priority pollutants of the US EPA (US EPA, 2020) is often determined. The quality of assessment and forecasting is limited by a number of factors, including the relevance of generally accepted methods for determining the mass fraction of pollutants in soil. It is generally

: https://doi.org/10.18393/ejss.1472489
: http://ejss.fesss.org/10.18393/ejss.1472489
Publisher : Federation of Eurasian Soil Science Societies
e-ISSN : 2147-4249

accepted that the most complete extraction of PAHs from soils takes place in the Soxhlet device (up to 99%) (Guerin, 1999; Castro-Guijarro et al., 2021; Silalahi et al., 2021). A significant disadvantage of the method is the 24 hours required for extraction, which significantly slows down the analysis and rapid assessment of the ecological status of soils. In general, organic solvent-based extraction methods are widely used in the analysis of PAH content from solid matrices (Wu et al., 2019; Mukhopadhyay et al., 2020). The simplest and most efficient methods of organic pollutants extraction include ultrasonic and microwave extraction of solid PAHs in solvent media (methanol, hexane, dichloromethane, acetone, etc.) (Zhang et al., 2020; Nowakowski et al., 2022). In Russia, the standard method in the study of environmental objects is the saponification method, in which the pre-interfering lipid fraction of soils, coastal and bottom sediments and plants is removed by boiling the sample in alkali followed by solvent ejection (IPA F 16.1:2.2:2.3:3.62-09, 2009). A common disadvantage of such methods is the high consumption of toxic volatile and semi-volatile reagents such as hexane, dichloromethane, methanol, acetone, acetonitrile etc. (Wu et al., 2019; Soursou et al., 2023). Extraction of pollutants from soils in subcritical water is an alternative to these extraction methods (Sushkova et al., 2014).

Subcritical water is water in the liquid state at a temperature above 100°C and pressure above saturated vapor (Figure 1). As we know, water at room temperature (23°C) and pressure of 1 atm. is a polar solvent with the density of 1000 kg m^{-3}, its dielectric permittivity is ε = 79.73 and its ionic product (Kw) = 10-14. As water temperature and pressure increase, water changes its properties from being a polar solvent to a non-polar solvent. The properties of water as a solvent change due to changes in its dielectric permittivity, ionic product, and hydrogen bond distribution. Changes in viscosity, heat capacity, diffusion coefficients and density affect the transport characteristics of aqueous solutions. At temperatures above 100°C but below 373°C, which is characteristic of the critical point of water, and pressures above 1 atm but below 218 atm (the region of the pre-critical state, respectively), water has an interface but changes its properties, becoming a highly efficient solvent. At constant temperature, the density of water changes continuously, within the existence of each of these phases, and only at the interface is there a density jump. At the critical point (373°C, 218 atm), the interface between the liquid and gaseous phases disappears, and the density of water becomes equal to 300 kg/m^3. However, near the critical point, water has unlimited compressibility, therefore, by varying (even in minor limits) the temperature and pressure in this area, it is possible to change the density of water in a wide range (Figure 1) (Touba and Mansoori, 1998; Islam et al., 2013). As a consequence, water in the subcritical state is a universal medium for chemical reactions.

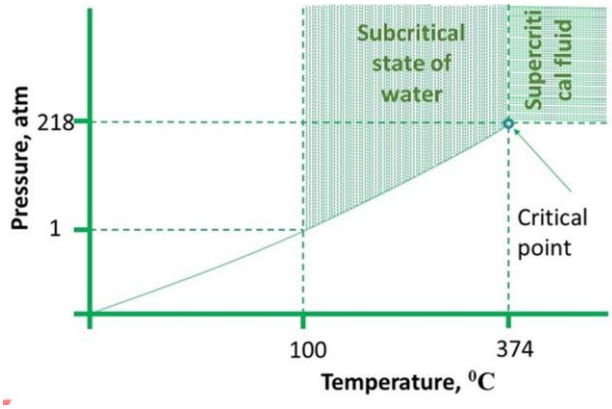

Figure 1. Phase state diagram of water at different pressure and temperature parameters

The efficiency of using water in sub- and supercritical state in the production of biologically active compounds has been repeatedly confirmed (Gbashi et al. 2017; Kim and Lim, 2020). In addition, along with almost complete elimination of toxic non-ionized solvents, the cost of extraction and time spent on this process are significantly reduced (Cheok et al., 2014). Subcritical aqueous method of processing chicken manure allowed to obtain a liquid extract containing organic acids, characterized by the presence of basic functional groups, high content of organic carbon and trace elements (Sushkova et al., 2021). Subcritical and supercritical states of water were used as extractants in the extraction of some individual PAH compounds (benz(a)pyrene, phenanthrene, fluoranthene, pyrene) from Calcic Chernozems, Andosols, sandy substrates and sewage sludge (Islam et al., 2013; Sushkova et al., 2013, 2014, 2015; Yabalak et al., 2024).

The development of pollutant extraction technology for qualitative assessment of ecosystem ecological state requires selecting conditions and testing the method of subcritical water extraction of the entire pool of priority PAHs for soils most vulnerable to pollution. In this regard, the aim of the study was to investigate the possibility of using subcritical water for extracting polycyclic aromatic hydrocarbons from soils of the dry-steppe zone.

Material and Methods

The object of the study were Gleyic Kastanozems, Endosalic Kastanozems, Kastanozems Sodic and Solonets sampled from the territory of the "Rostovsky" Natural Biosphere Reserve located in the dry-steppe zone of the Rostov region. Soil samples for the study were taken according to GOST 17.4.4.02-2017 (GOST 17.4.4.02-2017, 2019) at a depth of 0-20 cm. The studied soils are characterized as heavy loams, differing in the degree of salinization. Properties of soils are given in Table 1.

Table 1. Physical and chemical properties of soils in the dry steppe zone

Corg	Granulometric fractions		pH	$CaCO_3$	Solid residue	Exchange cations		
	<0.01 mm	<0.001 mm				Ca^{2+}	Mg^{2+}	Na^{+}
%				%		cmol (Eq) kg^{-1}		
Gleyic Kastanozems								
2,4±0,2	59,1±2,0	33,5±1,5	7,2±0,04	0,3±0,02	0,055±0,003	22,12±1,68	8,68±0,42	1,18±0,06
Endosalic Kastanozems								
2,8±0,1	54,2±0,9	30,4±1,4	7,8±0,04	0,6±0,02	0,040±0,001	16,49±1,13	6,86±0,52	1,13±0,18
Kastanozems Sodic								
2,1±0,1	57,4±2,3	31,2±1,1	7,8±0,03	0,7±0,03	0,030±0,002	17,75±1,24	5,33±0,47	1,20±0,11
Solonets								
1,5±0,2	59,2±2,0	32,9±1,5	8,5±0,04	0,7±0,05	0,221±0,001	17,17±1,16	5,89±0,33	4,11±0,26

Methods

Procedure for subcritical aqueous extraction of PAHs

The primary step of the PAH extraction procedure consisted of sample preparation by air-drying the soil, cleaning it of plant residue, and sieving it through a sieve with a 1 mm hole diameter. Extraction of PAHs from soil samples was carried out in a continuous pressurized water stream, which allows to extract more polyarenes than extractions in a closed loop cartridge using deionized water as solvent. The repetition of the experiment is 9-fold. After the extraction cell, the obtained extract was passed through a cooling system and then the cartridge was opened and the contents were filtered three times until the solution was clear. The obtained aqueous extract was mixed with 5 mL of n-hexane (99.9% w/w Aquatest, Russia) and placed on a shaker for 15 minutes. The layers were separated on a separating funnel in three successive steps with another portion of hexane (5 mL). The combined hexane extract was passed through a funnel with anhydrous sodium sulfate into a clean dry round bottom flask, evaporated on a rotary evaporator at a water bath temperature of 40-49°C to a dry residue. The resulting dry residue was dissolved in 1 mL acetonitrile (99.9%, b.w., Cryochrom, Russia) for further quantitative analysis.

The study tested different parameters of temperature (200°C, 250°C and 300°C) and extraction time (10, 20 and 30 minutes). The tested range of temperature and pressure is most commonly found as a recommendation for performing the extraction of organic compounds, including PAHs in subcritical water media (Sushkova et al., 2015, 2016; Taki et al., 2018; Yabalak et al., 2024; Zhu et al., 2024).

Comparison of PAH extraction results from soils by different methods

Comparison of extraction results of 16 prioritized PAHs from soils of dry-steppe zone with different degree of salinization (Gleyic Kastanozems, Endosalic Kastanozems, Kastanozems Sodic and Solonets) was carried out via subcritical water extraction with widely used methods: 1) ultrasonic extraction (US EPA, 2007), based on extracting pollutants with acetonitrile:dichloromethane (1:1) mixture (dichloromethane: h.p.a., ChemMed, Russia) under ultrasound; 2) saponification method (IPA F 16.1:2.2:2.2:2.3:3.62-09), which hydrolyzes the lipid fraction of the test sample with a 2% solution of KOH (99.8% p.o.a. Aquatest, Russia) in ethanol (99.8% p.o.a. Aquatest, Russia) followed by 3-fold extraction of hydrocarbons with n-hexane.

Assessment of PAH extraction completeness

In order to establish the completeness of extraction of priority PAHs (naphthalene, anthracene, acenaphthene, acenaphthylene, fluorene, phenanthrene, benz(a)anthracene, fluoranthene, pyrene, chrysene, benz(b)fluoranthene, benz(k)fluoranthene, benz(a)pyrene, dibenz(a, h)anthracene, benz(g,h,i)perylene, indeno(1,2,3-cd)pyrene) from soil by the methods under consideration, a blank experiment was additionally carried out with the application of solutions of a given concentration (10, 20, 40 and 80 ng g^{-1}) of each polyarene into soil (additive method). For this purpose, 16 priority PAH STANDARD was purchased. The

additive was injected with an acetonitrile solution of each PAH into a 1 g soil sample placed in a rotary evaporator flask. After the evaporation of acetonitrile (at room temperature), the sample with the introduced additive was processed according to the proposed method of subcritical aqueous extraction. The experiment was repeated nine times.

The correction factor for PAH recovery in subcritical water was calculated according to the following formulas:

$$k = C1/C2 \quad (1)$$

$$C1 = Cst + Cs \quad (2)$$

where C1 is the total concentration of each PAH in the soil sample, μg kg^{-1}; C2 is the concentration of each PAH in the soil determined by the method used, ng g^{-1}; Cst is the concentration of each PAH in the soil due to the application of its standard solution, ng g^{-1}; Cs is the average concentration of each PAH in the soil sample, ng g^{-1}.

Quantitative analysis of PAHs in the extracts

Quantitative analysis of PAHs in the extracts was performed by high-performance liquid chromatography (HPLC) with an HPLC system equipped with UV and fluorescence detectors (Agilent Model 1260, USA, 2015). The limits of detection (LOD) and limits of quantification (LOQ) of PAHs are presented in Table 2.

Table 2. Limits of detection (LOD) and limits of quantification (LOQ) for 16 priority PAHs

No	PAHs	LOD	LOQ	Holding Time
1	Naphthalene	0.17	0.09	5.26
2	Acenaphthylene	0.08	0.12	6,58
3	Acenaphthene	0.05	0.10	7,11
4	Fluorene	0.08	0.26	8.05
5	Phenanthrene	0.09	0.17	8,90
6	Anthracene	0.01	0.05	9.20
7	Fluoranthene	0.08	0.20	10.30
8	Pyrene	0.10	0.28	11.92
9	Chrysene	0.03	0.15	13.75
10	Benz(a)anthracene	0.03	0.19	16.38
11	Benz(b)fluoranthene	0.03	0.07	22.82
12	Benz(l)fluoranthene	0.02	0.06	24.90
13	Benz(a)pyrene	0.01	0.06	26.80
14	Dibenz(a,h)anthracene	0.04	0.04	32.45
15	Benz(g,h,i)perylene	0.19	0.56	39.48
16	Indeno(1,2,3-cd)pyrene	0.11	0.31	44.51

Statistical treatment of the results obtained

The results were processed statistically using descriptive statistics, multivariate and single factor analysis of variance followed by Tukey's posterior criterion in STATISTICA 8. Visualization of the results is presented using Sigmaplot 12.5.

Results and Discussion

The methodology of extraction of 16 priority PAHs in subcritical water for soils of chestnut-solonetz complex was adapted. It was found that the yield of polyarenes in the extract depends on the temperature and extraction time, as well as on the type of PAHs and soil properties. For low molecular weight 2-ringed naphthalene and 3-ringed acenaphthene, acenaphthylene, anthracene, phenanthrene and fluorene, the optimal extraction conditions correspond to 10 minutes at a temperature of 200°C. For high molecular weight 4- and 5-ringed benz(a)anthracene, fluoranthene, pyrene, chrysene, benz(b)fluoranthene, benz(k)fluoranthene, dibenz(a,h)anthracene, as well as the pollutant of the first hazard class - benz(a)pyrene, the optimal extraction time reached 20 minutes at a temperature of 250°C. Similar results were demonstrated in the extraction of BaP from Calcic Chernozems (Sushkova et al., 2016) For 6-ring benz(g,h,i)perylene and indeno(1,2,3-cd)pyrene, the optimal extraction time increases up to 30 min and the temperature increases up to 300°C (Figure 2). At the same time, treatment of samples with water at 300°C for 30 minutes reduces the yield of less nuclear PAHs, especially their 2- and 3-ringed representatives, which is most likely due to the destruction of less stable pollutant molecules (Islam et al., 2012; Khanjari et al., 2016; Yabalak et al., 2023).

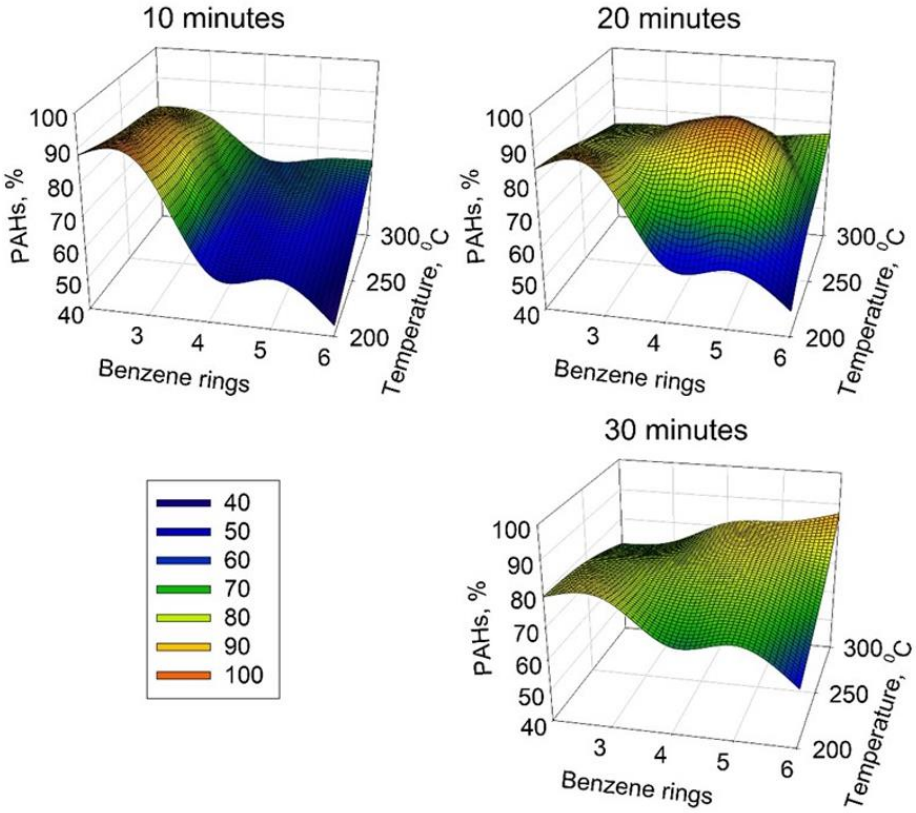

Figure 2. Content of 16 priority PAHs in soil depending on temperature and extraction time in subcritical water medium, ng g^{-1} (n=9)

In order to unify the method of PAH extraction in subcritical water, the conditions chosen as optimal were the 250°C temperature and 20 minute time, as the highest yield of a wide pool of the most toxic and widespread substances was recorded at these parameters (Chaplygin et al., 2022; Sushkova et al., 2020; Dudnikova et al., 2023a,b). The results of PAH content in soils of the dry-steppe zone obtained by extracting pollutants under optimal conditions of temperature and time are presented in Figure 3. It is shown that the studied soils of the natural territory of the dry-steppe zone are characterized by the predominance of low-molecular compounds, first of all, naphthalene and phenanthrene, the content of which exceeds 40 ng g^{-1} in almost all cases. Among high molecular weight compounds pyrene dominates, its amount in soils of the dry-steppe zone varies from 29 ng g^{-1} to 54 ng g^{-1} (Figure 3).

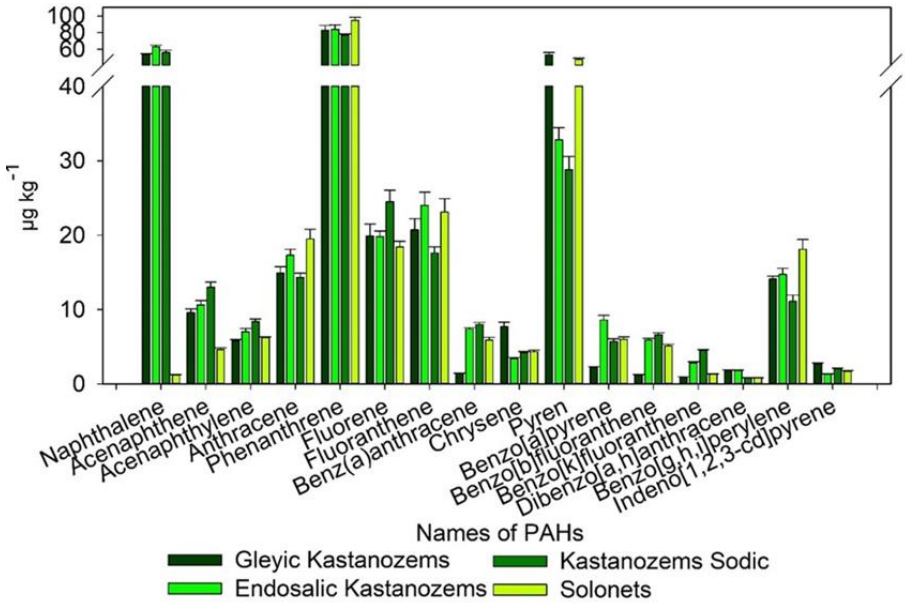

Figure 3. PAH content in soils of the dry-steppe zone based on the results of extraction with subcritical water at a temperature of 250°C for 20 minutes

According to the results of multivariate analysis of dispersion, it was found that the yield of PAHs in the extract depends on the type of PAH, type of extraction, and soil properties (Table 3). The coefficient value is actually an empirical value obtained during the development and approximation of PAH extraction methods. It is necessary for leveling the incompleteness of PAH extraction and it represents the number by which the obtained analytical data should be multiplied. In this regard, an increase in the value of the PAH extraction factor from soils indicates a decrease in the extraction efficiency of pollutants. According to the value of the extraction coefficient of priority PAHs from the studied soil types, the extraction methods can be arranged in the following descending order: ultrasonic extraction (1.05) > subcritical extraction (1.13) > saponification method (1.25). The differences between the methods are significant, which was confirmed using Tukey's posterior criterion at $p<0.05$ (Figure 4).

Table 3. Results of one-factor analysis of dispersion. Variation of PAH extraction coefficient depending on extraction method, soil type, and pollutant type

Factor	SS	MS	F	p
PAH	0.162	0.011	6.7	<0.000001
Extraction	5.137	2.568	1602.8	<0.000001
Soil type	0.049	0.016	10.1	0.000002
PAH*Extraction	0.416	0.014	8.7	<0.000001
PAH*Soil type	0.057	0.001	0.8	0.836616
Extraction*Soil type	0.160	0.027	16.6	<0.000001
PAH*Extraction*Soil type	0.134	0.001	0.9	0.654836

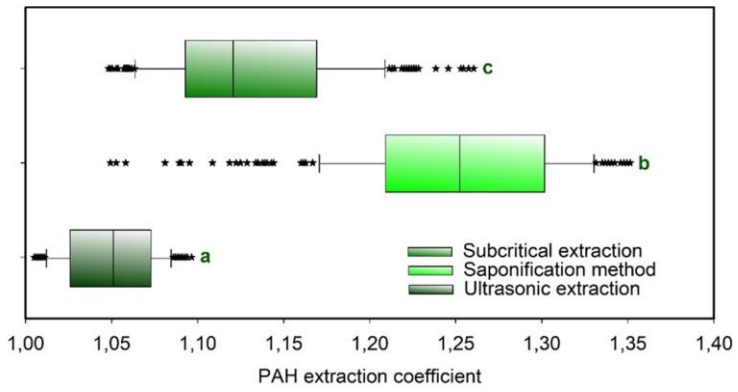

Figure 4. PAH extraction coefficient from soils of the dry-steppe zone depending on the extraction method. Letters indicate differences in PAH extraction coefficient for different extraction methods calculated using Tukey's apposterior criterion at $p<0.05$.

Using multivariate analysis of dispersion it is shown that at PAH extraction by methods based on the use of organic solvents (ultrasonic extraction and saponification method), soil properties do not significantly affect the degree of extraction of pollutants. On the contrary, at subcritical aqueous extraction there is a tendency towards an increase in the degree of PAHs extraction depending on the level of soil salinity in the series: Gleyic Kastanozem > Endosalic Kastanozem > Kastanozem Sodic > Solonets. At the same time, the PAH extraction coefficient from Solonets is significantly higher than from less saline soils (Figure 5), which is due to a decrease in dialectic permittivity of water under the influence of sodium salts (Patel et al. 2021).

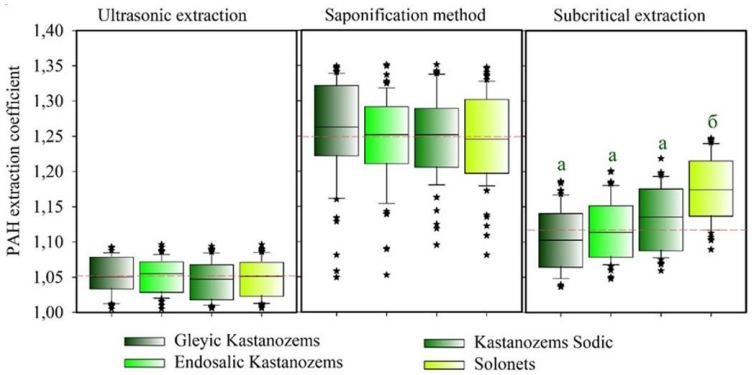

Figure 5. PAH extraction coefficient from dry-steppe zone soils depending on extraction method. Letters indicate differences in PAH extraction coefficient from soils of different types calculated using Tukey's apposterior criterion at $p<0.05$.

Differences between the extraction rates of individual compounds were not established when the pollutants were extracted with solvents in ultrasonic or saponification methods. For subcritical water extraction, the extraction ratio of 4- and 5-ringed compounds is significantly lower than that of low molecular weight and 6-ringed compounds (Figure 6). This because as the number of benzene rings in the PAH molecule increases, their molecular weight, lipophilicity and binding affinity to soil increases, the energy cost of desorption of pollutant from soil particles increases (Liang et al. 2016).

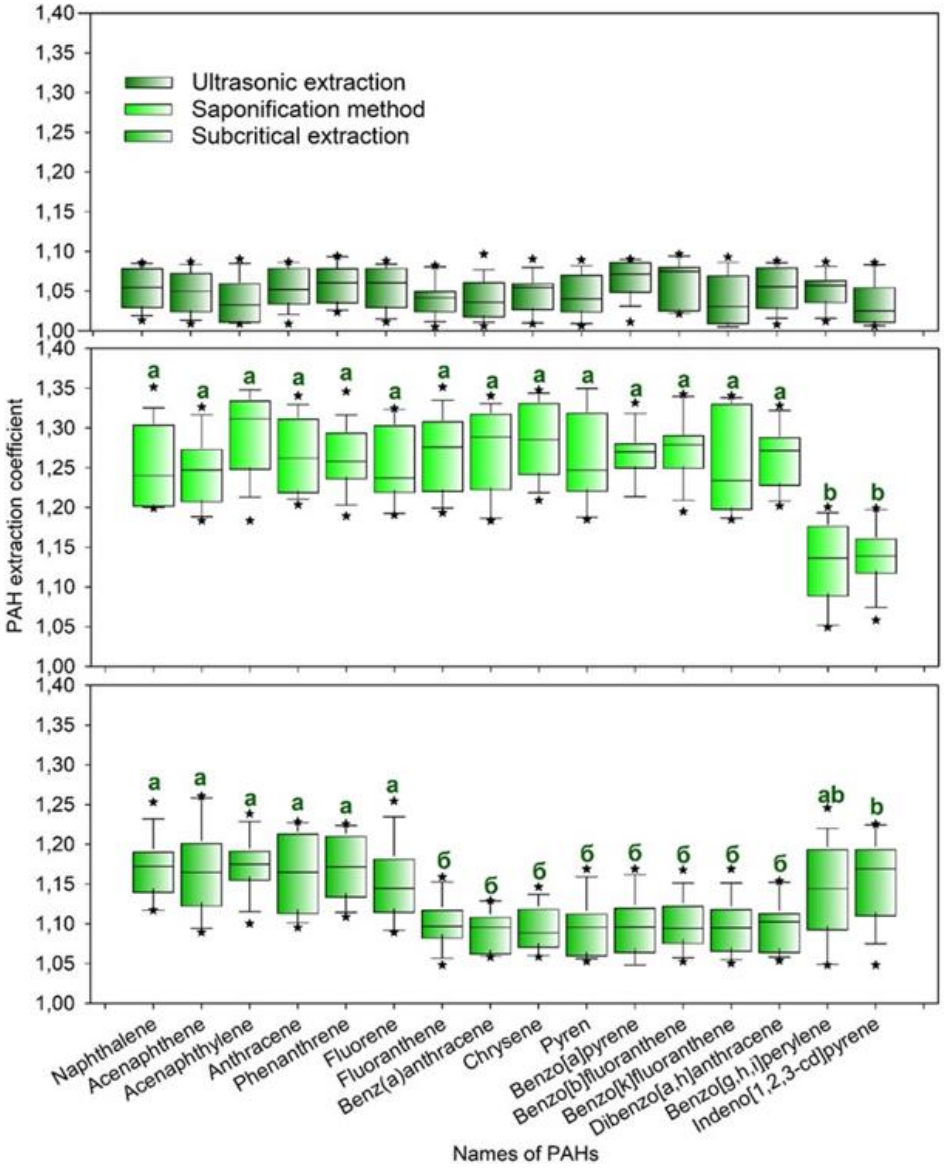

Figure 6. PAH extraction coefficient from soils of the dry-steppe zone depending on the extraction method. Letters indicate differences in the extraction coefficient of individual PAHs at different methods of their extraction from soils, calculated using Tukey's apposterior criterion at $p<0.05$.

Based on the results of a model experiment using soils of the dry-steppe zone, the optimal conditions for extraction of 16 priority PAHs in subcritical water were determined. It is shown that PAH extraction in subcritical water allows to significantly reduce the time spent on analysis, as well as almost completely exclude the use of toxic organic solvents. At the same time, the adapted method is more effective than the saponification method and is comparable to ultrasonic extraction for the most common and hazardous high-molecular-weight 4- and 5-ringed PAHs (Table 4).

Table 4. Comparison of methods for extraction of PAHs from natural objects

Comparison parameters		Subcritical extraction	Saponification method	Ultrasonic extraction
Time, min			240	30
Solvent, mL	Hexane	15	60	45
	Acetonitrile	1	1	2
	Dichloromethane	-	-	45
Average extraction coefficient			1.25	1.05

Conclusion

The optimal conditions of extraction of priority PAHs in subcritical water medium from soils of chestnut-solonetz complex of dry-steppe zone were determined using Gleyic Kastanozems, Endosalic Kastanozems, Kastanozems Sodic, and Solonets as examples. It was shown that for low molecular weight compounds of 2- and 3-ringed PAHs, the optimal extraction conditions correspond to 10 minutes at a temperature of 200°C, for high molecular weight 4- and 5-ringed PAHs - 20 minutes at a temperature of 250°C, for 6-ringed PAHs - 30 minutes at a temperature of 300°C. In order to unify the method of extraction of pollutants in subcritical water medium, the conditions corresponding to the temperature of 250°C for 20 minutes were chosen as optimal, since at these parameters the highest yield of a wide pool of the most toxic and widespread PAHs was recorded. Using the proposed parameters it was established that naphthalene, phenanthrene and pyrene dominate in the studied soils of the dry-steppe zone.

The efficiency of PAH extraction by widely used methods based on the use of organic solvents and subcritical extraction was compared. By means of multifactor dispersion analysis performed based on the results of calculating the PAH extraction coefficient, it was found that the peculiarities of soil properties and the type of pollutant significantly affect the degree of extraction of pollutants from soils during subcritical extraction in optimal parameters of temperature and time. The efficiency of subcritical water extraction decreases with increasing number of benzene rings in the PAH molecule, as well as with increasing soil salinity in the series: Gleyic Kastanozems < Endosalic Kastanozems < Kastanozems Sodic < Solonets. According to the extraction coefficient value of priority PAHs from the studied soil types, the extraction methods can be placed in the following descending row: ultrasonic extraction (1.05) > subcritical extraction (1.13) > saponification method (1.25). Despite the more complete extraction of PAHs from soils by ultrasonic extraction, subcritical extraction significantly reduces the time and the amount of toxic organic solvents spent on analysis.

Acknowledgments

The study was supported by the Russian Science Foundation (project No. 19-74-10046) at the Southern Federal University.

References

ATSDR, 1995. Toxicological profile for polycyclic aromatic hydrocarbons. Washington, DC, U.S. Department of Health and Human Services. Agency for Toxic Substances and Disease Registry. Available at [Access date: 02.09.2023]: https://wwwn.cdc.gov/tsp/ToxProfiles/ToxProfiles.aspx?id=122&tid=25

Castro-Guijarro, P.A., Álvarez-Vázquez, E.R., Fernández-Espinosa, A.J., 2021. A rapid Soxhlet and mini-SPE method for analysis of polycyclic aromatic hydrocarbons in atmospheric particles. *Analytical and Bioanalytical Chemistry* 413: 2195-2206.

Chaplygin, V., Dudnikova, T., Chernikova, N., Fedorenko, A., Mandzhieva, S., Fedorenko, G., Sushkova, S., Nevidomskaya, D., Minkina, T., Sathishkumar, P., Rajput, V.D., 2022. Phragmites australis cav. As a bioindicator of hydromorphic soils pollution with heavy metals and polyaromatic hydrocarbons. *Chemosphere* 308: 136409.

Cheok, C.Y., Salman, H.A.K., Sulaiman, R., 2014. Extraction and quantification of saponins: A review. *Food Research International* 59: 16-40.

Dudnikova, T., Minkina, T., Sushkova, S., Barbashev, A., Antonenko, E., Konstantinova, E., Shuvaev, E., Nevidomskaya, D., Ivantsov, A., Bakoeva, G., Gorbunova, M., 2023. Background content of polycyclic aromatic hydrocarbons during monitoring of natural and anthropogenically transformed landscapes in the coastal area soils. *Water* 15(13): 2424.

Dudnikova, T., Sushkova, S., Minkina, T., Barbashev, A., Ferreira, C.S.S., Antonenko, E., Shuvaev, E., Bakoeva, G., 2023. Main factors in polycyclic aromatic hydrocarbons accumulations in the long-term technogenic contaminated soil. *Eurasian Journal of Soil Science* 12(3): 282-289.

Gbashi, S., Adebo, O.A., Piater, L., Madala, N.E., Njobeh, P.B., 2017. Subcritical water extraction of biological materials. *Separation & Purification Reviews* 46 (1): 21-34.

GN 2.1.7.2041-06, 2006; 2017. Resolution of the Chief State Sanitary Doctor of the Russian Federation dated 01/23/2006 No. 1 (ed. dated 06/26/2017) "On the introduction of hygienic standards GN 2.1.7.2041-06" (together with "GN 2.1.7.2041-06. 2.1.7. Soil, cleaning of populated areas, waste of production and consumption, sanitary protection of soil. Maximum permissible concentrations (MPC) of chemicals in the soil. Hygienic standards", approved by Chief State Sanitary Doctor of the Russian Federation on 19.01.2006) (Registered with the Ministry of Justice of the Russian Federation on 07.02.2006 N7470).

GOST 17.4.4.02-2017, 2019. Protection of Nature. Soils. Methods of sampling and preparation of samples for chemical, bacteriological, helminthological analysis. Moscow. Standartinform, Russia. 12p.

Guerin, T.F., 1999. The extraction of aged polycyclic aromatic hydrocarbon (PAH) residues from a clay soil using sonication and a Soxhlet procedure: a comparative study. *Journal of Environmental Monitoring* 1 (1): 63-67.

IARC, 2020. List of classifications, volumes 1-123. IARC Monographs on the Evaluation of Carcinogenic Risks to Humans. Lyon: International Agency for Research on Cancer. Available at [Access date: 02.09.2023]: https://monographs.iarc.fr/list-of-classifications-volumes/

IPA F 16.1:2.2:2.3:3.62-09, 2009. Quantitative chemical analysis of soils. Methodology for measuring the mass fractions of polycyclic aromatic hydrocarbons in soils, bottom sediments, sewage sludge and production and consumption waste by high–performance liquid chromatography. Standartiform, Moscow, Russia, 11p.

Islam, M.N., Jo, Y.T., Jung, S.K., Park, J.H., 2013. Thermodynamic and kinetic study for subcritical water extraction of PAHs. *Journal of Industrial and Engineering Chemistry* 19 (1): 129-136.

Islam, M.N., Jo, Y.T., Park, J.H., 2012. Remediation of PAHs contaminated soil by extraction using subcritical water. *Journal of Industrial and Engineering Chemistry* 18(5): 1689-1693.

Kalinitchenko, V.P., Glinushkin, A.P., Minkina, T.M., Mandzhieva, S.S., Sushkova, S.N., Sukovatov, V.A., Il'ina, L.P., Makarenkov, D.A., Zavalin, A.A., Dudnikova, T.S., Barbashev, A.I., Bren, D.V., Rajput, P., Batukaev, A.A., 2022. Intra-soil waste recycling provides safety of environment. *Environmental Geochemistry and Health* 44 (4): 1355-1376.

Khanjari, Y., Eikani, M.H., Rowshanzamir, S., 2016. Remediation of polycyclic aromatic hydrocarbons from soil using superheated water extraction. *The Journal of Supercritical Fluids* 111: 129-134.

Kim, D.S., Lim, S.B., 2020. Kinetic study of subcritical water extraction of flavonoids from citrus unshiu peel. *Separation and Purification Technology* 250: 117259.

Liang, X., Zhu, L., Zhuang, S., 2016. Sorption of polycyclic aromatic hydrocarbons to soils enhanced by heavy metals: perspective of molecular interactions. *Journal of Soils and Sediments* 16: 1509-1518.

Mukhopadhyay, S., Dutta, R., Das, P., 2020. A critical review on plant biomonitors for determination of polycyclic aromatic hydrocarbons (PAHs) in air through solvent extraction techniques. *Chemosphere* 251: 126441.

Nowakowski, M., Rykowska, I., Wolski, R., Andrzejewski, P., 2022. Polycyclic aromatic hydrocarbons (PAHs) and their derivatives (O-PAHs, N-PAHs, OH-PAHs): Determination in suspended particulate matter (SPM)–A review. *Environmental Processes* 9:2.

Patel, L.A., Yoon, T.J., Currier, R.P., Maerzke, K.A., 2021. NaCl aggregation in water at elevated temperatures and pressures: Comparison of classical force fields. *The Journal of Chemical Physics* 154 (6): 064503.

Qu, Y., Gong, Y., Ma, J., Wei, H., Liu, Q., Liu, L., Wu, H., Yang, S., Chen, Y., 2020. Potential sources, influencing factors, and health risks of polycyclic aromatic hydrocarbons (PAHs) in the surface soil of urban parks in Beijing, China. *Environmental Pollution* 260: 114016.

Silalahi, E.T.M.E., Anita,S., Teruna, H.Y., 2021. Comparison of extraction techniques for the determination of polycyclic aromatic hydrocarbons (PAHs) in soil. *Journal of Physics: Conference Series* 1819: 012061.

Soursou, V., Campo, J., Picó, Y., 2023. Revisiting the analytical determination of PAHs in environmental samples: An update on recent advances. *Trends in Environmental Analytical Chemistry* 37: e00195.

Sushkova, S., Minkina, T., Chaplygin, V., Nevidomskaya, D., Rajput, V., Bauer, T., Mazarji, M., Bren, A.B., Popov, I., Mazanko, M., 2021. Subcritical water extraction of organic acids from chicken manure. *Journal of the Science of Food and Agriculture* 101(4): 1523-1529.

Sushkova, S., Minkina, T., Mandzhieva, S., Tjurina, I., Bolotova, O., Vasilyeva, G., Orlović-Leko, P., Varduni, T., Kizilkaya, R., Akca, I., 2015. Solubility of benzo[a]pyrene and organic matter of soil in subcritical water. *Croatica Chemica Acta* 88(3): 247-253.

Sushkova, S., Minkina, T., Tarigholizadeh, S., Antonenko, E., Konstantinova, E., Gülser, C., Dudnikova, T., Barbashev, A., Kızılkaya, R., 2020. PAHs accumulation in soil-plant system of Phragmites australis Cav. in soil under long-term chemical contamination. *Eurasian Journal of Soil Science* 9 (3): 242-253.

Sushkova, S., Minkina, T., Tarigholizadeh, S., Rajput, V., Fedorenko, A., Antonenko, E., Dudnikova, T., Chernikova, N., Yadav, B.K., Batukaev, A., 2021. Soil PAHs contamination effect on the cellular and subcellular organelle changes of *Phragmites australis* Cav. *Environmental Geochemistry and Health* 43: 2407-2421.

Sushkova, S.N., Minkina, T.M., Mandzhieva, S.S., Tjurina, I.G., 2013. Elaboration and approbation of methods for benzo[a]pyrene extraction from soils for monitoring of the ecological state in technogenic landscapes. *World Applied Sciences Journal* 25(10): 1432-1437.

Sushkova, S.N., Minkina, T.M., Mandzhieva, S.S., Vasilyeva, G.K., Borisenko, N.I., Turina, I.G., Kızılkaya, R., Bolotova, O.V., Varduni, T.V., 2016. New alternative method of benzo[a]pyrene extractionfrom soils and its approbation in soil under technogenic pressure. *Journal of Soils and Sediments* 16: 1323-1329.

Sushkova, S.N., Vasilyeva, G.K., Minkina, T.M., Mandzhieva, S.S., Tjurina, I.G., Kolesnikov, S.I., Kizilkaya, R., Askin, T., 2014. New method for benzo[a]pyrene analysis in plant material using subcritical water extraction. *Journal of Geochemical Exploration* 144: 267-272.

Taki, G., Islam, M.N., Park, S.J., Park, J.H. 2018. Optimization of operating parameters to remove and recover crude oil from contaminated soil using subcritical water extraction process. *Environmental Engineering Research* 23(2): 175-180.

Touba, H., Mansoori, G.A., 1998. Structure and property prediction of sub-and supercritical water. *Fluid phase equilibria* 150-151: 459-468.

Tsibart, A.S., Gennadiev, A.N., 2013. Polycyclic aromatic hydrocarbons in soils: sources, behavior, and indication significance (a review*). Eurasian Soil Science* 46(7): 728-741.

US EPA, 2007. SW-846 Test Method 3550C: Ultrasonic Extraction. US Environmental Protection Agency, Washington DC, USA. Available at [Access date: 02.09.2023]: https://www.epa.gov/hw-sw846/sw-846-test-method-3550c-ultrasonic-extraction

US EPA, 2020. IRIS Assessments. Integrated Risk Information System (IRIS). US Environmental Protection Agency, Washington DC, USA. Available at [Access date: 02.09.2023]: https://cfpub.epa.gov/ncea/iris_drafts/AtoZ.cfm

Wu, L., Sun, R., Li, Y., Sun, C., 2019. Sample preparation and analytical methods for polycyclic aromatic hydrocarbons in sediment. *Trends in Environmental Analytical Chemistry* 24: e00074.

Yabalak, E., Akay, S., Kayan, B., Gizir, A.M., Yang, Y., 2023. Solubility and decomposition of organic compounds in subcritical water. *Molecules* 28 (3): 1000.

Yabalak, E., Aminzai, M.T., Gizir, A.M., Yang, Y., 2024. A Review: Subcritical water extraction of organic pollutants from environmental matrices. *Molecules* 29 (1): 258.

Zhang, Q., Liu, P., Li, S., Zhang, X., Chen, M., 2020. Progress in the analytical research methods of polycyclic aromatic hydrocarbons (PAHs). *Journal of Liquid Chromatography and Related Technologies* 43 (13-14): 425-444.

Zhu, M.H., Yin-Dong, L., Wang, L.T., Huang, Z.B., Yuan, P.Q. 2024. Selective extraction of aromatics from residual oil with subcritical water. *Chemical Engineering Research and Design* 202: 444-454.

Eurasian Journal of Soil Science 2024, 13(3), 234 - 246

Eurasian Journal of Soil Science

Journal homepage : http://ejss.fesss.org

Tea plantation shade tree leaf influences the susceptibility of rhizosphere microbial consortium: A comprehensive study on their leaf extract cross tolerance

Arindam Ghosh [a], Arnab Nag [a], Sukanya Acharyya [a], Sumedha Saha [a], Soumya Majumder [a], Sourav Chakraborty [a,b], Malay Bhattacharya [a,*]

[a] Molecular Biology and Tissue Culture Laboratory, Department of Tea Science, University of North Bengal. Rajarammohanpur, Siliguri, Darjeeling- 734013, India

[b] Post Graduate Department of Botany, Darjeeling Government College, Darjeeling, West Bengal, 734101, India

Article Info

Received : 02.11.2023
Accepted : 26.04.2024
Available online: 30.04.2024

Author(s)

A.Ghosh
A.Nag
S.Acharyya
S.Saha
S.Majumder
S.Chakraborty
M.Bhattacharya*

* Corresponding author

Abstract

Leguminous shade trees are ubiquitous parts of tea plantations of the Terai region. However, their shed leaves might have an effect on the soil microflora under those shade trees, so it is important to find out how leaf litter affect the soil microflora. Isolation of soil microbial consortia followed by downstream experiments were conducted to observe the tolerance/susceptible pattern of those soil microflora against the fallen leaves. Sample from under *Albizia odoratissima* has higher organic carbon, organic matter and nitrogen content but the same property was found to be low in the sample collected under *Melia azedarach*. Isolation of consortia was done on nutrient agar. *In vitro* tolerance assay was conducted to find out the tolerance pattern against leaf extracts, heavy metal salts, pesticides, antibiotics and antifungals. Heavy metals salts like Arsenic trioxide (AS_2O_3) and Cupric chloride ($CuCl_2$); and pesticides like Thiamethoxam; Spiromesifen; Phorate etc. showed no inhibition against all the isolated consortia. Co-Trimoxazole and Augmentin have not showed any inhibition except consortia under *Derris robusta*, whereas no antifungals but Itraconazole had an impact over all the consortia. Shade trees, being a crucial member of the tea plantations, cannot be removed but replacement of these with other species could be a probable option, besides this limited use of chemical pesticides and fertilizers should be taken into consideration strictly to restrain the microbial population in tea garden soil. So, this study has disclosed the acceptability of each and every shade tree used in this region.

Keywords: Shade tree, tea plantation, rhizosphere, soil microbes, tolerance.

© 2024 Federation of Eurasian Soil Science Societies. All rights reserved

Introduction

The Tea plant [*Camellia sinensis* (L.) Kuntze], is cultivated for the production of tea. Tea is the 2nd most consumed beverage worldwide and boasts an aromatic flavor as well as beneficial to the drinker. The Tea industry is one of the oldest agro-based industries in India and it is greatly valued for its economic significance as it contributes 1% of the GDP of the country (Sharma et al., 2019). Tea plantations generally employ shade trees to protect their bushes from scorching sunlight. They also help in the betterment of the soil nutrient profile by hosting symbiotic nitrogen-fixing microorganisms and a range of nutrients being added through the degradation of leaf litter from these trees (Ghosh et al., 2021; Ghosh et al., 2022). The shade trees along with tea bushes create a microclimate that improves soil microbial population with an increase in soil organic carbon and moisture (Ghosh et al., 2022). Organic matter supplementing soil microbes is involved in several ecological, biodegradable cycles (Malviya et al., 2021) and mitigates heavy metal toxicity (Pandey et al., 2019). Soil rhizosphere contains diverse microbes, of which plant growth promoting ones improve soil fertility.

To meet the rising demand for tea, the use of fertility management techniques, high yielding clones, longer pruning cycle etc. have been introduced. The microflora hosted by the soil in these gardens may be subject to

: https://doi.org/10.18393/ejss.1476125
: http://ejss.fesss.org/10.18393/ejss.1476125
Publisher : Federation of Eurasian Soil Science Societies
e-ISSN : 2147-4249

a variety of factors including but not limited to exposure to the phytochemical effects of leaf litters, pesticides, antibiotics etc., resulting in the acquisition of tolerance to said irritants. So, in order to find out whether or not these factors are affecting the soil microflora we explored their antibiotic, antifungal, heavy metal and pesticide tolerance abilities. As this region lies under the Himalayan foothills, anthropogenic activities and the use of chemical fertilizers and pesticides are to be expected.

Shade tree leaf litter is a pool of secondary metabolites that may promote or restrict soil microbes (Saha et al., 2022). Shade trees vary in secondary metabolite content, so there must be differential antagonism toward soil microbes. Not much work has been done on this particular issue. Though the inhibitory effect of tea plantation shade tree leaf extract on phosphate solubilizing bacteria (PSB) has been studied by Saha et al. (2022), where it was found that metabolites like 1-heptanol, 2-propyl-, neophytadiene, phytol and squalene from shade trees like *Albizia odoratissima*, *Albizia chinensis*, *Albizia procera* exhibited antimicrobial activity as they showed *in vitro* inhibition zones in PSB culture collected from tea gardens. But much in this context remains to be explored.

So, this research intended to isolate microbial consortia from the soil of the tea plantation of Terai region and explore their tolerance ability against leaf litters, pesticides, heavy metal salts as well as various antibiotic and antifungal agents. Thus, this study was aimed to gain an understanding of the growing resistance ability of microflora and their adaptability that may ultimately help in maintaining soil fertility which is an indispensable part of proper plant growth and development.

Material and Methods

Collection of soil samples

Seven Shade trees viz. *Albizia odoratissima* (L.f.) Benth. (AO), *Albizia chinensis* (Osbeck)Merr. (AC), *Acacia lenticularis* Benth. (AL), *Dalbergia sissoo* Roxb. (DS), *Derris robusta* (DC.) Benth. (DR), *Leucaena leucocephala* (Lam.) de Wit (LL) and *Melia azedarach* L. (MA) were selected and considered for the present study. Vacant land (VL) as well as shade tree free (WST) areas were used as control plots for the study. All the collection sites were from NBU tea plantations (26.713006 N, longitude 88.3480252 E). Soil samples were collected from the cover area of the shade tree by following the protocol of Saha et al. (2020) with slight modifications. Soil sampling was done early in the morning after the pre-monsoon showers.

Soil analysis

Soil parameters like pH, organic carbon (OC), organic matter (OM) content, total nitrogen, available phosphorus, potassium and Sulphur contents were evaluated from the collected sample. Before analysis soil samples were air-dried and sieved (Mukherjee et al., 2020; Saha et al., 2020).

Isolation of Consortia

Soil microbial consortia were isolated by mixing 500mg of soil sample in 1 ml of sterile distilled water. 500µl of the soil solution was added to the pre-autoclaved nutrient broth and was incubated overnight at 37º C. The isolates were preserved at 4ºC for downstream experiments (Saha et al., 2021).

Effect of shade tree leaf extract on the growth of Rhizopsheric Microbial Consortia (RMC)

Antimicrobial study was conducted with shade tree leaf extracts on the isolated consortia. Pour plate inoculation followed by well diffusion addition of leaf extracts of AO, AC, AL, DS, DR, LL and MA was employed for the study (Ghosh et al., 2021), where 200µl of cultures (RMC) were inoculated and 100µl (250 mg/ml) of leaf extracts were added in the wells of the semisolid agar. The Petri dishes were incubated at 37ºC for 24 hours.

Heavy Metal tolerance assay

To determine the heavy metal tolerance test, we followed the disc diffusion method proposed by Acharyya et al. (2021) with slide modification, where we took five different heavy metal salts like $CuCl_2$, As_2O_3, $Pb(NO_3)_2$, $CdCl_2$ and $HgCl_2$with the concentration of 2.5 mg/ml. To test the isolated culture, we prepared semi-solid nutrient media with 100µl of culture being spread throughout via the spread plate technique. After that, the disc was dipped in different heavy metal salts and placed on the petri dish.

Antibiotic and antifungal tolerance assay of Consortia

In vitro, antibacterial tolerance assay was conducted by following the protocol of Saha et al. (2020) against the selected isolated culture by using antibiotic discs. 200µl of isolated culture was pour plated in nutrient agar media. After the hardening of the agar, common antibiotic hexa-discs of Bacitracin (B10), Chloramphenicol (C30), Penicillin-G (P10), Polymixin B (PB300), Gentamicin (Gen10), Neomycin (N30), Cefotaxime (CTX30), Augmentin (AMC30), Erythromycin (E10), Ofloxacin (OF5) and Co-Trimoxazole (COT25), of HiMedia

(Catalogue No. HX032 and HX038) were were aseptically placed on top of the agar and then incubated these plates at 35°C for 24 hours. After 24 hours, inhibition zones around the discs were recorded.

To assess the tolerance activity of the fungal population in the soil, we followed the protocol of Saha et al. (2020), where 200µl of culture sample was inoculated in the plate with the pour plate technique. And six common antifungals like Amphotericin-B (AP100), Clotrimazole (CC10), Fluconazole (FLC25), Itraconazole (IT10), Ketoconazole (KT10) and Nystatin (NS100) from HiMedia (Catalogue No HX104) were used against consortia and incubated for 96 hours at 35°C. After incubation, the inhibition zones around the discs were recorded.

Pesticide tolerance assay

To determine their pesticide tolerance ability, we followed the protocol of Saha et al. (2020), where nine common pesticides like Emamectin benzoate, Fipronil, Phorate, Deltamethrin, Flubendiamide, Spiromesifen, Thiamethoxam, Fenazaquin, Quinalphos being usually applied in the tea plantation to get rid of pests were chosen. Pour plate and well diffusion method was followed to assess this test, where 200 µl of isolated culture was poured in petri dish with 2.8% nutrient agar media. Different concentrations like 2.5, 5, 10 and 20 mg/ml of the nine pesticides were chosen whereas the recommended value was 2.5mg/ml, and 100 µl of each concentrated different pesticide were added in the wells of the petri dishes followed by incubation of the plates at 30ºC for 48 hours.

Results

Soil analysis

pH and EC

Changes in soil pH mean a tenfold change in the amount of acidity or alkalinity. Tea Board of India proposed that the pH of the soil of tea plantations should be between 4.5-5.5 (Mukherjee et al., 2020). In this study, we found that the pH of the soil collected from underneath the tea plantation shade trees range between 4.5 to 6.1. Maximum soil pH was recorded in MA (6.1) while lowest pH was recorded in DR (4.5).

Electrical conductivity (EC), typically used to enumerate the charged particles present in particular soil samples, was also found to vary between plant species. The maximum EC (172 µS/cm) was found in the soil sample of DR plant species and the lowest EC (103.3 µS/cm) was detected in the soil of MA plant species (Table 1).

Table 1. Results of soil physicochemical properties

	pH	EC, µS/cm	OC,%	OM,%	Total N, %	Available K, mg/kg	Available S, mg/kg	Available P, mg/kg
AC	5.21±0.29	124.00±6.24	6.66±0.44	11.45±0.76	0.57±0.04	49.00±1.73	24.00±6.07	52.33±9.50
AO	4.89±0.07	145.00±2.65	10.37±1.31	17.84±2.25	0.89±0.11	42.67±5.86	16.27±2.16	37.33±9.71
AL	4.73±0.07	132.33±17.24	9.34±2.63	16.07±4.52	0.80±0.23	31.33±2.52	16.67±2.54	29.00±11.27
DS	4.88±0.12	143.33±32.65	7.70±1.16	13.24±1.99	0.66±0.10	41.00±3.61	19.80±2.25	24.33±6.66
DR	4.58±0.17	172.00±4.58	7.19±0.37	12.36±0.64	0.62±0.03	30.33±3.51	17.30±2.93	11.33±4.04
LL	5.31±0.10	145.00±11.27	6.93±0.36	11.93±0.63	0.60±0.03	59.33±6.51	18.97±4.41	40.67±15.01
MA	6.12±0.19	103.33±21.50	5.97±0.72	10.27±1.24	0.51±0.06	60.67±8.08	17.93±5.09	21.67±10.69
VL	4.86±0.07	111.67±1.53	6.59±0.59	11.33±1.02	0.57±0.05	44.00±2.65	17.30±4.03	0.67±1.15
NS WST	5.24±0.05	132.67±4.04	7.15±0.36	12.29±0.62	0.61±0.03	50.67±10.79	19.37±1.44	20.33±2.89

Albizia chinensis (AC), *Albizia odoratissima* (AO), *Acacia lenticularis* (AL), *Dalbergia sissoo* (DS), *Derris robusta* (DR), *Leucaena leucocephala* (LL), *Melia azedarach* (MA), Vacant land (VL) and WST (Without shade tree)

Organic carbon and Organic matter

Soil organic matter is an aggregation of all organic components present in the soil including plant and animal matter excluding mineral carbon. Organic matter (OM) makes up just 2-10% of most of the soil's mass. Organic carbon (OC) content should be 1-2% as recommended by the Tea Board of India. In this study, the average organic carbon was found to be about 7.73%. Whereas maximum organic content was recorded at 10.37% for AO and the minimum was found in MA (5.96%).

Moreover, non-shaded areas (WST) showed a moderate level of organic matter and organic carbon content due to the presence of shaded tea leaf litter on it while the vacant land (VL) portrayed a low trend in OC and OM content compared to others. Interestingly, MA resulted in the lowest OC and OM values in its cover region where possible explanation can be found only after future comparative nutrient analysis on shed leaves in particular.

Nitrogen, Phosphorous, Potassium and Sulphur

Nitrogen, phosphorous, potassium and sulfur are the macronutrients for plants that help plants regulate essential physiological processes, growth and development etc. (Mukherjee et al., 2020). In our study, we

found that 0.665% of nitrogen (N) was present in analyzed samples which were ideal. The highest nitrogen content was recorded in AO (0.892%) and the minimum in MA (0.513%).

Phosphorous (P) is present in the soil as phosphate (P_2O_5) and the ideal level recommended by the Tea Board of India is 10 to 20 mg/kg. But in our study, we found the highest phosphate content was in AC with an amount of 52.34 mg/kg and the lowest was detected in DR. Surprisingly, in vacant land (VL) phosphate level was very low (0.67 mg/kg).

The optimum level of potassium (K) as potash in soil recommended by the Tea Board of India is 60 to 80 mg/kg. Our results revealed that the average potassium level was lower than the optimum. However, the maximum potash level was found in MA (60.67 mg/kg) and the minimum potash level was recorded in DR (30.34 mg/kg). Whereas soils from non-shaded areas (WST) and vacant land (VL) showed an ideal level of potash i.e., 50.67 mg/kg and 44 mg/kg respectively.

Sulphur (S) is present in the soil as sulphate (SO_4) and the average sulphate level was recorded to be 18.71 mg/kg. The maximum value was recorded in AC (24 mg/kg) and the lowest was recorded in AO (16.27). Table 1 indicates that non-shaded soil or soil without shade trees (WST) contained a huge amount of sulphate compared to other samples.

Effect of shade tree leaf extract on the growth of Rhizospheric Microbial Consortia (RMC)

Aqueous extracts of shade tree leaf from AO, AC, DS, DR, Alen, LL and MA showed variable inhibition zones against consortia isolated from soil under different shade trees of tea gardens including vacant land and shade tree free areas (Table 2 and Figure 1). In this study, we found that leaf extracts of DR showed an inhibitory effect on six consortia collected from under six regions whereas DS, AO and AC showed an inhibitory effect on consortia of five areas respectively. In most of the cases, consortia showed resistance towards leaf extract with a percentage of 53.96%, whereas, 46.03% of consortia were found to be susceptible. All the consortia from under each shade tree except DS (negligible inhibition zone 6mm), VL and WST, have shown resistance against their respective leaf extracts. This might be due to either the developed resistance of microbes present in soil which has been exposed to leaf litter year after year or it can be assumed that the leaf extracts do not possess any kind of antimicrobial compound. Most of the maximum inhibition zones were found on the consortia collected from under LL, meaning the consortia under this tree were susceptible to all the leaf extracts except its own leaf. Apart from the LL consortia, leaving behind the consortia from LL, the highest inhibition zones were seen on the consortia of AC and AO, created by the extract of DS (17mm and 15mm respectively), followed by MA, VL which was inhibited by AO leaf extract 15mm respectively. So, leaf extracts of DS and AO possess some antimicrobial compounds, due to which some microbes of the consortia are susceptible.

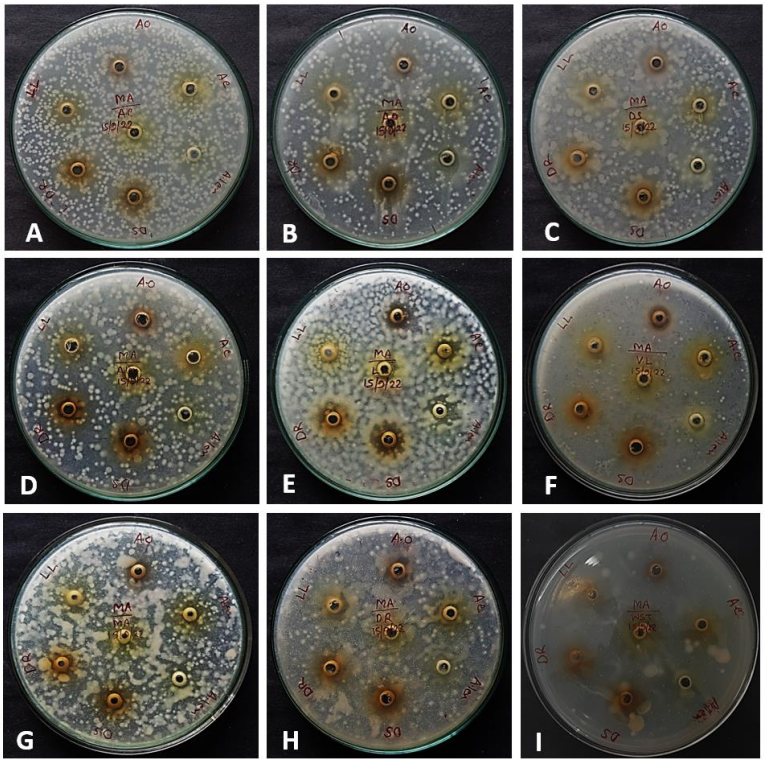

Figure 1. Resistance and susceptibility of consortia against different shade tree leaves extract where (A-I) represents the Consortia culture collected from under the AC, AO, DS, AL, LL, VL, MA, DR, WST respectively

Table 2. Inhibition zone (mm) created by leaf extracts on different consortia

	AC	AO	AL	DS	DR	LL	MA	VL	WST
AC	0	6	0	6	6	16	0	6	0
AO	0	0	0	6	0	18	15	15	13
AL	0	6	0	6	0	21	0	6	0
DS	17	15	7	6	0	18	0	0	0
DR	7	7	14	6	0	7	0	6	13
LL	0	0	0	0	0	0	0	0	0
MA	0	0	6	6	0	14	0	0	0

Albizia chinensis (AC), *Albizia odoratissima* (AO), *Acacia lenticularis* (AL), *Dalbergia sissoo* (DS), *Derris robusta* (DR), *Leucaena leucocephala* (LL), *Melia azedarach* (MA), Vacant land (VL) and WST (Without shade tree)

Heavy metal tolerance assay

Contamination occurring from metals like mercury (Hg), arsenic (As), and cadmium (Cd) etc. poses a serious toxic threat to all living organisms as it can cause cancer in humans when present in small quantities (Acharyya et al., 2021). These traumatic and stressful surroundings often encourage microbial populations to adapt and gain tolerance toward the metals. As this region is under the Himalayan range, it is prone to exposure to elevated levels of heavy metals which encourage microbes to build tolerance towards them. Therefore, we intended to study the heavy metal tolerance ability of the consortium presence in this region. The inhibition zones formed by selected heavy metals salt on isolated consortia from the tea plantations are shown in Figure 2 and Figure 3. Inhibition zones created by As_2O_3, $CdCl_2$, $CuCl_2$, and Pb $(NO_3)_2$ were less but in case of $HgCl_2$, the inhibition zones were much higher compared to other heavy metal salts (Table 3). Almost all the consortia have shown tolerance or are gaining tolerance against Lead nitrate, Arsenic trioxide and Cupric chloride, whereas the salts of cadmium and mercury produced inhibition zones against all the consortia.

Table 3. Inhibition zones (mm) exhibited by heavy metals on different consortia Colour code: 0 =Tolerant (Red), 6-9= mildly tolerant (Yellow), 10-17= moderately susceptible (Blue), 18 and above= Susceptible (green))

	Lead nitrate $Pb(NO_3)_2$	Arsenic trioxide AS_2O_3	Cadmium chloride $CdCl_2$	Cupric chloride $CuCl_2$	Mercuric chloride $HgCl_2$
AC	14	0	17	0	25
AO	0	0	12	0	25
AL	0	0	9	0	13
DS	6	0	7	0	20
DR	6	0	20	6	16
LL	0	0	10	0	15
MA	0	6	6	0	10
VL	6	6	10	0	31
WST	0	0	11	0	32

Albizia chinensis (AC), *Albizia odoratissima* (AO), *Acacia lenticularis* (AL), *Dalbergia sissoo* (DS), *Derris robusta* (DR), *Leucaena leucocephala* (LL), *Melia azedarach* (MA), Vacant land (VL) and WST (Without shade tree)

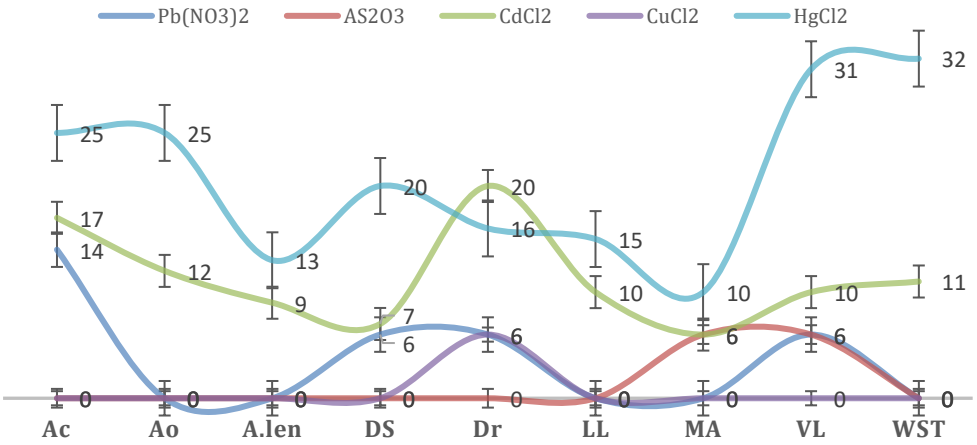

Figure 2. Graphical representation of resistance and susceptibility pattern of consortia against five heavy metal salts (x axis representing different consortia and y axis representing inhibition zones)

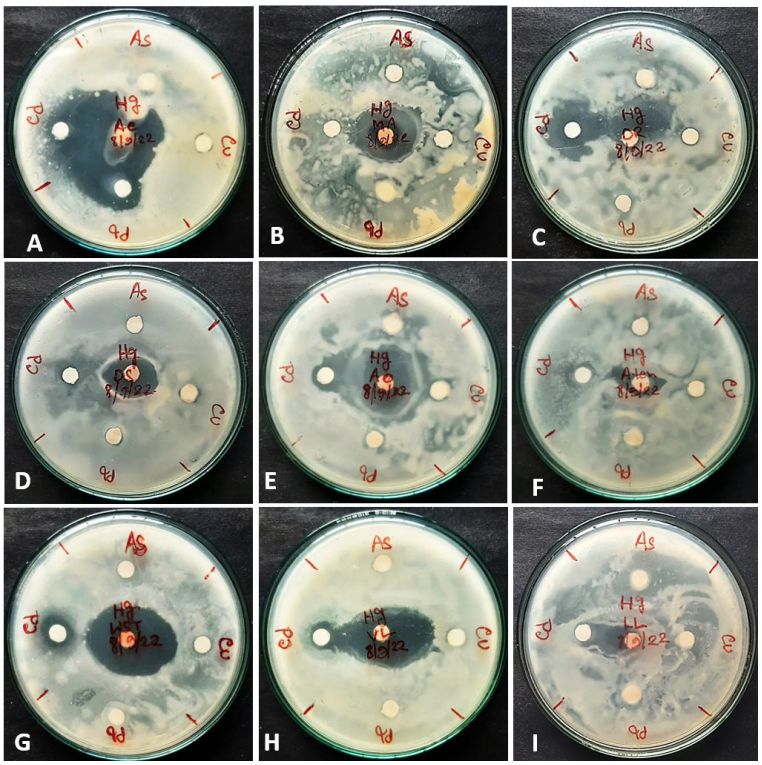

Figure 3. Resistance and susceptibility of consortia culture against five different heavy metal salts, where (A-I) represents the Consortia, culture collected from under the different areas of AC; MA; DR; DS; AO; AL; WST; VL; LL respectively

Antibiotic tolerance assay

Bacteria and fungi are the main biotic components of the microflora of soil consortia. Since its discovery, antibiotics have been used extensively. These antibiotics tend to accumulate in soil and water, eliciting an effect on beneficial microorganisms harbored in these regions (Saha et al., 2020). In recent years, antibiotics have become very handy for treatment against various bacterial infections, be it as medication for humans to livestock rearing. The use of antibiotics in agricultural fields has also gained momentum as a means to rid the fields of unwanted, harmful bacterial invasions. Improper knowledge of dosage can often lead to a disastrous end. With the development in the field of science, synthetic antibiotics have become a convenient choice. The secondary metabolites from the leaves and pods, often contain antimicrobial (antibacterial or antifungal) compounds. Hence, this study was carried out to understand the behaviour of the isolates in the face of some common antibiotics. Eleven different antibiotics were used for this study.

Studies revealed that different antibiotics act differently on consortia. Results of the antibiotic tolerance assay have been expressed in Table 4 and Figure 4. In Table 4 of the nine samples which had been tested against eleven different antibiotics indicated that 35.35 % of samples were tolerant against above mentioned antibiotics, while 22.22 % of samples were susceptible to those antibiotics. Besides these, 16.16 % of samples exhibited mild tolerance and 26.26 % of samples showed moderate tolerance levels. Among the different shade tree cover soil microbes, AC, MA and LL showed tolerance against maximum antibiotics. On the contrary, DR showed a more or less susceptible nature against all used antibiotics.

Table 4. Inhibition zone (cm) of different samples tested against different antibiotics (Colour code: 0 =Tolerant (Red), 0.1-1= mildly tolerant (Yellow), 1.1-2= moderately susceptible (Blue), 2 and above= Susceptible (green))

	AC	AO	AL	DS	DR	LL	MA	VL	WST
Chloramphenicol	0.5	1.3	0.9	0.6	1.6	0.7	0.8	0.8	0.4
Ofloxacin	2.3	2.5	2.6	2.4	2	2.5	2.6	2.4	2.2
Cefotaxime	1	2.5	2.6	1.5	2.5	2	0	0.9	1.6
Erythromycin	0	2.5	2.5	0.8	2	0	0	0.9	0
Co-Trimoxazole	0	0	0	0	1.6	0	0	0	0
Augmentin	0	0	0	0	2.3	0	0	0	0
Bacitracin	0	0	1.1	0	0.9	0	1	0	1
polymyxin B	1.1	1.3	1.2	1	1.5	1.3	1.2	1.2	0.9
Gentamicin	0.8	2.5	1.2	2.3	1.5	1	1.5	0.8	1.8
Neomycin	0	2.4	2	2	0	1.3	1	0.8	2.2
Penicillin G	0	0	1.3	0	0	0	0	0	1.1

Albizia chinensis (AC), *Albizia odoratissima* (AO), *Acacia lenticularis* (AL), *Dalbergia sissoo* (DS), *Derris robusta* (DR), *Leucaena leucocephala* (LL), *Melia azedarach* (MA), Vacant land (VL) and Without shade tree (WST)

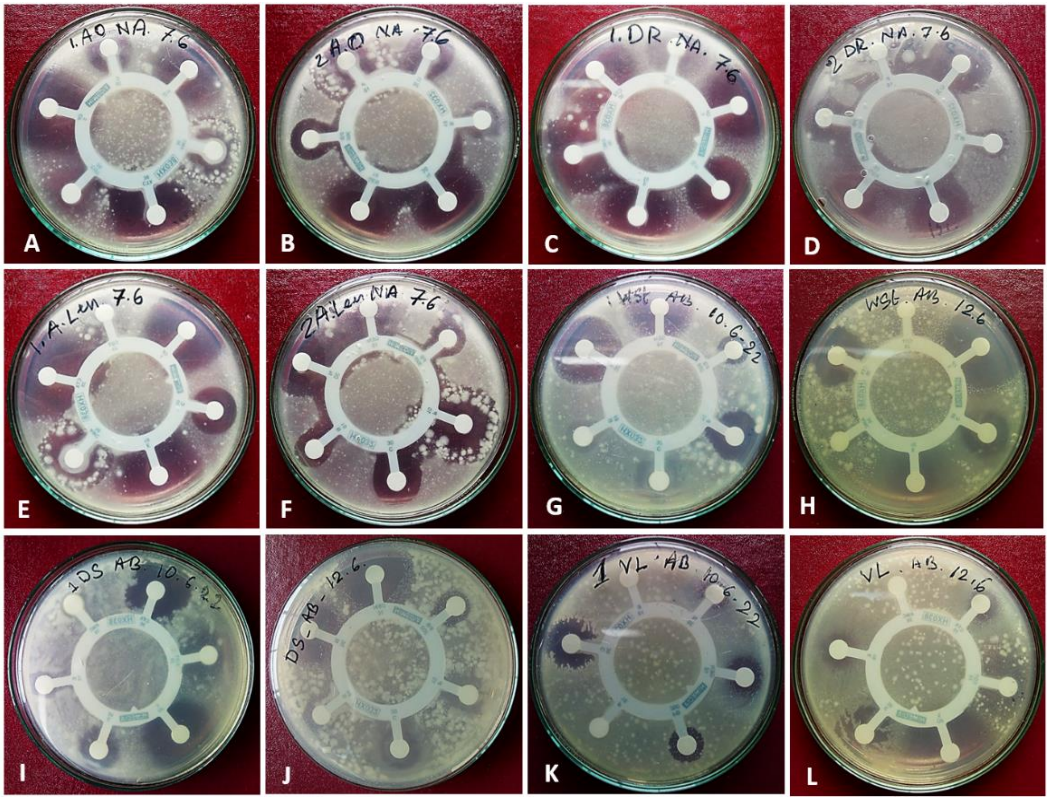

Figure 4. Antibiotic susceptibility and resistance of different consortia where (A-L) represent the consortia culture of under from AO; DR; AL; WST; DS; VL respectively

Co-Trimoxazole and Augmentin exhibited the lowest efficacy in inhibiting the *in vitro* growth of the bacterial populations isolated from the soil samples under the cover of all the shade trees selected for this study, except for DR, which showed considerable susceptibility as seen from the graph Figure 4. On the other hand, Ofloxacin showed the highest efficacy in terms of inhibition zone against the bacterial populations isolated from the cover region of all the shade trees.

Out of the eleven antibiotics tested OF5 (2.388±0.19 cm) showed average maximum and COT25 (0.177 ± 0.53 cm) showed minimum inhibition zone. So, it can be considered that COT25 was the least effective and OF5 was the most effective for the isolated consortia. The increasing order of tolerance observed in our study is COT25; AMC30; P10; B10; C30; E10; PB300; N30; Gen10; CTX30; OF5 (Table 4).

Antifungal tolerance assay

Fungal invasions are also a great threat to plants. Thus, needless to say, the use of antifungals in agriculture is an inevitable solution that people reach for to get rid of fungal infections/fungi. With the application of antifungals, there comes a possibility of developing antifungal tolerance by the fungal populations. Also, the antimicrobial components present in the dropped plant parts may play a role too just as in the case of antibiotics mentioned above. Therefore, the study of antifungal tolerance by the isolates has become an absolute necessity. Antifungals used in the assay have different target patterns for different fungi present in the consortia. The data for the antifungal assay are represented in Table 5 and Figure 5 concerning their tolerance ability. The data represents the tolerance pattern of the fungal population isolated from the soil samples of the respective shade trees. Fungicides having azole groups are the most widely used antifungals against fungal plant pathogens (Saha et al., 2020). In this study, we have used four antifungals viz. CC10, FLC25, IT10 and KT10 have azole groups. All the samples have full resistance against the five antifungals i.e., Amphotericin-B (AP100), Clotrimazole (CC10), Fluconazole (FLC25), Ketoconazole (KT10), and Nystatin (NS 100) i.e., they have not shown any inhibitory effect in the consortia. Itraconazole (IT10), on the other hand, has shown an inhibitory effect in all the consortia, wherein the sample of AC, MA and VL, it showed a full inhibition zone of 3.5cm each, followed by 3cm; 2.4cm; 2.3cm in AL, WST and DS respectively and 2.2 cm in three samples of AO; DR and LL.

Pesticide tolerance assay

Based on the application of pesticides in tea plantations, the nine most regularly used pesticides were selected and *in vitro* tolerance assay was done to find out the level of tolerance in isolated consortia. Over a period of time, chemical pesticides in tea plantations accumulate in an area of soil where microbial diversity is at its

maximum level. In our study, our consortia showed variable levels of tolerance against different concentrations of each pesticide (Table 6 and Figure 6). Four pesticides viz. Spiromesifen; Thiamethoxam, Phorate and Flubendiamide showed no inhibition zone in any of the consortia at the studied concentrations. So, consortia isolated from underneath all the shade trees, vacant land and without shade trees are tolerant to all concentrations of pesticides. All the pesticides, except Fenazaquin, showed inhibition zones only above 5mg/ml concentrations. So, this concludes that all the consortia from tea plantations are highly tolerant against these pesticides (excluding Fenazaquin) at these concentrations. Fenazaquin showed a gradual increase in inhibition zone with an increase in concentration against consortia of AO, AL and WST, whereas against the consortia of AC and DS, this pesticide showed a density gradient increase in inhibition zones in all the higher concentrations but no inhibition zone was found at the lowest concentration. Deltamethrin also showed a gradual increase in inhibition zones in all the higher concentrations against the consortia collected from under AC, AO and DS but with the concentration of 2.5mg/ml, there were zero inhibition zones.

Table 5. Inhibition zone (cm) of different samples tested against different antifungals (Colour code: 0=Tolerant (Red), 2.1-3= moderately susceptible (Blue), 3.5 and above= Susceptible (green))

	AC	AO	AL	DS	DR	LL	MA	VL	WST
Amphotericin B	0	0	0	0	0	0	0	0	0
Clotrimazole	0	0	0	0	0	0	0	0	0
Fluconazole	0	0	0	0	0	0	0	0	0
Itraconazole	3.5	2.2	3.0	2.3	2.2	2.2	3.5	3.5	2.4
Ketoconazole	0	0	0	0	0	0	0	0	0
Nystatin	0	0	0	0	0	0	0	0	0

Albizia chinensis (AC), *Albizia odoratissima* (AO), *Acacia lenticularis* (AL), *Dalbergia sissoo* (DS), *Derris robusta* (DR), *Leucaena leucocephala* (LL), *Melia azedarach* (MA), Vacant land (VL) and Without shade tree (WST)

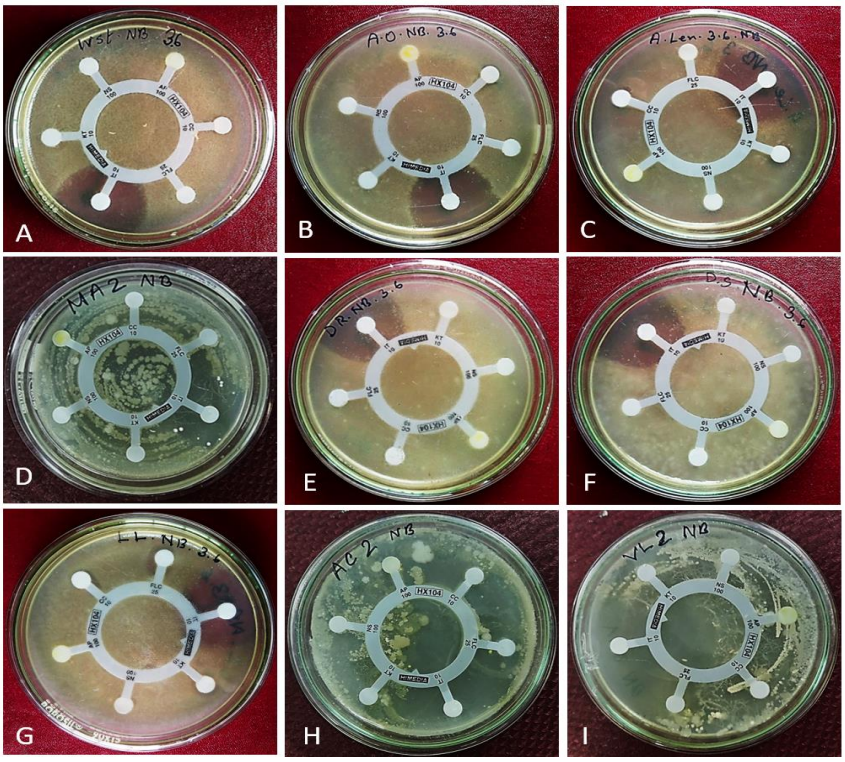

Figure 5. Tolerance and susceptibility of consortia against six different Antifungal agents where (A-I) represents the consortia culture under from WST, AO, AL, MA, DR, DS, LL, AC, VL respectively

Discussion

In this study we have found that all the soil are found to be acidic the possible reason behind this because that maximum shade trees belong to the Fabaceae family that characteristically shed their leaves once a year and contribute to the accumulation of a massive amount of organic matter and simultaneously increases organic carbon and nitrogen content in the soil. Being a non-leguminous plant, MA shade tree cannot form root nodules; thus, nitrogen content was also low in its cover soil. In the presence of a good amount of mineral nutrition and organic matter, microorganisms thrive and produce humic acid in the soil consequently decreasing the pH. Table 1 reveals that the MA shade tree contributes the least amount of organic matter to the soil. Furthermore, the shed leaves of MA may contain some chemical compounds that can inhibit the

growth of microorganisms, thereby limiting the pH drop that would otherwise have resulted from the profuse growth of microbes as previously discussed.

The maximum quantity of phosphate also came from leaf litter and organic matter. Leaves of certain shade tree species like AC, LL, AO and AL may provide a good amount of phosphorus (Table 1) which leads the phosphate solubilizing microorganisms to digest the phosphorus as substrate to produce an available form of phosphate for plant uptake, while, DR (11.33) and DS (24.33) might have some antagonistic effect (antibacterial effect) on these microorganisms as the results suggest. Recently, Ghosh et al. (2021) reported the antibacterial activities of these leaves against microorganisms. Table 1 shows that where electrical conductivity is higher, consequently potassium level is lower, it is because of the leaching of potassium ions into subsoil. Lack of nutrient management system and fertilizer application in tea gardens could be the reason behind unfamiliar results (unlike other nutrient parameters) or the high amount of sulphate present in non-shade areas or without shade tree regions.

Based on our heavy metal tolerance assay, it can be presumed that the isolated consortia are tolerant or slightly tolerant towards metals like Pb, As and Cu but susceptible towards Cd and Hg. The tolerance property of these consortia towards heavy metal salts like As_2O_3, $CuCl_2$, and $Pb(NO_3)_2$ is a serious concern as it may have been stimulated by the persistence of these salts in soil.

Table 6. Inhibition zones (mm) exhibited by concentrations of pesticide on different consortia (Colour code: 0= Tolerant (Red), 10-12= moderately susceptible (Yellow), 13 and above= Susceptible (green).)

Pesticides	Time	Concentration	AC	AO	DS	DR	Al	LL	MA	VL	WST
Emamectin benzoate	x	2.5mg/ml	0	0	0	0	0	0	0	0	0
	2x	5mg/ml	0	0	13	0	0	0	0	0	0
	4x	10mg/ml	0	11	16	0	0	0	0	0	0
	8x	20mg/ml	0	12	17	0	15	0	0	0	0
Fipronil+Imidacloprid	x	2.5mg/ml	0	0	0	0	0	0	0	0	0
	2x	5mg/ml	0	0	0	0	0	0	0	0	0
	4x	10mg/ml	0	11	0	0	0	0	0	0	0
	8x	20mg/ml	0	13	0	11	12	12	0	0	0
Spiromesifen	x	2.5mg/ml	0	0	0	0	0	0	0	0	0
	2x	5mg/ml	0	0	0	0	0	0	0	0	0
	4x	10mg/ml	0	0	0	0	0	0	0	0	0
	8x	20mg/ml	0	0	0	0	0	0	0	0	0
Thiamethoxam	x	2.5mg/ml	0	0	0	0	0	0	0	0	0
	2x	5mg/ml	0	0	0	0	0	0	0	0	0
	4x	10mg/ml	0	0	0	0	0	0	0	0	0
	8x	20mg/ml	0	0	0	0	0	0	0	0	0
Deltamethrin	x	2.5mg/ml	0	0	0	0	0	0	0	0	0
	2x	5mg/ml	12	11	11	0	0	0	0	0	0
	4x	10mg/ml	16	13	12	0	14	0	0	0	0
	8x	20mg/ml	16	14	15	14	16	0	0	0	0
Phorate	x	2.5mg/ml	0	0	0	0	0	0	0	0	0
	2x	5mg/ml	0	0	0	0	0	0	0	0	0
	4x	10mg/ml	0	0	0	0	0	0	0	0	0
	8x	20mg/ml	0	0	0	0	0	0	0	0	0
Flubendiamide	x	2.5mg/ml	0	0	0	0	0	0	0	0	0
	2x	5mg/ml	0	0	0	0	0	0	0	0	0
	4x	10mg/ml	0	0	0	0	0	0	0	0	0
	8x	20mg/ml	0	0	0	0	0	0	0	0	0
Quinalphos	x	2.5mg/ml	0	0	0	0	0	0	0	0	0
	2x	5mg/ml	0	10	0	0	0	0	0	0	0
	4x	10mg/ml	10	11	0	0	11	0	0	0	0
	8x	20mg/ml	11	12	0	0	11	0	0	0	0
Fenazaquin	x	2.5mg/ml	0	11	0	0	11	0	0	0	11
	2x	5mg/ml	11	13	11	0	13	0	0	0	12
	4x	10mg/ml	12	14	12	0	13	0	0	0	15
	8x	20mg/ml	14	14	14	0	15	0	0	0	17

Albizia chinensis (AC), *Albizia odoratissima* (AO), *Acacia lenticularis* (AL), *Dalbergia sissoo* (DS), *Derris robusta* (DR), *Leucaena leucocephala* (LL), *Melia azedarach* (MA), Vacant land (VL) and Without shade tree (WST)

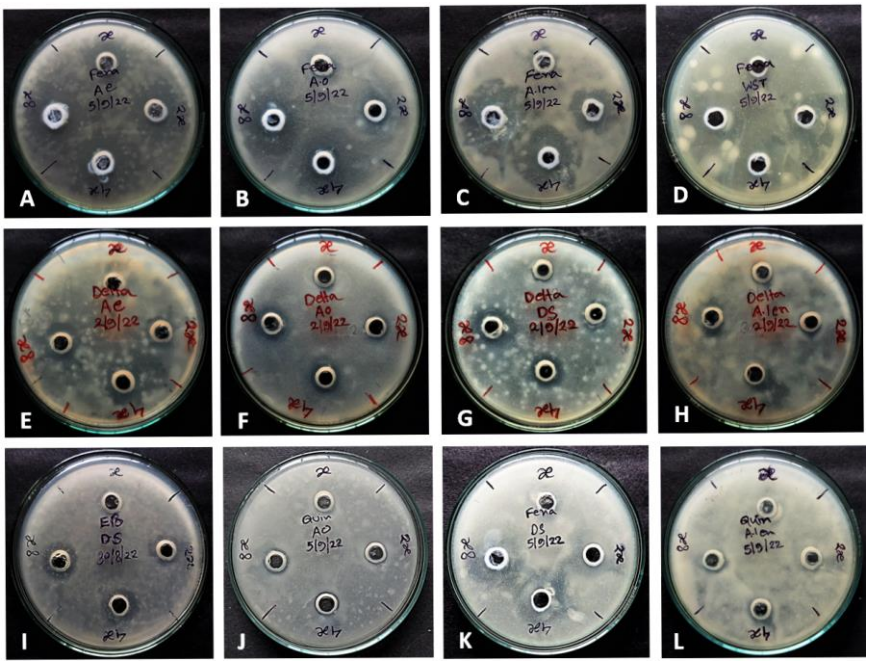

Figure 6. Resistance and susceptibility of consortia culture against different pesticides with different concentrations where (A-L) represents the Consortia culture collected from under the different shade trees AC; AO, AL; WST; DS

The exploitation of antibiotics/antifungals in agricultural fields can lead to the eradication of the useful bacterial/fungal populations that inhabit the soil and thereby have an effect on the nutrient uptake processes of plants. There also lies the risk of developing antibiotic/antifungal tolerance by the bacterial/fungal population. Initially, these compounds were isolated from the secondary metabolites produced by microorganisms such as bacteria and fungi. In this antibiotic tolerance assay, though a few antibiotics were found to be ineffective against some of the microbes, most of them elicited a considerable range of susceptibility from the microbes. Their pattern of tolerance is mainly based on the respective shade tree cover region from where the soil sample was collected, as we can see in case of DR.

On an average farmers use antibiotics in their agricultural fields with the intention of getting rid of the harmful bacteria that may affect the plants (Saha et al., 2020). But while doing this, it also increases the chances of developing antibiotic resistant microbes. This could be the possible reason for the acquisition of tolerance by some of the bacterial populations. Another reason for such tolerance may have to do with antimicrobial components detected in the shed parts of the trees. Photographs of some plates have been attached below (Figure 4).

In the antifungal assay, a resistance pattern towards all the antifungals except IT10 has been found which may be a result of the unsupervised overuse of fungicides in tea plantations or another plausible reason may be the possible co-selection of resistance genes under selective pressure of survival related to other elements like heavy metals (Sun et al., 2021). Hence, we could conclude that IT10 is probably not used as much or use of this is close to nil in this tea plantation.

Pesticides are very toxic and harmful to the ecosystem as they accumulate in soil. It brings changes in soil microflora by killing and reducing the microflora count or diversity or may even modify tolerance towards the pesticides for resisting pesticides. Pesticides have a half-life and the half-life of Phorate is more than Emamectin Benzoate and the mixture of Fipronil and Imidacloprid. Phorate is slightly soluble in water when kept over time and 2g of this is added to the soil during the plantation of plantlets and is not spread further in later years. Prolonged use of cultural practices like the use of chemical pesticides could be the reason for tolerance observed in the microbial population.

Probable candidates of leaf extracts for growth inhibition validates by GC-MS

To find out the probable reason for getting inhibition zone in the different cultures of consortia by the shade tree leaf extracts, we have done Gas chromatography and mass spectrometry analysis. In our GC-MS analysis, we found a total of 74 compounds in the leaf extracts of seven shade trees having microbial properties, where 11 compounds were from each extract of AO, DS, AL and MA comprising 14.86%, 13 compounds from DR adding up to 17.56%, 9 in AC at 12.16%; and 8 compounds in LL of 10.81% (Table 7).

Phytol, an acyclic diterpene, has an antimicrobial effect against *Pseudomonas aeruginosa*, *Maphomina phaseolina* and triterpene compound squalene also has antimicrobial activity (Saha et al., 2022). Both of these compounds have been detected in all the leaf extracts (Table 7). Neophytadiene, another antimicrobial component has been found in all the extracts except MA (Non-leguminous). 1-Heptanol, 2-propyl-; .gamma. -

Linolenic acid, methyl ester; Cyclopentadecanone, 2-hydroxy-; Dehydroabietylamine; Longifolene; Longiborneol (activity against *Candida albicans, Trichophyton rubrum, Aspergillus fumigatus*, *Staphylococcus aureus*); 9,12-Octadecadienoic acid, methyl ester was only found in AO and are reported to have antimicrobial property, only found in AO, whereas in the extracts of AC, 13-Hexyloxacyclotridec-10-en-2-one; Dehydroabietic acid and its TMS derivative; Ethanone, 1-phenyl-; and Menthol were unique. Tetradecane and 9-octadecenal, (z)- were only found in DS. Four reportedly antimicrobial compounds, (2e)-3,7,11,15-tetramethyl-2-hexadecene; 9-Octadecenoic acid, methyl ester, (E)-; Hexadecanoic acid; and Methyl abieta-8,11,13-trien-18-oate were only distinguished in DR. beta- amyrin; Octadecane and Methyl commate d with 22.58% area were detected in AL. 2-methyloctacosane is the only compound found in MA, reported to have antimicrobial properties. In the leaf extract of LL, no particular compounds were found to be unique but two compounds Phenol, 2,4-bis(1,1-dimethylethyl)-, phosphite (3:1) and vitamin E with antimicrobial activity were found with a high percentage of 20.75 and 12.88 peak area respectively. Antimicrobial compounds worth 17.56% were found in the leaf of DR. In the consortia of DR, we found almost no inhibition. With a percentage of 10.81 in the leaf extracts of LL, it showed the lowest number of antimicrobial compounds (Figure 7). The consortium of LL was found to be susceptible except to the extract of LL. Thus, it can be said that leaf litter do have an impact on the growth of microflora and can restrict the beneficial microorganisms of soil.

Table 7. GC-MS detected compounds with peak area percentage and antimicrobial activity

Compounds with antimicrobial activity	**GC-MS (Peak area %)**							**References**
	AO	**AC**	**DS**	**LL**	**DR**	**AL**	**MA**	
1-Heptanol, 2-propyl-	3.69	8.7						Saha et al., 2022
13-Hexyloxacyclotridec-10-en-2-one		1.34						Saha et al., 2022
Beta-Amyrin						8.64		Elfadil et al., 2015
Gamma. -Linolenic acid, methyl ester	1.4							Saha et al., 2022
Cyclopentadecanone, 2-hydroxy-	0.61							Saha et al., 2022
Dehydroabietic acid and its TMS derivative		1.42						Saha et al., 2022
Dehydroabietylamine	0.81							Saha et al., 2022
Ethanone, 1-phenyl-		1.27						Saha et al., 2022
Neophytadiene	4.94	1.27	6.67	2.29	10.30	5.71		Singh et al., 2012
Phytol	5.64	1.77	29.48	0.52	23.46	7.15	47.14	Islam et al., 2018
Squalene	5.59	8.7	7.80	5.99	3.95	14.73	1.42	Rautela et al., 2017
Longifolene	1.04							Saha et al., 2022
Longiborneol	3.14							Saha et al., 2022
1,2-Benzenedicarboxylic acid, diethyl ester	2.55	1.45						Premjanu and Jaynthy, 2014
9,12-Octadecadienoic acid, methyl ester	2.13							Saha *et al*., 2022
Heptadecane			1.29		0.85		2.54	Adeyemi et al., 2017
Tetradecane			1.80					Nambi and Raju, 2017
Dodecane, 4,6-dimethyl-			1.22	1.07	0.72	1.34	1.85	Añides et al., 2019
Heneicosane			5.51	0.75	1.62	2.38	2.17	Vanitha et al., 2020
Eicosane			8.75	2.61	1.62	0.87	5.84	Octarya et al., 2021
9-octadecenal, (z)-			1.69					Subavathy and Thilaga, 2016
Gamma.-sitosterol			6.12				7.89	Akpuaka et al., 2013
Methyl Commate b			10.86			3.76		Arora and Kumar, 2017
Menthol		1.80						Freires et al., 2015
Phenol, 2,4-bis(1,1-dimethylethyl)-, phosphite (3:1)				20.75			2.32	Tyagi et al., 2021
Trimethylsilyl 2,6-bis[(trimethylsilyl)oxy] benzoate					0.22		0.33	Ajala et al., 2020
(2e)-3,7,11,15-tetramethyl-2-hexadecene					0.37			Mickymaray and Alturaiki, 2018
9-Octadecenoic acid, methyl ester, (E)-					1.90			Muflihunna et al., 2021
Hexadecanoic acid					0.63			Hameed et al., 2015
Methyl abieta-8,11,13-trien-18-oate					0.42			Burčová et al., 2018
Octadecane						0.65		Adeyemi et al., 2017
Methyl commate d						22.58		Bihana et al., 2018
2-methyloctacosane							0.80	Pelo et al., 2021
Vitamin E				12.88	9.08	15.61	2.94	Hartmann et al., 2020
% Of total antimicrobial compounds detected through GC-MS	31.54	27.72	81.19	46.86	55.14	83.42	75.24	

Albizia chinensis (AC), *Albizia odoratissima* (AO), *Acacia lenticularis* (AL), *Dalbergia sissoo* (DS), *Derris robusta* (DR), *Leucaena leucocephala* (LL), *Melia azedarach* (MA)

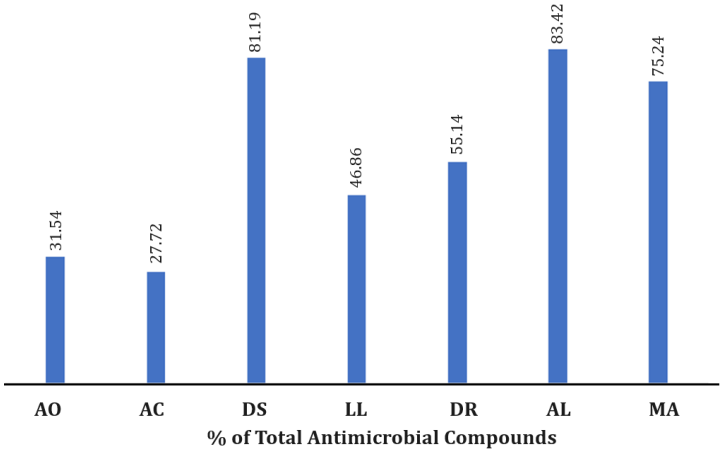

Figure 7. Percentage of total reported antimicrobial compounds detected by GC-MS in each extract

Conclusion

This research was conducted to investigate the effects of shed leaves on the soil microflora; as well as, to analyze important parameters like soil physicochemical properties, antibiotic, antifungal, heavy metal and pesticide tolerance abilities to characterize the tea garden soil covered by different shade trees. Variations in the results have been detected among soil samples (under shade trees, non-shade tree areas and vacant land) and after comparative study bring about an interesting conclusion. Shed leaf litter from these deciduous trees surely adds a huge amount of organic matter to the soil of tea gardens. Leguminous shade trees can also increase nitrogen fixation, but due to the antimicrobial effects of leaf litter or otherwise, the soil microflora can be adversely affected which is detrimental to the soil of tea plantations. However, as these shade trees are an indispensable part of the tea plantations in the plains of North Bengal they cannot be removed from the plantation. Replacement of these shade plants with other shade trees could be a probable option although further studies are needed as well. Besides these, other factors should be given thorough consideration to maintain a thriving and diverse system of beneficial microflora in tea garden soil; such as limited use of chemical pesticides and fertilizers. So, the results of this study give us a detailed understanding of the continued use of each and every shade tree in this region to inform our judgment about the overall impact of the studied shade trees on these plantations

References

Acharyya, S., Saha, S., Majumder, S., Bhattacharya, M., 2021. Characterization of a mercury tolerant strain of *Staphylococcus arlettae* from Darjeeling hills with an account of its antibiotic resistance pattern and metabolome. *Archive in Microbiology* 203: 5745-5754.

Adeyemi, M.A., Ekunseitan D.A., Abiola S.S., Dipeolu M.A., Egbeyale L.T., Sogunle, O.M., 2017. Phytochemical analysis and GC-MS determination of *Lagenaria breviflora* R. fruit. *International Journal of Pharmacognosy Phytochemical Research* 9: 1045-1050.

Ajala, E.O., Ajala, M.A., Tijani, I.A., Adebisi, A.A., Suru, I., 2020. Kinetics modelling of acid hydrolysis of cassava (*Manihot esculanta* Cranz) peel and its hydrolysate chemical characterisation. *Journal of King Saud University- Science* 32: 2284-2292.

Akpuaka, A., Ekwenchi, M.M., Dashak, D.A., Dildar, A., 2013. Biological activities of characterized isolates of n-hexane extract of *Azadirachta indica* A. Juss (Neem) leaves. *Nature and Science*. 11: 141-147.

Añides, J.A., Dapar, M.L.G., Aranas, A.T., Mindo, R.A.R., Manting, M.M.E., Torres, M.A.J., Demayo, C.G., 2019. Phytochemical, antioxidant and antimicrobial properties of the white variety of 'Sibujing'(*Allium ampeloprasum*). *Pharmacophore* 10: 1-12.

Arora, S., Kumar, G., 2017. Gas Chromatography-Mass Spectrometry (GC-MS) determination of bioactive constituents from the methanolic and ethyl acetate extract of *Cenchrus setigerus* Vahl (Poaceae). *The Pharma Innovation Journal* 6(11): 635-640.

Bihana, S., Dhiman, A., Singh, G., Satija, S., 2018. Gas chromatography-mass spectroscopy analysis of bioactive compounds in the whole plant parts of ethanolic extract of *Asclepias Curassavica* L. *International Journal of Green Pharmacy* 12(2): 107-114. .

Burčová, Z., Kreps, F., Greifová, M., Jablonský, M., Ház, A., Schmidt, Š., Šurina, I., 2018. Antibacterial and antifungal activity of phytosterols and methyl dehydroabietate of Norway spruce bark extracts. *Journal of Biotechnology* 282: 18-24.

Elfadil, H., Fahal, A., Kloezen, W., Ahmed, E.M., van de Sande, W., 2015. The *in vitro* antifungal activity of Sudanese medicinal plants against *Madurella mycetomatis*, the eumycetoma major causative agent. *PLoS Neglected Tropical Disease* 9: e0003488.

Freires, I.A., Denny, C., Benso, B., Alencar, S.M.D., Rosalen, P.L., 2015. Antibacterial activity of essential oils and their isolated constituents against cariogenic bacteria: a systematic review. *Molecules* 20: 7329–7358.

Ghosh, A., Majumder, S., Saha, S., Chakraborty, S., Bhattacharya, M., 2021. Leaves and barks of *Albizia* shade trees in tea plantation shows both insect attractant and pesticidal properties: a GC-MS based investigation. *Asian Journal of Agriculture* 5: 84-89.

Ghosh, A., Majumder, S., Sarkar, S., Bhattacharya, M., 2022. Insights into physicochemical assessment of shade tree litter biomass in tea plantations of Terai region. *International Journal of Sustainable Agricultural Research* 9: 46-54.

Hameed, I.H., Hussein, H.J., Kareem, M.A., Hamad, N.S., 2015. Identification of five newly described bioactive chemical compounds in methanolic extract of *Mentha viridis* by using gas chromatography-mass spectrometry (GC-MS). *Journal of Pharmacognosy and Phytotherapy* 7: 107-125.

Hartmann, M.S., Mousavi, S., Bereswill, S., Heimesaat, M.M., 2020. Vitamin E as promising adjunct treatment option in the combat of infectious diseases caused by bacterial including multi-drug resistant pathogens–Results from a comprehensive literature survey. European *Journal of Microbiology and Immunology* 10: 193-201.

Islam, M.T., Ali, E.S., Uddin, S.J., Shaw, S., Islam, M.A., Ahmed, M.I., Shill, M.C., Karmakar, U.K., Yarla, N.S., Khan, I.N., Billah, M., Pieczynska M.D., Zengin, G., Malainer, C., Nicoletti, F., Gulei, D., Neagoe, L.B., Apostol, A., Banach, M., Yeung, A.W.K., Atanasov, A.G., 2018. Phytol: A review of biomedical activities. *Food and Chemical Toxicology* 121: 82-94.

Malviya, M.K., Solanki, M.K., Li, C.N., Htun, R., Singh, R.K., Singh, P., Li, Y.R., 2021. Sugarcane microbiome: role in sustainable production. In: Microbiomes and Plant Health. Kumari, B., Solanki, M.K., Kashyap, P.L., Ansari, R.A., Academic Press, Elsevier pp. 225-242.

Mickymaray, S., Alturaiki, W., 2018. Antifungal efficacy of marine macroalgae against fungal isolates from bronchial asthmatic cases. *Molecules* 23: 3032.

Muflihunna, A., Mu'nisa, A., Hala, Y., 2021. Gas chromatography-mass spectrometry (GC-MS) analysis and antioxidant activity of sea-cucumber (*Holothurian atra* and *Holothurian edulis*) from Selayar Island. Journal of Physics Conference Series, IOP Publishing. 1752, 012057.

Mukherjee, M., Chakraborty, S., Sarkar, S., Saha, S., Majumder, S., Ghosh, A., Bhattacharya, M., 2020. Soil nutritional status of tea plantations in plains of sub–Himalayan West Bengal, India. *Current Agricultural Research* 8(3): 239-246.

Nambi, S.K., Raju, R., 2017. GC-MS analysis of n-Hexane Extract of Fruits of *Trichopus zeylanicus* ssp. travancoricus Burkill ex K. Narayanan. *Pharmacognosy Journal* 9: 99-102.

Octarya, Z., Novianty, R., Suraya, N., Saryono, S., 2021. Antimicrobial activity and GC-MS analysis of bioactive constituents of *Aspergillus fumigatus* 269 isolated from Sungai Pinang Hot Spring, Riau, Indonesia. *Biodiversitas Journal of Biological Diversity* 22: 75-85.

Pandey, A., Tripathi, A., Srivastava, P., Choudhary, K.K., Dikshit, A., 2019. Plant growth-promoting microorganisms in sustainable agriculture, In: Role of plant growth promoting microorganisms in sustainable agriculture and nanotechnology. Kumar, A., Singh, A.K., Choudhary, K.K. (Eds.). Elsevier Science. Amsterdam, pp. 1-19.

Pelo, S.P., Adebo, O.A., Green, E., 2021. Chemotaxonomic profiling of fungal endophytes of *Solanum mauritianum* (alien weed) using gas chromatography high resolution time-of-flight mass spectrometry (GC-HRTOF-MS). *Metabolomics* 17: 1-13.

Premjanu, N., Jaynthy, C., 2014. Antimicrobial activity of diethyl phthalate: an *in-silico* approach. *Asian Journal of Pharmaceutical and Clinical Research* 7: 141-142.

Rautela, I., Sharma, M.D., Sharma, N., Kishor, K., Singh, K., Sharma, N., 2017. Comparative GC-MS analysis of leaf and root extract of medicinal plant *Withania somnifera*. *World of Journal Pharmaceutical Research* 7: 956-972.

Saha, S., Acharyya, S., Sarkar, S., & Bhattacharya, M., 2021. Study of tolerance ability in phosphate solubilising microorganisms isolated from tea plantations soil of lower Darjeeling hills. *Bulletin of the National Research Centre* 45: 109.

Saha, S., Chakraborty, S., Acharyya, S., Sahadeb, S., Majumder, S., Ghosh, A., Bhattacharya, M., 2020. Phosphate solubilizing microorganism consortium of virgin Tiger hill forest soil shows high level tolerance to pesticide, antibiotic, antifungal and heavy metals. *Ecobiotech* 3: 578-588.

Saha, S., Ghosh, A., Acharyya, S., Bhattacharya, M., 2022. Metabolites of *Albizia* inhibit *in vitro* growth of phosphate solubilizing microbial consortia isolated from tea garden soil of Darjeeling hills, India. *Biodiversitas Journal of Biological Diversity* 23: 2865-2870.

Sharma, A., Dutta, A.K., Bora, M.K., Dutta, P.P., 2019. Study of energy management in a tea processing industry in Assam, India. In: AIP Conference Proceedings: Current Trends in Renewable and Alternate Energy. 4–6 December 2018. Guwahati, India. 2091 (1): 020012.

Singh, R., Dar, S.A., Sharma, P., 2012. Antibacterial activity and toxicological evaluation of semi purified hexane extract of *Urtica dioica* leaves. *Research Journal of Medicinal Plants* 6: 123-135.

Subavathy, P., Thilaga, R.D., 2016. GC-MS analysis of bioactive compounds from whole body tissue methanolic extract of *Cypraea arabica* (L. 1758). *World Journal of Pharmaceutical Research* 5: 800-806.

Sun, F., Xu, Z., Fan, L., 2021. Response of heavy metal and antibiotic resistance genes and related microorganisms to different heavy metals in activated sludge. *Journal of Environmental Management* 300: 113754.

Tyagi, S., Singh, R.K., Tiwari, S.P., 2021. Anti-enterococcal and anti-oxidative potential of a thermophilic cyanobacterium, *Leptolyngbya* sp. HNBGU 003. *Saudi Journal of Biological Sciences* 28(7): 4022-4028.

Vanitha, V., Vijayakumar, S., Nilavukkarasi, M., Punitha, V.N., Vidhya, E., Praseetha, P.K., 2020. Heneicosane—A novel microbicidal bioactive alkane identified from *Plumbago zeylanica* L. *Industrial Crops and Products* 154: 112748.

Eurasian Journal of Soil Science 2024, 13(3), 247 - 253

Eurasian Journal of Soil Science

Journal homepage : http://ejss.fesss.org

Effect of fertilizer treatments on sugar beet cultivars: A comprehensive study on crop yield and nutrient contents of soil and plant in chestnut soil of Kazakhstan

Saira Kaliyeva [a,*], Beibut Suleimenov [b], Gulnissam Rvaidarova [c], Kerimkul Konysbekov [d], Sholpan S. Muminova [e], Baktigul Raimbekova [a]

[a] Kazakh National Agrarian Research University, Almaty, Kazakhstan
[b] U.U.Uspanov Kazakh Research Institute of Soil Science and Agrochemistry, Almaty, Kazakhstan
[c] Kazakh Scientific Research Institute for Plant Protection and Quarantine, Almaty, Kazakhstan
[d] Kazakh Research Institute of Agriculture and Crop Production Almaty, Kazakhstan
[e] University named after Zhumabek Akhmetuly Tashenev, Shymkent, Kazakhstan

Article Info
Received : 02.10.2023
Accepted : 01.05.2024
Available online: 07.05.2024

Author(s)
S.Kaliyeva *
B.Suleimenov
G.Rvaidarova
K.Konysbekov
S.S.Muminova
B.Raimbekova

* Corresponding author

Abstract

This study aimed to investigate the effects of different fertilizer treatments on the growth, yield, and nutrient content of two sugar beet cultivars, Aksu (Kazakhstan) and Yampol (Poland), cultivated in the Almaty region of Kazakhstan. The experiment was conducted using a complete randomized block design with three replicates, comprising six treatments: control (without fertilizer), $N_{120}P_{120}K_{90}$, and $N_{130}P_{130}K_{130}$ for both cultivars. The soil's physical and chemical properties were analyzed, revealing a foothill light chestnut soil with favorable nutrient levels. Results indicated that the $N_{130}P_{130}K_{130}$ treatment significantly increased soil available nitrogen, phosphorus, and potassium contents, leading to enhanced sugar beet growth, nutrient uptake, and yield. Both cultivars responded positively to the increased nutrient levels, with the $N_{130}P_{130}K_{130}$ treatment showing the highest yield of 785.6 tons/ha for Aksu and 802.5 tons/ha for Yampol. Furthermore, nutrient content in tubers and leaves was significantly higher in the $N_{130}P_{130}K_{130}$ treatment compared to other treatments. These findings underscore the importance of balanced nutrient management tailored to specific cultivars for optimizing sugar beet productivity and soil fertility in diverse agro-climatic conditions. Adopting balanced mineral nutrient management approaches could offer promising solutions to enhance sugar beet productivity and sustainability. Future research should focus on exploring long-term effects and integrated nutrient management strategies for sustainable sugar beet cultivation.

Keywords: Sugar beet, fertilizer treatments, mineral fertilizers, crop yield, nutrient contents.

© 2024 Federation of Eurasian Soil Science Societies. All rights reserved

Introduction

Sugar beet (Beta vulgaris L.) is an essential crop cultivated worldwide, predominantly for sugar production but also as a source of bioenergy and feedstock (Haankuku et al., 2015). Sugar beet cultivation spans across 41 countries worldwide, encompassing approximately 8.1 million hectares (Mall et al. 2011). Among these, the top ten sugar beet-producing countries include the Russian Federation, France, Germany, the United States of America, Turkey, Poland, China, Egypt, Ukraine, and the United Kingdom, as reported by FAO in 2019. Kazakhstan, with its diverse agro-climatic zones, holds significant potential for sugar beet cultivation due to its favorable soil and climatic conditions (Zhaksybayeva et al., 2022). Almaty, Zhetysu, and Zhambyl regions includes 14.5 thousand hectares of the fields for sugar beet cultivation, it is 99 per cent of all sugar beet sowing fields in Kazakhstan (Khusnitdinova et al., 2023). The Almaty region, in particular, offers suitable conditions for sugar beet growth, with its temperate climate and fertile soils.

Climatic factors, particularly temperature and precipitation, significantly influence sugar beet growth and

: https://doi.org/10.18393/ejss.1479830
: https://ejss.fesss.org/10.18393/ejss.1479830
Publisher : Federation of Eurasian Soil Science Societies
e-ISSN : 2147-4249

development (Sánchez-Sastre et al., 2018). Adequate temperature and water availability during the growing season are crucial for achieving optimal yields (Huang et al., 2022). Therefore, monitoring and understanding the climatic conditions during the crop's growth stages are essential for implementing appropriate irrigation and management practices (de Oliveira e al., 2015).

Soil fertility plays a pivotal role in determining the success of sugar beet cultivation (Tayyab et al., 2023). Understanding the physical and chemical properties of the soil is essential for implementing effective management practices that optimize soil health and crop productivity (Gülser et al., 2017; Onyegbule et al., 2023). The soil at the study site, characterized as a foothill light chestnut soil, was analyzed for its physical and chemical properties to provide insights into its fertility status and nutrient availability (Saparov, 2014; Ospanbayev et al., 2023).

Fertilization is a key management practice that significantly impacts sugar beet yield and quality (Pogłodziński et al., 2021; Kamzina et al., 2022). Proper nutrient management, including nitrogen (N), phosphorus (P), and potassium (K) application, is essential for promoting vigorous growth, improving yield, and enhancing sugar content in sugar beet plants. However, excessive or inadequate nutrient application can lead to nutrient imbalances, affecting crop health and productivity (El-Geddawy et al., 2008).

The choice of sugar beet cultivars is critical in determining the crop's performance and yield under specific environmental conditions (Taleghani e al., 2023). In this study, two sugar beet cultivars, Aksu (Kazakhstan) and Yampol (Poland), were selected to assess their performance under varying fertilizer treatments. These hybrids have been chosen based on their adaptability to the local climatic conditions and their potential to deliver high yields. Given the importance of soil fertility, climatic conditions, and fertilization practices in determining sugar beet yield and quality, this study aims to investigate the effects of different fertilizer treatments on the growth, yield, and nutrient content of two sugar beet hybrids (Aksu and Yampol) cultivated in the Almaty region of Kazakhstan. The findings from this study will contribute to the existing knowledge base on sugar beet cultivation practices in the region and provide valuable insights for farmers and researchers aiming to enhance sugar beet productivity and sustainability in similar agro-climatic conditions.

Material and Methods

Study site and Soil Properties

During the spring and summer of 2022, the current research was conducted at Kazakh Research Institute of Agriculture and Plant Growing located in Almalybak village, Karasai district, Almaty region, Kazakhstan on a foothill light chestnut soil. The sugar beet hybrids used in the experiment were Aksu (Kazakhstan) and Yampol (Poland). A soil sample was collected from the experimental field at the beginning of the experiment. Physical and chemical properties of the experimental soil were determined Kazakh National Agrarian Research University according to the Rowell (1996).

Climatic data

Based on meteorological data collected during the study period, temperature conditions for sugar beet crops were relatively consistent across the growing seasons. The most favorable temperature conditions were observed during the growing season, with an average temperature of approximately 17°C. Optimal distribution of heat and water resources was observed, attributed to consistent and favorable natural moisture supply during the sugar beet sowing period. Specifically, precipitation levels were 35.6 mm in April, 145.4 mm in May, 35.9 mm in June, 15.1 mm in July, 8.2 mm in August, and 2.1 mm in September and the first ten days of October. Overall, the total precipitation during the growing season closely aligned with the long-term average. The least precipitation was recorded during the sowing period, with a negative water balance observed during the period of intensive growth and development of sugar beet. To mitigate the moisture deficit, vegetative irrigations were implemented to ensure adequate water supply for the sugar beet crops.

Soil Preparation, Experimental design and Cultivation

As per standard commercial cultural practice for light chestnut soil. The field was plowed using a chisel plow. Thereafter, the experimental field was divided into 180 cm wide strips. For each fertilizer treatment described below. Total plot area was 288 m^2 (12 m x 4 m) to which mineral fertilizers. Fertilizers were then incorporated into the soil using a rotavator. Fertilizer treatments were arranged in a complete randomized block design with three replicates.

Sugar beet (*Beta vulgaris* L.) cultivar Aksu and Yampol were mechanically planted on 12 April 2022, with a planting density of 4kg/ha or 1.7 p.u./ha of dried seed in the 3.75-4.75 mm fraction using a four-row-planter in all plots.

The experiment consisted of six treatments as follows:

T1-Aksu	Control (without fertilizer)
T2-Aksu	$N_{120}P_{120}K_{90}$
T3-Aksu	$N_{130}P_{130}K_{130}$
T4-Yampol	Control (without fertilizer)
T5-Yampol	$N_{120}P_{120}K_{90}$
T6-Yampol	$N_{130}P_{130}K_{130}$

Fertilizers were applied at a rate of $N_{120}P_{120}K_{90}$ and $N_{130}P_{130}K_{130}$ for Aksu and Yampol cultivar. All amounts of phosphorus and potassium were applied manually during soil preparation in the form of Ammophos (46%P_2O_5, 10%N) and potassium sulfate (50% K_2O), while nitrogen was divided into two equal portions, and applied during soil preparation and 6 weeks after planting in the form of ammonium nitrate (33% N).

Harvesting of the crop was done treatment-wise on 15 October 2022. Firstly one border row from both sides and two plants from both ends were harvested to eliminate the border effect from each plot. Harvesting was done by digging of plants.

Agronomic Activities

Throughout the experimental period, a comprehensive set of agronomic activities was meticulously executed at the experimental site to optimize conditions for sugar beet growth and ensure accurate data collection. The soil was carefully prepared for planting, followed by furrow irrigation with a total water requirement of 600-700 m^3/ha, divided into four applications. Cultivation and weed control measures were consistently applied to maintain soil health and manage weed growth. During the active growth phase, disease and pest control strategies were implemented using systemic fungicides like Impact and Skor for powdery mildew and cercosporosis, and insecticides such as Kinmix, Rovikurt, Arrivo, and Cymbush for beet fleas, beet weevils, and leaf-eating moths. Harvesting was conducted at the optimal maturity stage to ensure maximum yield and quality, with all activities performed in strict adherence to recommended practices, highlighting the importance of ecological and agronomic parameters in the experimental setup.

Data collection

Soil Sampling and Analyses

After harvest, the soil samples collected from depth of 20 cm were naturally air-dried, milled and passed through 2.0 mm sieve. Available nitrogen (NH_4+NO_3) by the modified Kjeldahl method, available Phosphorus was determined by the 0.5M $NaHCO_3$ extraction method, available Potassium content were determined by the 1N NH_4OAc extraction method according to the Rowell (1996) and Jones (2001).

Plant Sampling and Analyses

After harvesting, tubers of sugar beet were separated according to the treatment and weighed on double pan balance for each treatment separately. After this, total tuber yield was calculated as the sum of the weights of tubers from the net plot area and transformed to ton per hectare. Leaves of sugar beet samples were analyzed for dry weight and nutrient (N, P and K) content in leaves and sugar beet tubers according to the Jones (2001).

Results and Discussion

The experimental site was characterized by foothill light chestnut soil formed on loess-like loams, presenting a well-defined fertile profile. The surface soil exhibited an organic matter content of 2.02%, total nitrogen (N) at 0.135%, a C/N ratio of 8.7, and a total carbonate content of 2.73%. Exchangeable cations were measured with Ca at 10.24 meq/100 g, Mg at 1.49 meq/100 g, and Na at 0.30 meq/100 g. Additionally, the soil contained 82.4 mg/kg of Available nitrogen (NH_4+NO_3), available P_2O_5 at 25 mg/kg, available K_2O at 442 mg/kg, with a soil pH of 8.2.

The study aimed to investigate the effects of different fertilizer treatments on the growth, yield, and nutrient content of two sugar beet cultivars, Aksu and Yampol, cultivated in the Almaty region of Kazakhstan. The results obtained shed light on the intricate relationship between fertilizer treatments, soil nutrient content, and crop yield. The application of different fertilizer treatments had a significant impact on the nutrient content of the soil. For the Aksu cultivar, the highest NH_4+NO_3 content was observed in the N130P130K130 treatment with 19.4 mg/kg, followed by the $N_{120}P_{120}K_{90}$ treatment with 16.7 mg/kg and the control with 11.7 mg/kg (Table 1). Similarly, the highest available P content was recorded in the $N_{130}P_{130}K_{130}$ treatment with 45.9 mg/kg, whereas the control had the lowest P content at 12.8 mg/kg. Regarding available K, the $N_{130}P_{130}K_{130}$ treatment led with 415 mg/kg, followed by $N_{120}P_{120}K_{90}$ with 378 mg/kg, and the control with 331 mg/kg. For the Yampol cultivar, the trend was consistent with the Aksu cultivar. The $N_{130}P_{130}K_{130}$ treatment

resulted in the highest NH_4+NO_3 content at 20.2 mg/kg, available P at 47.7 mg/kg, and available K at 422 mg/kg. The control treatment showed the lowest nutrient content across all parameters (Table 1).

Table 1. Effects of fertilizer treatments on soil nutrient content

Treatment	Aksu cultivar			Yampol cultivar		
	NH_4+NO_3, mg/kg	Available P, mg/kg	Available K, mg/kg	NH_4+NO_3, mg/kg	Available P, mg/kg	Available K, mg/kg
Control	11,7	12,8	331	12,0	13,1	342
$N_{120}P_{120}K_{90}$	16,7	27,2	378	17,7	28,5	382
$N_{130}P_{130}K_{130}$	19,4	45,9	415	20,2	47,7	422

The sugar beet plant's nutrient content, particularly in tubers and leaves, was significantly influenced by the fertilizer treatments. For the Aksu cultivar, the $N_{130}P_{130}K_{130}$ treatment exhibited the highest N, P, and K content in both tubers and leaves. The control treatment showed the lowest nutrient content across all parameters. Similarly, for the Yampol cultivar, the $N_{130}P_{130}K_{130}$ treatment had superior nutrient content, with higher N, P, and K values in both tubers and leaves compared to other treatments (Table 2).

Table 2. Effects of fertilizer treatments on sugar beet yield and plant nutrient content

Treatment	Yield, ton/ha	Tubers			Leaves		
		N, %	P, %	K, %	N, %	P, %	K, %
Aksu cultivar							
T1-Control	345,0	0,75	0,30	4,65	3,1	0,22	4,67
T2- $N_{120}P_{120}K_{90}$	634,2	1,52	0,32	4,22	4,3	0,47	5,55
T3-$N_{130}P_{130}K_{130}$	785,6	1,72	0,36	3,88	4,22	0,61	5,22
Yampol cultivar							
T4-Control	389,0	0,77	0,36	4,78	3,22	0,31	4,85
T5-$N_{120}P_{120}K_{90}$	683,5	1,55	0,34	4,36	4,4	0,52	5,62
T6-$N_{130}P_{130}K_{130}$	802,5	1,77	0,42	4,11	4,38	0,56	5,14

Soil nutrients play a pivotal role in determining plant growth, development, and yield productivity. The present study aimed to evaluate the effects of different mineral fertilizer treatments on soil agrochemical properties and sugar beet nutrient content, in line with the literature. In the current study, the application of mineral fertilizers at different rates significantly improved the soil's available nutrient contents. The treatment of $N_{130}P_{130}K_{130}$ notably increased available nitrogen, phosphorus and potassium compared to the control treatment. These findings are consistent with previous studies by Jabborova et al. (2019, 2020), McDowell et al. (2004), Fang et al. (2009), Monaco et al. (2008), and Wang et al. (2008), highlighting the positive impact of inorganic fertilizers on soil nutrient contents and other agrochemical properties. Dinesh et al. (2012) observed an enhancement in total N content of rainfed ginger soil with chemical nutrient management. Similarly, Yanthan et al. (2010) reported increased N, P, and K content in soil with NPK applications, corroborating our findings. However, it's noteworthy to mention the findings from Srinivasan et al. (2019), indicating that high mineral fertilizer decreased several nutrient contents in the soil, emphasizing the need for balanced fertilizer management. Furthermore, the mineral elements in soil, particularly N, P, and K, significantly influence plant growth, development, and yield. The present study found that the $N_{130}P_{130}K_{130}$ application rate significantly enhanced the sugar beet's nutrient content, including N, P, and K, in both tubers and leaves. These results align with the studies of Egamberdieva et al. (2018), and Thakur and Sharma (1997), emphasizing the positive effect of mineral fertilizers on nutrient uptake by plants. Interestingly, our study revealed high levels of NPK in sugar beet tubers and leaves, which underscores the plant's potential as a rich source of essential nutrients. These findings are in agreement with Ayaji et al. (2013), who reported the richness of ginger in various essential minerals.

The effects of fertilizer treatments on sugar beet yield varied significantly between the two cultivars, Aksu and Yampol. The yield data presented in Table 2 clearly demonstrate the substantial influence of nutrient management on sugar beet productivity. For the Aksu cultivar, the control group without fertilizer application yielded 345.0 tons/ha. However, with the application of $N_{120}P_{120}K_{90}$, the yield increased to 634.2 tons/ha, marking a significant improvement. The highest yield was observed with the $N_{130}P_{130}K_{130}$ treatment, reaching 785.6 tons/ha, indicating that the additional nutrients further enhanced sugar beet growth and yield. In contrast, the Yampol cultivar exhibited a different response to the fertilizer treatments. The control group yielded 389.0 tons/ha, which was surpassed by the $N_{120}P_{120}K_{90}$ treatment with a yield of 683.5 tons/ha. The highest yield for this cultivar was recorded with the $N_{130}P_{130}K_{130}$ treatment at 802.5 tons/ha, suggesting that the increased nutrient levels positively impacted the growth and yield of Yampol sugar beets. These results highlight the importance of selecting appropriate fertilizer treatments tailored to specific sugar beet cultivars

to maximize yield potential. The variability in yield responses between Aksu and Yampol cultivars underscores the necessity for cultivar-specific nutrient management strategies to optimize sugar beet production in diverse agro-climatic conditions. To further contextualize the findings of this study, a comparative analysis was conducted with recent researches focusing on the effects of different nutrient management practices on sugar beet cultivars. El-Mageed et al. (2022) explored the physio-biochemical and agronomic changes in two sugar beet cultivars (Romulus and Francesca) grown in saline soil under varying potassium (K) rates. The study found that a high potassium rate of 144 kg K/ha significantly enhanced cell membrane stability, relative water content, and performance index under high salinity conditions. Additionally, the maximum improvements in sugar yield and quality were observed at this potassium rate, emphasizing the importance of potassium fertilization in mitigating the adverse effects of saline soils and enhancing sugar beet productivity. Similarly, Demirbaş (2021) investigated the impact of different phosphorus (P) doses on sugar beet yield and nutrient uptake. The study reported that increasing phosphorus doses led to a significant yield increase, with the highest yield recorded at 30 kg P/ha. Furthermore, elevated concentrations of nitrogen, phosphorus, and potassium were observed at this phosphorus dose, highlighting the crucial role of phosphorus fertilization in optimizing sugar beet yield and nutrient uptake. In another study by Marajan et al. (2021), the combined application of compost and phosphorus fertilizer was assessed for its effect on sugar beet growth and yield components. The results revealed that the combination of compost and phosphorus fertilizer significantly increased various agronomic traits, including leaf number, leaf area index, leaf dry weight, root diameter, and root fresh weight. This suggests that integrating organic and mineral fertilizers can synergistically enhance sugar beet growth and yield. Comparing these studies with the current research, it is evident that nutrient management plays a pivotal role in determining sugar beet productivity across different environmental conditions. While the current study primarily focused on nitrogen (N), phosphorus (P), and potassium (K) fertilization, the aforementioned studies highlighted the importance of potassium in saline soils and the synergistic effects of combining compost with mineral fertilizers. In conclusion, these comparative insights emphasize the need for tailored nutrient management strategies based on soil conditions, cultivar characteristics, and environmental factors to optimize sugar beet yield and quality. Adopting integrated nutrient management approaches that combine organic and mineral fertilizers could offer promising solutions to enhance sugar beet productivity and sustainability in diverse agro-climatic conditions.

Conclusion

In conclusion, the present study provides comprehensive insights into the effects of different fertilizer treatments on the growth, yield, and nutrient content of two sugar beet cultivars, Aksu and Yampol, cultivated in the Almaty region of Kazakhstan. The results underscore the significant impact of nutrient management on sugar beet productivity and soil fertility, highlighting the importance of tailored fertilizer applications in optimizing crop performance. The application of mineral fertilizers, particularly the $N_{130}P_{130}K_{130}$ treatment, significantly enhanced the soil's available nitrogen, phosphorus, and potassium contents, leading to improved sugar beet growth, nutrient uptake, and yield. Both sugar beet cultivars responded positively to the increased nutrient levels, with the $N_{130}P_{130}K_{130}$ treatment demonstrating superior performance in terms of yield and nutrient content in tubers and leaves. The findings from this study corroborate previous research highlighting the positive effects of balanced nutrient management on crop productivity. Moreover, the variability in yield responses between the Aksu and Yampol cultivars underscores the necessity for cultivar-specific nutrient management strategies to maximize sugar beet production under diverse agro-climatic conditions. It is essential to emphasize the significance of soil fertility in determining crop yield and quality. The foothill light chestnut soil of the Almaty region exhibited favorable physical and chemical properties, emphasizing the region's potential for sugar beet cultivation. However, continuous monitoring and effective soil management practices are crucial to maintaining soil health and ensuring sustainable crop production.

Future research should focus on exploring integrated nutrient management approaches that combine organic and mineral fertilizers to enhance soil fertility, improve nutrient use efficiency, and promote sustainable sugar beet cultivation practices. Furthermore, investigating the long-term effects of different fertilizer regimes on soil health, microbial communities, and crop resilience will provide valuable insights for developing holistic and sustainable agricultural strategies. In conclusion, the findings from this study contribute to the existing knowledge base on sugar beet cultivation practices in Kazakhstan and offer practical recommendations for farmers and researchers aiming to enhance sugar beet productivity, soil fertility, and sustainability in similar agro-climatic conditions. Adopting science-based nutrient management strategies is imperative for achieving sustainable agricultural intensification and ensuring food security in the face of changing climatic conditions and increasing demand for agricultural products.

References

Ajayi, O.B., Akomolafe,1S.F., Akinyemi, F.T., 2013. Food value of two varieties of ginger (Zingiber officinale) commonly consumed in Nigeria. *International Scholarly Research Notices* Article ID 359727.

de Oliveira, R.A., Ramos, M.M., de Aquino, L.A., 2015. Irrigation Management. In: Sugarcane. Santos, F., Borém, A., Caldas, C. (Eds.). Academic Press, pp. 161-183.

Demirbaş, A., 2021. The effect of different phosphorus doses application on yield and nutrient uptake of sugar beet (Beta Vulgaris L.) plant. *Turkish Journal of Agriculture - Food Science and Technology* 9(2): 420–424.

Dinesh, R., Srinivasan, V., Hamza, S., Manjusha, A., Kumar, P.S., 2012. Short-term effects of nutrient management regimes on biochemical and microbial properties in soils under rainfed ginger (Zingiber officinale Rosc.) *Geoderma* 173: 192-198.

Egamberdieva, D., Jabborova, D., Wirth, S., Alam, P., Alyemeni, M.N., Ahmad, P., 2018. Interaction of magnesium with nitrogen and phosphorus modulates symbiotic performance of soybean with Bradyrhizobium japonicum and its root architecture. *Frontiers in Microbiology* 9: 1000.

El-Geddawy, I.H., Kheiralla, K.A., Darweish, Y.Y.I., Sharaf, E.A.M., 2008. Agricultural practices in relation to yield and quality of sugar beet: Yield and yield components. *Sugar Tech* 10: 227–233.

El-Mageed, T.A.A., Mekdad, A.A.A., Rady, M.O.A. Abdelbaky, A.S., Saudy, H.S., Shaaban, A., 2022. Physio-biochemical and agronomic changes of two sugar beet cultivars grown in saline soil as ınfluenced by potassium fertilizer. *Journal of Soil Science and Plant Nutrition* 22: 3636–3654.

Fang, H.J., Yu, G.R., Cheng, S.L., Mo, J.M., Yan, J.H., Li, S., 2009. 13C abundance, water-soluble and microbial biomass carbon as potential indicators of soil organic carbon dynamics in subtropical forests at different successional stages and subject to different nitrogen loads. *Plant and Soil* 320: 243–254.

FAO, 2019. Food and Agriculture Statistics. Available at [Access date: 02.10.2023]: https://www.fao.org/

Gülser, C, Minkina, T., Sushkova, S., Kizilkaya, R., 2017. Changes of soil hydraulic properties during the decomposition of organic waste in a coarse textured soil. *Journal of Geochemical Exploration* 174: 66-69.

Haankuku, C., Epplin, F.M., Kakani, V.G., 2015. Industrial sugar beets to biofuel: Field to fuel production system and cost estimates. *Biomass and Bioenergy* 80: 267-277.

Huang, N., Song, Y., Wang, J., Zhang, Z., Ma, S., Jiang, K., Pan, Z., 2022. Climatic threshold of crop production and climate change adaptation: A case of winter wheat production in China. *Frontiers in Ecology and Evolution* 10: 1019436.

Jabborova, D., Baboev, S., Davranov, K., Jabbarov Z., 2019. Improvement of plant growth, nodulation, and yield of common bean (Phaseolus vulgaris L.) by microbiological preparations *Journal of Biological and Chemical Research* 36: 52-57.

Jabborova, D., Wirth, S., Kannepalli, A., Narimanov, A., Desouky, S., Davranov, K., Sayyed, R.Z., El Enshasy, H., Malek, R.A., Syed, A., Bahkali, A.H., 2020. Co-Inoculation of Rhizobacteria and biochar application ımproves growth and nutrientsin soybean and enriches soil nutrients and enzymes. *Agronomy* 10(8): 1142.

Jones, J.B., 2001. Laboratory guide for conducting soil tests and plant analyses. CRC Press, New York, USA. 363p.

Kamzina, G., Seilgazina, S., Suleimenova, S., Zakieva, A., Zhamangarayeva, A., 2022. The effects of NPK fertilization on hay production and some yield components of crested wheatgrass (Agropyron cristatum) in the dry steppe zone of Eastern Kazakhstan. *Eurasian Journal of Soil Science* 11(4): 337-344.

Khusnitdinova, M., Abdrakhmanova, A., Pozharskiy, A., Kapytina, A., Kerimbek, N., Nizamdinova, G., Taskuzhina, A., Adilbayeva, K., Kolchenko, M., Gritsenko, D., 2023. Problems and prospects of sugar beet cultivation in Kazakhstan. *Agronomy Research* 21(3): 1174–1185.

Mall, A.K., Misra, V., Santeshwari, Pathak, A.D., Srivastava, S., 2021. Sugar beet cultivation in India: Prospects for bio-ethanol production and value-added co-products. *Sugar Tech* 23: 1218–1234.

Marajan, W.A., Idris, B.E.M., Adam, A.H.M., 2021. Response of sugar beet (Beta vulgaris L.) growth, yield and yield components to compost and phosphorus fertilizers. *journal of Agronomy Research* 4(1): 14-22.

McDowell, W.H., Magill, A.H., Aitkenhead-Peterson, J.A., Aber, J.D., Merriam, J.L., Kaushal, S.S., 2004. Effects of chronic nitrogen amendment on dissolved organic matter and inorganic nitrogen in soil solution. *Forest Ecology and Management* 196 (1): 29-41.

Monaco, S., Hatch, D.J., Sacco, D., Bertora, C., Grignani, C., 2008. Changes in chemical and biochemical soil properties induced by 11-yr repeated additions of different organic materials in maize-based forage systems. *Soil Biology and Biochemistry* 40(3): 608-615.

Onyegbule, U., Onwudike, S., Opara-Nadi, N., Opara-Nadi, O., 2023. Soil fertility evaluation and land-use effects on soil properties, carbon and nitrogen sequestration in the rainforest of Nigeria. *Eurasian Journal of Soil Science* 12(4): 310 - 319.

Ospanbayev, Z., Doszhanova, A., Abdrazakov, Y., Zhapayev, R., Sembayeva, A., Zakieva, A., Yertayeva, Z., 2023. Tillage system and cover crop effects on organic carbon and available nutrient contents in light chestnut soil. *Eurasian Journal of Soil Science* 12(3): 238-243.

Pogłodziński, R., Barłóg, P., Grzebisz, W., 2021. Effect of nitrogen and magnesium sulfate application on sugar beet yield and quality. *Plant, Soil and Environment* 67(9): 507-513.

Rowell, D.L., 1996. Soil Science: methods and applications. Longman, UK. 350p.

Sánchez-Sastre, L.F., Martín-Ramos, P., Navas-Gracia, L.M., Hernández-Navarro, S., Martín-Gil, J., 2018. Impact of climatic variables on carbon content in sugar beet root. *Agronomy* 8(8): 147.

Saparov, A., 2014. Soil Resources of the Republic of Kazakhstan: Current status, problems and solutions. In: Novel Measurement and Assessment Tools for Monitoring and Management of Land and Water Resources in Agricultural Landscapes of Central Asia. Mueller, L., Saparov, A., Lischeid, G., (Eds.). Environmental Science and Engineering. Springer International Publishing. Switzerland. pp. 61-73.

Srinivasan, V., Thankamani, C.K., Dinesh, R., Kandiannan, K., Hamza, S., Leela, N.K., Zachariah, T.J., 2019. Variations in soil properties, rhizome yield, and quality as influenced by different nutrient management schedules in rainfed ginger. *Agricultural Research* 8(2): 218-230.

Taleghani, D., Rajabi, A., Saremirad, A., Fasahat, P., 2023. Stability analysis and selection of sugar beet (Beta vulgaris L.) genotypes using AMMI, BLUP, GGE biplot and MTSI. *Scientific Reports* 13: 10019.

Tayyab, M., Wakeel, A., Mubarak, M.U., Artyszak, A., Ali, S., Hakki, E.E., Mahmood, K., Song, B., Ishfaq, M., 2023. Sugar beet cultivation in the tropics and subtropics: Challenges and opportunities. *Agronomy* 13(5): 1213.

Thakur, S.K., Sharma, S.K., 1997. Response of ginger to nitrogen and phosphorus in the sub-tropical zone of Himachal Pradesh. *Indian Journal of Agricultural Research* 31(3): 195-198.

Yanthan, L., Singh, A.K., Singh, V.B., 2010. Effect of INM on yield, quality, and uptake of N, P, and K by ginger. *Agropedology* 20: 74-79.

Zhaksybayeva, G., Balgabayev, A., Vassilina, T., Shibikeyeva, A., Malimbayeva, A., 2022. Yield of sugar beet and changes in phosphorus fractions in relation to long term P fertilization in chestnut soil of Kazakhstan. *Eurasian Journal of Soil Science* 11(1): 25-32.

Eurasian Journal of Soil Science 2024, 13(3), 254 - 262

Eurasian Journal of Soil Science

Journal homepage : http://ejss.fesss.org

Efficacy of nano-zinc oxide and iron oxide formulations on shelf life of strawberry

Lakhwinder Singh [a,*], Ramesh Kumar Sadawarti [a], Shailesh Kumar Singh [a], Vishnu D. Rajput [b], Tatiana Minkina [b], Svetlana Sushkova [b]

[a] Department of Horticulture, School of Agriculture, Lovely Professional University, Phagwara, 144-411, Punjab, India
[b] Academy of Biology and Biotechnology, Southern Federal University, Rostov-on-Don, Russia

Article Info
Received : 20.02.2024
Accepted : 13.05.2024
Available online: 15.05.2024

Author(s)
L.Singh *
R.K.Sadawarti
S.K.Singh
V.D.Rajput
T.Minkina
S.Sushkova

* Corresponding author

Abstract

The research investigates the transformative impact of nano-zinc oxide and iron oxide formulations on prolonging the shelf life of strawberries. A total of 16 distinct treatments were applied through foliar application, and a nano-zinc oxide (ZnO) and iron oxide (FeO) formulations were administered. Each square meter received 42 ml of the solution in triplicate, ensuring a comprehensive exploration of the formulations' impact on shelf-life enhancement. Notably, the combined application of ZnO and FeO NPs at 150 mg/l, specifically T_{15} (Z_3F_3), exhibited superior effectiveness in preserving the crop. T_{11} (Z_2F_2), featuring 100 mg/l ZnO and 100 mg/l FeO, closely trailed T_{15}, showcasing significant improvements in parameters such as ascorbic acid content (49.66 mg/100g), and anthocyanin content (39.82 mg/l), etc. at nine days after harvesting. Besides this, TSS (7.25 ^{o}brix) in T_{14} and acidity (0.65%) in T_5 and T_9 at nine days intervals. These findings advancing the strawberry preservation methods in the agriculture and food industries and establishes the superiority of simultaneous applications of nano-formulations in T_{15} (150 mg/l ZnO + 150 mg/l FeO) and T_{11} (100 mg/l ZnO + 100 mg/l FeO). These formulations emerge as optimal solutions for extending the shelf life of strawberry fruits, particularly the Cv. Winter Dawn under Punjab Region, India, and could implement in similar climatic condition around world.

Keywords: Strawberry, winter dawn, nano-fertilizers, ZnO, FeO, shelf life, anthocyanin content.

© 2024 Federation of Eurasian Soil Science Societies. All rights reserved

Introduction

Strawberry fruits are vibrant, with significant minerals and vitamins, plants can reach a height of 20–22 cm (8-10 inches) and have 2-4 years of economic life before replacing plants (Menzel, 2023). China dominates global strawberry production in every aspect with production of 3.336.690 tons during the 2021-22 period, whereas the USA follows with a production of 1.055.963 tons of strawberries (FAO, 2023). Strawberry is an aggregate accessory fruit formed through the enlargement of the receptacle. Typically, the fruit's external surface is adorned with diminutive seeds referred to as achenes, which protrude slightly from its flesh (Barakhov et al., 2023). Strawberries are preferably grown in soil having a pH range of 4.6-6.5 (Cankurt and İpek, 2023).

The soil beneath the strawberry plants provides the foundation for their growth, bearing the responsibility of supplying essential nutrients, maintaining proper pH levels, and ensuring adequate drainage (Al-Mamun et al., 2021). As such, soil nutrition is central to the success of strawberry production. It not only influences the plant's growth, vigor, and disease resistance but also plays a pivotal role in determining the fruit's quality, flavor, and shelf life (Duralija et al., 2021). Among the various essential nutrients strawberries require for optimal growth, two micronutrients, zinc (Zn) and iron (Fe), have emerged as critical players in shaping fruit quality and shelf life.

: https://doi.org/10.18393/ejss.1484756
: https://ejss.fesss.org/10.18393/ejss.1484756
Publisher : Federation of Eurasian Soil Science Societies
e-ISSN : 2147-4249

The shelf life of strawberries is significantly influenced by the presence of zinc oxide and iron oxide in the soil. These minerals play crucial roles in various physiological processes within the strawberry plant, ultimately impacting the quality and longevity of the fruit (Jatav et al., 2021) Zinc oxide and iron oxide are essential micronutrients required for the proper growth and development of strawberry plants. ZnO-NPs improve biochemical indices of strawberry plants (Singh et al., 2024a,b,c). Adequate levels of zinc and iron in the soil promote optimal nutrient absorption and act as cofactors for antioxidant enzymes such as superoxide dismutase (SOD) and catalase, which play critical roles in scavenging reactive oxygen species (ROS) and protecting plant cells from oxidative damage (Singh et al., 2022a,b). Iron is involved in the synthesis of phytoalexins, which are compounds produced by plants in response to microbial attack, while zinc enhances the activity of defense-related enzymes and strengthens cell walls (Panigrahi et al., 2019). By bolstering the plant's immune system, zinc oxide and iron oxide help reduce the incidence of diseases that could otherwise compromise fruit quality and shelf life (Mohapatra et al., 2022). This research delves into the intricate relationship between soil nutrition, particularly the impact of zinc oxide and iron oxide on shelf life of strawberries under Punjab region of India.

Nano-fertilizers are more sensitive and can penetrate the epidermis, empowering them to promote nutrient consumption efficiency while reducing nutrient overabundance (Al Tawaha et al., 2024). NPs also stimulate root hair development, increasing nutrient absorption capacity. Furthermore, ZnO-NPs influence ion transporters and channels (Singh et al., 2024a,b,c) Advances in nanotechnology research could improve fundamental aspects of food security, including agricultural productivity, soil progress, use of safe water, food dispersal in stores, and food quality (Singh et al., 2024a,b,c). These micronutrients, although required in small quantities, have a disproportionate impact on the overall health and productivity of the strawberry crop. Their influence on synthesizing vital biomolecules, enzyme activities, and redox processes makes them indispensable contributors to the various stages of strawberries from blossom to harvest (Bayat et al., 2019). Zinc, an essential micronutrient, participates in numerous enzymatic reactions within the plant, including those related to hormone regulation, protein synthesis, and nucleic acid metabolism (Meyer et al., 2021). Understanding the specific role of zinc in strawberries is critical for farmers and horticulturists seeking to maximize the visual appeal and nutritional value (Bandeira et al., 2020). Iron, another micronutrient, plays an equally pivotal role in the life cycle of strawberry plants. Iron is a fundamental component of chlorophyll, the pigment responsible for photosynthesis, and is essential for electron transfer reactions within the plant (Warang et al., 2023). In strawberries, adequate iron availability is closely linked to healthy foliage, efficient photosynthesis, and the synthesis of vital compounds like phenolic compounds and anthocyanins, contributing to fruit color and antioxidant content. As such, unraveling the specific role of iron in strawberries is paramount for those aiming to enhance fruit quality and health benefits (Duralija et al., 2021).

By focusing on the specific roles of zinc and iron, present study aimed to intricate interplay of soil nutrition and shelf life of strawberry fruits. The mechanisms underlying the effects of zinc and iron on strawberries, strategies to optimize the availability of these nutrients in the soil and to cultivate strawberries that exhibit not only visual appeal but also enhanced nutritional richness and prolonged shelf life.

Material and Methods

Description of the location and plants

The present research was conducted at Lovely Professional University, School of Agriculture, Horticulture Research Farm, Punjab, India (2022-2023). Experimental site which is nearly 237m (768 ft.) above mean sea level. It is located in the Punjab state at 31.2232°N latitude and 75.7670°E longitudes, with an average annual rainfall of 816 mm. The runners of strawberry cv. Winter Dawn (one month old) were transplanted by the 7th and 8th of November 2022 under protected and open field conditions with three replications. A summary of materials and methodology are mentioned below,

Field preparation

Before the transplanting of strawberry runners, urea was applied in two splits at a concentration of 23.9 g per square meter, while DAP was applied at 21.7 g and MOP at 20 g per square meter as per the recommendation of package practice provided by state agriculture university (Punjab). Phosphorus and potash were applied prior to planting and drip irrigation method was used for irrigation at discharge rate of 2 liters/hour, total 6 irrigation were applied to the field for both conditions from transplanting to harvesting stage.

Characterization of ZnO and FeO

Nano zinc oxide can enhance nutrient uptake, induce systemic acquired resistance, and act as an antioxidant in strawberry plants, promoting growth and stress tolerance Similarly, iron oxide nanoparticles can improve photosynthesis efficiency, bolster plant defense mechanisms, and potentially increase disease resistance in strawberries. Zinc and iron enhance the shelf life of strawberries by promoting enzymatic activity, which aids in maintaining fruit freshness and delaying decay processes. Additionally, these minerals contribute to the stabilization of cellular structures, extending the longevity of the fruit during storage (Chaplygin et al., 2020).

Preparation of ZnO and FeO doses

Nanoform of ZnO and FeO were prepared at a concentration of 50, 100 and 150 mg/l. Zinc oxide and iron oxide using digital weighing scale in micrograms and place it in a weighing dish. The 0.05 g of ZnO and FeO separately were used in order to make a 50 mg/l solution then dissolve the weigh calculated ZnO and FeO in 10ml ethanol after that mix the 10 ml of prepared stock solution to 90 ml distilled water to make 100 ml solution and same for the 100 mg/l and 150 mg/l concentration. Commercial grade nano zinc oxide and iron oxide fertilizers were used in foliar applications (1000 ml) on leaves of each strawberry plant. These NPs were obtained from ad-nano Technologies Pvt. Ltd., and prepared by the chemical precipitation method, and had a purity rate of 99.9%, average particle size of 30–80 nm, and bulk density of 0.58 g/cm^3.

Observations, Analysis and Treatment details

Procedure for determination of biochemical constituents

Spoilage

Shelf-life parameters was monitored at 0-, 3-, 6- and 9-days interval and fruits were stored at ambient room temperature conditions. The spoilage was calculated by as the total number of spoiled units, divided by the total units produced, and multiplied by hundred.

Total soluble solids (TSS)

Total soluble solids (TSS) were calculated with a digital refractometer, and ascorbic acid content was estimated using a modified procedure from A.O.A.C. Titratable acidity was determined by titration with 0.1N NaOH and phenolphthalein as an indicator.

Physiological Loss in eight (PLW)

The physiological loss in weight was calculated by subtracting the final weight of the fruit from the initial weight of the fruit and determine in percentage.

Anthocyanin

Differential method of pH has been used to determine the anthocyanin content and the absorbance was measured using UV- spectrophotometer and absorbance was read at 520 nm.

Total sugars and reducing sugars

Lane and Eynon method were used to estimate the total sugars and reducing sugars.

Data analysis

Statistical analysis was conducted on shelf-life parameters and treatments were computed using SPSS software for randomized block design (RBD).

Soil analysis

Total nitrogen was determined through the micro-kjeldahl (Jackson, 1973), while total phosphorus was estimated by the Vandomolybdophospheric yellow color method (Jackson, 1973), and total potash was estimated on Flame photometer (Jackson, 1973). The available nitrogen in the soil is 225.8 kg/ha, phosphorous levels ranging between 12-22 kg/ha with an average of 16.5 kg/ha, mean available potassium is about 158.32 kg/ha-221.04 kg/ha with an average of 179.20 kg/ha respectively.

Experimental setup

The experiment consists of sixteen various treatments: T_0 (100 % RDF), T_1 (500 mg/l ZnO NPs), T_2 (100 mg/l ZnO NPs), T_3 (150 mg/l ZnO NPs), T_4 (50 mg/l FeO NPs), T_5 (100 mg/l FeO NPs), T_6 (150 mg/l FeO NPs), T_7 (50 mg/l ZnO NPs + 50 mg/l FeO NPs), T_8 (50 mg/l ZnO NPs + 100 mg/l FeO NPs), T_9 (50 mg/l ZnO NPs + 150 mg/l FeO NPs), T_{10} (100 mg/l ZnO NPs + 50 mg/l FeO NPs), T_{11} (100 mg/l ZnO NPs+ 100 mg/l FeO NPs), T_{12} (100 mg/l ZnO NPs + 150 mg/l FeO NPs), T_{13} (150 mg/l ZnO NPs + 50 mg/l FeO NPs), T_{14} (150 mg/l ZnO NPs + 100 mg/l FeO NPs), T_{15} (150 mg/l ZnO NPs + 150 mg/l FeO NPs) and conducted in Randomized block design.

Results and Discussion

Spoilage

Spoilage (%) of strawberry was affected by the different doses of Nano-ZnO and FeO, as presented in Table 1 respectively. Minimum Spoilage (0.73%) was observed in T_{15} significantly at 3 days interval and maximum spoilage (2.79%) was recorded in T_0 after six days interval minimum spoilage (1.51%) was observed in T_{15} and maximum (5.85%) was recorded in T_0 and at 9 days interval spoilage was observed minimum in T_{15} and maximum was observed in T_0 (8.39%). Spoilage percent of strawberry was observed from 0.73% - 8.39% respectively as shown in Figure 1 and Table 1. Numerous studies observed that applying Zn and Fe significantly influences crops' plant growth, shelf life, quality, and productivity of strawberry crop. For instance, de la Rosa et al. (2013) observed, increased shelf life and minimum spoilage and decay percentage in strawberry fruits are due to the application of $ZnSO_4$ in tomato, which might impute the availability of the appropriate quantity of Zn within the system of plants as the element elevates ribosome and ribonucleic acid (de la Rosa et al., 2013). Iron's influence on the spoilage percentage by the foliar application may be related to its availability and involvement in photosynthesis, which boosts the photosynthetic rate in the plant and produces more quality fruit for guava crop (Yogeesha et al., 2005). A study by Raliya and Tarafdar (2013) observed that various concentrations of NPs were applied to cucumber, alfalfa, and tomato to decrease the mass decay percentage of the fruits (Raliya and Tarafdar, 2013). Based on a study, it was noted that the simultaneous application of Zn and Fe nanoparticles at different concentrations led to an enhanced life span of strawberry fruits at various concentrations in comparison with the control (Kumar et al., 2017). Sing et al. (2005) discovered that $ZnSO_4$ by foliar application method in papaya plants, accelerated blooming in the papaya and more fruit having more life span compared with the control (Singh et al., 2005).

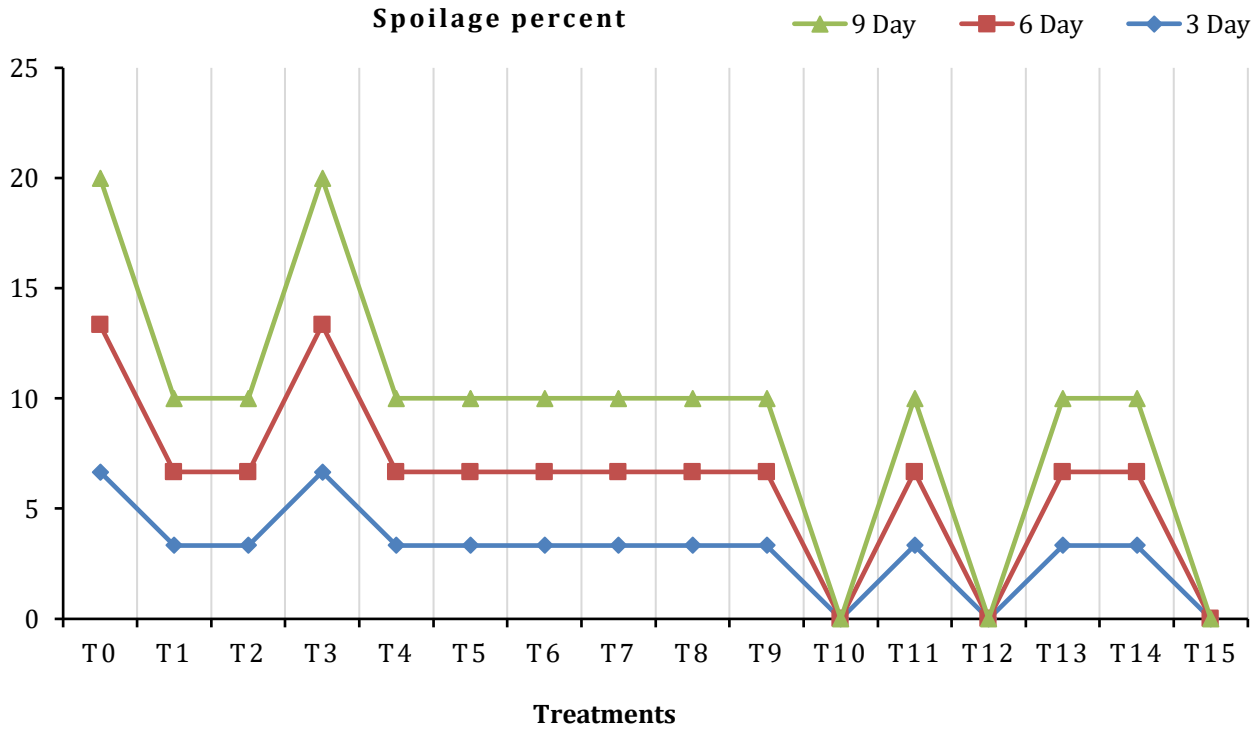

Figure 1. Effect of zinc oxide and iron oxide on spoilage percentage of strawberry

Total Soluble solids

In comparison, the minimum TSS was recorded at 3 days interval in T_0 having a value of (5.53 ^{o}brix) and maximum was recorded in T_7 (6.99 ^{o}brix) after 6 days interval the maximum value for TSS in ^{o}brix was observed in 7.15 and minimum was observed in T_0 (6.25 ^{o}brix) and at 9 days interval the value for TSS is 7.25 ^{o}brix in T_{14} and minimum in T_{12} (7.10 ^{o}brix) as shown in Table 1. TSS ^{o}brix of strawberry was observed from 5.53 ^{o}brix-7.25 ^{o}bix respectively. Same finding was observed by Chaturvedi et al. (2005) that maximum 9.42^0 Brix was recorded with a lower concentration of ferrous sulfate (0.2%), closely trailed by 0.4% zinc sulfate (9.32^0 Brix). Zinc and iron sprays demonstrated significant support for photosynthesis, thereby enhancing fruit quality. Additionally, zinc plays a pivotal role in regulating enzymatic activity, facilitating the conversion of carbon compounds into glucose (Chaturvedi et al., 2005).

Table 1. Effect of zinc oxide and iron oxide on spoilage, tss, acidity and ascorbic acid of strawberry

Treatments	Spoilage % (Days Interval)			TSS °Brix (Days Interval)			Acidity % (Days Interval)			Ascorbic acid mg/100g (Days Interval)		
	3 Day	6 Day	9 Day	3 Day	6 Day	9 Day	3 Day	6 Day	9 Day	3 Day	6 Day	9 Day
T_0	2.79^{b}	5.85^{d}	8.39^{d}	5.53^{a}	6.25^{ab}	7.28^{a}	0.53^{abc}	0.50^{abc}	0.47^{ab}	49.35^{ab}	47.93^{a}	46.63^{a}
T_1	1.22^{ab}	2.68^{abc}	3.99^{bc}	5.58^{a}	5.98^{a}	7.22^{a}	0.49^{a}	0.47^{a}	0.45^{a}	49.14^{a}	48.65^{ab}	46.81^{a}
T_2	1.08^{ab}	2.27^{ab}	3.40^{ab}	5.69^{ab}	6.13^{a}	7.18^{a}	0.60^{cde}	0.58^{cd}	0.56^{cd}	50.18^{abcde}	49.10^{abc}	47.20^{a}
T_3	1.22^{ab}	2.76^{abc}	3.83^{bc}	6.05^{bc}	6.20^{ab}	7.23^{a}	0.61^{cde}	0.59^{cde}	0.58^{cd}	50.98^{bcde}	49.93^{bcd}	48.61^{a}
T_4	1.97^{ab}	2.58^{ab}	3.37^{ab}	6.23^{cde}	6.74^{cd}	7.24^{a}	0.65^{def}	0.63^{def}	0.61^{cd}	51.36^{de}	50.44^{cd}	47.59^{a}
T_5	1.09^{ab}	2.23^{ab}	3.04^{ab}	6.09^{bcd}	6.38^{abc}	7.18^{a}	0.70^{f}	0.68^{ef}	0.65^{d}	51.61^{e}	50.38^{cd}	48.13^{ab}
T_6	1.54^{ab}	2.26^{ab}	3.12^{ab}	5.75^{ab}	6.17^{a}	7.12^{a}	0.62^{def}	0.60^{ab}	0.57^{d}	51.07^{cde}	49.69^{bcd}	48.00^{ab}
T_7	1.35^{ab}	2.74^{abc}	4.21^{bc}	6.99^{f}	7.15^{d}	7.15^{a}	0.50^{a}	0.49^{def}	0.47^{ab}	49.52^{abc}	48.37^{ab}	46.59^{ab}
T_8	1.91^{ab}	3.53^{abc}	4.31^{bc}	5.60^{a}	5.95^{a}	7.16^{a}	0.62^{def}	0.60^{def}	0.57^{cd}	50.48^{abcde}	49.19^{abc}	47.00^{ab}
T_9	2.19^{ab}	4.65^{cd}	5.63^{c}	6.81^{fg}	6.95^{d}	7.22^{a}	0.70^{f}	0.68^{f}	0.65^{d}	51.82^{e}	50.69^{cd}	47.12^{a}
T_{10}	1.92^{ab}	3.03^{abc}	4.89^{bc}	6.40^{cdef}	6.67^{bcd}	7.15^{a}	0.58^{bcd}	0.56^{bcd}	0.54^{bc}	49.85^{abcd}	49.15^{abc}	47.18^{a}
T_{11}	1.61^{ab}	0.11^{bc}	3.98^{bc}	6.41^{cdef}	6.77^{cd}	7.23^{a}	0.63^{def}	0.61^{def}	0.59^{cd}	51.18^{cde}	49.96^{bcd}	47.89^{a}
T_{12}	1.81^{ab}	3.00^{abc}	3.66^{ab}	6.50^{def}	6.84^{cd}	7.10^{a}	0.61^{cde}	0.60^{def}	0.57^{cd}	51.71^{e}	50.68^{cd}	48.75^{a}
T_{13}	1.29^{ab}	2.93^{abc}	3.95^{bc}	6.78^{fg}	7.00^{d}	7.24^{a}	0.67^{def}	0.64^{def}	0.61^{cd}	50.99^{bcde}	49.52^{abcd}	48.15^{a}
T_{14}	1.17^{ab}	3.44^{abc}	4.45^{bc}	6.61^{efg}	6.78^{cd}	7.25^{a}	0.61^{cde}	0.58^{cd}	0.56^{c}	50.36^{abcde}	49.13^{abc}	46.90^{ab}
T_{15}	0.73^{ab}	1.51^{a}	1.91^{a}	6.28^{cde}	6.39^{abc}	7.17^{a}	0.68^{ef}	0.65^{def}	0.63^{cd}	51.59^{e}	50.99^{d}	49.66^{b}

T_0 (Control 100% RDF), T_1 (50mg/l ZnO NPs), T_2 (100 mg/l ZnO NPs), T_3 (150 mg/l ZnO NPs),T_4 (50 mg/l FeO NPs), T_5(100 mg/l FeO NPs), T_6 (150 mg/l FeO NPs), T_7 (50mg/l ZnO NPs + 50mg/l FeO NPs), T_8 (50pm ZnO NPs + 100mg/l FeO NPs), T_9 (50mg/l ZnO NPs+ 150mg/l FeO NPs), T_{10} (100mg/l ZnO NPs + 50mg/l FeO NPs), T_{11} (100mg/l ZnO NPs+ 100mg/l FeO NPs), T_{12} (100mg/l ZnO NPs + 150mg/l FeO NPs), T_{13} (150mg/l ZnO NPs + 50mg/l FeO NPs), T_{14} (150mg/l ZnO NPs + 100mg/l FeO NPs), T_{15} (150mg/l ZnO NPs + 150mg/l FeO NPs)

Acidity

Readings on acidity percentage of strawberry fruits Cv. Winter Dawn significant variations were found between different treatments. The data showed that maximum acidity (0.70%) was observed in T_5 and T_9, and minimum (0.49%) was recorded in T_0 at 3 days interval after 6 days interval maximum acidity was observed in T_9 (0.68%) and minimum in T_1 (0.47%). At 9 days interval maximum acidity percentage was noted in T_5 and T_9 (0.65%) respectively and minimum was recorded T_1 (0.45%) as shown in Table 1. Acidity (%) of strawberry fruits was observed from 0.45%-0.70% respectively shown in Figure 1 and Table 1. The maximum contents of acidity (0.968%) was observed with 0.4 per cent zinc sulphate, closely followed by 0.2 per cent ferrous sulphate (65.94 mg and 0.967%). This increase might be due to the fact that zinc works as stimulant of amino acids and appears to be helpful in the process of photo synthesis and accumulation of carbohydrates (Kumar et al., 2022).

Ascorbic Acid

Significant variations were found among all the treatments on the 3, 6 and 9 days interval after harvesting regarding ascorbic acid of fruits; maximum ascorbic acid content at 3 days interval was observed in T_{12} (51.71 mg/100g) and minimum was recorded in T_1 (49.14 mg/100 g) after 6 days interval maximum ascorbic acid was noted in T_{15} (50.99 mg/100g) and minimum was noted in T_0 (47.93 mg/100g). At 9 days interval maximum content of ascorbic acid was observed in T_{15} (49.66 mg/100g) and minimum was recorded in T_0 (46.63 mg/100g) as shown in Table 1 and Figure 2. Ascorbic acid (mg/100g) of strawberry fruits was observed from 46.63 mg/100g-51.71 mg/100g respectively. Highest levels of ascorbic acid (66.10 mg) were observed with 0.4% zinc sulfate, closely followed by 0.2% ferrous sulfate (65.94 mg and 0.967%, respectively). This augmentation could be attributed to the role of zinc as a stimulant for amino acids, contributing to the process of photosynthesis and carbohydrate accumulation. In guava, the highest levels of ascorbic acid was recorded with 0.4% zinc sulfate (Sharma et al., 1991). Furthermore, the shelf life of berries increased with 0.6% zinc sulfate when stored at ambient temperature (Jurgens, 1990). By the Foliar application of micronutrient mixture (1%) (Ca, Fe and Zn) on banana cv. Grand Naine recorded maximum amount of ascorbic acid (0.70 mg/100 g) (Yadlod and Kadam, 2003).

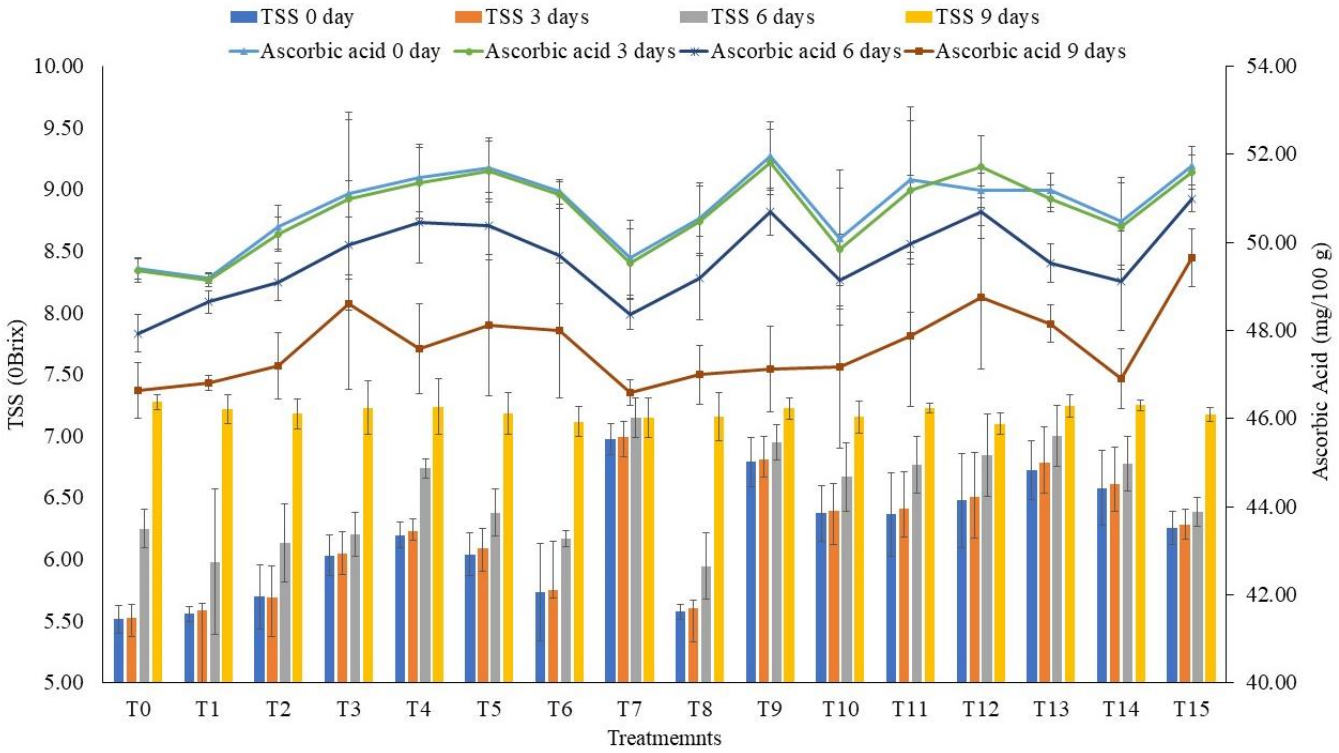

Figure 2. Effect of Zinc oxide and Iron oxide on TSS ºBrix and Ascorbic acid content (mg/100g) of strawberry

Anthocyanin Content

Concerning the anthocyanin content (mg/l), variations were found amongst all the treatments. Maximum anthocyanin content at 3 days interval was observed in T_{15} (41.12 mg/l) and minimum in T_0 (32.28 mg/l) after 6 days interval maximum ascorbic acid was noted down in T_{15} (41.56 mg/l) and minimum in T_0 (32.56 mg/l) after 9 days interval same findings was observed maximum anthocyanin content was observed in T_{15} (39.82 mg/l) and minimum in T_0 (31.44 mg/l). The value of anthocyanin content was varying from 31.44 mg/l-41.56 mg/l as shown in Figure 3. and Table 2. In 2019 Panigrahi observed that with the foliar application of ferrous sulphate at 0.2-0.6 per cent alone in plants promote the development of vibrant colors and desirable anthocyanin content. Fruits with well-developed color and flavor appeal more to consumers and have a longer shelf life. Iron is involved in synthesizing pigments, such as anthocyanins and flavonoids, which contribute to the color and flavor of fruits (Panigrahi et al., 2019).

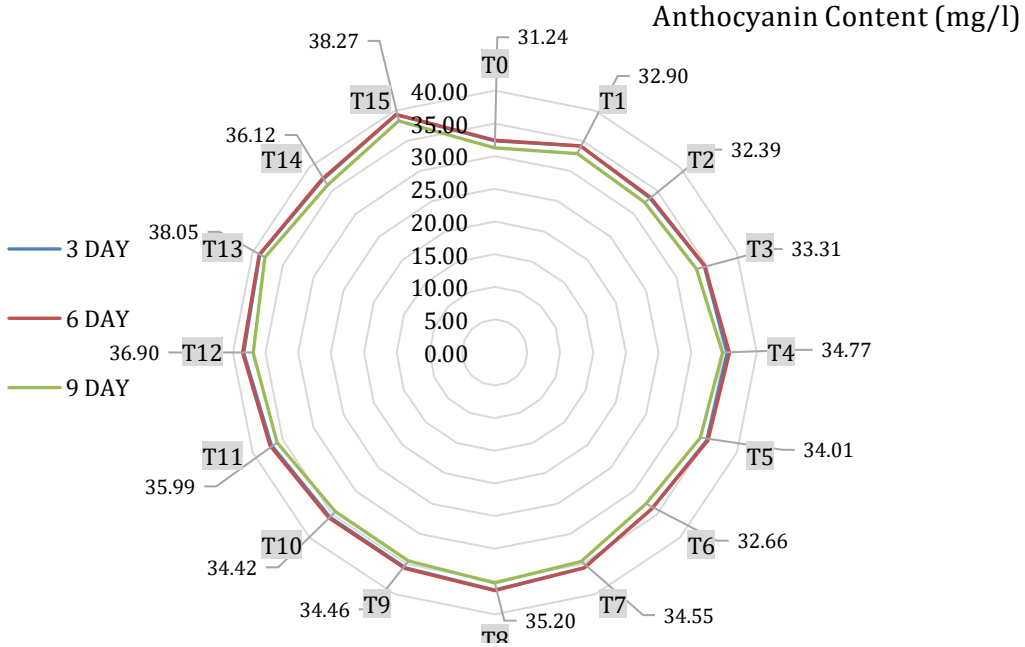

Figure 3. Effect of ZnO and FeO on Anthocyanin content (mg/100g) of strawberry

Table 2. Effect of zinc oxide and iron oxide on anthocyanin content, total sugars, and reducing sugars of strawberry at different days interval

Treatments	Anthocyanin Content (mg/l) (Days Interval)			Total Sugars (%) (Days Interval)			Reducing Sugars (%) (Days Interval)		
	3 Day	6 Day	9 Day	3 Day	6 Day	9 Day	3 Day	6 Day	9 Day
T_0	32.28^{a}	32.56^{a}	31.44^{a}	7.15^{bc}	7.53^{bcde}	8.40^{e}	4.48^{bcd}	4.54^{bcd}	4.77^{bcde}
T_1	33.59^{ab}	33.76^{ab}	32.91^{ab}	7.19^{bc}	7.42^{bcd}	7.71^{bc}	4.21^{bc}	4.31^{bc}	4.39^{abc}
T_2	33.43^{ab}	33.65^{ab}	32.72^{ab}	6.54^{a}	6.75^{bcde}	7.08^{a}	3.56^{a}	3.61^{a}	3.83^{a}
T_3	34.57^{abcd}	34.82^{abc}	33.94^{abcd}	7.21^{bc}	7.46^{bcd}	7.82^{bc}	4.52^{bc}	4.55^{bcd}	4.76^{bcde}
T_4	34.64^{abcd}	34.85^{abc}	33.82^{abcd}	7.34^{bcd}	7.56^{a}	7.82^{a}	4.33^{bcd}	4.40^{a}	4.52^{bcd}
T_5	37.77^{cdef}	38.11^{cde}	37.26^{cdef}	7.66^{bcde}	7.82^{bcd}	8.03^{bcd}	4.62^{bcd}	4.68^{bcd}	4.83^{bcde}
T_6	33.97^{abc}	34.15^{ab}	33.41^{abc}	7.17^{bc}	7.32^{bcde}	7.54^{ab}	4.13^{ab}	4.20^{b}	4.38^{abc}
T_7	36.73^{bcde}	36.95^{bcd}	36.18^{bcdef}	7.98^{de}	8.10^{bcde}	8.34^{de}	4.95^{bcd}	4.99^{cd}	5.16^{e}
T_8	34.56^{abcd}	34.82^{abc}	33.90^{abcd}	7.38^{bcd}	7.57^{bc}	7.80^{bc}	4.34^{bcd}	4.41^{bcd}	4.54^{bcde}
T_9	36.16^{abcde}	36.46^{abcd}	35.34^{abcde}	7.88^{de}	8.01^{e}	8.17^{cde}	4.83^{d}	4.88^{cd}	5.03^{cde}
T_{10}	38.61^{ef}	38.83^{de}	37.93^{ef}	7.78^{cde}	7.90^{cde}	8.08^{bcd}	4.76^{bcd}	4.82^{bcd}	4.98^{cde}
T_{11}	38.25^{def}	38.50^{cde}	37.52^{def}	7.55^{bcde}	7.75^{de}	8.04^{cde}	4.50^{bcd}	4.58^{bcd}	4.76^{bcde}
T_{12}	35.73^{abcde}	35.97^{abcd}	35.25^{abcde}	7.10^{bc}	7.27^{cde}	7.63^{bc}	4.13^{ab}	4.22^{bc}	4.33^{ab}
T_{13}	40.61^{f}	40.94^{e}	39.36^{f}	7.64^{bcde}	7.74^{bcde}	8.05^{bcde}	4.52^{bcd}	4.58^{bcd}	4.73^{bcde}
T_{14}	37.90de^{f}	38.36^{cde}	37.48^{def}	7.21^{bc}	7.33^{ab}	7.71^{bc}	4.22^{bc}	4.28^{bc}	4.39^{abc}
T_{15}	41.12^{f}	41.56^{e}	39.82^{f}	7.56^{bcde}	7.66^{bcde}	7.84^{bcd}	4.50^{bcd}	4.60^{bcd}	4.71^{bcde}

T_0 (Control 100% RDF), T_1 (50mg/l ZnO NPs), T_2 (100 mg/l ZnO NPs), T_3 (150 mg/l ZnO NPs),T_4 (50 mg/l FeO NPs), T_5(100 mg/l FeO NPs), T_6 (150 mg/l FeO NPs), T_7 (50mg/l ZnO NPs + 50mg/l FeO NPs), T_8 (50pm ZnO NPs + 100mg/l FeO NPs), T_9 (50mg/l ZnO NPs+ 150mg/l FeO NPs), T_{10} (100mg/l ZnO NPs + 50mg/l FeO NPs), T_{11} (100mg/l ZnO NPs+ 100mg/l FeO NPs), T_{12} (100mg/l ZnO NPs + 150mg/l FeO NPs), T_{13} (150mg/l ZnO NPs + 50mg/l FeO NPs), T_{14} (150mg/l ZnO NPs + 100mg/l FeO NPs), T_{15} (150mg/l ZnO NPs + 150mg/l FeO NPs

Total Sugars and Reducing Sugars

At 3 days interval the maximum value for total sugars was observed in T_7 (7.98%) and maximum reducing sugars was also noted in T_7 (4.95%) while minimum total sugars and reducing sugars was observed in T_2 (6.54%, 3.56%) and after 6 days interval the maximum total sugars was recorded in T_7 (8.10%) and reducing sugars (4.99%) and minimum in T_2 (6.75% and 3.61%). At 9 days interval the maximum value for total suagrs and reducing sugars was recorded maximum in T_7 (8.34% and 5.16%) and T_2 having minimum values (7.08% and 3.83%). Total sugars (%) of strawberry fruits was observed from 6.54%-8.34% and reducing sugars was noted from 3.16%-4.99% respectively as shown in Table 2. In 1983, Singh and Chhonkar conducted research and observed that total soluble solids and total sugars were recorded maximum in guava by foliar spray of 0.2% $ZnSO_4$ (Singh and Chhonkar 1983). With the application of 0.4% $ZnSO_4$ (T_4) recorded highest total sugar (5.42%) and reducing sugar (4.19%). As a component of proteins, zinc acts as a functional, structural, or regulatory cofactor of a large number of enzymes and involved in carbohydrate metabolism (Mousavi et al., 2013).

Conclusion

Present research showed the efficacy of various treatments on the shelf life of strawberry fruits with the application of nano-form of ZnO and FeO, with a specific focus on cv. Winter Dawn. Notably, treatments T_{15} Z_3F_3 (150mg/l ZnO NPs + 150mg/l FeO NPs) and T_{11} Z_2 F_2 (100mg/l ZnO NPs + 100mg/l FeO NPs) have emerged as particularly promising avenues. The concurrent application of ZnO and FeO NPs has demonstrated notable benefits, as evidenced by microbial analysis highlighting the antimicrobial properties of ZnO NPs, thereby contributing significantly to the prolonged shelf life of the fruits. When combined with ZnO, FeO substantially enhances the shelf life of fruits. Zinc oxide at a concentration of 150mg/l fulfills essential functions such as chlorophyll production, thylakoid synthesis, and chloroplast maintenance, while iron oxide at the same concentration complements these processes, further enhancing the fruits' longevity. It can be recommended that the combining ZnO and FeO (150 mg/l) could enhance the shelf life of strawberry.

List of Abbreviations

ZnO-Zinc oxide, FeO- Iron oxide, NPs- Nanoparticles, DAT- Days after transplanting, g- Gram, $ZnSO_4$- Zinc sulphate, mg/l- Milligram per litre, Cv.- Cultivar, DAP-Diammonium phosphate, MOP-Muriate of Potassium, g/cm^3- Gram per centimeter cube, nm-Nanometer.

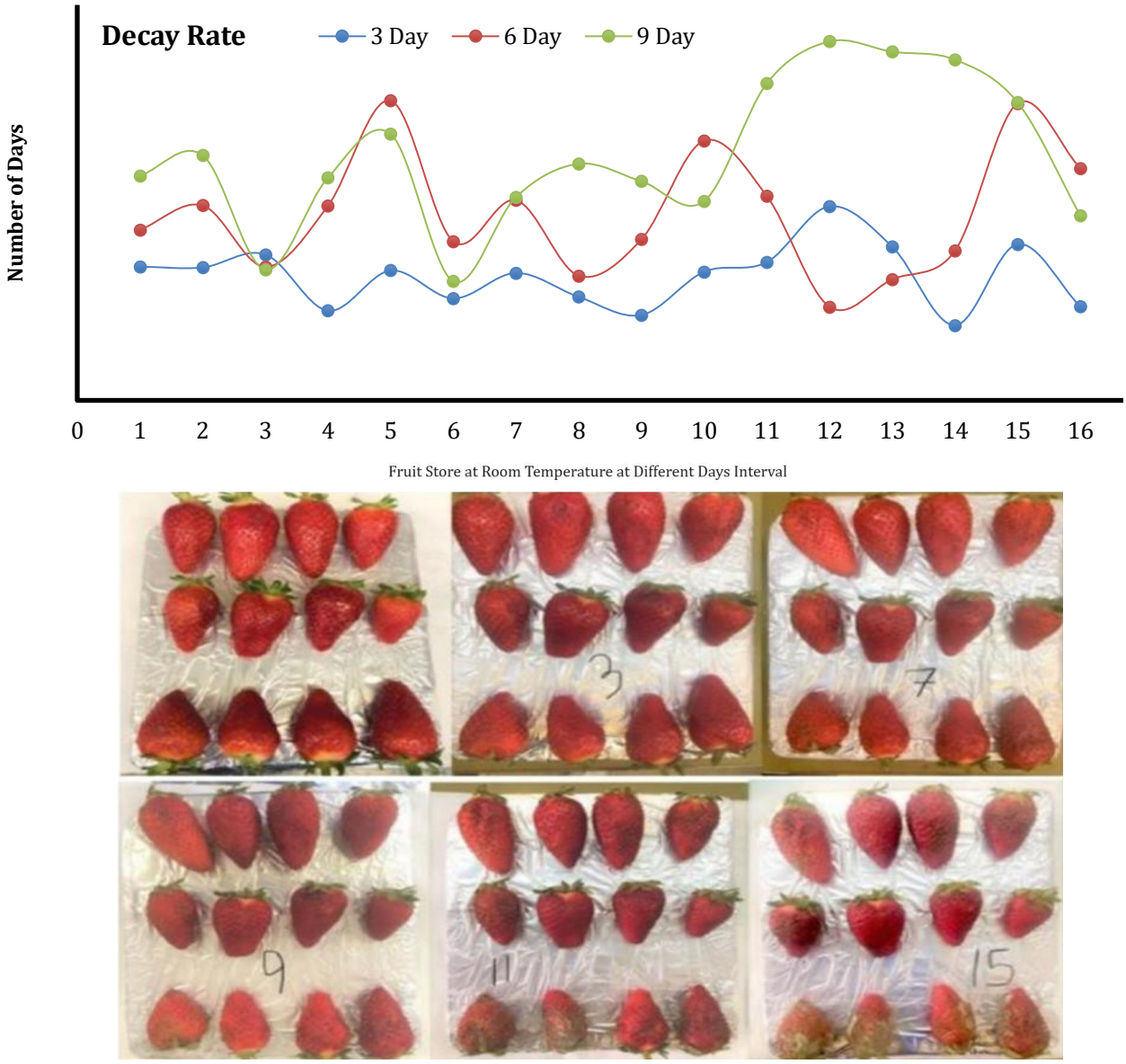

Figure 4. Effect of ZnO and FeO on decay rate with storage time in days (0-15) of

Acknowledgement

We greatly acknowledge Lovely Professional University (School of Agriculture) for providing the facilities to conduct this research experiment. VDR, TM and SS acknowledge the support by the Strategic Academic Leadership Program of the Southern Federal University ("Priority 2030").

References

Al Tawaha, A.R.M., Singh, A., Rajput, V. D., Varshney, A., Agrawal, S., Ghazaryan, K., Minkina, T., Al Zoubi, O.M., Habeeb, T., Dionis, L., Hasan, H.A., Shawaqfeh, S., 2024. Green nanofertilizers – The need for modern agriculture, intelligent, and environmentally-friendly approaches. *Ecological Engineering & Environmental Technology* 25(1): 1-21.

Al-Mamun, M. R., Hasan, M.R., Ahommed, M.S., Bacchu, M.S., Ali, M.R., Khan, M.Z.H., 2021. Nanofertilizers towards sustainable agriculture and environment. *Environmental Technology & Innovation* 23: 101658.

Bandeira, M., Giovanela, M., Roesch-Ely, M., Devine, D. M., da Silva Crespo, J., 2020. Green synthesis of zinc oxide nanoparticles: A review of the synthesis methodology and mechanism of formation. *Sustainable Chemistry and Pharmacy* 15: 100223.

Barakhov, A., Chernikova, N., Dudnikova, T., Barbashev, A., Sushkova, S., Mandzhieva, S., Rajput, V.D., Kizilkaya, R., Konstantinova, E., Bren, D., Minkina, T., Konstantinov, A., 2023. Role of sorbents in early growth of barley under copper and benzo(a)pyrene contaminated soils. *Eurasian Journal of Soil Science* 12(1): 1–9.

Bayat, M., Pakina, E., Astarkhanova, T., Sediqi, A. N., Zargar, M., Vvedenskiy, V., 2019. Review on agro-nanotechnology for ameliorating strawberry cultivation. *Research on Crops* 20(4): 731-736.

Cankurt, K., İpek, M., 2023. The Effects of some organic compounds on yield and fruit quality in albion strawberry (Fragaria x ananassa Duch) ultivar. *Selcuk Journal of Agriculture and Food Sciences* 37(1):19-24.

Chaplygin V., Mandzhieva S., Minkina T., Sushkova S., Barahov A., Nevidomskaya D., Kızılkaya, R., Gülser C., Chernikova, N., Mazarji M., Iljina L., Rajput V., 2020. Accumulating capacity of herbaceous plants of the Asteraceae and Poaceae families under technogenic soil pollution with zinc and cadmium. *Eurasian Journal of Soil Science* 9(2):165–172.

Chaturvedi, O.P., Singh, A.K., Tripathi, V.K., Dixit, A.K., 2003. Effect of zinc and iron on growth, yield and quality of strawberry cv. Chandler. *Acta Horticulturae* 696: 237-240.

de la Rosa, G., López-Moreno, M.L., de Haro, D., Botez, C.E., Peralta-Videa, J.R., Gardea-Torresdey, J.L., 2013. Effects of ZnO nanoparticles in alfalfa, tomato, and cucumber at the germination stage: root development and X-ray absorption spectroscopy studies. *Pure and Applied Chemistry* 85(12): 2161-2174.

Duralija, B., Mikec, D., Jurić, S., Lazarević, B., Maslov Bandić, L., Vlahoviček-Kahlina, K., Vinceković, M., 2021. Strawberry fruit quality with the increased iron application. *Acta Horticulturae* 1309: 1033-1040.

FAO, 2023. Production: Crops and livestock products. Food and Agriculture Organization of the United Nations. Available at [Access date: 15.02.2024]: https://www.fao.org/faostat/en/#data/QCL

Jackson, M.L., 1973. Soil Chemical Analysis. Prentice Hall of India Pvt. Ltd., New Delhi, India. 498p.

Jatav, H., Singh, S., Jatav, S., Rajput, V.D., Sushkova, S., 2021. Feasibility of sewage sludge application in rice-wheat cropping system. *Eurasian Journal of Soil Science* 10(3): 207-214.

Jurgens, J., 1990. Foliar fertilization in strawberry cultivation. *Erwerbsobstbau* 32(4): 104-107.

Kumar, U.J., Bahadur, V., Prasad, V.M., Mishra, S. and Shukla, P.K., 2017. Effect of different concentrations of iron oxide and zinc oxide nanoparticles on growth and yield of strawberry (Fragaria x ananassa Duch) cv. Chandler. *International Journal of Current Microbiology and Applied Sciences* 6(8):2440-2445.

Kumar, U.J., Bairwa, M., Rolaniya, M., 2022. Effect of different concentrations of iron oxide and zinc oxide nano-particles on quality of strawberry (Fragaria x ananassa Dutch) cv. chandler. *The Pharma Innovation* 11(2): 1259-1263.

Menzel, C.M., 2023. A review of fruit development in strawberry: high temperatures accelerate flower development and decrease the size of the flowers and fruit. *The Journal of Horticultural Science and Biotechnology* 98(4):409-431.

Meyer, M., Diehl, D., Schaumann, G.E., Muñoz, K., 2021. Multiannual soil mulching in agriculture: Analysis of biogeochemical soil processes under plastic and straw mulches in a 3-year field study in strawberry cultivation. *Journal of Soils and Sediments* 21: 3733-3752.

Mohapatra, K., Singh, S., Patra, A., Jatav, S., Rajput, V., Popova, V., Puzikova, O., Nazarenko, O., Sushkova, S., 2022. Biogeoaccumulation of zinc in hybrid rice (Oryza sativa L.) in an inceptisol amended with soil zinc application and its bioavailability to human being. *Eurasian Journal of Soil Science* 11(3): 184 – 197.

Panigrahi, H. K., Lodhi, Y., Saha, M., 2019. Growth, yield and quality improvement in strawberry through foliar application of calcium, iron and zinc: A review. *Journal of Pharmacognosy and Phytochemistry* 8(6):734-737.

Raliya, R., Tarafdar, J.C., 2013. ZnO nanoparticle Biosynthesis and Its Effect on Phosphorous-Mobilizing Enzyme Secretion and Gum Contents in Clusterbean (Cyamopsis tetragonoloba L.). *Agricultural Research* 2: 48-57.

Sharma, R. K., Kumar, R., Thakur, S., 1991. Effect of foliar feeding of potassium, calcium and zinc on yield and quality of guava. *Indian Journal of Horticulture* 48(4): 312-314.

Singh, A., Rajput, V. D., Varshney, A., Sharma, R., Ghazaryan, K., Minkina, T., El-Ramady, H., 2024b. Revolutionizing crop production: Nanoscale wonders - current applications, advances, and future frontiers. *Egyptian Journal of Soil Science* 64(1): 221-258.

Singh, A., Rajput, V.D., Lalotra, S., Agrawal, S., Ghazaryan, K., Singh, J., Alexiou, A., 2024a. Zinc oxide nanoparticles influence on plant tolerance to salinity stress: insights into physiological, biochemical, and molecular responses. *Environmental Geochemistry and Health 46*(5):148.

Singh, A., Sengar, R. S., Rajput, V. D., Al-Ghzawi, A. L., Shahi, U. P., Ghazaryan, K., Habeeb, T., 2024c. Impact of salinity stress and zinc oxide nanoparticles on macro and micronutrient assimilation: unraveling the link between environmental factors and nutrient uptake. *Journal of Ecological Engineering* 25(2): 1-9.

Singh, A., Sengar, R. S., Rajput, V. D., Minkina, T., Singh, R. K., 2022a. Zinc oxide nanoparticles improve salt tolerance in rice seedlings by improving physiological and biochemical indices. *Agriculture* 12(7):1014.

Singh, A., Sengar, R. S., Shahi, U. P., Rajput, V. D., Minkina, T., Ghazaryan, K. A., 2022b. Prominent effects of zinc oxide nanoparticles on roots of rice (Oryza sativa L.) grown under salinity stress. *Stresses* 3(1): 33-46.

Singh, D. K., Paul, P. K., Ghosh, S.K., 2005. Response of papaya to foliar application of boron, zinc and their combinations. *Research on Crops* 6(2): 277-280.

Warang, O., Sante, P., Dhole, R., 2023. Nanofertilizers for efficient fruit production: A review. *The Pharma Innovation Journal* 12(4): 2603-2607.

Yadlod, S.S., Kadam, B.A., 2003. Effect of plant growth regulators and micronutrients on growth, yield and storage life of banana (Musa sp.) cv. Grand Naine. *The Asian Journal of Horticulture* 36(2):114-117.

Yogeesha, L., 2005. Effect of Iron on yield and quality of Grape (Vitis Vinifera L) in Calcareous vertisol. University of Agricultural Sciences (Bangalore). Soil Science & Agricultural Chemistry. M.Sc.Thesis.

Eurasian Journal of Soil Science 2024, 13(3), 263 - 272

Eurasian Journal of Soil Science

Journal homepage : http://ejss.fesss.org

Effective strategies for reclaiming soda-saline soils: Field experimentation and practical applications in Southeast Kazakhstan

Askhat Naushabayev [a], Nurzikhan Seitkali [a,*], Karlyga Karayeva [a], Shynar Mazkirat [b], Meirambay Toilybayev [a], Tursunay Vassilina [a]

[a] Kazakh National Agrarian Research University, Abay Avenue 8, Almaty, Kazakhstan

[b] Kazakh Research Institute of Agriculture and Plant Growing, Almaty District, Almalybak 040909, Kazakhstan

Article Info

Received : 07.12.2023

Accepted : 23.05.2024

Available online : 03.06.2024

Author(s)

A.Naushabayev

N.Seitkali *

K.Karayeva

S.Mazkirat

M.Toilybayev

T.Vassilina

* Corresponding author

Abstract

Soda-saline soils pose significant challenges to agricultural productivity, particularly in regions like the foothill plain of the Ili Alatau in southeast Kazakhstan. In this study, we examined the effectiveness of different ameliorants, including phosphogypsum, elemental sulfur, and sulfuric acid, in reclaiming soda-saline soils and enhancing crop yields. The study was conducted under real climatic and production conditions at the "Amiran" LLP farm. Using a randomized complete block design, we assessed the impact of these ameliorants on soil composition and alfalfa yield over two cutting cycles. The experiment involved the application of phosphogypsum, elemental sulfur, and sulfuric acid to designated plots within the farm, each covering an area of 15m2. Soil samples were collected before and after treatment to assess changes in soil composition and salinity. Alfalfa, a resilient perennial crop, was selected for cultivation due to its tolerance to adverse soil conditions. Our findings reveal that all tested ameliorants successfully neutralized the toxic environment of soda-saline soils, resulting in improved soil conditions and increased crop productivity. Phosphogypsum treatment led to a reduction in bicarbonate and carbonate ions, an increase in sulfate ion concentration, and improved soil structure. Elemental sulfur incubation decreased bicarbonate and carbonate ions, further reducing absorbed sodium levels and enhancing soil fertility. Sulfuric acid treatment provided rapid results in reducing alkalinity and increasing sulfate ion concentration, leading to significant improvements in soil quality and crop yield. However, the reclamation of soda-saline solonetzes presented challenges related to soil heterogeneity and poor water permeability. To address these challenges, we recommend the implementation of mechanical destruction of the solonetz soil horizon and deep soil loosening, accompanied by the addition of ameliorants. In conclusion, our study demonstrates the potential of phosphogypsum, elemental sulfur, and sulfuric acid as effective ameliorants for reclaiming soda-saline soils and improving agricultural productivity in challenging environments. By adopting recommended reclamation strategies, farmers can overcome soil limitations and achieve sustainable crop production in regions affected by soda-saline soil degradation.

Keywords: Soil reclamation, soda-saline soils, elemental sülfür, phosphogypsum, sulfuric acid, agricultural productivity.

© 2024 Federation of Eurasian Soil Science Societies. All rights reserved

Introduction

Soil salinization and sodification remain significant challenges worldwide, particularly in arid and semi-arid regions. These phenomena not only hinder agricultural productivity but also jeopardize global food security (Negacz et al., 2022). The prevalence of saline and soda-affected soils continues to expand, driven by both natural processes and human activities such as unsustainable irrigation and drainage practices (FAO, 2015;

: https://doi.org/10.18393/ejss.1491206

: https://ejss.fesss.org/10.18393/ejss.1491206

Publisher : Federation of Eurasian Soil Science Societies

e-ISSN : 2147-4249

Ivushkin et al., 2019). The consequences of soil salinization and sodification extend beyond diminished crop yields, disrupting vital soil processes and undermining soil biodiversity (Doula and Sarris, 2016).

Of particular concern are alkaline soda soils, which present formidable obstacles to reclamation due to their elevated levels of sodium, magnesium, and sodium carbonates and bicarbonates in the pore solution (FAO, 1984). In Kazakhstan, where fertile lands are interspersed with areas affected by soil salinity and sodicity, the need for effective reclamation strategies is paramount. In the foothill plains of southeast Kazakhstan, characterized by meadow, meadow-gray soil, and meadow-chestnut soils, substantial yield losses of 15% to 45% due to soda salinity have been observed (Funakawa et al., 2000; Saparov, 2014; Pachikin et al., 2014; Otarov, 2014; Laiskhanov et al., 2016; Suska-Malawska et al., 2019, 2022; Zhang et al., 2019; Ma et al., 2019; Yertayeva et al., 2019; Kussainova et al., 2020; Liu et al., 2022).

Efforts to address soil salinity and sodicity in Kazakhstan have focused on the application of ameliorative techniques such as phosphogypsum, elemental sulfur, and sulfuric acid. Previous laboratory research has provided valuable insights into the physicochemical processes involved in soil reclamation, laying the groundwork for field experimentation (Hopmans et al., 2021). However, the translation of laboratory findings to real-world conditions is essential for developing effective soil reclamation strategies tailored to local environmental and climatic conditions (Shankar and Evelin, 2019).

This article presents the outcomes of a field experiment conducted in southeast Kazakhstan to evaluate the efficacy of various ameliorants in reclaiming soda-saline soils. Building upon the insights gained from laboratory studies, the field experiment aimed to elucidate the dynamics of ameliorant influence on soil salt regimes in actual environmental settings. By effectively managing the fertility of infertile soda-saline soils, the study contributes to the advancement of sustainable land management practices and agricultural productivity in saline-affected regions (Qadir and Schubert, 2002; Schirawski and Perlin, 2018). In summary, the field evaluation of ameliorants for reclaiming soda-saline soils represents a crucial step towards addressing the pressing challenge of soil salinity and sodicity in Kazakhstan. The findings offer practical insights into soil reclamation strategies tailored to the unique characteristics of saline-affected lands, paving the way for sustainable agricultural development and enhanced food security in the region.

Material and Methods

Site description

The field experimentation and soil sampling were conducted in the Talgar region of the Almaty province in Kazakhstan. The selection of the experimental site was based on comprehensive analyses of small, medium, and large-scale soil maps, emphasizing the distribution of alkaline soda-saline soils within the region. The specific coordinates of the site are N 43°39'7858, E 77°18'2917 (Figure 1). This area falls within the halogeochemical province characterized by the accumulation of sodic-sulfate salts from the Balkhash Lake basin. The climate in this region exhibits characteristics of continental and drought-prone conditions, with dry and hot summers. July typically sees average temperatures ranging from 22-25°C, while January averages range between 9-12°C. Annual precipitation averages around 250-300 mm, with an average annual air temperature of 9.8°C. The predominant soils in the study area are light meadow gray soils, with particular focus directed towards semi-hydromorphic heavy loamy solonetzes exhibiting sulfate-sodic, sodic-sulfate, and pure sodic chemistries. These soils cover approximately 10% of the total area under investigation.

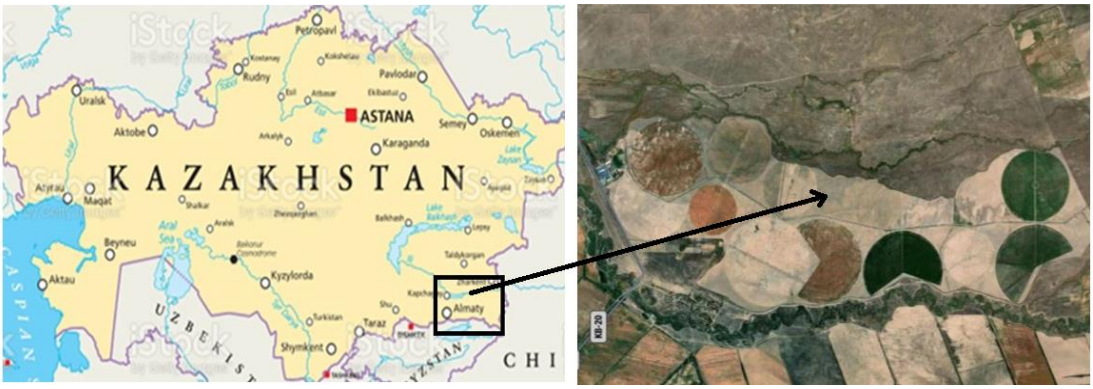

Figure 1. Location of the study area

Field Experiment and Soil Sampling

The field experiment was conducted at Amiran Farm in experimental field №8, dedicated to corn silage production within a crop rotation system. The area's soils exhibit diverse characteristics, ranging from meadow gray soils to light northern, weakly solonchakous-slightly solonchakous, and medium to strongly

solonetzic types, with chloride-soda and soda-sulfate chemistry covering an expanse of 77 hectares. Notably, heavy loamy medium-salt semi-hydromorphic solonetzes, comprising approximately 10% (8 hectares) of the field, occur in the form of spots on microdepressions, displaying sulfate-soda, soda-sulfate, and pure soda chemistry. Solonetzes are marked by a dense clay horizon B, rich in adsorbed (exchangeable) Na^+ and occasionally Mg^{2+}. These soils also contain free soda (Na_2CO_3), contributing to a highly alkaline environment, which adversely affects corn growth, leading to sparse or complete absence in affected areas.

Figure 2. Condition of corn plants on the spotted soda-saline solonetz of the experimental plot

An experimental site was designated within one of these spots to evaluate the effectiveness of various ameliorants, including phosphogypsum, elemental powdered sulfur, and a 1% solution of sulfuric acid. The experiment was replicated four times to ensure robustness of results. Before initiating the field experiment, soil samples were collected from each plot and replicate at depths of 0-20 cm, 20-40 cm, and 40-60 cm to determine initial content of water-soluble salts, pH, and composition of absorbed bases (Ca, Mg, Na, K). Subsequent plowing and leveling prepared the experimental plot for further proceedings. Based on the experimental design, the plot was divided into randomly distributed plots, each covering an area of $5\times3=15m^2$. Following this, calculated doses of ameliorants were applied to the soil of the plots and thoroughly mixed. Periodic moistening was carried out to maintain optimal soil moisture levels.

Utilizing data on the initial physicochemical composition of semi-hydromorphic heavy loamy solonetzes, a comprehensive field experiment scheme was devised, incorporating phosphogypsum, powdered elemental sulfur, and a 1% solution of sulfuric acid. These were applied based on an equivalent dose of 1 ton of gypsum.

№	Variants	Doses of Ameliorating Substances
1	Control	-
2	Phosphogypsum	17.5 kg (per 15 m2) / 11.67 tons (per hectare)
3	Elemental Sulfur	6.66 kg (per 15 m2) / 2.22 tons (per hectare)
4	Sulfuric Acid, 1% Solution	9.97 kg (per 15 m2) / 6.652 tons (per hectare)

The fertility restoration of the 0-40 cm soil layer was determined using the formula:

$$G= 0.086\times(Na^+ - 0.1xCEC) + [(CO_3^{2-} + HCO_3^-) - 1.0] \times H \times Bd;$$

here:

G represents the amount of pure gypsum (100% $CaSO_4\cdot2H_2O$).

Na^+ is the amount of exchangeable sodium (me $100g^{-1}$).

H stands for the thickness of the reclamed layer (cm).

Bd indicates the bulk density (g cm^3).

CEC signifies the cation exchange capacity (me $100g^{-1}$).

0.086 is the coefficient of conversion of calcium to gypsum.

1.0 represents the amount of (CO_3^{2-} + HCO_3^-) in the water extract that is not harmful to plants (me $100g^{-1}$).

0.1 is the coefficient allowing the preservation of 10% of exchangeable sodium in the soil absorbing complex of solonetzes.

The concentration of these ions (CO_3^{2-} + HCO_3^-) in the water extract is measured in me $100g^{-1}$. The presence of free soda in the soil necessitates an increase in ameliorating substances due to the presence of sodium carbonates and bicarbonates. Equivalent amounts of sulfur and sulfuric acid, in tons equivalent to 1 ton of pure gypsum, are 0.19 and 0.57, respectively. Calculations revealed that for medium and strong solonetz, the reclamation of a 0-40 cm layer requires 11.67 t/ha of gypsum or phosphogypsum, 2.22 t/ha of elemental sulfur, and 6.652 t/ha of sulfuric acid. The concentration of the latter was adjusted by diluting it with water to a 1% solution. In the variants utilizing phosphogypsum, sulfur, and sulfuric acid, the soil underwent plowing

and washing with 1.5-2 volumes of water, equal to the total moisture capacity of the soil (5 m^3) with a volume of 4500 m^3/ha. Water supply was repeated three times every 5-6 days to ensure effective leaching after each release of the reclaimed soil layer from gravitational water (water of large and medium pores). The rinsing rate of water was determined using the formula of Volobuev (1975).

$$Q = Q1 + Q2 + Q3$$

where:

Q represents the leaching rate (m^3/ha).

Q1 denotes the amount of water in percentage that saturates the soil above natural moisture to the lowest moisture capacity (LMC), calculated as LMC-m.

mm signifies the reserve of natural humidity (in percentage).

Q2 indicates the amount of water (in percentage) saturating the soil above the LMC to the full moisture capacity (FMC), calculated as FMC-LMC.

Q3 represents the amount of water in m^3/ha filtered through the soil after it is completely saturated, expressed as a multiple of FMC or LMC by coefficient n, depending on salinity, water-physical, and physicochemical properties of the soil, i.e. Q3=n x FMC x (LMC)

Before and after leaching, mixed soil samples from the experimental plots were collected and subjected to laboratory analysis, including the determination of the ionic composition (HCO3-, CO_3^{2-}, Cl^-, SO_4^{2-}, Ca^{2+}, Mg^{2+}, Na^+, K^+) of water extract from soils, salt content, pH levels, and the composition of absorbed cations (USDA, 2014; 2022). The toxicity threshold for individual ions in aqueous extracts from soil was used for classification according to Bazilevich and Pankov (1969). Statistical analysis was performed using one-way ANOVA and Tukey's multiple comparison tests to determine the significance of differences between the different ameliorants. The analysis was conducted in the R statistical software (v4.1.3).

Results and Discussion

Reclamation efficiency of phosphogypsum incubation, sulfur, and sulfuric acid application, and leaching on soda-saline soils

The geological dynamics within the middle segment of the Ili Depression have instigated a desalinization process within the upper layers of carbonate sulfate solonchaks. These solonchaks, primarily formed under effusive water regimes in preceding epochs, underwent transformation into solonchakous meadow gray soils due to prolonged and gradual infiltration of sodium sulfate-rich solutions through carbonate strata. This phenomenon eventually led to the development of soda semi-hydromorphic solonetzes (Sarybaeva and Naushabayev, 2021). The perpetual generation of soda compounds (Na_2CO_3, $NaHCO_3$) within the soil profile, facilitated by exchange reactions between sodium colloids and the soil solution, is intricately linked with groundwater dynamics. Consequently, any chemical reclamation endeavors targeting soda-saline soils within the saz zone of the foothill plain yield short-term efficacy.

Field experiments were conducted to investigate the initial ion composition in pore solutions and soil-absorbing complexes within a designated area. Ameliorants were applied to experimental variants characterized by mild to moderately saline conditions (Table 1). The soluble salt content in soil variants treated with phosphogypsum measured 0.578%, 0.492%, and 0.645% at three depths, while elemental sulfur-treated variants exhibited contents of 0.142%, 0.157%, and 0.304%, and sulfuric acid-treated variants had contents of 0.143%, 0.437%, and 0.487%. Notably, these alternatives displayed a salinity chemistry comprising sulfate-soda, soda-sulfate, and pure soda components. Moreover, the presence of ions (HCO_3^-, CO_3^{2-}) responsible for soil alkalinity ranged from 1.36 to 3.80 me $100g^{-1}$ and 0.16 to 0.88 me $100g^{-1}$soil within the 0-20 cm upper layer. The elevated levels of these ions, surpassing plant-toxic thresholds, contribute to a high alkalinity environment (pH~9.0). Additionally, the soil solution harbored sulfates exceeding toxicity thresholds (1.7 me $100g^{-1}$), while chlorine ions remained at insignificant levels below toxicity thresholds (<0.3 me $100g^{-1}$). Sodium ions predominated in the cationic composition, exceeding toxicity thresholds (>2.0 me $100g^{-1}$) by several folds (3.24–8.21 me $100g^{-1}$).

Analysis of absorbed exchangeable cations revealed that soils within experimental variants exhibited characteristics of sodium-magnesium solonetzes (Sn). These soils predominantly absorbed magnesium, followed by sodium, with their proportions ranging from 30.00 to 63.69% and from 10.78 to 19.00% of the cation exchange capacity (CEC) within the surface layer of experimental variants. The average absorption capacity varied from 10.83 to 17.95 me $100g^{-1}$ soil across experimental variants.

Table 1. Influence of incubation of ameliorants and leaching of soda-saline soils of semi-hydromorphic solonetzes of the experimental site on their salt regime

Ameliorants	Variants	Total salt, %	(me 100g^{-1})								pH	Salinity chemistary	Degree of salinity
			HCO_3^-	CO_3^{2-}	Cl^-	SO_4^{2-}	Ca^{2+}	Mg^{2+}	Na^+	K^+			
At the depth of 0-20 cm													
PG	C	0,578a	3,80a	0,88a	0,11ab	3,56b	0,24a	0,24bc	6,79a	0,20bc	9,15a	S/Sd	moderate
	BL	0,34bcd	0,82cde	0,10bcd	0,05b	3,94ab	1,71a	0,61abc	2,24bc	0,26ab	7,90cde	S	low
	AL	0,363bc	0,73cde	0,06cd	0,21a	4,15ab	1,00a	0,60abc	3,21bc	0,29ab	8,41bc	S	low
S/r	C	0,142d	1,48b	0,32b	0,11ab	0,16c	0,10a	0,19c	1,32c	0,15c	8,98ab	Sd	low
	BL	0,35bcd	0,69de	0,06cd	0,07ab	4,09ab	1,03a	0,52abc	3,04bc	0,27ab	7,70de	S	low
	AL	0,276cd	0,47e	0,02cd	0,12ab	3,39b	1,62a	1,00a	1,05c	0,33a	8,28cd	S	low
SA, 1%	C	0,143d	1,36bc	0,16bcd	0,11ab	0,35c	0,10a	0,38bc	1,21c	0,14c	9,22a	Sd	low
	BL	0,534ab	0,66de	0,10bcd	0,10ab	6,77a	1,67a	0,73ab	4,83ab	0,30a	7,40e	S	moderate
	AL	0,226cd	1,13bcd	0,22bc	0,07ab	1,81bc	0,22a	0,29bc	2,35bc	0,15c	8,47bc	Sd/S	low
At the depth of 20-40 cm													
PG	C	0,492ab	2,76a	1,04a	0,11a	3,56b	0,10b	0,10b	6,08ab	0,16bc	9,03bcd	Sd/S	moderate
	BL	0,432ab	1,89abc	0,40bc	0,03a	3,84b	0,12b	0,33ab	5,18ab	0,138bc	9,60ab	Sd/S	moderate
	AL	0,381b	0,82d	0,14c	0,09a	4,35ab	0,36ab	0,48ab	4,16b	0,26a	8,77cd	S	low
S/r	C	0,157c	1,36cd	0,32bc	0,11a	0,55c	0,10b	0,38ab	1,43c	0,11bc	8,90cd	Sd/S	low
	BL	0,427ab	1,72bc	0,28bc	0,05a	3,97b	0,14ab	0,35ab	5,08ab	0,17b	9,60ab	Sd/S	moderate
	AL	0,359b	1,01cd	0,10c	0,12a	3,80b	0,50a	0,48ab	3,71bc	0,24a	8,50de	Sd/S	low
SA, 1%	C	0,437ab	1,80bc	0,56b	0,07a	3,98b	0,10b	0,29ab	5,37ab	0,10c	9,24abc	Sd/S	moderate
	BL	0,595a	1,60bcd	0,58b	0,13a	6,45a	0,27ab	0,55a	7,2a	0,17b	9,85a	S	moderate
	AL	0,472ab	2,42ab	0,90a	0,07a	3,73b	0,10b	0,24ab	5,74ab	0,14bc	7,96e	Sd/S	moderate
At the depth of 40-60 cm													
PG	C	0,645a	2,48a	1,20a	0,15ab	6,03a	0,10bc	0,19b	8,21a	0,16ab	9,03d	Sd/S	strong
	BL	0,453bc	2,35ab	0,68bcd	0,04cd	3,60bc	0,12abc	0,38ab	5,36bc	0,14abc	10,1a	Sd/S	moderate
	AL	0,441bc	1,82abc	0,58cd	0,07bcd	4,01abc	0,12abc	0,22ab	5,38bc	0,17ab	9,69b	Sd/S	moderate
S/r	C	0,304c	1,72bc	0,56cd	0,11abc	2,20c	0,19a	0,48a	3,24c	0,13bc	8,92d	Sd/S	low
	BL	0,455bc	2,07abc	0,48d	0,02d	3,95abc	0,09c	0,26ab	5,54bc	0,15abc	10,0a	Sd/S	moderate
	AL	0,397bc	1,50c	0,32d	0,11abc	3,74bc	0,17ab	0,36ab	4,65bc	0,18a	9,12cd	Sd/S	low
SA, 1%	C	0,49abc	2,28ab	1,04ab	0,11abc	4,08abc	0,10bc	0,19b	6,08abc	0,10c	9,28c	Sd/S	moderate
	BL	0,565ab	1,78abc	0,64bcd	0,16a	5,74ab	0,10bc	0,39ab	7,03ab	0,17ab	10,0abc	Sd/S	moderate
	AL	0,47abc	2,16abc	0,94abc	0,07bcd	3,96abc	0,12abc	0,198b	5,74abc	0,14abc	11,46a	Sd/S	moderate
Toxicity threshold, me		0,1	0,8	0,03	0,3	1,7	-	-	2,0	-	-	-	-

PG – Phosphogypsum, S/r – sulfur, SA – sulfuric acid, C – control, BL – before leaching, AL – after leaching, S – sulfate, Sd – sodic

Table 2. Effect of incubation and leaching on the composition of absorbed cations of reclaimed soda-saline semi-hydromorphic solonetz of the experimental site

Ameliorants	Variants	me100g^{-1}					Solonetz degree
		Ca^{2+}	Mg^{2+}	Na^+	K^+	CEC	
At the depth of 0-20 cm							
Phosphogypsum	C	3,96b	10,40a	1,76abc	0,21a	16,33ab	SN
	BL	15,10a	4,83c	0,77bc	0,19a	20,89a	SRn1Msh
	AL	9,16ab	5,20c	0,51bc	0,18a	15,05ab	SRn1Msh
Sulfur	C	4,95b	6,93bc	1,83ab	0,21a	13,92b	SN
	BL	10,15ab	7,55abc	0,96abc	0,21a	18,87ab	SRn1Msh
	AL	9,90ab	7,06bc	0,31c	0,12a	17,39ab	SRn1Msh
Sulfuric acid 1%	C	6,44b	8,91ab	2,28a	0,32a	17,95ab	SN
	BL	9,16ab	7,79abc	1,11abc	0,26a	18,32ab	SRn1Msh
	AL	6,08b	5,44c	1,37abc	0,33a	13,22b	SRn1Msh
At the depth of 20-40 cm							
Phosphogypsum	C	3,47c	7,43a	4,24a	0,51a	15,65ab	SN
	BL	4,46bc	7,31a	2,29abc	0,27abc	14,33ab	SN
	AL	8,54a	7,06a	0,76c	0,19bc	16,55a	SRn1Msh
Sulfur	C	3,96bc	7,43a	2,00abc	0,00c	13,39ab	SN
	BL	5,32bc	7,18a	2,15abc	0,37ab	15,02ab	SN
	AL	6,81ab	7,06a	0,36c	0,22bc	14,45ab	SRn1Msh
Sulfuric acid 1%	C	3,96bc	7,92a	1,14bc	0,35ab	13,37ab	SN
	BL	4,70bc	6,06a	1,78bc	0,43ab	13,47ab	SN
	AL	3,09c	5,20a	3,28ab	0,39ab	11,96b	SN
At the depth of 40-60 cm							
Phosphogypsum	C	1,98c	8,42a	1,21a	0,47a	12,08a	SN
	BL	2,11c	7,31ab	1,88a	0,30abc	11,60a	SN
	AL	2,85bc	6,19ab	1,49a	0,31abc	10,84a	SN
Sulfur	C	4,46b	5,94b	1,87a	0,16c	12,43a	SN
	BL	3,10bc	6,44ab	2,21a	0,25bc	12,00a	SN
	AL	3,84bc	6,93ab	0,71a	0,29abc	11,77a	SN
Sulfuric acid 1%	C	6,93a	3,46c	1,62a	0,25bc	12,26a	SRn1Msh
	BL	3,59bc	6,43ab	1,51a	0,39ab	11,92a	SN
	AL	3,09bc	5,19bc	2,78a	0,40ab	11,46a	SN
Solonetz threshold		-	-	-	-	-	

C – control, BL – before leaching, AL – after leaching, SN – solonetz, SRn_1Msh – meadowish sierozem northern

Overall, the soils at the experimental site were identified as heavy loamy sodium-magnesium solonetzes with mixed sulfate-soda, soda-sulfate, and pure soda chemistry, exhibiting weak to moderate salinity levels. Following the application of calculated equivalent doses of sulfur, phosphogypsum, and sulfuric acid to soda-saline solonetzes, their reclamation efficiency was assessed based on water extracts and absorbed base compositions before leaching (Table 1 and 2).

Investigation of the effects of incubation of phosphogypsum, sulfur, and sulfuric acid and leaching of reclaimed soils on alfalfa yield

The study aimed to assess the impact of incubation and leaching of reclaimed soils with phosphogypsum, elemental sulfur, and sulfuric acid on perennial grass yield (Figure 3). Alfalfa variety "Kokorai" was sowed in the spring at a seeding rate of 26 kg/ha. Variants treated with phosphogypsum and sulfur showed relatively good alfalfa green mass yield, crucial considering the challenge of obtaining a harvest on the soda-saline solonetzes of the experimental plot without ameliorants. The zero yield in the control variant underscored the necessity of ameliorants. The impediments to alfalfa seed germination included toxic soda and sulfates in the soil solution, adverse water-physical properties, and the formation of a dense crust.

Figure 3. Overview of the experimental plot and the alfalfa cultivated within

The control variant's soils, where alfalfa failed to grow, exhibited high levels of carbonate, bicarbonate ions, and sulfates. These ions' concentrations in the 0-40 cm soil layer averaged 0.59, 2.66, and 2.83 me $100g^{-1}$ soil, respectively, indicating a sulfate-soda and soda-sulfate salinity chemistry. Sodium dominated the cationic composition of the soil solution, averaging 5.00 me $100g^{-1}$ soil, indicating sodium-magnesium heavy solonetzes. The soil environment in the control plots was highly alkaline (pH 9.0). To facilitate alfalfa growth and development, the experimental variants received abundant irrigation.

Alfalfa seedlings sprouted across all replicates of variants with phosphogypsum, sulfur, and sulfuric acid, primarily in cracks after soil surface drying. Field germination averaged 80-85% per plot area unit ($15m^2$). The alfalfa leaves displayed varying shades of green. Within a year, a two-cutting yield of alfalfa green mass was achievable using the experimental variants.

Table 3 illustrates the effect of incubation of equivalent doses of phosphogypsum, sulfur, and sulfuric acid, and soil washing on alfalfa yield. The phosphogypsum-treated variant showed an average alfalfa fresh yield of 4.40 tons/ha for the first cutting cycle, with a corresponding dry matter yield of 2.948 tons/ha. Similarly, the sulfur-treated variant yielded 4.09 tons/ha of fresh alfalfa and 2.740 tons/ha of dry matter.

Table 3. Impact of incubation with phosphogypsum, sulfur, and sulfuric acid, and soil washing on alfalfa yield (2023)

№	Variants	Average alfalfa yield, ton/ha					
		Forage fresh yield		∑ for 1 year	Forage dry matter yield		∑ for 1 year
		Cutting cycle1	Cutting cycle2		Cutting cycle1	Cutting cycle2	
1	Control	0.00c	0.00b	0.00b	0.00a	0.000a	0.000a
2	Phosphogypsum	4.40ab	3.82a	8.22a	2.95b	2.559b	5.507b
3	Sulfur	4.09b	3.37ab	7.46a	2.74b	2.258b	4.998ab
4	Sulfuric acid 1%	6.54c	5.88c	12.42c	4.38c	3.940c	8.322c

The second cutting's alfalfa yield slightly decreased in the phosphogypsum and sulfur-treated variants, averaging 3.82 and 3.37 tons/ha, respectively. Notably, the sulfuric acid-treated variant demonstrated a higher yield of 6.54 tons/ha for the first cutting and 5.881 tons/ha for the second, with dry matter yields of 4.382 and 3.94 tons/ha, respectively. This resulted in an annual yield of 12.42 tons/ha of green mass and 8.322 tons/ha of dry hay, highlighting sulfuric acid's potential as a treatment option.

In summary, the experimental plot soils exhibited unfavorable compositions and properties, rendering vegetation growth nearly impossible without ameliorants. Reclamation efforts enabled satisfactory alfalfa harvest, with sulfuric acid proving the most effective among the tested ameliorants in terms of productivity.

Influence of ameliorant incubation and alfalfa cultivation on soil salt regime and absorbed cation composition

The efficacy of ameliorant incubation, including phosphogypsum, sulfur, and sulfuric acid, along with soil leaching and alfalfa cultivation during the summer-autumn growing season, was assessed to understand their impact on the ionic composition of soil water extracts at the experimental site. The results indicated a notable reduction in salinity towards weak levels. In contrast to post-leaching data, sulfate content decreased nearly twofold in the phosphogypsum variant, reaching 2.13 and 2.05 me $100g^{-1}$ soil in the upper layers (0–20 and 20–40 cm). Sulfur incubation similarly reduced sulfate content in the 20–40 cm layer to 2.66 me $100g^{-1}$ soil (from 3.80 me after leaching). Notably, sulfur treatment created more favorable conditions for alfalfa growth compared to phosphogypsum, despite retaining sulfate ions in the solution.

Incubation of sulfuric acid during alfalfa ontogenesis in the summer-autumn period led to an increase in hydrocarbonate and carbonate ions in weakly soda-saline and saline meadow gray soils, accompanied by a decrease in harmful sulfate and sodium ions below their toxicity thresholds compared to post-leaching data. However, there was a general trend of decreasing water-soluble salt content in the soil solution, counteracted by increased ion concentration due to environmental factors such as elevated air and soil temperatures and intensified plant evaporation. The impact of ameliorant incubation, leaching, and alfalfa cultivation on soil salt regime was further evaluated through Table 4, showing variations in salt content across different treatments and depths. Phosphogypsum and sulfur incubation, along with alfalfa cultivation, contributed to sodium neutralization in the soils, approaching non-solonetz levels. However, the proportion of absorbed magnesium increased, indicating changes in soil-absorbing complex composition. Similar trends were observed with elemental sulfur, albeit with a higher proportion of magnesium.

Table 4. Effect of incubation of ameliorants, leaching and cultivation of alfalfa on the salt regime of soils in the experimental plot, me, August 2023

Ameliorants	Variants	Total salt, %	me $100g^{-1}$ soil								pH	Salinity chemistry	Degree of salinity
			HCO_3^-	CO_3^{2-}	Cl^-	SO_4^{2-}	Ca^{2+}	Mg^{2+}	Na^+	K^+			
PG	C	0,210a	0,73cd	0,10de	0,07a	2,13ab	1,12ab	0,62ab	1,01bc	0,19ab	8,6d	Sd/S	Low
	BL	0,276a	1,6abcd	0,50abcd	0,07a	2,05ab	0,12b	0,88a	2,58abc	0,15b	9,7ab	Sd/S	Low
	AL	0,260a	1,89ab	0,60abc	0,08a	1,39ab	0,10b	0,34ab	2,80a	0,14b	9,9ab	S/Sd	Low
S/r	C	0,288a	0,54d	0,00e	0,06a	3,54a	2,09a	0,96a	0,86c	0,24a	8,7cd	S	Low
	BL	0,273a	1,04bcd	0,24cde	0,06a	2,66ab	0,58ab	0,72ab	2,28abc	0,19ab	9,3bc	Sd/S	Low
	AL	0,260a	1,77abc	0,62abc	0,09a	1,52ab	0,10b	0,39ab	2,77a	0,13b	10,1a	S/Sd	Low
SA, 1%	C	0,162a	1,37abcd	0,28dcde	0,06a	0,69b	0,18b	0,69ab	1,13abc	0,13b	8,6d	S/Sd	Low
	BL	0,220a	2,10ab	0,66ab	0,06a	0,61b	0,15b	0,43ab	2,08abc	0,13b	10,0ab	Sd	Low
	AL	0,247a	2,26a	0,84a	0,05a	0,78b	0,10b	0,22b	2,66ab	0,12b	10,3a	Sd	Low
Toxicity threshold, me		0,1	0,8	0,03	0,3	1,7	-	-	2,0	-	-	-	-

PG – Phosphogypsum, S/r – sulfur, SA – sulfuric acid, C – control, BL – before leaching, AL – after leaching, S – sulfate, Sd – sodic

Table 5 illustrates the effect of ameliorant incubation and phytomelioration on absorbed bases of mixed soda-saline meadow gray soils. Notably, long-term sulfuric acid addition significantly decreased absorbed sodium while increasing absorbed magnesium in the upper soil layers, emphasizing its potential in altering soil cation composition.

Table 5. Effect of incubation of equivalent doses of ameliorants and phytomelioration on the absorbed bases of mixed soda-saline meadow gray soils, August 2023

Ameliorants	Variants	Absorbed cations, me $100g^{-1}$				CEC, me $100g^{-1}$	Solonetz degree	
		Ca^{2+}	Mg^{2+}	Na^+	K^+		Mg^{2+}	Na^+
Phosphogypsum	C	9,04a	7,06a	0,16ab	0,23bc	16,49a	SN	SRn1Msh
	BL	6,19abc	7,18a	0,65b	0,24bc	14,26a	SN	SRn1Msh
	AL	5,94abc	6,56a	1,01b	0,22bc	13,73a	SN	$SRn1Msh^{SN1}$
Sulfur	C	10,03a	8,42a	0,20b	0,21c	18,86a	SN	SRn1Msh
	BL	7,31ab	8,17a	1,17b	0,24bc	16,89a	SN	$SRn1Msh^{SN'}$
	AL	2,60cd	9,16a	1,41ab	0,28abc	13,45a	SN	$SRn1Msh^{SN"}$
Sulfuric acid 1%	C	6,31abc	7,31a	0,79b	0,27abc	14,68a	SN	$SRn1Msh^{SN'}$
	BL	4,21bcd	7,31a	1,67b	0,31a	13,50a	SN	$SRn1Msh^{SN"}$
	AL	1,74d	9,28a	3,00a	0,29ab	14,31a	SN	SN
Solonetz threshold		-	-	-	-	-	-	-

C – control, BL – before leaching, AL – after leaching, SN – solonetz, SRn_1Msh – meadowish sierozem nothern

Overall, these findings underscore the efficacy of ameliorant incubation and alfalfa cultivation in mitigating soil salinity and altering absorbed cation composition, highlighting their potential for soil reclamation and sustainable agriculture practices.

The study aimed to evaluate the comparative effectiveness of phosphogypsum, elemental sulfur, and sulfuric acid in reclaiming soda-saline solonetzes, focusing on their impact on soil salt regimes during incubation, leaching, and alfalfa cultivation. Overall, the results indicate that all tested ameliorants effectively altered the ion composition of the soil solution compared to the control group, suggesting their potential for soil reclamation.

Phosphogypsum, sulfur, and sulfuric acid treatments led to a notable reduction in bicarbonate and carbonate ions, thus mitigating soil alkalinity. However, distinct differences were observed in sulfate ion concentrations among the treatments. Particularly, sulfuric acid treatment significantly increased sulfate ion levels in the soil solution by displacing absorbed sodium with calcium ions, transforming the soil chemistry to a pure sulfate composition. This highlights sulfuric acid's effectiveness in reducing soil salinity.

Among the ameliorants, sulfuric acid demonstrated exceptional efficacy in shifting the soil's salinity chemistry towards a pure sulfate composition. This was attributed to the displacement of absorbed sodium by calcium ions from the soil-absorbing complex (SAC), resulting in an increased sulfate ion concentration in the solution. Additionally, sulfuric acid facilitated the leaching of reaction products, leading to a notable decrease in sulfate ion content in the soil solution. In contrast, sulfur treatment showed significant potential in reducing bicarbonate and normal carbonate ion levels in the soil solution, particularly in the upper layer. Despite retaining sulfate ions, sulfur-treated soils exhibited favorable conditions for alfalfa growth, indicating its effectiveness in ameliorating soil alkalinity. Phosphogypsum also showed promising outcomes, albeit with slight variations in ion composition compared to sulfur and sulfuric acid treatments. While phosphogypsum led to a higher sulfate ion content, it demonstrated properties conducive to improving soil structure, as observed during field observations. The reduction in absorbed sodium proportion relative to other cations in treated soils indicated the creation of more favorable conditions for crop growth and development. Alfalfa cultivation, particularly in phosphogypsum and sulfur-treated soils, not only enhanced soil structure but also improved soil nutritional regimes. However, the increased proportion of absorbed magnesium in almost all experimental variants warrants further investigation into its implications for soil fertility and crop productivity. Among the ameliorants, sulfuric acid emerged as the most efficient option in terms of incubation time and alfalfa yield, suggesting its potential for soil reclamation in sodic soils.

Given the unique characteristics of solonetzic soils, mechanical interventions such as deep soil destruction and loosening using specialized equipment are essential for effective ameliorant incorporation. This approach facilitates the penetration of ameliorants, such as phosphogypsum and sulfur, into deeper soil horizons, thereby enhancing their efficacy in soil reclamation.

Conclusion

The study addressed the pressing challenge of soil salinity and sodicity, particularly in arid and semi-arid regions, by evaluating the effectiveness of various ameliorants in reclaiming soda-saline solonetzes in southeast Kazakhstan. Against the backdrop of expanding saline and soda-affected soils globally, including in Kazakhstan, where these soils threaten agricultural productivity and food security, our research aimed to contribute to the development of effective soil reclamation strategies. Through a comprehensive field experiment, incorporating phosphogypsum, elemental sulfur, and sulfuric acid, we observed promising outcomes in altering the ion composition of the soil solution and mitigating soil alkalinity. All tested ameliorants effectively reduced bicarbonate and carbonate ions, thus alleviating soil alkalinity, which is detrimental to crop growth.

Sulfuric acid emerged as a particularly efficient option, demonstrating exceptional efficacy in transforming the soil's salinity chemistry into a pure sulfate composition. By displacing absorbed sodium with calcium ions and facilitating leaching, sulfuric acid not only reduced soil salinity but also improved soil structure, as evidenced by field observations. Sulfur and phosphogypsum treatments also showed promising results, albeit with slight variations in ion composition compared to sulfuric acid. While sulfur effectively reduced bicarbonate and carbonate ion levels, phosphogypsum contributed to improving soil structure, enhancing soil nutritional regimes, and reducing absorbed sodium proportion. The successful cultivation of alfalfa in treated soils further underscored the effectiveness of the reclamation strategies, with sulfuric acid exhibiting the most significant impact on alfalfa yield. However, the increased proportion of absorbed magnesium in treated soils warrants further investigation into its implications for soil fertility and crop productivity. Mechanical interventions such as deep soil destruction and loosening are essential for effective ameliorant incorporation, particularly in

solonetzic soils. These interventions facilitate the penetration of ameliorants into deeper soil horizons, enhancing their efficacy in soil reclamation and paving the way for sustainable agricultural development in saline-affected regions.

In conclusion, our study offers practical insights into soil reclamation strategies tailored to the unique characteristics of saline-affected lands, contributing to the advancement of sustainable land management practices and agricultural productivity in Kazakhstan and similar regions worldwide.

Acknowledgments

This research was funded by the Kazakhstan Ministry of Science and Education (Project No. AP13068643). We gratefully acknowledge their support. We also extend our appreciation to the anonymous reviewers for their valuable feedback and contributions to the improvement of this study.

References

Bazilevich, N.I., Pankova, E.I., 1969. Classification of soils according to their chemistry and degree of salinization. *Agrokémia és talajtan* 18 (sup). pp. 219-226. [in Russian].

Doula, M.K., Sarris, A., 2016. Soil environment. In: Environment and Development : Basic Principles, Human Activities, and Environmental Implications. Poulopoulos, S.G., Inglezakis, V.J. (Eds.). Elsevier, pp. 213-286.

FAO, 1984. Prognosis of salinity and alkalinity. FAO Soils Bulletins No. 31. Food and Agriculture Organization of the United Nations. Rome, Italy, 260p. Available at [Access date: 07.12.2023]: https://www.fao.org/4/ar112e/ar112e.pdf

FAO, 2015. Status of the World's Soil Resources: Main Report. Food and Agriculture Organization of the United Nations and Intergovernmental Technical Panel on Soils (ITPS), Rome, Italy, 650p. Available at [Access date: 07.12.2023]: https://openknowledge.fao.org/server/api/core/bitstreams/6ec24d75-19bd-4f1f-b1c5-5becf50d0871/content

Funakawa, S., Suzuki, R., Karbozova, E., Kosaki, T., Ishida, N., 2000. Salt-affected soils under rice-based irrigation agriculture in Southern Kazakhstan. *Geoderma* 97(1-2): 61–85.

Hopmans, J. W., Qureshi, A. S., Kisekka, I., Munns, R., Grattan, S. R., Rengasamy, P., Ben-Gal, A., Assouline, S., Javaux, M., Minhas, P.S., Raats, P.A.C., Skaggs, T.H., Wang, G., De Jong van Lier, Q., Jiao, H., Lavado, R.S., Lazarovitch, N., Li, B., Taleisnik, E., 2021. Critical knowledge gaps and research priorities in global soil salinity. *Advances in Agronomy* 169: 1-191.

Ivushkin, K., Bartholomeus, H., Bregt, A. K., Pulatov, A., Kempen, B., de Sousa, L., 2019. Global mapping of soil salinity change. *Remote Sensing of Environment* 231: 111260.

Kussainova, M., Spaeth, K., Zhaparkulova, E., 2020. Efficiency of using the rangeland hydrology and erosion model for assessing the degradation of pastures and forage lands in Aydarly, Kazakhstan. *Eurasian Journal of Soil Science* 9(2): 186 - 193.

Laiskhanov, S.U., Otarov, A., Savin, I.Y., Tanirbergenov, S.I., Mamutov, Z.U., Duisekov, S.N., Zhogolev, A., 2016. Dynamics of soil salinity in irrigation areas in South Kazakhstan. *Polish Journal of Environmental Studies* 25(6): 2469–2476.

Liu, W., Ma, L., Smanov, Z., Samarkhanov, K., Abuduwaili, J., 2022. Clarifying soil texture and salinity using local spatial statistics (Getis-Ord Gi* and Moran's I) in Kazakh–Uzbekistan Border Area, Central Asia. *Agronomy* 12: 332.

Ma, L., Abuduwaili, J., Smanov, Z., Ge, Y., Samarkhanov, K., Saparov, G., Issanova, G., 2019 Spatial and vertical variations and heavy metal enrichments in irrigated soils of the Syr Darya River watershed, Aral Sea Basin, Kazakhstan. *International Journal of Environmental Research and Public Health* 16(22):4398.

Negacz, K., Malek, Ž., de Vos, A., Vellinga, P., 2022. Saline soils worldwide: Identifying the most promising areas for saline agriculture. *Journal of Arid Environments* 203: 104775.

Otarov, A., 2014. Concentration of heavy metals in irrigated soils in Southern Kazakhstan. In: Novel measurement and assessment tools for monitoring and management of land and water resources in agricultural landscapes of Central Asia. Mueller, L., Saparov, A., Lischeid, G. (Eds.). Environmental Science and Engineering. Springer, Cham. pp 641–652.

Pachikin, K., Erokhina, O., Funakawa, S., 2014. Soils of Kazakhstan, their distribution and mapping. In: Novel measurement and assessment tools for monitoring and management of land and water resources in agricultural landscapes of Central Asia. Mueller, L., Saparov, A., Lischeid, G. (Eds.). Environmental Science and Engineering. Springer, Cham. pp 519–533.

Qadir, M., Schubert, S., 2002. Degradation processes and nutrient constraints in sodic soils. *Land Degradation & Development 13*(4): 275-294.

Saparov, A., 2014. Soil resources of the Republic of Kazakhstan: Current status, problems and solutions. In: Novel measurement and assessment tools for monitoring and management of land and water resources in agricultural landscapes of Central Asia. Mueller, L., Saparov, A., Lischeid, G. (Eds.). Environmental Science and Engineering. Springer, Cham. pp 61–73.

Sarybaeva, G.M., Naushabayev, A.K., 2021. Formation of Soda-Saline Semi-Hydromorphic Solonetz of The Ili Depression. *Izdenister Natigeler* 2(90): 192–204. [in Russian].

Schirawski, J., Perlin, M.H., 2018. Plant–microbe interaction 2017—the good, the bad and the diverse. *International Journal of Molecular Sciences 19*(5): 1374.

Shankar, V., Evelin, H., 2019. Strategies for reclamation of saline soils. In: Microorganisms in Saline Environments: Strategies and Functions. Giri, B., Varma, A. (Eds.). Soil Biology, vol 56. Springer, Cham. pp. 439-449.

Suska-Malawska, M., Sulwiński, M., Wilk, M., Otarov, A., Metrak, M., 2019. Potential eolian dust contribution to accumulation of selected heavy metals and rare earth elements in the aboveground biomass of Tamarix spp. from saline soils in Kazakhstan. *Environmental Monitoring and Assessment* 191: 57.

Suska-Malawska, M., Vyrakhamanova, A., Ibraeva, M., Poshanov, M., Sulwiński, M., Toderich, K., Metrak, M., 2022. Spatial and in-depth distribution of soil salinity and heavy metals (Pb, Zn, Cd, Ni, Cu) in arable irrigated soils in Southern Kazakhstan. *Agronomy* 12: 1207.

USDA, 2014. Soil Survey Field and Laboratory Methods Manual. Soil Survey Investigations Report No. 51, Version 2. United States Department of Agriculture (USDA), Natural Resources Conservation Service, Kellogg Soil Survey Laboratory. 457p. Available at [Access date: 07.12.2023]: https://www.nrcs.usda.gov/sites/default/files/2023-01/SSIR51.pdf

USDA, 2022. Kellogg Soil Survey Laboratory Methods Manual. Soil Survey Investigations Report No. 42, Version 6.0. Part 1: Current Methods. Kellogg Soil Survey Laboratory, National Soil Survey Center, Natural Resources Conservation Service, United States Department of Agriculture (USDA). 796p. Available at [Access date: 07.12.2023]: https://www.nrcs.usda.gov/sites/default/files/2022-10/SSIR42-v6-pt1.pdf

Volobuev, V.R., 1975. Calculation of washing saline soils. Kolos, Moscow.

Yertayeva, Z. , Kızılkaya, R., Kaldybayev, S., Seitkali, N., Abdraimova, N., Zhamangarayeva, A., 2019. Changes in biological soil quality indicators under saline soil condition after amelioration with alfalfa (Medicago sativa L.) cultivation in meadow Solonchak. *Eurasian Journal of Soil Science* 8 (3): 189-195.

Zhang, W., Ma, L., Abuduwaili, J., Ge, Y., Issanova, G., Saparov, G., 2019. Hydrochemical characteristics and irrigation suitability of surface water in the Syr Darya River, Kazakhstan. *Environmental Monitoring and Assessment* 191: 572.

Eurasian Journal of Soil Science 2024, 13(3), 273 - 283

Eurasian Journal of Soil Science

Journal homepage : http://ejss.fesss.org

Aggregate stability and carbon and N dymamics in macroaggregate size fractions with different soil texture

Mahtali Sbih [a,*], Zohra Bounouara [b], Zoubeir Bensid [a], Djenette Chergui [a], Abbes Zerari [a,c], Souhila Meziane [a], Antoine Karam [d]

[a] Batna 1 University, Institute of Agronomic and Veterinary Sciences, Department of Agronomy, 05000, Batna, Algeria
[b] University of Skikda, Institute of Agronomic Sciences, Department of Agronomy, 21000, Skikda, Algeria
[c] FERTIAL SPA, Route des Salins, El-Hadjar, 23000, Annaba, Algeria
[d] Laval University, Department of Soils and Agri-Food Engineering, Sainte-Foy, Quebec. G1V0A6 Canada

Article Info

Received : 27.12.2023
Accepted : 27.05.2024
Available online: 03.06.2024

Author(s)

M.Sbih *
Z.Bounouara
Z.Bensid
D.Chergui
A.Zerari
S.Meziane
A.Karam

* Corresponding author

Abstract

Soil nutrient cycling, the distribution of soil aggregates, and their stability are directly influenced by soil texture. Different sizes of soil aggregates provide microhabitats for microorganisms and therefore influence soil carbon (C) and nitrogen (N) mineralization. The purpose of the present study was to assess the aggregate stability and dynamics of carbon and nitrogen in macroaggregate size fractions (1-8 mm) with different clay content from meadow soils. Surface soil samples (0-15 cm) were collected from 4- to 5-year-old forage crops. Four macroaggregate size classes were isolated by dry sieving and analyzed for their mass proportions: fine macroaggregates (FM) (less than 1 mm), medium-fine macroaggregates (MFM) (1-2 mm), medium-coarse macroaggregates (MCM) (2-4 mm), and large-coarse macroaggregates (LCM) (4-8 mm). The dry mean weight diameter (MWD), organic carbon (OC), total nitrogen (TN), carbon and nitrogen of microbial biomass (C-MB, N-MB) were determined. CO2 emission and net nitrogen mineralized (NM) were measured after 14 weeks of incubation. The amounts of FM were significantly lower than those of intermediate macroaggregates (MCM and MFM) and decreased markedly with increasing clay content within soil macroaggregates. In general, the amounts of macroaggregate size fractions were lowest in soils with high clay content. MWD exhibited a significant correlation with particle size distribution, OC, and MB-C. OC, TN, MB-C, and MB-N contents within macroaggregates increased with decreasing macroaggregate size and increasing clay content of macroaggregate fractions. The CO2 emission and NM content increased with increasing macroaggregate size, indicating higher organic C and N mineralization activity in larger macroaggregates. Mineralization of OC was lowest in macroaggregate fractions with the highest clay content. We conclude that clay content can increase the protection of microbial biomass in meadow soils. Small macroaggregates tend to contain more recalcitrant organic matter compared to larger macroaggregates.

Keywords: Soil aggregates, aggregate stability, soil texture, soil organic matter.

© 2024 Federation of Eurasian Soil Science Societies. All rights reserved

Introduction

The mineralization of organic carbon (C) and nitrogen (N) in soils has been reported to enhance soil fertility and thus can directly affect different levels of soil quality (Thomsen et al., 2012; Cai et al., 2016). Soil properties, soil aggregation, microbial biomass associated with aggregates, and agricultural management practices play key roles in the C and N dynamics (de Moraes Sá et al., 2014; Abbasi et al., 2015; Naresh et al., 2018) and the distribution of N and C among soil aggregate fractions (Bimüller et al., 2016; Xiao et al., 2017; Xie et al., 2017; Mitran et al., 2018). Gupta and Germida (2015) highlighted the role of soil fungal biomass in changing soil macroaggregates, carbon and nutrient flush following crop cultivation. Similarly, Ogunwole et

: https://doi.org/10.18393/ejss.1494595
: https://ejss.fesss.org/10.18393/ejss.1494595
Publisher : Federation of Eurasian Soil Science Societies
e-ISSN : 2147-4249

al. (2014) indicated that soil organic carbon, aggregate-associated organic carbon, and aggregate size are important soil quality indicators. A better understanding of the mineralization of organic C and N in different particle-size fractions is necessary to improve the management of soil fertility and ultimately enhance agricultural sustainability (Cai et al., 2016; Ghimire et al., 2017; Xie et al., 2017).

It is generally known that the addition of organic materials/wastes contributes to enhancing the formation of aggregates in the soil. Awad et al. (2018) found that biochar and biopolymer amended with oyster shell powder increased the proportion of micro-aggregates (<0.25 mm) relative to the control soil, while the proportion of large macro-aggregates (1–2 mm) increased with the addition of polyacrylamide alone. Wang et al. (2011) showed that in a reddish paddy soil based on a long-term fertilization experiment, the application of organic materials decreased the proportion of small water-stable aggregates (WSA) (<1 mm) and increased the proportion of large WSA (>2 mm), resulting in an increase in the mean weight diameter of WSA, whereas the application of chemical fertilizer had little effect.

It is widely observed that organic matter (OM) biodegradation is faster in coarse- than in fine-textured soils (van Veen and Kuikman, 1990; Saggar et al., 1996), which was associated with faster OM turnover in soil macro-aggregates and lower organic C and N in coarse-textured soils (Six et al., 2000). Bossuyt et al. (2001) found that the formation of water-stable macroaggregates (>250 μm) was not significantly influenced by residue quality or bacterial activity; however, fungal activity positively influenced the stability of these macroaggregates. Ouyang et al. (2013) reported that biochar produced from dairy manure significantly improved macroaggregate formation in two contrasting textured soils (clay and sandy soil) at a ratio of 2% (w/w, dry weight). Cai et al. (2016) reported that in long-term experiments of manure application with or without chemical fertilization, OC and TN content significantly increased and C and N mineralization were enhanced in the three particle-size fractions. The amount of C and N mineralization followed the order 0.053 mm > 0.20-0.053 mm > 2.00-0.25 mm fraction, whereas the amount of OC and TN in different aggregate fractions followed the reverse order. In manure fertilization experiments, Hao et al. (2017) found that long-term manure use significantly increased the amount of coarse fractions and their associated OC and TN stocks in the soils. Also, P-fertilization increased the OC and TN in soil aggregates >2 mm and decreased the loss of N from chemical fertilizers in the legume-grain rotation system. Amellal et al. (2001) showed that the mineralization of organic substances in the larger sand- and silt-sized fractions (50–2000 μm and 2–50 μm, respectively) in petroleum hydrocarbon-contaminated soils was more significant than in the finer (clay-rich) aggregate size fractions (<2 μm). Six et al. (2000) also found that the C content of macroaggregates (0.250-2.00 mm and >2 mm fractions) was higher than that of microaggregates (<0.250 mm fractions) in soils dominated by illite and chlorite. However, they did not observe increased C concentrations with increasing aggregate size in soil with mixed mineralogy (Fe- and Al-oxides and kaolinite). There is little available information on the dynamics of C and N in different aggregate fractions of meadow soils. According to Naresh et al. (2018), there is limited consensus on the pattern of changes in soil OM mineralization and nutrient release across aggregates of different sizes. The present study was conducted with the hypothesis that (i) large-sized macroaggregates (8-4 mm) can mineralize more C and N than fine macroaggregates (<1 mm), (ii) soil fine fraction (clay+ silt) would increase soil aggregation and affect the C, N, and MB dynamics in different aggregate fraction sizes, and (iii) the distribution of microbial biomass carbon (MBC) and nitrogen (MBN) in different aggregate classes affects SOM mineralization in each aggregate size. The objectives of the present study were to quantify the relative rates of C and N mineralization in different particle-size fractions and to examine the effects of clay content and soil aggregation on C and N storage in aggregate-size classes.

Material and Methods

Soil sampling

The soils used in this study were collected from twelve dairy farms located in Sainte-Croix de Lotbinière, in eastern Quebec, Canada. A total of 34 plots spread over 380ha are cultivated in meadow crops. These farms are in transition from conventional management to a low input organic management system. Solid cattle manure is applied on the basis of 132 kg N ha^{-1} which is 20 Mg ha^{-1} on a wet basis. The soil series represents gleyed humo-ferric podzols, samples are taken from the soil layer from 0 to 15 cm. these soils were plowed every 4 to 5 years. Finally, only 14 samples were retained, the other soils are sandy and do not present the different categories of aggregates.

Aggregate-size fractionation

Undisturbed soil samples were taken under wet conditions in the field. Composite samples for each site were formed from nine wet field subsamples. The soils were sampled with a special spade. Special care was applied

in order to maintain the natural structure of the soil samples. Parts of the samples showed signs of deformation due to the smoothing of the spade-cut surface during the process.

Aggregates were separated by dry sieving of moist soil (10 to 14%) as described by Mendes et al. (1999). Dry sieving is simple, rapid and valid method for aggregate separation when examining biologycally active N pools in aggegrates (Sainju, 2006). Field-moist soils were stored at 4°C for 7 to 10 d until they reached a gravimetric water content of 10% (Sainju, 2006). Drying the soil samples at 4 °C reduces its impact on microbial communities and activities within aggregates (Mendes et al., 1999). Soil aggregates were separated by placing 200-g soil fragments (<8 mm, air dried at 4°C) on the top of a set of sieves in decreasing order of mesh sizes: 8.00, 4.00, 2.00, and 1.00 mm (Miller et al., 2009). The aggregates of 8.00-4.00 mm, 4.00-2.00 mm, 2.00-1.00 mm and < 1 mm were referred to as large-coarse macroaggregate (LCM), medium-coarse macroaggregate (MCM) (4-2 mm), medium-fine macroaggregate (MFM), (2-1 mm) and fine macroaggregates (FM) (<1 mm), respectively. After gentle manual crumbling, fragments such as roots and stones constituted a negligible share and were removed. Then the sieves were attached to a Tyler To-Tap sieve shaker and shaken at 200 oascillations/min for 3 min (Sainju, 2006). The aggregates (8.00-4.00, 4.00-2.00, 2.00-1.00, and <1.00 mm) retained and passed through the sieves were weighed (Mendes et al., 1999; Sainju, 2006), maintained at field-moist, and stored in plastic bags at 4 °C before experimentation.

Mean weight diameter

Subsamples of the aggregate fractions (8.00-4.00, 4.00-2.00, 2.00-1.00, and <1.00 mm) were oven-dried at 60°C for 48 hours and weighed for the fraction percentage measurement and soil texture determination. Particle size analysis was performed by mechanical dispersion of the aggregate fractions after OM removal. Particle-size analysis was completed through the adaptation of hydrometer method outlined by Kroetch and Wang (2008). Mean weight diameter (MWD) of aggregates was calculated (Hillel, 2004; Liu et al., 2019) as follows:

$$MWD = \sum_{i=1}^{n} x_i w_i$$

where i is aggregate size (k = 1, 2, 3 indicate macro-aggregate, micro-aggregate and silt + clay-sized fraction); x_i (mm) is the mean diameter of any particular size range of aggregates separated by sieving; wi (%) is the weight of the aggregates in that size range as a fraction of the total dry weight of soil used. MWD is commonly used to express aggregate stability (Blair, 2010). High MWD values indicate lower erodability of soil (Ciric et al., 2012) and larger aggregate size fractions in the soil and, therefore, greater aggregate stability (Piccolo et al., 1997).

Organic C and total N in soil fractions

A sub-sample of each aggregate size fraction was ground to 0.15 mm for organic carbon (OC) and total N (TN) content measurement. The OC content was determined by the Walkley-Black potassium dichromate oxidation procedure (Allison, 1965) and TN was analyzed by Kjeldahl digestion method (Rutherford et al., 2008).

Microbial biomass C and N in soil fractions

Soil microbial biomass (SMB) C and N in different particle-size fractions (8.00-4.00, 4.00-2.00, 2.00-1.00, and <1.00 mm) were determined according to the method modified by Vance et al. (1987). This method was described by Sbih et al. (2012). Briefly, the amounts of C and N deriving from SMB were extracted with 0.5 M K_2SO_4 from non-fumigated and fumigated soil fractions and in the extracts were determined respectively by wet dichromate oxidization technique and standard Kjeldahl digestion method (Rutherford et al., 2008). The microbial biomass C (MB-C) and the microbial biomass N (MB-N) are determined according to Joergensen (1996) and Brookes et al. (1985) respectively. Data were expressed in mg kg^{-1} dry soil aggregate and represented the average of two replicates.

Organic C and N mineralization in soil fractions

Organic C and N mineralization in bulk soil and different particle-size fractions (8.00-4.00, 4.00-2.00, 2.00-1.00, and <1.00 mm) was determied according to Sbih et al. (2003). Briefly, two 50-g soil samples (oven-dried at 60°C, not ground) were moistened with demineralized water at 85% field capacity and placed in a 1-L polyethylene flask. Soil fractions were incubated in the flask at room temperature (25 ± 2°C) for 4 wk and the incubation periodes were 1, 2, 3 and 4wk soil moisture was maintained constant. In order to traped evolved CO_2 vials containing 1 M NaOH were introduced in flask, during incubation. At the end of each period, vials containing NaOH were sampled to measure the CO_2 content. Soil aggerates were then sampled (20 g) to measure mineralized N. The CO_2 evolved was determined by titration of excess NaOH and reported as C-CO_2 emision (mgC/ g aggregate- C) (Ross et al., 1995). NH_4^+ and NO_3^- were extracted with 2 M L^{-1} KCl (soil-solution

ratio of 1:4) and determined by Autoanalyser. The amount of N mineralized was calculated as the difference between the final and initial extractable inorganic N concentrations, after adjustment soil from fresh dry weight. The net N mineralized (%) is calculated as N-min (%) = [(NH_4^+-N + NO_3^--N)$_f$ / total N_f] x 100, where, f represent either bulk soil or aggregate fraction (Xie et al., 2017).

Data Analysis

Statistical calculations were performed with the full data set of all soils. the relationships between the various parameters and the effect of clays on the aggregates and their sizes was evaluated by ANOVA (PROC GLM procedure of XLSTAT software). Mean separation was done with an *F*-protected LSD test, and the Pearson's correlation is used to find the relationship between the different parameters.

Results and Discussion

Aggregate size distribution

The amount of different macroaggregate size fractions is expressed as a percentage of total soil mass. In general, FM (<1mm) represented the lowest fraction whereas intermediate macroaggregates class (1-4 mm) represented the greatest proportion for all soils (Table 1). The same observation was reported by Xie et al. (2017) who examined the OC stock over 20 cm depth of aggregates, its mineralization under the effect of organic and inorganic inputs in intensive wheat-maize cultivation in northern China. The large-coarse macroaggregate size fraction >2 mm was the most abundant, suggesting that LCM (as determined by dry sieving) comprised the bulk of the macroaggregates within the soil studied.

Table 1. Amounts of different macroaggregate size fractions, expressed as percentage of total soil mass.

	Clay content (g kg^{-1})										
Macroaggregate size fractions	150	-	200	(n=7)	201	-	300	(n=5)	301	-	400	(n=2)
<8-4 mm range mean	20.8	-	28.8	(25.3) bc	30.2	-	35.9	(32.9) a	36.6	-	38.6	(37.6) a
<4-2 mm range mean	28.5	-	41.0	(33.5) a	30.2	-	42.0	(35.3) a	27.8	-	33.7	(30.8) b
<2-1 mm range mean	17.6	-	26.2	(19.7) c	13.9	-	22.1	(18.8) b	18.5	-	25.2	(21.8) c
<1 mm range mean	12.1	-	26.5	(21.5) c	8.2	-	17.4	(13.0) c	9.3	-	10.3	(9.8) d
LSD (0.05)			3.5		4.23						5.7	

Different letters in each column indicate significant differences between different treatments n: number of soil samples; Means with the same letter are not significantly different at *P*<0.05 according to the LS means test.

In general, the amounts of macroaggregate size fractions were lowest in soils with high clay content (Table 1). The amount of FM (<1mm) decreased markedly with increasing clay content within soil aggregates (Table 1). These results are in agreement with the findings of Kristiansen et al. (2006), who also found that the proportion of soil recovered in aggregates> 2 mm increased with increasing clay content of the whole soil, while those <1 mm decreased. The results of the correlation analysis (Figure 1) showed that the amounts of clay+silt-sized particles within macroaggregate fractions were positively correlated with the mass proprotion of LCM (<8-4 mm) (r=0.75; *P*≤0.01) and negatively correlated with the mass proportion of FM (<1 mm) (r=0.90; *P*≤0.001).

Dry mean weight diameter

The dry MWD of macroaggregate size fractions varied between 2.80 and 3.70 mm (Figure 2). It increases as the proportion of small particles increases. The clay particles affect the mean value of MWD in the following order: 2.98 mm for soils with 150-200 g clay particules kg^{-1} soil < 3.40 mm for soils with 201-300 g clay particules kg^{-1} soil < 3.58 mm for soils with 301-400 g clay particules kg^{-1} soil. MWD exhibited significant correlation with particle size distribution. From figure 2, it is notable that the values of dry. Contrasting correlations between MWD and soil texture components, indeed, MWD were positively correlated with clay content (r = 0.88; P ≤ 0.01) and negatively correlated with sand content (r = -0.79; *P* ≤ 0.01). When the amounts of clay+silt-sized particles were considred, the correlation became more strong (r=0.90; *P* <0.001), suggesting that clay+silt-sized particles promotes the formation of stable aggregates in meadow soils. Khaledian et al. (2013) examined the effect of soil texture on soil permanganate organic carbon in somes soils fron deforested areas in Northern Iran. They concluded that clay and silt particles could provide some degree of physical protection for oxidizable C groups in lignin. In addition, positive correlations were obtained between MWD and soil OC (r=0.66; *P*<0.05) and MB-C (r=0.64; *P*<0.05). Different experiments have demonstrated that aggregate stability increases when clay and organic matter accumulation increase, confirming the role of these soil properties in soil aggregation (Norton et al., 2006; Nweke and Nnabude, 2015). Aziz and Karim (2016) monitored in the climatological region of Iraqi Kurdistan region with different uses of agricultural land certain soil properties in relation to soil aggregates. They obtained a positive correlation between aggregate stability

(MWD) and clay content and organic matter content of soils. Khaledian et al. (2013) obtained very highly positive correlations (P<0.001) between stable carbon and MWD. These relationships are in agreement with the fact that organic matter and clay content of soils acts as cementing and binding agent (Kemper and Koch, 1966; Kemper and Rosenau, 1986; Golchin et al., 1997; Seybold and Herrik, 2001). The stabilization of clay-organic complexes is the main mechanism of soil preservation, this is due to the soil clay content which seems to be the determining factor in the chemical stabilization of this complex (Blanco-Moure et al., 2016).

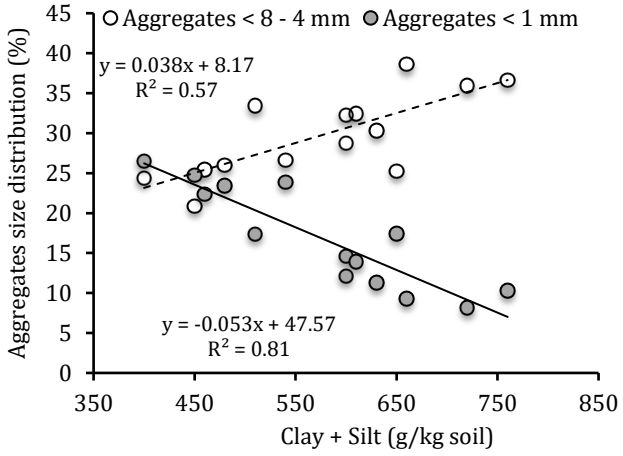

Figure 1. Mass proportion of two macroaggregate size fractions with different clay +silt contents

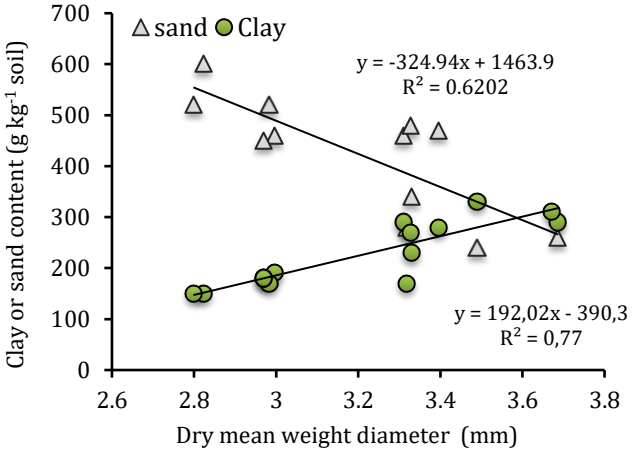

Figure 2. Values of dry mean weight diameter of soils with different sand and clay contents

Soil macroaggregate sizes markedly affected soil OC stock (Figure 3) and consequently, the distribution of microbial biomass C (Figure 4) and mineralization of OC (Figure 5) within soil macroaggregates.

Total oganic carbon

The OC content within soil macroaggregates increased with decreasing macroaggregate size from LCM (8-4 mm) to FM (<1 mm) (Figure 3). The OC content varied between 34.9 to 42.1 g kg^{-1} in soil fractions with lower clay content (150-200 g kg^{-1}) and from 37.6 to 56.4 g kg^{-1} in soil fractions with highest clay content (301-400 g kg^{-1}). Thus, the mean OC content in LCM class with highest clay content was 7.7% higher than in LCM with lowest clay content. However, the OC content of FM fraction with highest clay content was 55% higher than in FM fraction with lowest clay content. These results indicate that the OC is more concentrated or sequestered in the finest soil aggregate fraction of meadow soils. Clay particles provide a greater ability to chemically stabilize SOM due to the greater reactive surface area of clay particles and also to physically protect SOM by incorporation into aggregates (Feller and Beare, 1997; Six et al., 2002). This implies that as the clay content increases, the proportion of small pores increases, therefore decomposing microbes are excluded which stabilizes the OC (Mtambanengwe et al., 2004; Strong et al., 2004).

Microbial biomass carbon

The content of MB-C within soil macroaggregates increased as follows: FM (<1 mm) > MFM (2-1 mm) > (CMM) (4-2 mm) > LCM (8-4 mm) (Figure 4). These results indicate that MB-C is more concentrated in the finer fraction of soil macroaggregates. This is probably due to the fact that fine macroaggregates can have a high-water holding capacity and become a preferential microhabitat for MB. Seech and Beauchamp (1988), Miller and Dick (1995) reported that C-MB is mainly concentrated in microaggregates and as FM is a set of micraggregates that is why they contain more C-MB. The MB-C content within soil macroaggregates increased with increasing soil clay content (Figure 4). Microbial biomass C content was significantly correlated to OC content (r=0.70; P<0.05), and strongly correlated to soil clay+silt content (r=0.889; P<0.001). These results suggest that MB-C is concentrated mostly in the smallest macroaggregate sizes and the finest textured meadow soils. When investigated the relationship between soil clay content and soil organic matter turnover Müller and Höper (2004) found strong relationship between clay content and soil microbial biomass-C and concluded that clay particles might render some degree of protection for microbial biomass. Particles less than 2 µm (clay) are generally considered as protective microhabitats and provide protection for microbial biomass against desiccation (Heijnen and van Veen, 1991). Sainju et al. (2009) found greater MB-C at 0 to 5 cm or greater MB-C and MB-N at 5 to 20 cm in the <0.25 mm than in the 4.75 to 2.00-mm size class of soils from different cropping sequences. They concluded that microaggregates can protect microbial biomass from predators.

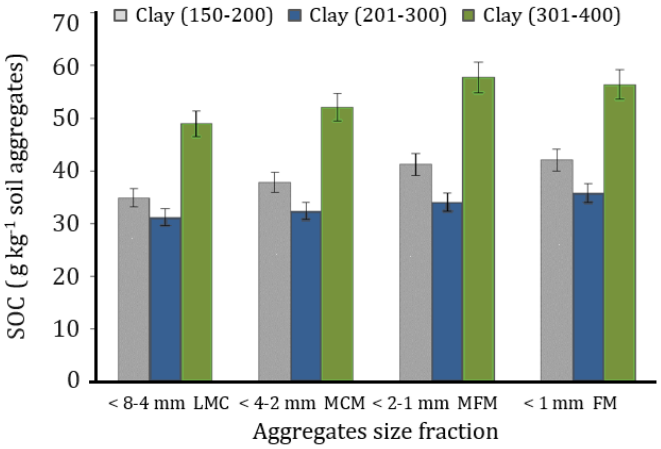

Figure 3. Organic carbon (OC) content of macroaggregate fractions with different clay contents.
(Lower case letters in Figure represent differences between same aggregates at different clay level are significantly different at P <0.05 by least squares means test. Uppercase letters represent differences between the same clay level in different soil aggregates are significantly different at P <0.05 by least square means test).

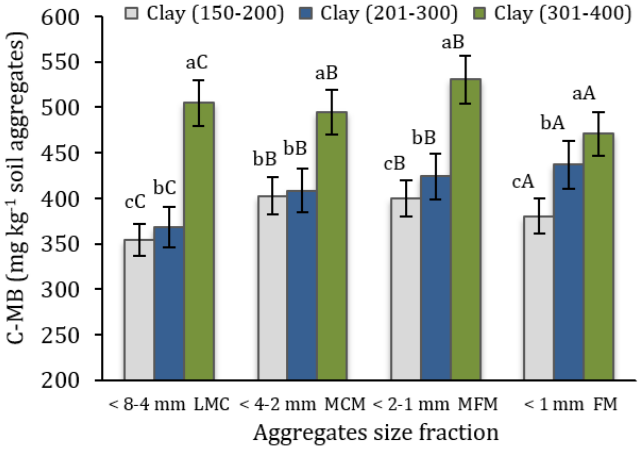

Figure 4. Microbial biomass carbon (C-MB) content of macroaggregate fractions with different clay contents
(Lower case letters in Figure represent differences between same aggregates at different clay level are significantly different at P <0.05 by least squares means test. Uppercase letters represent differences between the same clay level in different soil aggregates are significantly different at P <0.05 by least square means test).

Mineralization of organic carbon

Because microorganisms related to C and N dynamics could be heterogeneously distributed throughout pores of various sizes and within aggregates (Watteau and Villemin, 2018), it is expected that OC mineralization will vary among soil macroaggregates. The CO_2 emission during the 28-d incubation (Figure 5) was expressed as mg C g^{-1} aggregate C content.

As we can see from figure 5, the C-CO_2 emission increased with increasing macroaggregate size as follows: LCM (8-4 mm) > (MC) (4-2 mm) > (MFM (2-1 mm) > FM (<1 mm). These results indicate a higher organic C mineralization activity in coarse macroaggregates. Several studies have shown that OM decomposition is faster in coarse-textured soils than in fine-textured soils (vanVeen and Kuikman, 1990; Strong et al., 2004) because clay soils are better able to protect OM from decomposition (Mtambanengwe et al., 2004). Fernández et al. (2010) found highest CO_2 production at 15 days of soil incubation in the 1-4 mm aggregate fraction, however, the aggregates <1, >4 mm and undisturbed soil, their respiration was 59, 56 and 72% lower respectively, compared with the 1-4 mm class. Under three contrasting land uses of the topsoil from Dermosol sites (Acrisols in the FAO soil classification), Rabbi et al. (2014) show that the cumulative C mineralization (C-CO_2 gkg^{-1} aggregate) of the < 53 µm fraction was 28% lower than that of macroaggregates (250–2000 µm) and microaggregates (250–53 µm). However, because of the insignificant difference in C mineralization, slow soil OC pool sizes and mean residence time of slow soil OC pool between macro-aggregates and micro-aggregates, they concluded that soil OC mineralization rate and thus the protection of soil OC was similar in both macroaggregates and microaggregates. In another study, Rabbi et al. (2016) investigated the influence of pore geometry on the OC decomposition rate and bacterial diversity in both macroaggregates (250–2000 µm) and microaggregates (53–250 µm) using field samples. They found that the OC decomposition rate constant was similar in aggregate size ranges. In general, the C-CO_2 emission increased with decreasing clay content of soil macroaggregate fractions (Figure 5). Protection of OM within stable aggregates is potentially stabilized by a high clay content (Six et al., 2002). In general, OM compounds could be stabilized by interaction with soil clay fraction, as soil organic compounds binds chemically to clay minerals or Fe/Al oxides (Saidy et al., 2012; Torres-Sallan et al., 2017; Singh et al., 2018). Chen et al. (2018) concluded that organic C-mineral associations in soils could retard the decomposition of biochemically labile organic compounds like carbohydrates and peptides. Several studies reported that the stabilization of soil OC is influenced by the type of phyllosilcates present in soils (Goh, 2004; Gartzia-Bengoetxea et al., 2017; Singh et al., 2018). Meena et al. (2017) reported that smectic clays are more potent in accumulation and sequestration of SOC in black cotton soils of India. Jones and Singh (2014) highlighted the potential of mineral surfaces in influencing the stability of OM in organo-mineral interactions.

Dynamic of nitrogen within soil macroaggregates

Total nitrogen and microbial biomass nitrogen

Figure 6 shows TN associated with different sizes of macroaggregates. The distribution of TN followed the same pattern as OC among the four macroaggregate classes. The size of macroaggregates markedly affected TN stock within soil macroaggregates. The content of TN increased with decreasing macroaggregate size fractions as follows: LCM (8-4 mm) < MCM (4-2 mm) < MFM (2-1 mm) < FM (1 mm) (Figure 6), indicating that smaller-size macroaggregate fraction was the main pool of total N.

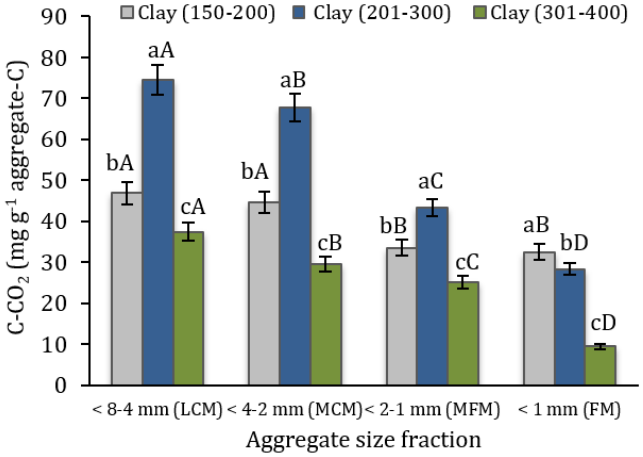

Figure 5. C-CO_2 emission from incubated macroaggregate fractions with different clay content.
(Lower case letters in Figure represent differences between same aggregates at different clay level are significantly different at P <0.05 by least squares means test. Uppercase letters represent differences between the same clay level in different soil aggregates are significantly different at P <0.05 by least square means test).

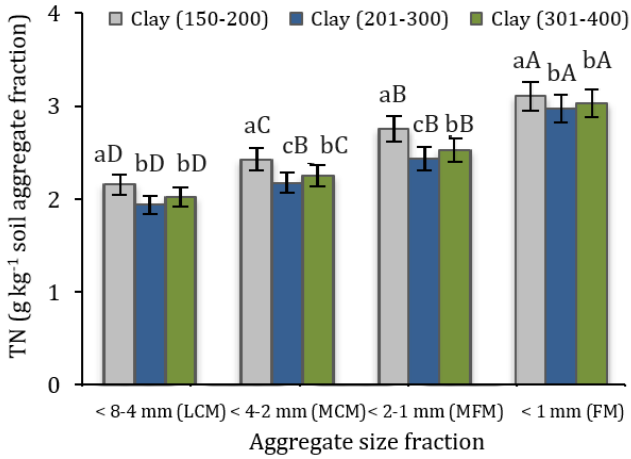

Figure 6. Total nitrogen (TN) content of macroaggregate fractions with different clay contents
(Lower case letters in Figure represent differences between same aggregates at different clay level are significantly different at P <0.05 by least squares means test. Uppercase letters represent differences between the same clay level in different soil aggregates are significantly different at P <0.05 by least square means test).

The amount of TN varied from 2.3 g kg^{-1} to 3.3 g kg^{-1} in macroaggregates with 150-200 g clay particules kg^{-1} soil and from 3.0 g kg^{-1} to 4.4 g kg^{-1} in macroaggregates with 301-400 g clay particules kg^{-1} soil. On average, the amount of TN in <8-4 mm size fraction in macroaggregates with 301-400 g clay particules kg^{-1} soil was 43% higher than that in macroaggregates with 150-200 g clay particules kg^{-1} soil. These results indicate that N is more concentrated or sequestered in the finest soil macroaggregate fraction.

The distribution of MB-N among soil aggregates showed the same pattern as the macroaggregate total N (Figure 7). This observation is in accord with the findings of Egan et al. (2018) who reported that long-term grazing and inorganic nutrient fertilization could contribute to greater N and C pools of smaller soil fractions. Several studies found that soil management practices can alter the aggregate associated organic C and N fractions with different clay contents (Sodhi et al., 2009; Tripathi et al., 2014).

Organic nitrogen mineralization

In general, N mineralization increased with increasing aggregate size, with the <4-2 mm aggregate size mineralizing more N, compared to smaller sized aggregates (<2–1 and <1 mm). The amount of N-mineralzed increased with increasing aggregate size as follows (Figure 8): LCM and MCM (4-2 mm) > MFM (2-1 mm) > FM (<1 mm), suggesting that larger macroaggregate fractions contain a larger proportion of readily mineralizable organic N than smaller macroaggregate fractions in meadow soils. Similarly, Muruganandama et al. (2008) found that N mineralization enzymes increased with increasing aggregate size of soils. They found that the potential activities of NAG, l-glutaminase, and arylamidase were significantly greater ($P < 0.05$) in the intermediate (0.5–1 mm) aggregate size than in other size fractions (<0.25, 0.25–0.5, 1–2, and 2–4 mm). In general, an increasingly greater proportion of the organic N within soil aggregate fractions was mineralized as the mineral particle size decreased, except for the small macro-aggregate (<1 mm) (Figure 8), which released less than 3 mg N g^{-1} aggregate N after 28 d of incubation. This indicates that in the small macro-aggregate fraction, OM was not available for microbial degradation and was therefore physically protected against decomposition (Hassink et al., 1993; Bimüller et al., 2014).

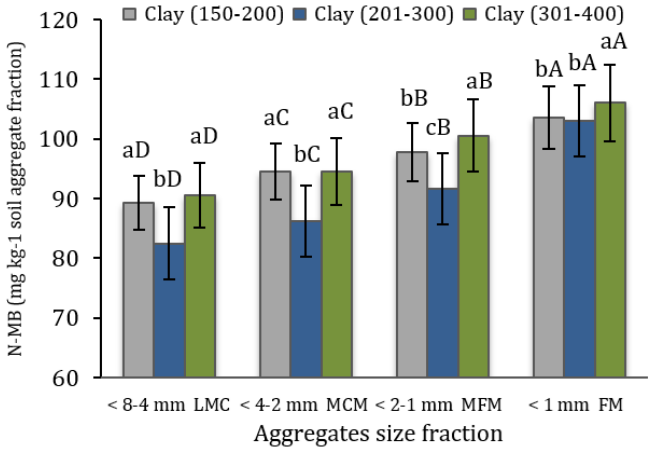

Figure 7. Microbial biomass nitrogen (N-MB) content of macroaggregate with different clay contents (Lower case letters in Figure represent differences between same aggregates at different clay level are significantly different at P <0.05 by least squares means test. Uppercase letters represent differences between the same clay level in different soil aggregates are significantly different at P <0.05 by least square means test).

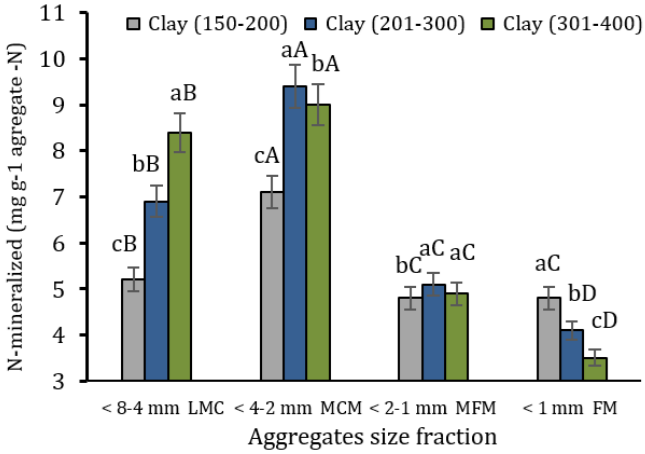

Figure 8. Nitrogen mineralization within macroaggregate fractions with different clay contents (Lower case letters in Figureure represent differences between same aggregates at different clay level are significantly different at P <0.05 by least squares means test. Uppercase letters represent differences between the same clay level in different soil aggregates are significantly different at P <0.05 by least square means test).

Nitrogen mineralization pattern in soil aggregate size fractions seems to be similar to CO_2 emission pattern. Indeed, a significant positive correlation was found between N-min and CO_2 emission (r=0.66, P<0.001). Unlike what we have seen with C-CO_2 emission, the C/N of both soil OM and microbial biomass are very highly correlated (r=0.62, P<0.001) to N-min at aggregates size <8-4 mm. Also, C-MB and N-MB were highly correlatd to N-min (r =0.84, P<0.001; r =0.67, P<0.001 repectively). However, these parameters are less correlated in the other aggregate sizes. It seems that LCM are more accessible to microbial and contain a larger proportion of readily mineralizable organic N than smaller aggregates. In contrast to our findings, other researchers have reported higher N mineralization in small aggregates (Craswell et al., 1970; Cameron and Posner, 1979).

Conclusion

Soil aggregates of different sizes provide diverse microhabitats for microorganisms and therefore influence soil activities. The clay content of soil aggregate fractions affects the mean weight diameter of macroaggregate size fractions. Generally, a greater proportion of the organic carbon (C) and organic nitrogen (N) within soil aggregate fractions is mineralized as the mineral particle size decreases. Clay content can increase the protection of microbial biomass in meadow soils. This study suggests that the mean weight diameter (MWD) should be considered in routine soil testing because it determines the particle size distribution of aggregates and essentially measures the stability of macroaggregates, maintaining high stability. Aggregates in soils are important for sustainable soil maintenance, as they are essential for preserving agricultural production, reducing soil erosion and degradation, and reducing environmental pollution. A well-aggregated soil creates favorable conditions for biological activity, resulting in an increase in the bioavailability of nutrients, thus improving plant growth conditions.

References

Abbasi, M.K., Tahir, M.M., Sabir, N., Khurshid, M., 2015. Impact of the addition of different plant residues on nitrogen mineralization-immobilization turnover and carbon content of a soil incubated under laboratory conditions. *Solid Earth* 6(1): 197-205.

Allison L.E. 1965. Organic carbon. In: Methods of soil analysis. Part 2. Chemical and microbiological properties. Black, C.A., Evans, D.D., White, J.L., Ensminger, L.E., Clark F.E. (Eds.), Soil Science Society of America. Madison, Wisconsin, USA. pp 1367-1378.

Amellal, N., Portal, J.M., Berthelin, J., 2001. Effect of soil structure on the bioavailability of polycyclic aromatic hydrocarbons within aggregates of a contaminated soil. *Applied Geochemistry* 16(14): 1611-1619.

Awad, Y.M., Lee, S.S., Kim, K.H., Ok, Y.S., Kuzyakov, Y., 2018. Carbon and nitrogen mineralization and enzyme activities in soil aggregate-size classes: Effects of biochar, oyster shells, and polymers. *Chemosphere* 198: 40-48.

Aziz, S.A., Karim, S.M., 2016. The effect of some soil physical and chemical properties on soil aggregate stability in different locations in Sulaimani and Halabja Governorate. *Open Journal of Soil Science* 6(4): 81-88.

Bimüller, C., Kreyling, O., Kölbl, A., von Lützow, M., Kögel-Knabner, I., 2016. Carbon and nitrogen mineralization in hierarchically structured aggregates of different size. *Soil Tillage Research* 160: 23-33.

Bimüller, C., Mueller, C.W., von Lützow, M., Kreyling, O., Kölbl, A., Haug, S., Schloter, M., Kögel-Knabner, I., 2014. Decoupled carbon and nitrogen mineralization in soil particle size fractions of a forest topsoil. *Soil Biology and Biochemistry* 78: 263-273.

Blair, N., 2010. The impact of soil water content and water temperature on wet aggregate stability. What answer do you want? 19th World Congress of Soil Science, Soil Solutions for a Changing World. 1 – 6 August 2010, Brisbane, Australia. pp 106-109.

Blanco-Moure, N., Gracia R., Bielsa, A.C., López, M.V., 2016. Soil organic matter fractions as affected by tillage and soil texture under semiarid Mediterranean conditions. *Soil and Tillage Research* 155: 381-389.

Bossuyt, H., Denef, K., Six, J., Frey, S.D., Merckx, R., Paustian, K., 2001. Influence of microbial populations and residue quality on aggregate stability. *Applied Soil Ecology* 16: 195-208.

Brookes, P.C., Powlson, D.S., Jenkinson, D.S., 1985. The microbial biomass in soil. In: Ecological interactions in soil. Fitter, A.H. (Ed.), Special Publication No. 4 British Ecological Society. Blackwell Scientific, Oxford. pp. 123-125.

Cai, A., Xu, H., Shao, X., Zhu, P., Zhang, W., Xu, M., Murphy, D.V., 2016. Carbon and nitrogen mineralization in relation to soil particle-size fractions after 32 years of chemical and manure application in a continuous maize cropping system. *PLoS One* 11(3): e0152521

Cameron, R.S., Posner, A.M., 1979. Mineralisable organic nitrogen in soil fractionated according to particle size. *European Journal of Soil Science* 30(3): 565-577.

Chen, C., Leinweber, P., Eckhardt, K.U., Sparks, D.L., 2018. The decomposition and stability of clay-associated organic matter along a soil profile. *Soil Systems* 2(1): 16.

Ciric, V., Manojlovic, M., Nesic, Lj., Belic, M., 2012. Soil dry aggregate size distribution: effects of soil type and land use. *Journal of Soil Science and Plant Nutrition* 12(4): 689-703.

Craswell, E.T., SafFigurena, P.G, Waring, S.A., 1970. The mineralization of organic nitrogen in dry soil aggregates of different sizes. *Plant and Soil* 33: 383-392.

de Moraes Sá, J.C., Tivet, F., Lal, R., Briedis, C., Hartman, D.C., dos Santos, J.Z., dos Santos, J.B., 2014. Long-term tillage systems impacts on soil C dynamics, soil resilience and agronomic productivity of a Brazilian Oxisol. *Soil and Tillage Research* 136: 38-50.

Egan, G., Crawley, M.J., Fornara, D.A., 2018. Effects of long-term grassland management on the carbon and nitrogen pools of different soil aggregate fractions. *Science of The Total Environment* 613–614: 810–819.

Feller, C., Beare, M.H., 1997. Physical control of soil organic matter dynamics in the tropics. *Geoderma* 79(1-4): 69-116.

Fernández, R., Quiroga, A., Zorati, C., Noellemeyer, E., 2010. Carbon contents and respiration rates of aggregate size fractions under no-till and conventional tillage. *Soil and Tillage Research* 109(2): 103-109.

Gartzia-Bengoetxea, N., Fernandez-Ugalde, O., Virto, I., Arias-Gonzalez, A., 2017. Clay minerals, metallic oxides and oxy-hydroxides and soil organic carbon distribution within soil aggregates in temperate forest soils. 19th EGU General Assembly, EGU2017, 23-28 April, 2017. Vienna, Austria. p.13807.

Ghimire, R., Lamichane, S., Acharya, B.S., Bista, P., Sainju, U.M., 2017. Tillage, crop residue, and nutrient management effects on soil organic carbon in rice-based cropping systems; a review. *Journal of Integrative Agriculture* 16(1):1-15.

Goh, K.M., 2004. Carbon sequestration and stabilization in soils: implications for soil productivity and climate change. *Soil Science and Plant Nutrition* 50(4): 467-476.

Golchin, A., Baldock, J.A., Oades, J.M. 1997. A model linking organic matter decomposition, chemistry, and aggregate dynamics. In: Soil processes and the carbon cycle. Lal, R., Kimble, J.M., Follett, R.F., Stewart, B.A. (Eds.). CRC Press, Boca Raton. p. 245-266.

Gupta, V.S.R., Germida, J.J., 2015. Soil aggregation: Influence on microbial biomass and implications for biological processes. *Soil Biology and Biochemistry* 80: A3-A9.

Hao, Y., Wang, Y., Chang, Q., Wei, X., 2017. Effects of long-term fertilization on soil organic carbon and nitrogen in a highland agroecosystem. *Pedosphere* 27(4): 725-736.

Hassink, J., Bouwman, L.A., Zwart, K.B., Bloem, J., Brussaard, L., 1993. Relationships between soil texture, physical protection of organic matter, soil biota, and C and N mineralization in grassland soils. *Geoderma* 57(1-2): 105-128.

Heijnen, C.E., van Veen, J.A., 1991. A determination of protective microhabitats for bacteria introduced into soil. *FEMS Microbiology Letters* 85(1): 73-80.

Hillel, D., 2004. Introduction to Environmental Soil Physics. Elsevier, Amsterdam, 494 p.

Joergensen, R.G., 1996. The fumigation-extraction method to estimate soil microbial biomass: calibration of the k_{EC} value. *Soil Biology and Biochemistry* 28(1): 25-31.

Jones, E., Singh, B. 2014. Organo-mineral interactions in contrasting soils under natural vegetation. *Frontiers in Environmental Sciences* 2:2.

Kemper, W.D., Koch, E.J. 1966. Aggregate stability of soils from Western USA and Canada. USDA Technical Bulletin No. 1355, US Government Printing Office, Washington DC.

Kemper, W.D., Rosenau, R.C., 1986. Aggregate stability and size distribution. In: Methods of Soil Analysis: Part 1 Physical and Mineralogical Methods, 5.1, Second Edition. Klute, A. (Ed.). American Society of Agronomy, Soil Science Society of America, WI, Madison, USA. pp. 425-442.

Khaledian, Y., Kiani, F., Weindorf, D.C., Ebrahimi, S., 2013. Relationship of potentially labile soil organic carbon with soil quality indicators in deforested areas of Iran. *Soil Horizons* 54(4):1-11.

Kristiansen, S.M., Schjønning, P., Thomsen, I.K., Olesen, J.E., Kristensen, K., Christensen, B.T., 2006. Similarity of differently sized macro-aggregates in arable soils of different texture. *Geoderma* 137(1-2): 147-154.

Kroetch D., Wang C. 2008. Particle size distribution. In: Soil sampling and methods of analysis. Carter, M.R., Gregorich, E.G. (Eds.). 2nd ed. CRC Press, Boca Raton. pp. 713-725.

Liu, M., Han, G., Zhang, Q., 2019. Effects of soil aggregate stability on soil organic carbon and nitrogen under land use change in an erodible region in Southwest China. *International Journal of Environmental Research and Public Health* 16(20): 3809.

Meena, R.K., Verma, A.K., Kumawat, C., Yadav, B., Pawar, A.B., Trivedi, V.K., 2017. Impact of clay mineralogy on stabilization of soil organic carbon for long-term carbon sequestration. *International Journal of Current Microbiology and Applied Sciences* 6(5): 2157-2167.

Mendes, I.C., Mandick, A.K., Dick, R.P., Bottomley, P.J., 1999. Microbial biomass and activities in soil aggregates affected by winter cover crops. *Soil Science Society of America Journal* 63(4): 873-881.

Miller, M., Dick, R.P., 1995. Dynamics of soil carbon and microbial biomass in whole-soil and aggregates in two cropping systems. *Applied Soil Ecology* 2(4): 253-261.

Miller, M.N., Zebarth, B.J., Dandie, C.E., Burton, D.L., Goyer, C., Trevors, J.T., 2009. Denitrifier community dynamics in soil aggregates under permanent grassland and arable cropping systems. *Soil Science Society of America Journal* 73(6): 1843-1851.

Mitran, T., Mani, P.K., Ganguly, K., 2018. Distribution of soil organic carbon within water stable soil aggregates in long-term fertilized and manured rice-wheat rotation. *International Journal of Academic Research and Development* 3 (1): 22-28.

Mtambanengwe, F., Mapfumo, P., Kirchmann, H., 2004. Decomposition of organic matter in soil as influenced by texture and pore size distribution. In: Managing nutrient cycles to sustain soil fertility in sub-saharan Africa. Bationo, A. (Ed.). Academy Science Publishers in association with the Tropical Soil Biology and Fertility Institute of CIAT, Nairobi, Kenya. pp. 261-275.

Müller, T., Höper, H., 2004. Soil organic matter turnover as a function of the soil clay content: consequences for model applications. *Soil Biology and Biochemistry* 36(6): 877-888.

Muruganandama, S., Israel D.W., Robargea, W.P., 2008. Activities of nitrogen-mineralization enzymes associated with soil aggregate size fractions of three tillage systems. *Soil Science Society of America Journal* 73(3): 751-759.

Naresh, R.K., Tyagi, S., Ghasal, P.C., Mahajan, N.C., Kumar, M., Jat, L., Singh, S., Kumar, R., 2018. Microbial biomass associated with aggregates; aggregate associated carbon and soil aggregate dynamics in rice-wheat cropping system: A review. *International Journal of Chemical Studies* 6(5): 1265-1283.

Norton, L.D., Mamedov, A.I., Huang C.H., Levy, G.J. 2006. Soil aggregate stability as affected by long-term tillage and clay mineralogy. *Advances in GeoEcology* 39: 422-429.

Nweke, I.A., Nnabude, P.C., 2015. Aggregate stability of four soils as evaluated by different indices. *Journal of Experimental Biology and Agricultural Sciences* 3(3): 246-252.

Ogunwole, J.O., Sharma, B.R., McCartney, M.P., Zemadim, B., Leta, G., 2014. Land use impact on soil physical quality and soil structure in three highland watersheds of Ethiopia. *Advances in Plants and Agriculture Research* 1(4):111-119.

Ouyang, I., Wang, F., Tang, J., Yu, L., Zhang, R., 2013. Effects of biochar amendment on soil aggregates and hydraulic properties. *Journal of Soil Science and Plant Nutrition* 13 (4): 991-1002.

Piccolo, A., Pietramellara, G., Mbagwu, J.S.C., 1997. Use of humic substances as soil conditioners to increase aggregate stability. *Geoderma* 75(3-4): 267-277.

Rabbi, S.M.F., Daniel, H., Lockwood, P.V., Macdonald, C, Pereg, L., Tighe, M., Wilson, B.R., Young, I.M., 2016. Physical soil architectural traits are functionally linked to carbon decomposition and bacterial diversity. *Scientific Reports* 6: 33012.

Rabbi, S.M.F., Wilson, B.R., Lockwood, P.V., Daniel, H., Young, I.M., 2014. Soil organic carbon mineralization rates in aggregates under contrasting land uses. *Geoderma* 216: 10-18.

Rutherford, P.M., McGill, W.B., Arocena, J.M., Figureueiredo, C.T., 2008. Total nitrogen. In: Soil sampling and methods of analysis. Carter, M.R., Gregorich, E.G., (Eds.). 2nd ed. CRC Press Inc., Boca Raton. pp. 239-250.

Saggar, S., Parshotam, A., Sparling, G.P., Feltham, C.W., Hart, P.B.S., 1996. ^{14}C-labeled ryegrass turnover and residence times in soils varying in clay content and mineralogy. *Soil Biology and Biochemistry* 28(12): 1677- 1686.

Saidy, A.R., Smernik, R.J., Baldock, J.A., Kaiser, K., Sanderman, J., Macdonald, L.M., 2012. Effects of clay mineralogy and hydrous oxides on labile organic carbon stabilization. *Geoderma* 173-174: 104-110.

Sainju, U.M., Caesar-TonThat, T., Jabro, J.D., 2009. Carbon and nitrogen fractions in dryland soil aggregates affected by long-term tillage and cropping sequence. *Soil Science Society of America Journal* 73(5): 1488-1495.

Sainju, U.M., 2006. Carbon and nitrogen pools in soil aggregates separated by dry and wet sieving methods. *Soil Science* 171(12): 937-949.

Sbih M., N'Dayegamiye, A., Karam, A., 2003. Evaluation of carbon and nitrogen mineralization rates in meadow soils from dairy farms under transit to biological cropping systems. *Canadian Journal of Soil Science* 83(1): 25-33.

Sbih, M., Karam, A., N'Dayegamiye, A., Bensid, Z., Boukaboub, A., 2012. Dynamic of the active fraction of organic matter in some meadow soils. *Eurasian Journal of Soil Science* 1(1): 22-27.

Seech, A.G., Beauchamp, E.G., 1988. Denitrification in soil aggregates of different sizes. *Soil Science Society of America Journal* 52(6): 1616-1621.

Seybold, C.A., Herrick, J.E., 2001. Aggregate stability kit for soil quality assessments. *Catena* 44(1): 37-45.

Singh, M., Sarkar, B., Sarkar, S., Churchman, J., Bolan, N., Mandal, S., Menon, M., Purakayastha, T.J., Beerling, D.J., 2018. Stabilization of soil organic carbon as influenced by clay mineralogy. *Advances in Agronomy* 148: 33-84.

Six, J., Conant, R.T., Paul, E.A., Paustian, K., 2002. Stabilization mechanisms of soil organic matter: implications for C-saturation of soils. *Plant and Soil* 241: 155-176.

Six, J., Paustian, K., Elliott, E.T., Combrink, C., 2000. Soil structure and organic matter I. Distribution of aggregate-size classes and aggregate-associated carbon. *Soil Science Society of America Journal* 64(2): 681-689.

Sodhi, G.P.S, Beri, V., Benbi, D.K., 2009. Soil aggregation and distribution of carbon and nitrogen in different fractions under long-term application of compost in rice–wheat system. *Soil and Tillage Research* 103(2): 412-418.

Strong, D.T., Wever, H.D., Merckx, R., Recous, S., 2004. Spatial location of carbon decomposition in the soil pore system. *European Journal of Soil Science* 55(4): 739-750.

Thomsen, M., Faber, J.H., Sørensen, P.B., 2012. Soil Ecosystem health and services–Evaluation of ecological indicators susceptible to chemical stressors. *Ecological Indicators* 16: 67-75.

Torres-Sallan, G., Schulte, R.P.O., Lanigan, G.J., Byrne, K.A., Reidy, B., Simó, I., Six, J., Creamera, R.E., 2017. Clay illuviation provides a long-term sink for C sequestration in subsoils. *Scientific Reports* 7: 45635.

Tripathi, R., Nayak, A.K., Bhattacharyya, P., Shukla, A.K., Shahid, M., Raja, R., Panda, B.B., Mohanty, S., Kumar, A., Thilagam, V.K., 2014. Soil aggregation and distribution of carbon and nitrogen in different fractions after 41 years long-term fertilizer experiment in tropical rice–rice system. *Geoderma* 213: 280-286.

van Veen, J.A., Kuikman, P.J., 1990. Soil structural aspects of decomposition of organic matter by micro-organisms. *Biogeochemistry* 11(3): 213-234.

Vance, E.D., Brookes, P.C., Jenkinson, D.S., 1987. An extraction method for measuring soil microbial biomass C. *Soil Biology and Biochemistry* 19(6): 703-707.

Wang, W., Chen, W.C., Wang, K.R., Xie, X.L., Yin, C.M., Chen, A.L., 2011. Effects of long-term fertilization on the distribution of carbon, nitrogen and phosphorus in water-stable aggregates in paddy soil. *Agricultural Sciences in China* 10(12): 1932–1940.

Watteau, F., Villemin, G., 2018. Soil microstructures examined through transmission electron microscopy reveal soil-microorganisms interactions. *Frontiers in Environmental Science* 6: 106.

Xiao, S., Zhang, W., Ye, Y., Zhao, J., Wang, K., 2017. Soil aggregate mediates the impacts of land uses on organic carbon, total nitrogen, and microbial activity in a Karst ecosystem. *Scientific Reports* 7: 41402.

Xie, J., Hou, M., Zhou, Y., Wang, R., Zhang, S., Yang, X., Sun, B., 2017. Carbon sequestration and mineralization of aggregate-associated carbon in an intensively cultivated Anthrosol in north China as affected by long term fertilization. *Geoderma* 296: 1-9.